593

HEAO-1
A-2 LED SOFT X-RAY SKY CATALOG
77-075A-02F

HEAO-3
HEAVY NUCLEI REDUCED DATA - GOLD
79-082A-03A
HEAVY NUCLEI REDUCED DATA - COBALT
79-082A-03B
HEAO C-3 VERIFY PROGRAM
79-082A-03C

HEAO-3
FIRST 28 FROM HEAO-3
79-082A-01A
HEAO3-A COMPRESSED DATA BASE
79-082A-01B
GAMMA RAY SPEC SHIELD
79-082A-06A

Table of Contents

----

1. INTRODUCTION:

The documentation for this data set was originally on paper, kept in NSSDC's Data Set Catalogs (DSCs). The paper documentation in the Data Set Catalogs have been made into digital images, and then collected into a single PDF file for each Data Set Catalog. The inventory information in these DSCs is current as of July 1, 2004. This inventory information is now no longer maintained in the DSCs, but is now managed in the inventory part of the NSSDC information system. The information existing in the DSCs is now not needed for locating the data files, but we did not remove that inventory information.

The offline tape datasets have now been migrated from the original magnetic tape to Archival Information Packages (AIP’s).

A prior restoration may have been done on data sets, if a requestor of this data set has questions; they should send an inquiry to the request office to see if additional information exists.

2. ERRATA/CHANGE LOG:

NOTE: Changes are made in a text box, and will show up that way when displayed on screen with a PDF reader.

When printing, special settings may be required to make the text box appear on the printed output.

Version	Date	Person	Page	Description of Change
01				
02				

3 LINKS TO RELEVANT INFORMATION IN THE ONLINE NSSDC INFORMATION SYSTEM:

http://nssdc.gsfc.nasa.gov/nmc/

[NOTE: This link will take you to the main page of the NSSDC Master Catalog. There you will be able to perform searches to find additional information]

4. CATALOG MATERIALS:

a. Associated Documents — To find associated documents you will need to know the document ID number and then click here.
http://nssdcftp.gsfc.nasa.gov/miscellaneous/documents/

b. Core Catalog Materials

HEAO 1

A-2 LED SOFT X-RAY SKY CATALOG

77-075A-02F ASXR-00064

THIS DATA SET HAS BEEN RESTORED. ORIGINALLY THERE WAS ONE 9-TRACK, 800 BPI TAPE WRITTEN IN EBCDIC. THERE IS ONE RESTORED TAPE. THE DR TAPE IS A 3480 CARTRIDGE AND THE DS TAPE IS 9-TRACK, 6250 BPI. THE TAPE WAS CREATED ON A 3033 COMPUTER. THE DR AND DS NUMBERS ALONG WITH THE CORRESPONDING D NUMBER IS AS FOLLOWS:

DR#	DS#	D#	FILES
DR03673	DS03673	D57541	1

B34901-000A DSC # 593
77-075A-02F

THE ASTROPHYSICAL JOURNAL SUPPLEMENT SERIES, 51:1–28, January 1983

HEAO A-2 SOFT X-RAY SOURCE CATALOG

J. J. NUGENT,[1] K. A. JENSEN,[1] J. A. NOUSEK,[2] G. P. GARMIRE,[2] K. O. MASON,[3] F. M. WALTER,[3]
C. S. BOWYER,[3] R. A. STERN,[4] AND G. R. RIEGLER[4]
Received 1981 December 28; accepted 1982 May 10

ABSTRACT

The *HEAO* A-2 low energy X-ray detectors have surveyed over 95% of the sky in the spectral bands 0.18–0.44 and 0.44–2.8 keV, down to a typical limiting sensitivity of 1×10^{-11} and 3×10^{-11} ergs cm^{-2} s^{-1} in each band, respectively. Using a significance criterion of 6 σ for existence, 114 sources are cataloged, of which 54 were previously undiscovered and 32 remain unidentified.

The catalog contains a listing of all counterpart identifications and a cross-reference to all *HEAO 1* A-2 low energy detector team publications on the catalog sources complete through the end of 1981.

Supplementary material allows the estimation of spectral parameters for simple spectral models from the observed intensities. Simple graphs allow the extraction of energy fluxes at the Earth, both with and without the effects of interstellar absorption.

The angular distribution of the cataloged sources in the 0.44–2.8 keV band is concentrated toward the galactic plane and resembles that seen at higher energy. The distribution in the 0.18–0.44 keV band is more uniform and contains many more newly discovered and unidentified sources.

Subject heading: X-rays: sources

I. INTRODUCTION

Before the launch of *HEAO 1* many surveys of the X-ray sky existed. These were the *Uhuru* catalog (Forman *et al.* 1978), the *OSO 7* catalog (Markert *et al.* 1979), the *Ariel* catalog (McHerdy *et al.* 1981), and the *SAS 3* RMC catalog (see Bradt, Doxsey, and Jernigan 1979). None of these surveys were sensitive to photon energies $\lesssim 1.5$ keV, rendering them relatively insensitive to sources whose spectra could be characterized by steep power laws (photon indexes $\lesssim -3$) or low temperatures ($\lesssim 1.5$ keV). Previous sounding rocket and satellite experiments that were sensitive to photons in the energy range 0.2–2.0 keV found a variety of objects that exhibited such spectra. Among them were supernova remnants (e.g., Cygnus Loop and Vela SNR), cataclysmic variables (e.g., SS Cygni), white dwarfs (e.g., HZ 43), and nearby stars (e.g., Capella and Sirius). An extragalactic source with a soft X-ray spectrum, Mrk 421, was discovered as well.

The *HEAO* A-2 experiment was primarily designed for studying the diffuse X-ray background; however, it was also capable of studying point sources with good sensitivity. The data collected from the part of the experiment known as the LED (low energy detectors) represent the most complete and sensitive sky survey below photon energies of 2 keV. All but 5% of the sky was systematically surveyed. In addition to providing information on the nature of the spectra of previously known sources, the LED was able to extend the list of known sources whose X-ray flux is predominantly below 2 keV by a factor of ~ 2.

Two spectral bands were employed in this survey. One was sensitive to photon energies between 0.18 and 0.44 keV, and the other was sensitive between 0.44 and 2.8 keV. For the purposes of this catalog, a conservative source existence criterion of 6.1 σ was used (1 σ, in this context, is defined with the intensity being the only interesting parameter; see § III for a more complete explanation). For a source to be detectable, at this significance, it would typically have to have a minimum flux of $\sim 1 \times 10^{-11}$ ergs cm^{-2} s^{-1} in the lower energy spectral band and $\sim 3 \times 10^{-11}$ ergs cm^{-2} s^{-1} in the higher energy range. These sensitivity levels may easily vary by an order of magnitude due to the nonuniform exposure in different points of the sky, the nonuniform nature of the soft X-ray background, and the different responses of the LED to different assumed spectral shapes of the hypothetical source. Section II of this paper briefly describes the LED experiment and the criteria used to select the data for the catalog. Section III outlines the source selection criteria. Section IV describes in detail the method of determining the positional error boxes and measured intensities of the sources that passed the selection criteria. There is also a discussion of the calibration of the angular offsets of the LED

[1]California Institute of Technology, Pasadena, California.
[2]Pennsylvania State University, University Park, Pennsylvania.
[3]University of California, Berkeley, Berkeley, California.
[4]Jet Propulsion Laboratory, Pasadena, California.

and efforts to verify our computing procedures. Section V is a guide for the understanding of the actual catalog table and the interpretation of the meaning of the intensity measurements. Finally, § VI discusses the attempts to identify both the soft sources found by the LED with previously known X-ray sources, the nature of the identified sources, and the angular distribution of sources seen in each spectral band.

II. EXPERIMENT DESCRIPTION

The data used to construct the catalog were taken from the narrowest of the four fields of view of the A-2 low energy experiment. This field of view is rectangular, with a triangular response of 1°55 full width at half maximum (FWHM) along the scan path and 2°95 FWHM perpendicular to the scan path. The on-axis geometric area of the detector over this field of view is 174 cm^2, providing an effective area of ~ 70–90 cm^2, depending on spectral shape. A more complete experimental description can be found in Rothschild *et al.* (1979).

Figure 1 shows the quantum efficiency as a function of incident photon energy for the first anode layer of the LED detector. Only events occurring in this layer were used in making the catalog. The absorption feature at 0.28 keV is due to the K shell of carbon in the polypropylene detector window. Since the pulse height of an event is roughly proportional to the incident photon energy, spectral bands can be established by setting pulse-height discriminators. For the purpose of the catalog, two spectral bands were defined. The location of the pulse-height discriminators that defined these two bands are represented in Figure 1 as vertical lines at 0.18, 0.44, and 2.8 keV. The band between 0.18 and 0.44 keV shall be referred to as the 0.25 keV band and the band between 0.44 and 2.8 keV will be referred to as the 1 keV band.

The spectral resolution of the LED detectors is modest, with $\Delta E/E$ equal to 73% (FWHM) at carbon Kα (277 eV) and is 32% at aluminum Kα (1486 eV). Because of resolution broadening, a photon with an energy corresponding to a given band has a probability to be counted in the other band. This has a significant—in some cases dominant—effect on the resultant count rate in the bands given an incident spectrum that is steeply rising or falling.

HEAO 1 was predominantly operated in a scanning mode, spinning at a constant angular velocity. Because of the location of the solar panels, the spin axis was constrained to remain pointed in the direction of the Sun. The view directions of the A-2 detectors were perpendicular to the spin axis; therefore, the fields of view of the experiment swept along lines of constant ecliptic longitude. Every 12 hr the spin axis moved ~ 0°5 along the ecliptic plane and thus incremented by the same amount the longitude scanned. In this way, a

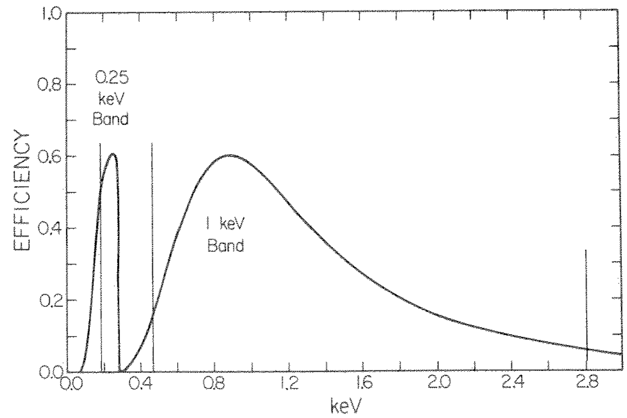

FIG. 1.—Quantum efficiency as a function of incident photon energy for the first anode layer of the LED detector. Vertical lines denote the setting of the pulse-height discriminators that define the 0.25 keV band and the 1 keV band.

raster scan was performed across any given point in the sky, except near the ecliptic poles where the scanning pattern resembled more the spokes of a wheel.

III. SOURCE SELECTION CRITERION

In the scanning mode, the spacecraft rotated once every ~ 33 minutes; thus, a given location on the great circle of observation might, in principle, be observed up to 44 times in 1 day. Unfortunately, most of these observations could not be used, either because the detectors were turned off, the Earth occulted the field of view, the particle background was high, or the high voltage setting differed from normal. Data taken in any of these conditions or other more minor exclusion criteria were automatically excluded. The remaining data were further culled by rejecting intervals with large deviations from the mean counting rate. Finally, the resultant data were examined by eye.

The remaining data from each single day were superposed into 0°5 azimuthal bins. Typically four scans of each bin survived the data inclusion criteria in a 1 day superposition, but some bins contain as many as 16 or as few as none.

Even after combining an entire day's worth of data, a typical azimuthal bin contained only ~ 25 counts. Thus, uncertainty in the sky intensity due to counting statistics produced a background noise obscuring the contributions of sources. To reduce this uncertainty, several days of observations have been combined for our source search.

The advantage of combining days is reduced as the ecliptic longitude of the daily scans moves away from the source ecliptic longitude because the source contribution is modulated by the 2°95 FWHM off-scan collimator response. If $\boldsymbol{Z}$ is a three-vector of unit length that defines the position of the spin axis in Cartesian coordinates and $\boldsymbol{P}$ is the position vector of a source in the sky, then the angle, θ, can be defined as follows:

$$\theta(\boldsymbol{Z},\boldsymbol{P}) = 90° - \cos^{-1}(\boldsymbol{Z}\cdot\boldsymbol{P});$$

θ shall also be referred to as the elevation angle, since it is the angular displacement of the given point off the scan plane for a given spin axis. As θ becomes larger, the source contribution becomes smaller until it vanishes for $\theta \gtrsim \theta_{\rm FWHM}$, where $\theta_{\rm FWHM}$ is the FWHM of the collimator in the off-scan direction. Background noise is introduced with each scan. In the idealized case with continuous angular coverage and flat background, the signal-to-noise ratio of a superposition which comprises an integration of the scanning data from $-\theta_I$ to $+\theta_I$ is given, in the weak source limit, by

$$\frac{S}{N}(\theta_I) = C\frac{[1-(\theta_I/2\theta_{\rm FWHM})]\theta_I}{\sqrt{\theta_I}}$$

$$= C\left(\theta_I^{1/2} - \frac{\theta_I^{3/2}}{2\theta_{\rm FWHM}}\right)\theta_I < \theta_{\rm FWHM}, \quad (1)$$

where C is a constant related to the source and background counting rates. Taking the derivative of equation (1) and setting it equal to zero determines that $\theta_{\rm max}$, the value of θ_I that maximizes the signal-to-noise ratio, is given by

$$\theta_{\rm max} = \frac{2}{3}\theta_{\rm FWHM}. \quad (2)$$

For $\theta_{\rm FWHM} \approx 3°$, equation (2) gives $\theta_{\rm max} \approx 2°$. As mentioned in § II, the spin axis of *HEAO 1* moved $\sim 0.5°$ every 12 hr along the ecliptic plane. For a given point near the intersection of the scan plane and the ecliptic plane, θ changed by $\sim 1°$ per day, and, hence, the optimum sensitivity could be obtained, in principle, by superposing 4 days of scanning data, 2 days on either side of the time of the on-axis transit. Further, since the observation periods scale as the secant of the ecliptic latitude, even larger number of days could be combined at high ecliptic latitudes.

In practice a running sum of three of the 1 day superpositions was employed. (These shall henceforth be referred to as 3 day superpositions.) As the spin axis of the satellite wandered $\sim 0.5°$, using 4 day sums would have, on average, extended the integrations beyond $\Theta_{\rm max}$. Even at high ecliptic latitudes, computational convenience and the desire to treat the data in a uniform way led us to use 3 day superpositions for fitting all sources. Most of the sky was only weakly affected by this less than optimum procedure. At the price of a minor sensitivity loss, the computation was greatly facilitated. For example, $\sim 71\%$ of the sky is contained between $+45°$ and $-45°$, but the percentage decrease from the optimum sensitivity at $\pm 45°$ is only $\sim 16\%$.

Restricting the source search to 3 day superpositions also has the advantage that it does not dilute as severely the sensitivity to strong transient sources. For example, if a source with an ecliptic latitude of 60° was in outburst for only 1 day, less background noise is added to the signal by using only 3 days rather than 6 days (= 3 sec 60°).

All 3 day superposition data sets were searched both automatically and by eye for pointlike features. To decide if the features should be included in the catalog, a model was fitted to the data by the method of least squares. The model consisted of a background component, parameterized by a second-order polynomial, and a source component whose free parameters were the position of the source along the scan plane and its intensity. In some cases a model including more than one source was required to fit the data adequately.

In order to accept the source we required that the source intensity must have been at least 4 times the 1 σ uncertainty in the intensity. To determine a 1 σ uncertainty, the intensity parameter was perturbed from the best fit value until the change in χ^2 from the best fit was 2.3. This was done by increasing and decreasing the intensity parameter with every other parameter left free so as to minimize χ^2. This procedure found the extent of the 68% confidence region for the intensity with two interesting parameters—intensity and position (see Lampton, Margon, and Bowyer 1976). One half of this extent was taken as 1 σ. A confidence level of 4 σ by the above definition corresponds to $\sim 6\ \sigma$ level for estimation of the intensity alone.

Those features which passed the 4 σ (or 99.99%) criterion were also subjected to other criteria in an attempt to exclude the possibility of UV contamination and confused or extended regions. Because polypropylene becomes partially transparent to radiation at ~ 2000 Å, a large flux of UV radiation is admitted to the counter when a bright UV emitting star is traversed. This large flux manifests itself as soft X-ray pulses, in the lowest pulse-height channel, by means of "pulse pile up." UV-induced events occur not only in the first layer of anode wires, where the data for this catalog were taken, but, because propane is fairly transparent to UV, they also occur in the back anode layers. This is in contrast to 0.25 keV photons which interact almost exclusively in the front layer. By modeling the response of the detectors to reasonable X-ray spectra, it was possible to exclude intensity ratios of the front to back anode layers that cannot be produced by an X-ray spectrum. In this way we were able to flag certain 0.25 keV band sources (a total of four sources) that were contaminated by UV-induced events.

A second problem is source confused and extended regions. The soft X-ray sky is known to contain a number of extended features. It is possible that some of the features we observe are not truly pointlike but are too small ($\lesssim 1^\circ\!.55$) for the A-2 detectors resolve. Similarly, our experiment has difficulty differentiating between a feature with an extent of $\lesssim 1^\circ\!.55$ and two point sources with similar spatial separation.

In order to deal with this problem, the following ground rules concerning the fit to the feature in the 3 day superposition were adopted:

1. The reduced χ^2 describing the goodness of fit of our data to the model must have been < 2.0. If the variation from our model was purely statistical, then one in 200 fits to true point sources would fail this condition.

2. Fits using multiple sources where the source to be cataloged was between $1^\circ\!.55$ and $3^\circ\!.0$ of another source were included in the catalog with a comment mentioning possible confusion.

3. Features that required two sources within $1^\circ\!.55$ of each other were not cataloged.

One difficulty with rule 1 arose from the deviation of the true collimator transmission function from the idealized triangles used in the fitting model. This is particularly severe in the collimator wings, i.e., far from the peak transmission. The triangular source model fails for only the brightest of sources ($\gtrsim 50$ counts s^{-1}) where these sources produce a systematically higher reduced χ^2. All such sources fall into the category of previously known X-ray sources, and with the exception of the supernova remnants are all known to be pointlike. Therefore, for bright known sources, we ignored the reduced χ^2 criterion discussed above.

IV. METHOD OF ANALYSIS

Once a source has met the criteria stated in § III, analysis was performed on the data to determine an error box and the source intensity. Because of the manner in which the satellite scans the sky, the problem of determining the position of a source can be—to a good approximation—separated into determining the position of the source along the scan plane and determining the position perpendicular to the scan plane. (This approximation begins to break down near the ecliptic poles.) To do the former, the data in the 3 day superposition that measured the intensity with the highest signal-to-noise ratio were fitted with a model as described in § III. To determine the uncertainty in this measurement, the position parameter was perturbed from the best fit while all other parameters were allowed to vary. The error region was defined for all those values of the position where the change in χ^2 from the best fit was less than 2.71. This corresponds to a 95% error region with only one interesting parameter (see Lampton, Margon, and Bowyer 1976; Cash 1976).

To determine the best position along the direction perpendicular to the scan plane, two methods were used. Both methods used the fact that the regular stepping of the satellite's spin axis along the ecliptical plane produced a raster scan across any point in the sky. The duration of the observation t is given by

$$t \approx 6 \sec l \,(\text{days}), \tag{3}$$

where l is the ecliptic latitude of the source.

The first method assumed that the source intensity remained constant during the observation time(s) (see the last paragraph of this section for a discussion of the validity of this assumption). The position was determined by using the observed intensity as a function of angular distance perpendicular to the scan plane. The previously mentioned 1 day superpositions were used to measure the source intensity on the day of maximum observed signal. The time corresponding to the middle of the 3 day superposition in which the source was observed with the highest signal-to-noise ratio was taken to be the midpoint of the nominal observation window. Equation (3) defines the extent of the window. For all 1 day superpositions, a fit was made to the source intensity by using the same model as was applied to the 3 day superposition. The only modification was that the position of the source along the scan plane was fixed to that measured in the 3 day superposition. In this case, 1 σ was defined as 68% confidence for only one interesting parameter. The intensity determined in this manner was discarded if the point source model was not a good fit to the data, i.e., with a reduced χ^2 of > 2.0. The remaining intensities were fitted to a model with the triangular response (FWHM of $2^\circ\!.95$) that characterizes the collimator transmission along the direction perpendicular to the scan plane. The uncertainty in the position was derived for a 95% confidence region with only one interesting parameter (position).

If the observing window implied by the best-fit position contained a different set of days than the nominal window, another iteration using the new set of days was performed.

After the final iteration, a χ^2 test was performed to evaluate the goodness of fit of a constant source intensity model to the data. If the reduced χ^2 was greater than the value corresponding to a 90% confidence level, the constant intensity hypothesis was considered questionable, and the best fit box was not included for that source.

A second, more conservative, method for determining an error region perpendicular to the scan plane results from arguing that the source must lie within the intersection of the fields of view when the source was detected. This error region is the common area or "overlap" of the projections of the field of views of the extreme days on which the source was detected. Explicitly, for a source to be "detected" on a given day, its intensity must have been measured at $> 2\,\sigma$, and the fit must have had a reduced $\chi^2 < 2.0$. Once the extreme days had been identified, a great circle, determined by

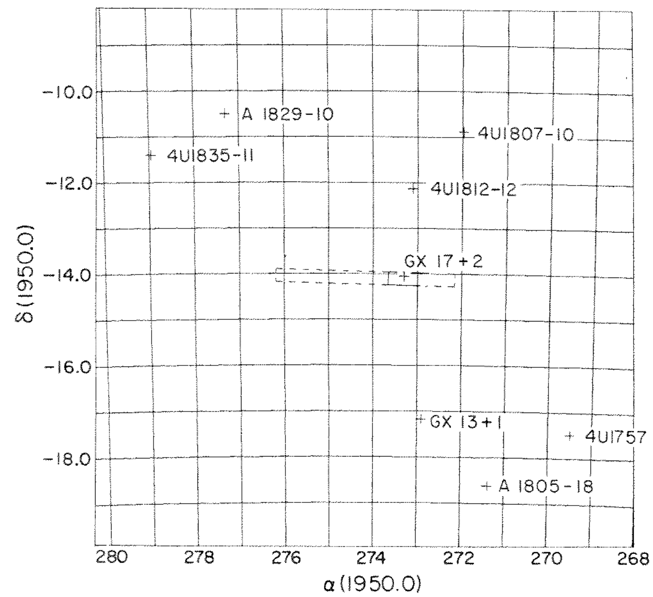

FIG. 2.—Error boxes for a typical source plotted on a tangent plane projection. Dotted line outlines the "overlap" error region, while solid line outlines the "best-fit" region. Crosses denote the position of known X-ray sources in the region.

the position of the spin axis on the highest signal-to-noise 3 day superposition and the best-fit position along the scan circle, is defined. The part of the circle that was observable during the transit on each of the two extremes was calculated next. Finally, the constraints on the position perpendicular to the scan plane were defined as the part of the great circle common to both observations.

The intensities in the 0.25 keV band and in the 1 keV band were calculated from fits to the one 3 day superposition with the highest signal to noise in either band. The uncertainty corresponds to a 68% confidence region with two interesting parameters.

Figure 2 shows the error boxes for typical source (H1813-14, more commonly known as GX17+2) plotted on a map along with the position of the known X-ray sources in the region. The dotted line shows the outline of the overlap error box, and the solid line outlines the best-fit error box. These error boxes display many of the typical features of the error boxes for a vast majority of source entries in the catalog. These are (1) two parallel sides common to both boxes that constrain the position along the scan plane representing the uncertainty in that direction; (2) the best fit box—when it exists—smaller and lying within the overlap box.

We tested the reliability of the method in various ways. First, to establish that the fitting procedures produce correct errors, Monte Carlo simulations of scans across idealized sources were performed. The resulting distribution was consistent with the predicted uncertainty. In order to eliminate any repeatable systematic problems (e.g., collimator offsets), previously measured pointlike X-ray sources whose position was known to $\lesssim 20''$ (much smaller than the typical uncertainty from the LED) were fitted using the above procedure. The average offset between our fit positions in the scan plane and the known source positions was $\lesssim 0\overset{\circ}{.}01$. The Crab Nebula, a bright, known, steady source, was used to calibrate the direction perpendicular to the scan plane. The systematic uncertainty in this direction was $\lesssim 0\overset{\circ}{.}05$. These systematic uncertainties are much smaller than the statistical uncertainties and were ignored in the calculation of the final error box.

A more uncertain aspect of the analysis is the determination of the nonsource contribution to the data used to fit for the position and intensity of catalog sources. In addition to the problem of source confusion common to mechanically collimated X-ray detectors at all energies, the diffuse X-ray background, particularly at 0.25 keV, is nonuniform. Our parameterization of the background by a second-order polynomial could prove inadequate in certain situations. For example, Monte Carlo simulations have shown that the use of this simplified background model, if the diffuse sky background near a source is discontinuous, could introduce systematic uncertainties in the source position on order of the size of the error box. No attempt was made to correct for this problem since to apply a proper model required an *a priori* knowledge of the background around each source. We are confident that these effects were ignorable for all but possibly a few sources, because our algorithm for computing errors based on counting statistics alone was successful in the case of sources with well-known positions. (While these well-known sources

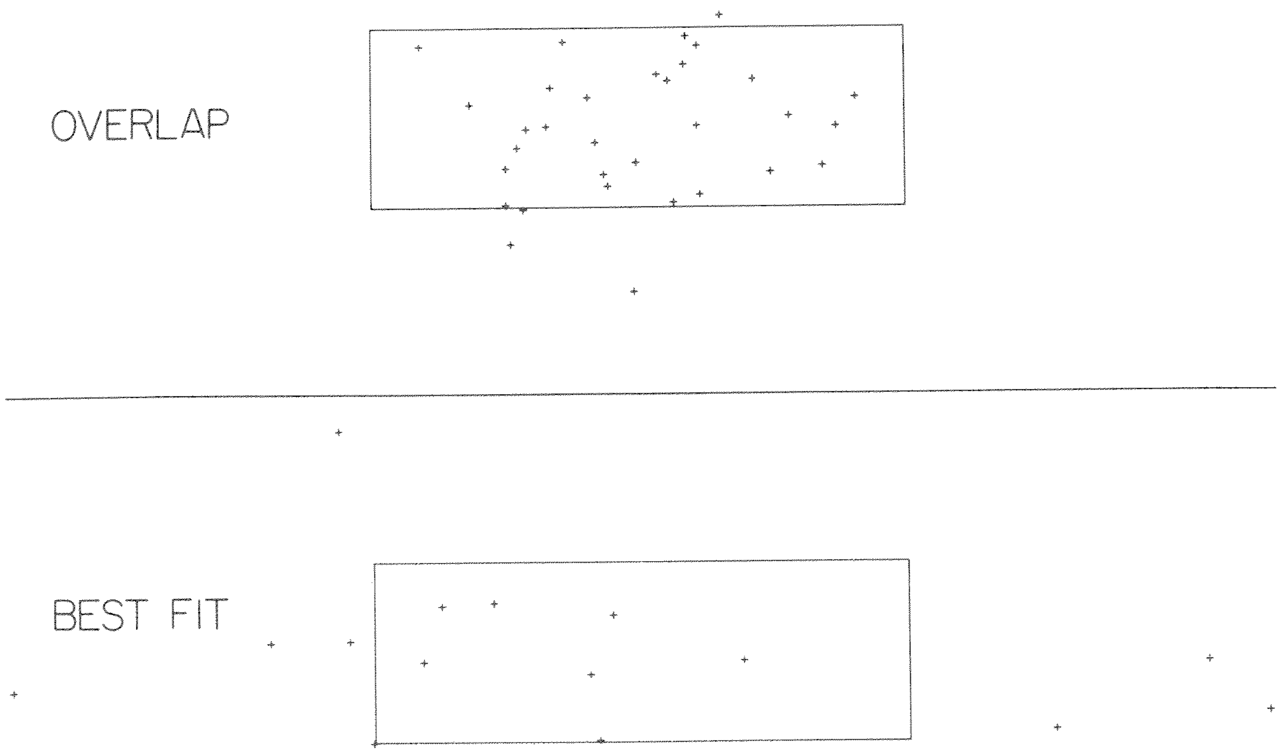

FIG. 3.—Summary of the result of the position analysis for previously known X-ray sources with positions accurate to $\lesssim 20''$. Dimensions of the error box are normalized to the size of the rectangle shown in each figure. True position is then plotted relative to this rectangle. In this way, any true position that lies within the corresponding error box will also lie within the plotted rectangle. (*a*) (*Top*) shows the overlap boxes; (*b*) (*bottom*) shows the best-fit boxes.

are, in general, comparatively bright, some are relatively faint in our bandpass and still are accurately positioned.)

A summary of the results of comparing the LED error boxes with known sources having positions accurate to $\lesssim 20''$ is displayed in Figure 3. The dimensions of the LED error box are normalized to the size of the rectangle shown in the picture. The true position is then plotted relative to this rectangle. In this way, any true position that lies within its corresponding LED error box will also lie within the plotted rectangle. This is done separately for the overlap error boxes and the best-fit error boxes. The best-fit part of the figure has fewer points due to the fact that—as was described above—not all source entries have best-fit boxes. For the overlap box, 29 out of 32 sources fell inside the error region. This is consistent with the expectation. However, for the best-fit box the scatter in the points is much larger than would be expected. This is most likely due to the weakness of the assumption of constant source intensity during the observation time.

V. RESULTS

Table 1 contains the results of the above analysis for all the sources that met the source selection criteria outlined in § III. There are a total of 114 catalog entries. They are organized in order of increasing right ascension.

The following is a description of the information contained in each entry of the catalog.

HEAO A-2 name.—This is the name assigned to the source based on the LED data. The names begin with the letter "H", followed by the right ascension and declination (in 1950 coordinates) of the center of the overlap box. This name is repeated in the last column.

Other names.—If the source has a positive identification or has been previously discovered in other X-ray surveys, its other aliases are given. If the alias is proceeded with the designation CGS, then it is to be found in *Positions and Identifications of Galactic X-ray Sources* (Bradt, Doxsey, and Jernigan 1979). The reader is referred there for any further catalog references.

Overlap box.—The top two lines of the six columns after "other names" give information concerning the position of the overlap error region for the source. The first and second line of the first column give the galactic coordinates, $l^{\rm II}$ and $b^{\rm II}$, respectively, of the geometric center of the overlap box. The second column gives the geometric center of the overlap box in 1950 celestial coordinates (right ascension is printed over declination). The next four columns display the positions of the

TABLE 1

HEAO A-2 Soft X-Ray Catalog

HEAO A-2 Name	Other Names	Center lII bII	Center RA (1950) Dec(1950)	Corners				Box Area	Int/Err	Comments	HEAO A-2 Name
		-------------	-------------	Overlap Box	-------------------				1 keV		
		-------------	-------------	Best Fit Box	-------------------				1/4 keV		
		120.00	5.48	3.72	6.68	7.30	4.34		8.1	SNR	
		1.17	63.61	63.11	64.39	64.09	62.83	.72	1.0		
H0021+63	TYCHO SNR										H0021+63
									<		
									1.6	Ref. 24	
		302.49	13.53	11.27	14.54	15.59	12.41		3.0	in SMC	
		-44.00	-73.40	-74.22	-72.40	-72.55	-74.39	.72	.5	SMC X-2 ?	
H0054-73											H0054-73
		302.03	14.58	13.70	14.39	15.45	14.77	.16	<		
		-44.60	-72.78	-72.91	-72.49	-72.64	-73.07		1.4		
		296.57	24.15	22.69	21.66	24.27	25.22		<	variable source	
		-48.09	-68.71	-70.15	-69.96	-68.18	-68.35	.80	.8		
H0136-68	3A0143-681										H0136-68
									2.6		
									.5		
		132.75	33.83	35.69	32.21	32.02	35.50		3.0	SNR	
		1.65	62.61	62.94	62.09	62.25	63.11	.33	.3		
H0215+62	HB3										H0215+62
									<		
									.5	Ref. 13	
		285.39	36.44	35.13	37.17	37.69	35.66		<	confused with H0305-65	
		-51.40	-62.57	-63.21	-61.76	-61.92	-63.37	.50	1.0	and H0248-63	
H0225-62											H0225-62
		284.97	36.77	36.19	36.82	37.34	36.71	.16	4.8		
		-51.50	-62.33	-62.48	-62.03	-62.18	-62.64		.7		
		136.24	41.81	44.33	40.08	39.31	43.64		1.4	QSO ?	
		2.84	62.37	62.45	61.53	62.24	63.18	1.76	.3		
H0247+62	3A0241+622										H0247+62
									<		
									1.0		
		145.77	41.87	39.16	44.22	44.60	39.60		3.6	AWM7	
		-16.12	41.20	40.97	42.28	41.36	40.08	3.82	.9	NGC1129 CD group	
H0247+41	3A0251+414										H0247+41
		145.81	41.93	41.10	42.36	42.76	41.51	.95	<		
		-16.08	41.22	41.50	41.83	40.92	40.60		2.7		
		283.01	42.15	42.16	41.35	42.14	42.93		<	confused with H0305-65	
		-49.15	-63.36	-62.92	-63.60	-63.79	-63.10	.30	1.0	and H0225-62	
H0248-63											H0248-63
									3.1		
									.7		
		283.07	46.30	45.57	46.23	47.02	46.36		<	confused with H0248-63	
		-46.55	-65.24	-65.48	-64.86	-65.00	-65.63	.25	1.8	and H0225-62	
H0305-65											H0305-65
		283.32	46.12	45.37	46.06	46.85	46.17	.25	3.2		
		-46.49	-65.41	-65.65	-65.02	-65.17	-65.80		.6		
		149.33	46.85	48.29	48.39	45.44	45.33			confused with H0316+41	
	ALGOL	-14.55	40.89	41.36	41.10	40.41	40.67	.63			
H0307+40	BETA PER										H0307+40
		149.41	47.00	46.61	46.72	47.40	47.29	.14	2.4	tf=1.20	
		-14.45	40.93	40.98	40.72	40.88	41.13		.3		
		150.62	49.16	49.51	49.52	48.82	48.80		21.9	confused with H0307+40	
	4U0316+41	-13.27	41.30	41.40	41.35	41.20	41.24	.03	.6		
H0316+41	PERSEUS CLUS										H0316+41
										Ref. 26	
		159.66	51.10	52.22	52.29	49.98	49.90		2.4	UV contaminated	
	H0323+28	-22.74	28.62	29.00	28.76	28.23	28.47	.52	.4		
H0324+28	UX ARI										H0324+28
		159.76	51.28	50.95	51.02	51.60	51.53	.13	3.3	tf=1.07	
		-22.61	28.66	28.71	28.47	28.61	28.85		.4	Ref. 37 38 9 7	
		237.15	53.35	50.74	55.74	55.91	50.89		5.4	NGC1365 ?	
		-54.27	-35.85	-36.53	-34.80	-35.11	-36.84	1.47	.8		
H0333-35											H0333-35
		237.02	53.55	53.15	53.78	53.95	53.32	.19	<		
		-54.11	-35.78	-35.73	-35.51	-35.83	-36.05		4.7		
		166.89	56.69	58.76	58.89	54.64	54.50		1.1		
		-22.92	24.21	24.92	24.35	23.48	24.04	2.29	.2		
H0346+24	PLEIADES										H0346+24
		166.46	55.94	54.84	54.99	57.03	56.90	1.10	.9		
		-23.50	24.05	24.11	23.55	23.98	24.54		.4	Ref. 3	

TABLE 1—*Continued*

HEAO A-2 Name	Other Names	Center lII / bII	Center RA (1950) / Dec(1950)	Corners				Box Area	Int/Err	Comments	HEAO A-2 Name
		Overlap Box / Best Fit Box							1 keV / 1/4 keV		
H0348+39		156.43	57.04	59.57	59.71	54.57	54.38		<	EPS PER?	H0348+39
		-10.90	39.83	40.54	40.00	39.06	39.60	2.26	1.4		
		156.24	56.64	55.86	56.03	57.42	57.26	.61	1.9		
		-11.15	39.76	39.90	39.36	39.61	40.15		.4		
H0353+30	CGS0352+309 X PER	163.30	58.35	59.48	59.63	56.17	56.00		1.7	X-ray pulsar	H0353+30
		-17.00	30.86	31.39	30.77	30.11	30.72	1.93	.4		
		163.25	58.26	57.65	57.81	58.86	58.70	.58	<	tf=1.08	
		-17.07	30.84	31.05	30.43	30.63	31.25		.7		
H0407-04		195.89	61.85	60.55	63.06	63.15	60.64		<	confused	H0407-04
		-37.37	-4.11	-4.15	-3.63	-4.06	-4.59	1.15	1.0		
		196.65	63.62	62.91	64.24	64.33	63.00	.59	1.7		
		-35.67	-3.75	-3.66	-3.40	-3.83	-4.09		.4		
H0410-07	H0405-08 40 ERI	200.63	62.71	64.73	64.83	60.68	60.58		1.8		H0410-07
		-38.56	-7.94	-7.22	-7.73	-8.60	-8.14	2.18	.4		
		200.31	61.87	61.21	61.31	62.52	62.42	.58	<	tf=1.23	
		-39.38	-8.12	-8.02	-8.48	-8.22	-7.76		2.8	Ref. 5	
H0416-12		206.39	64.03	63.68	64.33	64.38	63.73		<		H0416-12
		-39.40	-12.31	-12.26	-12.12	-12.36	-12.50	.16	1.2		
									4.3		
									.4		
H0447-43		248.59	71.88	68.59	74.94	75.11	68.73		<		H0447-43
		-39.98	-43.76	-44.24	-42.83	-43.19	-44.61	1.85	.4		
		248.59	71.88	71.62	71.99	72.14	71.78	.11	2.5		
		-39.98	-43.76	-43.62	-43.54	-43.91	-43.99		.3		
H0452+51		155.99	73.18	69.85	76.47	76.52	69.95		7.5		H0452+51
		5.36	51.66	51.51	52.06	51.72	51.18	1.40	1.3		
		156.24	73.93	73.73	74.07	74.14	73.80	.07	<		
		5.76	51.72	51.88	51.91	51.57	51.54		2.1		
H0456+46	HB9	160.64	74.22	71.31	77.12	77.15	71.37		8.6	SNR	H0456+46
		2.54	46.28	46.14	46.62	46.34	45.86	1.12	1.3		
		160.94	75.05	74.52	75.53	75.57	74.57	.20	<		
		3.02	46.34	46.44	46.52	46.24	46.16		2.1	Ref. 35	
H0513+45	CAPELLA	162.65	78.29	82.52	82.54	77.33	77.26		5.5		H0513+45
		4.56	45.89	46.31	45.83	45.59	46.07	1.75	.9		
		162.69	78.41	77.59	77.66	79.22	79.16	.53	4.0	tf=1.01	
		4.63	45.90	46.09	45.61	45.71	46.19		.8	Ref. 4 38 9 7	
H0513-40	CGS0512-401 NGC1851	244.48	78.44	76.93	79.83	79.94	77.03		4.8	globular cluster	H0513-40
		-34.78	-40.04	-40.02	-39.60	-40.04	-40.45	1.00	1.2	burster	
		244.48	78.34	77.69	78.87	78.98	77.79	.41	<	tf=1.09	
		-34.86	-40.05	-39.91	-39.75	-40.18	-40.35		4.8		
H0524-70		281.26	81.10	82.33	78.85	79.96	83.44		8.7	near LMC Bar	H0524-70
		-32.74	-70.49	-71.27	-70.03	-69.69	-70.91	.86	.7	confused with LMC X-1	
										and LMC X-2	
		280.84	79.90	79.77	78.93	60.03	80.88	.22	2.0		
		-33.21	-70.05	-70.38	-70.06	-69.72	-70.03		.4		
H0532-66	CGS0532-664 LMC X-4	276.17	83.15	82.56	82.82	83.70	83.50		11.4		H0532-66
		-32.56	-66.26	-67.09	-65.41	-65.43	-67.11	.61	1.5		
									2.8	tf=1.05	
									.5		
H0534+21	CGS0531+219 CRAB = TAU X-1	184.95	83.66	83.67	83.68	82.59	82.58		575.0	SNR	H0534+21
		-5.18	21.98	22.09	21.87	21.82	22.04	.23	6.0		
									24.2	tf=1.33	
									1.7	Ref. 8	
H0539-64		273.71	84.79	82.18	86.67	87.21	82.74		21.5	1 keV flux may be	H0539-64
		-32.02	-64.23	-65.30	-62.93	-63.11	-65.50	.95	1.1	contaminated by LMC X-3.	
		275.01	82.73	82.06	82.85	83.41	82.62	.16	3.4		
		-32.82	-65.27	-65.35	-64.98	-65.18	-65.56		.6		

TABLE 1—*Continued*

HEAO A-2 Name	Other Names	Center lII / bII	Center RA (1950) / Dec(1950)	Corners (Overlap Box / Best Fit Box)				Box Area	Int/Err (1 keV / 1/4 keV)	Comments	HEAO A-2 Name
		273.38	84.98	82.26	87.36	87.53	82.43		22.9		
	CGS0538-641	-31.95	-63.95	-64.81	-62.95	-63.04	-64.90	.35	1.4		
H0539-63	LMC X-3										H0539-63
									2.1	tf=1.08	
									.8		
		283.29	85.06	90.69	79.30	79.93	91.09		2.9		
	CGS0521-720	-31.20	-72.42	-73.21	-71.90	-71.49	-72.77	1.65	.6		
H0540-72	LMC X-2										H0540-72
									<	tf=1.65	
									.9		
		280.26	86.41	90.55	82.28	82.42	90.63		10.4		
	CGS0540-697	-31.03	-69.86	-70.21	-69.58	-69.41	-70.04	.52	1.0		
H0545-69	LMC X-1										H0545-69
									<	tf=1.19	
									2.0		
		200.54	92.88	94.90	94.90	92.30	92.30		31.0	burster	
		-3.99	9.15	9.15	9.06	9.12	9.20	.20	1.2		
H0611+09	CGS0614+091										H0611+09
									2.3	tf=1.31	
									.7		
		189.81	95.16	93.42	96.90	96.90	93.42		12.8	SNR	
	IC443	4.31	22.53	22.64	22.52	22.40	22.52	.38	.8		
H0620+22	4U0617+23										H0620+22
									<		
									.7	Ref. 14 10	
		198.32	100.43	101.41	99.41	99.45	101.46		<	associated with the Monocerous	
H0641+15		5.53	15.57	15.22	15.36	15.91	15.76	1.07	3.1	Ring	H0641+15
									5.3		
									1.3	Ref. 22	
		227.28	100.88	101.13	100.61	100.63	101.14		<		
		-8.76	-16.65	-16.75	-16.71	-16.55	-16.60	.08	1.1		
H0643-16	SIRIUS										H0643-16
		227.28	100.88	100.99	100.74	100.76	101.01	.04	9.7	tf=1.05	
		-8.76	-16.65	-16.74	-16.72	-16.56	-16.59		.9		
		206.92	103.22	104.67	101.71	101.77	104.73		<	confused with H0656+05	
		4.22	7.33	6.92	7.22	7.74	7.44	1.55	2.9		
H0652+07										associated with the	H0652+07
		207.36	104.01	104.25	103.71	103.77	104.31	.28	4.7	Monocerous Ring	
		4.88	7.25	6.96	7.02	7.54	7.48		1.1	Ref. 22	
		239.25	103.23	106.25	106.19	101.27	101.35		<	UV contaminated	
H0652-28	EPS CMA	-11.96	-28.65	-28.79	-29.22	-28.61	-28.17	1.90	.7		
											H0652-28
		239.94	104.60	103.90	103.82	105.31	105.39	.58	2.7	tf=1.06	
		-10.95	-28.84	-28.51	-28.95	-29.16	-28.73		.7		
		209.18	104.06	104.49	103.57	103.63	104.55		<	confused with H0652+07	
		4.01	5.23	4.94	5.04	5.52	5.42	.44	2.2		
H0656+05										associated with the	H0656+05
									5.4	Monocerous Ring	
									1.1	Ref. 22	
		280.91	108.69	110.98	107.10	105.80	109.94		<		
		-23.39	-69.67	-67.19	-72.24	-72.12	-67.09	2.17	.4		
H0714-69											H0714-69
		281.06	108.56	109.19	109.10	107.93	108.02	.04	1.1		
		-23.47	-69.83	-69.84	-69.94	-69.82	-69.72		.4		
		199.50	118.50	115.53	121.48	121.45	115.50		<	variable	
		23.76	22.03	22.61	21.54	21.40	22.46	.85	1.1	New MED source	
H0754+22	U GEM										H0754+22
									48.8	tf=1.18	
									1.4	Ref. 11 12 19 18	
		287.99	161.17	161.50	160.47	160.85	161.88		7.6	ETA CAR	
		-.95	-59.89	-60.27	-59.68	-59.51	-60.10	.20	.9	also near G287.8-0.5(SNR)	
H1044-59	3A1042-595										H1044-59
									<		
									1.0		
		180.24	166.29	162.74	169.87	169.70	162.59		4.8	BL Lac object	
	2A1102+384	65.81	38.07	39.54	36.76	36.51	39.28	1.78	.7		
H1105+38	MRK421										H1105+38
		179.83	164.87	164.53	165.37	165.21	164.37	.20	6.3	tf=1.37	
		64.58	38.62	38.91	38.59	38.33	38.66		.9		

TABLE 1—*Continued*

HEAO A-2 Name	Other Names	Center lII / bII	Center RA (1950) / Dec (1950)	Overlap Box / Best Fit Box Corners				Box Area	Int/Err 1 keV / 1/4 keV	Comments	HEAO A-2 Name
		359.54	245.18	242.28	248.11	248.09	242.27		1495.5		
	CGS1617-155	22.98	-15.72	-15.20	-16.12	-16.21	-15.29	.55	82.5		
H1620-15	SCO X-1										H1620-15
									53.3	tf=1.00	
									22.2	Ref. 15	
		30.99	246.13	245.64	246.66	246.62	245.60		1.3	Herc cluster ?	
		38.77	15.30	15.50	15.29	15.11	15.31	.19	.5	possible source confusion	
H1624+15										in 1/4 keV Band	H1624+15
									2.4		
									.5		
		53.04	246.64	244.66	248.82	248.59	244.46		<	confused	
		43.09	32.45	33.26	32.25	31.60	32.61	2.47	1.1		
H1626+32											H1626+32
		53.19	245.71	245.09	246.54	246.32	244.87	.86	1.9		
		43.90	32.67	33.17	32.83	32.17	32.51		.4		
		16.37	246.67	245.56	247.84	247.78	245.50		<		
		31.95	1.60	1.97	1.57	1.23	1.63	.80	2.2		
H1626+01											H1626+01
		16.38	246.69	246.13	247.30	247.25	246.07	.40	2.7		
		31.94	1.60	1.86	1.66	1.33	1.53		.5		
		333.19	250.35	253.02	247.66	247.72	253.05		20.5	confused	
		-5.45	-53.86	-54.18	-53.66	-53.48	-54.00	.59	2.1	burster	
H1641-53	CGS1636-536									bulge source	H1641-53
		333.01	249.76	250.29	249.18	249.24	250.34	.12	<	tf=1.07	
		-5.15	-53.80	-53.95	-53.84	-53.66	-53.77		1.9		
		29.22	250.56	247.41	253.76	253.69	247.36		5.4		
		33.41	11.80	12.47	11.47	11.10	12.10	2.35	.9		
H1642+11											H1642+11
		29.13	250.27	249.60	251.00	250.93	249.54	.52	3.8		
		33.69	11.85	12.15	11.92	11.55	11.78		.7		
		355.53	252.31	254.47	250.13	250.16	254.49		9.2	confused with H1650-28	
		11.29	-26.07	-26.41	-25.92	-25.71	-26.19	.84	2.0		
H1649-26											H1649-26
		355.26	251.73	252.11	251.33	251.36	252.14	.15	<		
		11.73	-26.01	-26.16	-26.07	-25.86	-25.95		5.0		
		63.57	252.49	250.62	254.42	254.33	250.55		2.2	BL Lac object	
	4U1651+39	3 39.29	39.86	40.36	39.55	39.33	40.13	.70	.3		
H1649+39	MRK501										H1649+39
	A1653+398	63.52	252.79	252.48	253.17	253.09	252.40	.13	2.4	tf=1.17	
		39.06	39.79	39.98	39.83	39.61	39.76		.4		
		353.38	252.50	254.12	250.85	250.89	254.15		9.1	confused with H1649-26	
		9.39	-28.91	-29.19	-28.84	-28.62	-28.97	.65	1.9	New MED source	
H1650-28											H1650-28
		353.33	252.39	252.95	251.81	251.84	252.98	.23	<		
		9.47	-28.90	-29.07	-28.95	-28.73	-28.85		3.1		
		75.66	253.75	249.52	257.96	257.79	249.39		.7		
		38.69	49.22	50.27	48.29	48.02	49.98	1.77	.3		
H1655+49											H1655+49
									2.9		
									.4		
		348.37	253.88	256.88	250.89	250.90	256.89		49.7	bulge source	
	CGS1702-363	3.93	-36.21	-36.50	-35.94	-35.85	-36.41	.44	2.5		
H1655-36	SCO X-2										H1655-36
									<	tf=1.56	
									2.2		
		58.01	254.44	252.44	256.49	256.43	252.38		5.0		
	CGS1656+354	37.14	35.24	35.66	35.07	34.79	35.38	.94	.7		
H1657+35	HER X-1										H1657+35
									6.9	tf=1.15	
									.9		
		69.64	254.91	254.31	255.66	255.50	254.15		<		
		37.84	44.49	44.82	44.54	44.15	44.43	.41	.6		
H1659+44											H1659+44
		69.69	254.69	254.23	255.31	255.15	254.08	.33	1.8		
		37.99	44.53	44.84	44.61	44.22	44.45		.4		
		75.14	257.13	255.34	259.04	258.89	255.21		<	star HD155638	
		36.48	48.81	49.34	48.54	48.26	49.05	.76	1.0	V=8.5	
H1708+48										RS Cvn/emission reversal	H1708+48
									2.4		
									.3	Ref. 30	

TABLE 1—*Continued*

HEAO A-2 Name	Other Names	Center lII / bII	Center RA (1950) / Dec(1950)	Corners				Box Area	Int/Err	Comments	HEAO A-2 Name
		------------- Overlap Box	-------------------						1 keV		
		------------- Best Fit Box	-------------------						1/4 keV		
		81.98	258.09	255.19	261.10	260.87	254.99		<	binary star (HD154905,06)	
H1712+54		35.85	54.33	55.20	53.69	53.40	54.90	1.20	.5	V=5.5	H1712+54
		82.28	257.19	256.73	257.86	257.64	256.52	.23	2.0		
		36.37	54.56	54.84	54.57	54.27	54.55		.3		
		7.90	260.75	257.71	263.80	263.80	257.70		45.7	bulge source	
H1722-16	CGS1728-169 GX9+9	10.31	-16.75	-16.48	-16.84	-16.97	-16.61	.76	3.2		H1722-16
									<	tf=1.47	
									4.1		
		345.71	262.73	260.51	264.97	264.96	260.49		37.1	burster	
H1730-44	CGS1735-444	-6.28	-44.33	-44.15	-44.32	-44.47	-44.30	.48	2.5	bulge source	H1730-44
		346.26	264.29	264.10	264.49	264.48	264.09	.04	2.9	tf=1.36	
		-7.26	-44.39	-44.31	-44.32	-44.47	-44.45		1.3		
		357.07	265.79	261.77	269.82	269.82	261.76		32.8	confused	
H1743-32	CGS1743-322	-1.99	-32.45	-32.22	-32.42	-32.55	-32.35	.88	1.9	transient	H1743-32
									2.1		
									.9		
		2.54	266.14	262.22	270.07	270.07	262.21		12.3	burster	
H1744-26	CGS1744-265 GX3+1	1.01	-26.22	-25.94	-26.13	-26.39	-26.20	1.84	1.7	bulge source	H1744-26
									<	tf=1.02	
									3.3		
		5.07	269.34	267.78	270.90	270.90	267.77		17.2	bulge source	
H1757-24	CGS1758-250 GX5-1	-.84	-24.99	-24.87	-24.88	-25.10	-25.08	.62	2.1		H1757-24
									<	tf=1.06	
									2.1		
		8.92	269.36	267.85	270.88	270.88	267.85		18.7	bulge source	
H1757-20	CGS1758-205 GX9+1	1.36	-20.56	-20.45	-20.47	-20.66	-20.64	.55	2.0		H1757-20
									<	tf=1.10	
									1.9		
		1.85	269.86	267.69	272.04	272.04	267.69		10.7	confused	
H1759-28		-3.23	-28.98	-28.77	-28.78	-29.15	-29.14	1.43	1.9	near CGS1743-288	H1759-28
									<		
									1.6		
		358.21	271.22	267.07	275.36	275.41	267.04		8.9	confused	
H1804-33	CGS1755-338	-6.59	-33.78	-33.39	-33.33	-34.02	-34.08	4.78	1.5		H1804-33
		357.49	269.45	268.79	270.11	270.11	268.78	.76	<	tf=3.04	
		-5.30	-33.78	-33.44	-33.44	-34.13	-34.13		1.3		
		93.25	273.50	270.53	275.96	276.66	271.25		1.6	New MED source ?	
H1814+63		28.19	63.74	62.86	64.93	64.55	62.51	1.53	.4	3C 383 ?	H1814+63
									1.4		
									.4		
		13.94	273.54	270.79	276.28	276.29	270.80		9.2	bulge source	
H1814-17	CGS1811-171 GX13+1	-.36	-17.02	-16.91	-16.79	-17.10	-17.22	1.63	1.4		H1814-17
		13.79	273.23	273.01	273.44	273.44	273.02	.13	<	tf=1.48	
		-.10	-17.03	-16.88	-16.87	-17.18	-17.19		2.5		
		77.95	274.08	273.40	274.75	274.75	273.41		2.2	variable	
H1816+49	CGS1814+498 AM HER	25.67	49.88	49.89	49.94	49.87	49.82	.06	.9	binary	H1816+49
									61.4	tf=1.08	
									2.2	Ref. 32 33 36	
		16.81	274.17	272.16	276.18	276.19	272.17		16.5	bulge source	
H1816-14	CGS1813-140 GX17+2	.51	-14.09	-13.99	-13.89	-14.18	-14.28	1.10	1.5		H1816-14
		16.36	273.25	272.84	273.66	273.66	272.85	.22	<	tf=1.21	
		1.29	-14.11	-13.98	-13.96	-14.25	-14.26		1.7		
		2.54	274.48	272.37	276.59	276.59	272.37		79.1	confused	
H1817-30	CGS1820-303 NGC6624	-7.42	-30.38	-30.39	-30.28	-30.32	-30.44	.19	1.8	burster	H1817-30
										globular cluster	
									2.7	tf=1.23	
									.8		

TABLE 1—*Continued*

HEAO A-2 Name	Other Names	Center lII bII	Center RA (1950) Dec(1950)	Corners				Box Area	Int/Err	Comments	HEAO A-2 Name
		Overlap Box							1 keV		
		Best Fit Box							1/4 keV		
		36.09	279.28	278.59	279.97	279.98	278.59		32.7	burster	
	CGS1837+049	4.93	5.01	4.99	5.10	5.02	4.91	.11	1.5		
H1837+05	SER X-1										H1837+05
									<	tf=1.03	
									2.0		
		90.79	283.24	287.73	288.16	279.46	279.00		<	transient	
		23.18	60.66	62.50	62.21	58.78	59.04	1.92	2.2	binary star HD173739,40 ?	
H1852+60											H1852+60
									4.6		
									.8	Ref. 31	
		34.92	286.25	285.58	286.88	286.93	285.63		4.7	burster	
		-3.51	.09	.20	.37	-.03	-.19	.52	.9	near AQL X-1	
H1905+00	CGS1905+000										H1905+00
		34.88	286.18	285.80	286.52	286.57	285.85	.29	<	tf=1.08	
		-3.46	.08	.23	.32	-.07	-.16		1.6		
		10.46	288.71	287.04	290.31	290.37	287.09		6.1	confused	
		-17.56	-27.60	-27.59	-27.21	-27.59	-27.97	1.12	1.1		
H1914-27											H1914-27
									<		
									1.5		
		75.42	289.69	286.25	293.00	293.19	286.49		3.1	cluster of galaxies	
	A2319	13.55	43.63	43.01	44.62	44.15	42.54	2.57	.6		
H1918+43	4U1919+44										H1918+43
									1.7	Ref. 27	
									.6		
		64.96	292.30	291.72	292.83	292.88	291.77		8.4	SNR	
		6.00	31.03	30.99	31.23	31.06	30.82	.17	.9	near Cygnus Superbubble	
H1929+31	G65.2+5.7										H1929+31
									5.9		
									.6	Ref. 20 6	
		51.34	299.32	297.81	300.79	300.83	297.85		14.9		
		-9.38	11.57	11.31	12.00	11.82	11.13	.55	1.3		
H1957+11	4U1956+11										H1957+11
									2.1	tf=1.02	
									.8		
		71.48	299.35	299.06	299.62	299.64	299.08		45.9		
	CGS1956+350	2.94	35.12	35.07	35.22	35.18	35.03	.02	1.3		
H1957+35	CYG X-1										H1957+35
									<	tf=1.07	
									1.7		
		336.61	300.28	299.71	300.65	300.86	299.91		<	extented region in Delphinus	
		-32.40	-60.56	-60.46	-60.32	-60.67	-60.30	.18	1.5	SNR?	
H2001-60											H2001-60
		336.76	301.27	300.73	301.60	301.81	300.94	.16	3.2		
		-32.89	-60.42	-60.31	-60.18	-60.53	-60.66		.6	Ref. 29	
		62.13	301.33	299.37	303.18	303.31	299.51		<		
		-5.03	22.97	22.68	23.68	23.23	22.24	1.67	1.9		
H2005+22											H2005+22
		62.14	301.34	300.90	301.66	301.79	301.03	.33	3.8		
		-5.04	22.97	23.09	23.29	22.85	22.65		.7		
		77.78	303.08	304.74	304.89	301.45	301.29		9.8	part of Cygnus A extended	
		3.49	40.71	41.42	41.15	39.97	40.23	.82	1.3	region?	
H2012+40										Cygnus Superbubble?	H2012+40
									<		
									1.6	Ref. 6	
		87.45	325.81	325.05	326.53	326.58	325.11		78.5		
	CGS2142+380	-11.37	38.12	37.81	38.50	38.43	37.74	.11	3.6		
H2143+38	CYG X-2										H2143+38
									4.0	tf=1.04	
									1.4		
		17.49	328.68	328.12	328.06	329.22	329.29		10.5	BL Lac object	
		-51.99	-30.58	-30.85	-30.69	-30.31	-30.46	.17	.9	New MED source	
H2154-30	PKS 2155-304										H2154-30
									14.1	tf=1.11	
									1.1	Ref. 1	
		117.73	347.90	350.11	347.62	345.97	348.23		1.1		
		16.05	77.64	78.49	76.68	76.78	78.60	.74	.2		
H2311+77											H2311+77
		118.19	348.85	350.24	349.32	347.51	348.34	.24	<		
		16.61	78.33	78.57	77.97	78.08	78.68		.8		

TABLE 1—*Continued*

HEAO A-2 Name	Other Names	Center lII / bII	Center RA (1950) / Dec(1950)	Corners				Box Area	Int/Err (1 keV / 1/4 keV)	Comments	HEAO A-2 Name
		Overlap Box							1 keV		
		Best Fit Box							1/4 keV		
		307.69	350.92	344.12	354.45	356.07	346.09		.8		
		-36.96	-79.65	-81.05	-77.98	-78.15	-81.26	1.32	.4		
H2323-79											H2323-79
									3.9		
									.5		
		113.94	353.59	348.96	358.14	358.81	349.64		4.4	SNR	
		-.76	60.52	58.46	62.78	62.41	58.13	3.03	.9		
H2334+60	CAS A										H2334+60
		114.32	354.23	352.24	355.61	356.30	352.92	1.09	<		
		-.56	60.82	60.19	61.78	61.42	59.85		1.9		

corners of the overlap error box in 1950 celestial coordinates.

Best-fit box.—The bottom two lines of the six columns after "other names" present information concerning the position of the best-fit error region for the source. The fourth and fifth line of the first column give the galactic coordinates, $l^{\rm II}$ and $b^{\rm II}$, respectively, of the geometric center of the best-fit box. The second column gives the geometric center of the best-fit box in 1950 celestial coordinates (right ascension is printed over declination). The next four columns provide the positions of the corners of the best-fit error box in 1950 celestial coordinates. This box is omitted if the data are inconsistent with a constant source. See § IV for details.

Box area.—This is the size of the error boxes in units of $\deg^2$. The number in the second line refers to the size of the overlap error box. If the best-fit error box exists, its size will be given on the fourth line.

INT/ERR.—This is the measured intensity, in units of counts s^{-1}, with its 1 σ uncertainty, for the two spectral bands defined in § II. The numbers on the first and second lines are the intensity and error for the 1 keV band, respectively. Likewise, the bottom two numbers refer to the measured intensity in the 0.25 keV band. When a < sign appears in the intensity position, it means that the number below is to be interpreted as a 2 σ upper limit. Discussion is given below on the conversion of these numbers to fluxes and on the relevance of the ratio of the intensities of the two spectral bands. The intensity is derived from the data in a uniform way, without regard to any source identification. To the extent that our source locations differ from the true source location, the quoted intensities are underestimates of the true source intensities. For known sources we include in the comments column a transmission factor based on the offset between our position and the source. Under the assumption that all the flux we detect is coming from the known source, the true source intensity is the product of the transmission factor and the quoted intensity.

Comments.—Comments include possible identifications, anomalies in the analysis of the LED data, and mention of unusual source characteristics. UV contamination refers to probable contamination of the 0.25 keV band by ultraviolet radiation from the object. The comment "confused" denotes a case that required a second source within 3° of the best-fit position of the cataloged source to adequately account for the data. "New MED source" denotes a previously unknown source that was detected by other *HEAO* A-2 detectors sensitive to photons with energies $\gtrsim$ 2 keV (see Marshall *et al.* 1979 for most information). "Transmission factor" (tf) is a correction factor for our intensities if the source identification is correct (see the preceding discussion of the INT/ERR column). If further discussion of the LED data analysis for a cataloged source appears in the literature, a reference number(s) is given. The actual reference that the number denotes can be found in Table 2.

The conversion of the measured intensity (in terms of counts s^{-1}) to a flux (in terms of ergs cm^{-2} s^{-1}) or a spectral density (in terms of μJy) is dependent on the incident spectrum. We define f_i as the conversion factor to flux for the ith band, using the spectrum as it appears at the top of the atmosphere (i.e., including interstellar absorption). It is given by

$$f_i = \left\{ \int_{E_{L_i}}^{E_{U_i}} E(dN/dE)(E) \exp\left[-\sigma(E) N_{\rm H}\right] dE \right\} \times \left\{ \int_{E_{L_i}}^{E_{U_i}} \int_0^\infty AT(E, E')(dN/dE)(E') \times \exp\left[-\sigma(E') N_{\rm H}\right] dE' dE \right\}^{-1}, \quad (4)$$

where A is the collecting area of the detector, E_{L_i} and E_{U_i} refer to the photon energies of the lower and upper pulse-height discriminators of the band i, respectively, $(dN/dE)(E)$ is the assumed source photon spectrum, $\sigma(E)$ is the interstellar absorption coefficient,[5] $N_{\rm H}$ is

[5] Throughout this paper the interstellar absorption cross sections are taken from Brown and Gould (1970).

TABLE 2

REFERENCE CROSS INDEX

Number	Reference
1..........	Agrawal and Riegler 1979
2..........	Agrawal and Riegler 1980
3..........	Agrawal, Riegler and Garmire 1980
4..........	Cash *et al.* 1978
5..........	Cash *et al.* 1979
6..........	Cash *et al.* 1980
7..........	Walter *et al.* 1980
8..........	Charles *et al.* 1979
9..........	Charles, Walter, and Cash 1979
10..........	Charles *et al.* 1981
11..........	Cordova 1979
12..........	Cordova *et al.* 1980
13..........	Galas, Tuohy, and Garmire 1980
14..........	Galas, Venkatesan, and Garmire 1981
15..........	Kahn *et al.* 1981
16..........	Lea *et al.* 1979
17..........	Lea *et al.* 1981
18..........	Mason *et al.* 1978
19..........	Mason, Cordova, and Swank 1979
20..........	Mason *et al.* 1979
21..........	Middleditch *et al.* 1981
22..........	Nousek *et al.* 1981
23..........	Nugent and Garmire 1978
24..........	Pravdo *et al.* 1980
25..........	Pravdo *et al.* 1981
26..........	Primini *et al.* 1981
27..........	Reichart *et al.* 1981
28..........	Riegler, Agrawal, and Gull 1980
29..........	Stern *et al.* 1980
30..........	Stern *et al.* 1981
31..........	Stern, Agrawal, and Riegler 1981
32..........	Tuohy *et al.* 1978*a*
33..........	Tuohy *et al.* 1978*b*
34..........	Tuohy *et al.* 1979
35..........	Tuohy, Clark, and Garmire 1979
36..........	Tuohy *et al.* 1981
37..........	Walter, Charles, and Bowyer 1978*a*
38..........	Walter, Charles, and Bowyer 1978*b*

neutral hydrogen column density to the source, and $T(E,E')$ gives the probability that a photon with energy E' impinging on the detector will cause an event with a pulse height corresponding to an energy between E and $E+dE$.

Many previous catalogs quote one nominal number for each band since for all but extreme types of spectra the conversion factors only vary by 10%–20% (see, for example, Forman *et al.* 1978). However, for the LEDs the nominal conversion factor can vary by 30 or more for a range of reasonable spectra. Thus, in order to convert our observed count rates into energy flux a specific spectral model must be assumed. To aid the reader we have calculated the conversion factors appropriate to three simple spectral types commonly used in X-ray astronomy: (*a*) thermal bremsstrahlung, $dN/dE \propto g(E)(e^{-E/kT}/E)$, where $g(E)$ is the energy dependent Gaunt factor, (*b*) power law spectra, $dN/dE \propto E^{-\gamma}$, where γ is the photon index; and (*c*) blackbody spectra, $dN/dE \propto E^2/(e^{E/kT}-1)$.

Conversion factors in units of 10^{-11} ergs cm^{-2} count^{-1} are displayed as contour plots in Figure 4 (thermal bremstrahlung), Figure 5 (power law), and Figure 6 (blackbody). The applicable conversion factor can simply be read off these plots by finding the intersection of the desired spectral shape parameter (temperature for thermal models or photon index for power-law models) along the *x*-axis and the intervening absorption column density along the *y*-axis. (Note: the contours are labeled with letters whose values are displayed to the right of each figure.)

The selection of an appropriate model is up to the reader, but some words of caution apply. Certain regimes of model space can produce pathological results. This is particularly true of highly absorbed spectra ($N_H \gtrsim 10^{21}$) in the 0.25 keV band and for extremely soft spectra ($T \lesssim 0.1$ keV) in the 1 keV band. In these cases the conversion factors are based on the extrapolated extreme wings of the detector energy response and are highly uncertain. If no independent means of estimating model parameters exist (say from measurements at higher energies), the ratio of the 1 keV band to the 0.25 keV band can be used to estimate spectral parameters. This ratio, called the hardness ratio, is displayed as a contour plot in Figure 7*a-c*. The area in Figure 10 with the observed hardness ratio corresponds to the allowed area in two-dimensional model parameter space (spectral parameter and N_H) which is consistent with the data.

Frequently the astrophysically interesting quantity is not the X-ray flux at the Earth, but at the source. Let d_i be the amount of flux in band i that would have been received if the interstellar medium were not present, then

$$d_i = \left[\int_{E_{L_i}}^{E_{U_i}} E(dN/dE)(E)\,dE\right] \times \left\{\int_{E_{L_i}}^{E_{U_i}}\int_0^\infty AT(E,E')(dN/dE)(E') \times \exp\left[-\sigma(E')N_H\right] dE'\,dE\right\}^{-1}. \quad (5)$$

Equation (5) is similar to equation (4), except that N_H is set to zero in the integral in the numerator. Figures 8, 9, and 10 are contour plots of d_i evaluated for thermal bremsstrahlung, power-law, and blackbody type spectra. The display is similar to Figures 4, 5, and 6, with the exception of a scale change for the contours.

A simple example may aid the reader in the use of Figures 4–10. The Crab Nebula ($=$ H0534+21) has a hardness ratio of 23.8 ± 1.7. Assuming a power-law spectrum, Figure 7*b* immediately reveals that N_H must be in the range 1–6×10^{21} cm^{-2}. For a photon index of -2

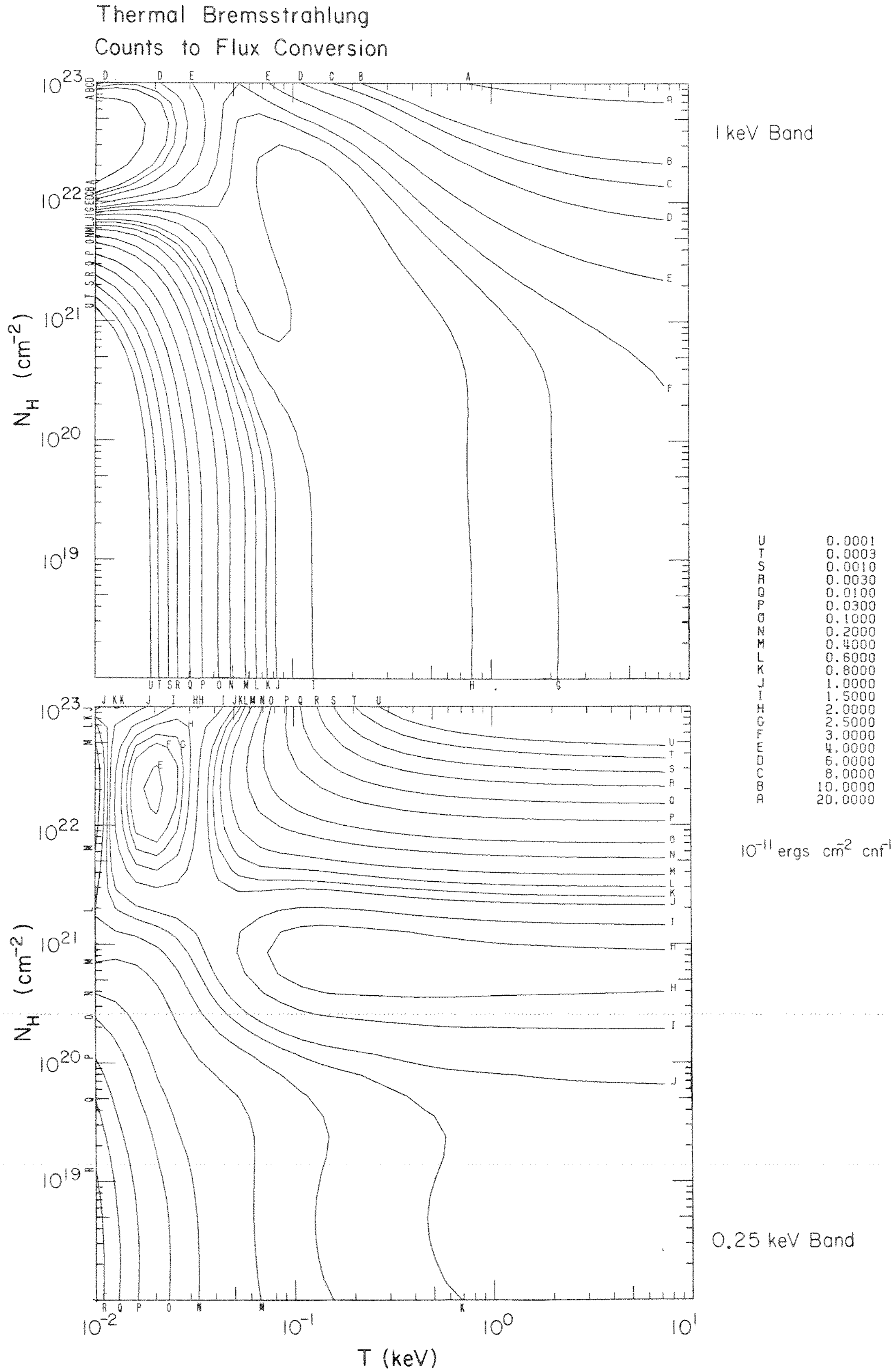

FIG. 4.—Factors to convert counts s^{-1} in the LED detector bands to an energy flux (in units of ergs cm^{-2} s^{-1}). Factors are for a thermal bremsstrahlung spectrum and are shown as a function of temperature and interstellar neutral hydrogen column density. These factors give the flux as it would appear at the top of the atmosphere. (*a*) (*Top*) is for the 1 keV band; (*b*) (*bottom*) is for the 0.25 keV band.

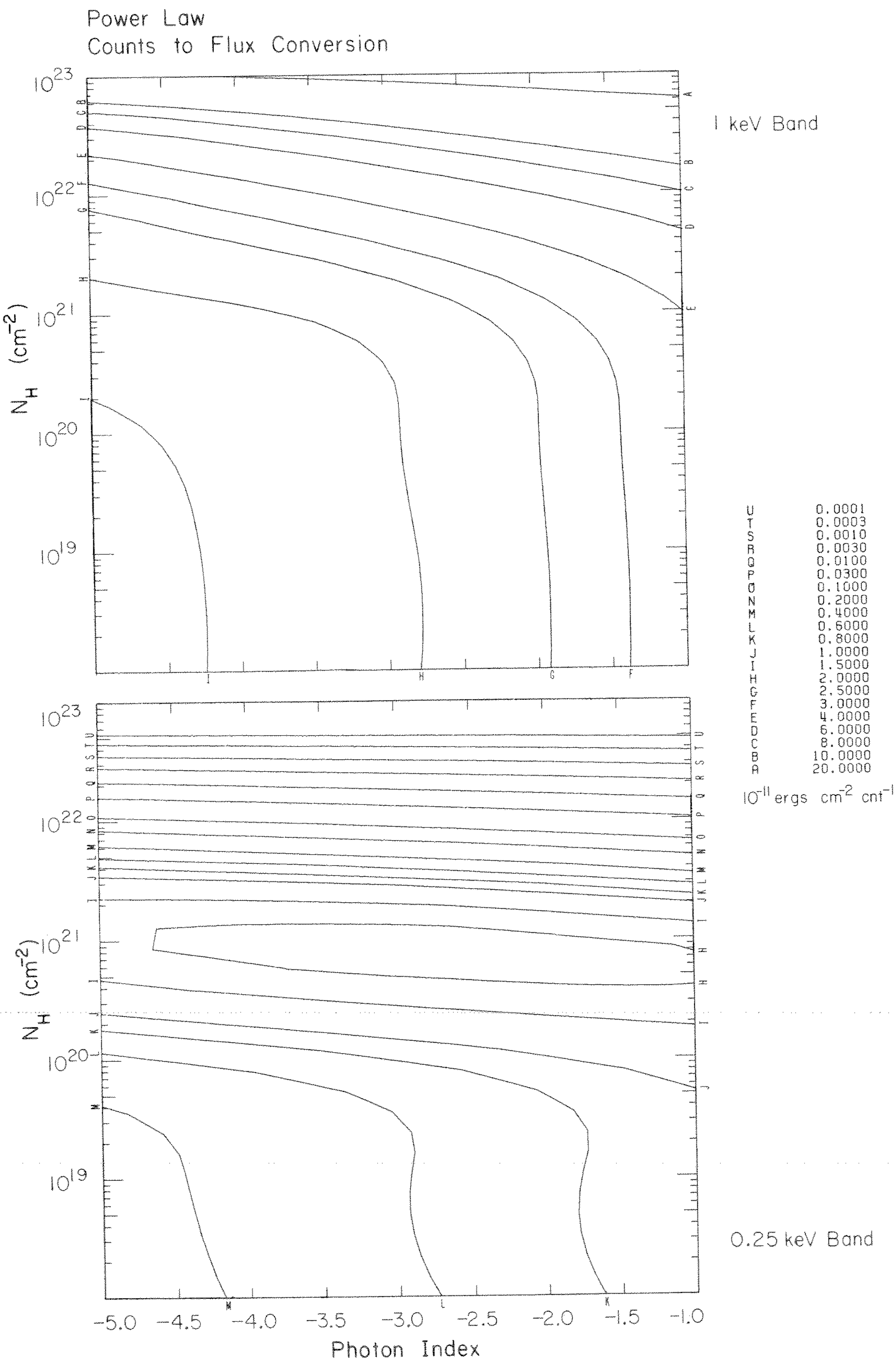

FIG. 5.—Factors to convert counts s^{-1} in the LED detector bands to an energy flux (in units of ergs cm^{-2} s^{-1}). Factors are for a power-law spectrum and are shown as a function of photon index and interstellar neutral hydrogen column density. These factors give the flux as it would appear at the top of the atmosphere. (*a*) (*Top*) is for the 1 keV band; (*b*) (*bottom*) is for the 0.25 keV band.

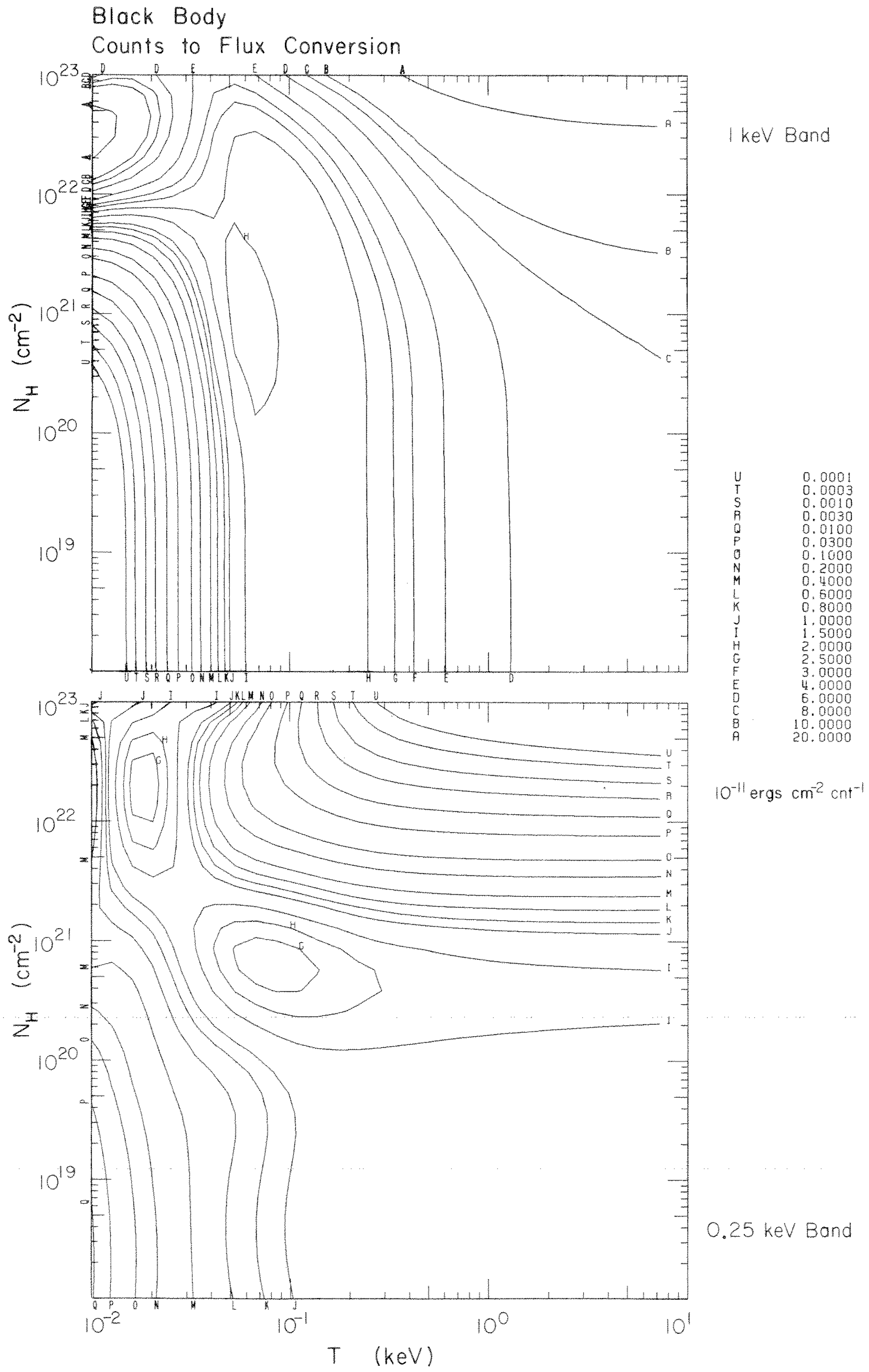

FIG. 6.—Factors to convert counts s^{-1} in the LED detector bands to an energy flux (in units of ergs cm^{-2} s^{-1}). Factors are for a blackbody spectrum and are shown as a function of temperature and interstellar neutral hydrogen column density. These factors give the flux as it would appear at the top of the atmosphere. (*a*) (*Top*) is for the 1 keV band; (*b*) (*bottom*) is for the 0.25 keV band.

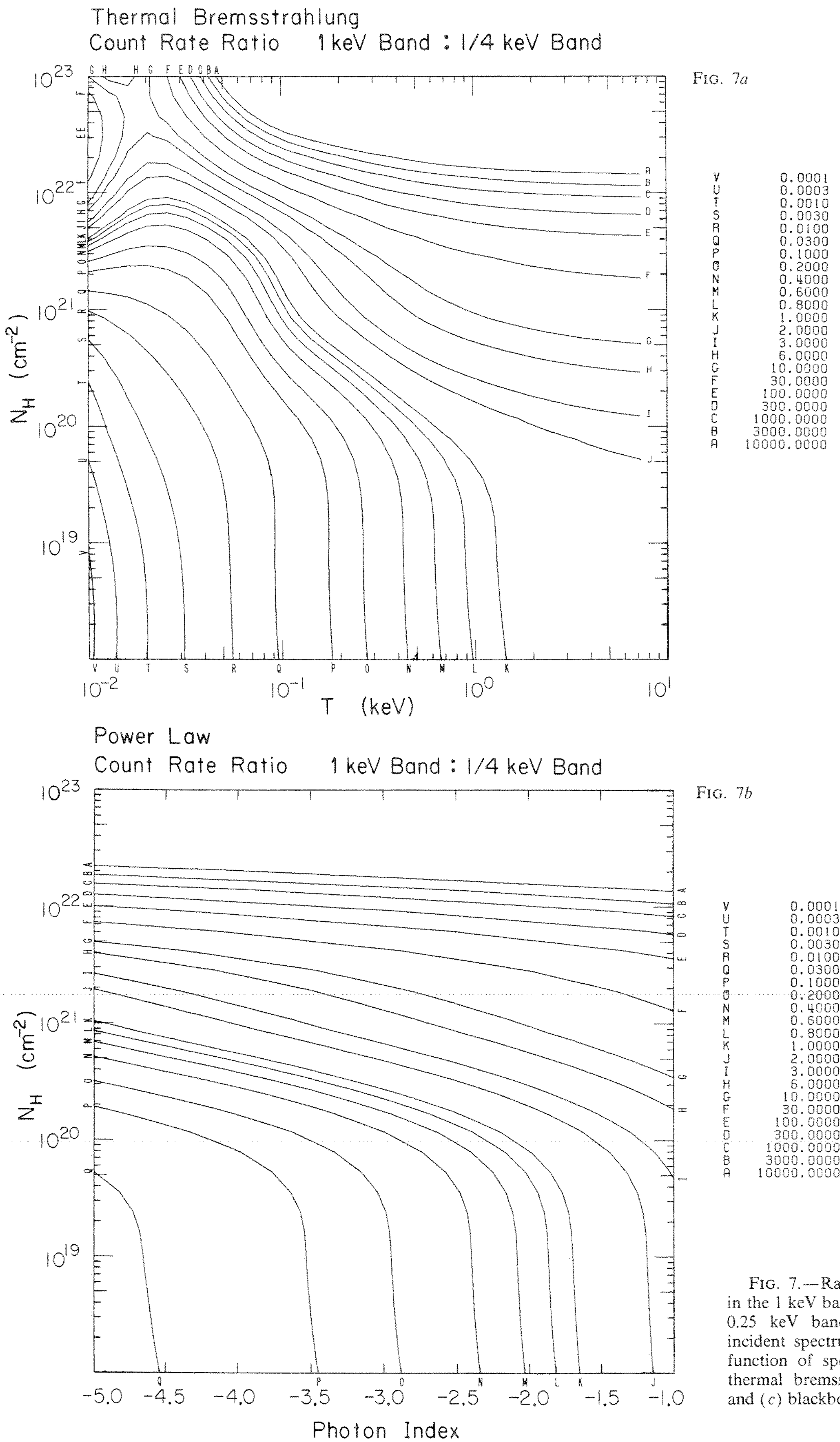

FIG. 7*a*

FIG. 7*b*

FIG. 7.—Ratio of expected count rate in the 1 keV band to the count rate in the 0.25 keV band as a function of the incident spectrum. Ratio is plotted as a function of spectral parameters for (*a*) thermal bremsstrahlung, (*b*) power-law, and (*c*) blackbody type spectra.

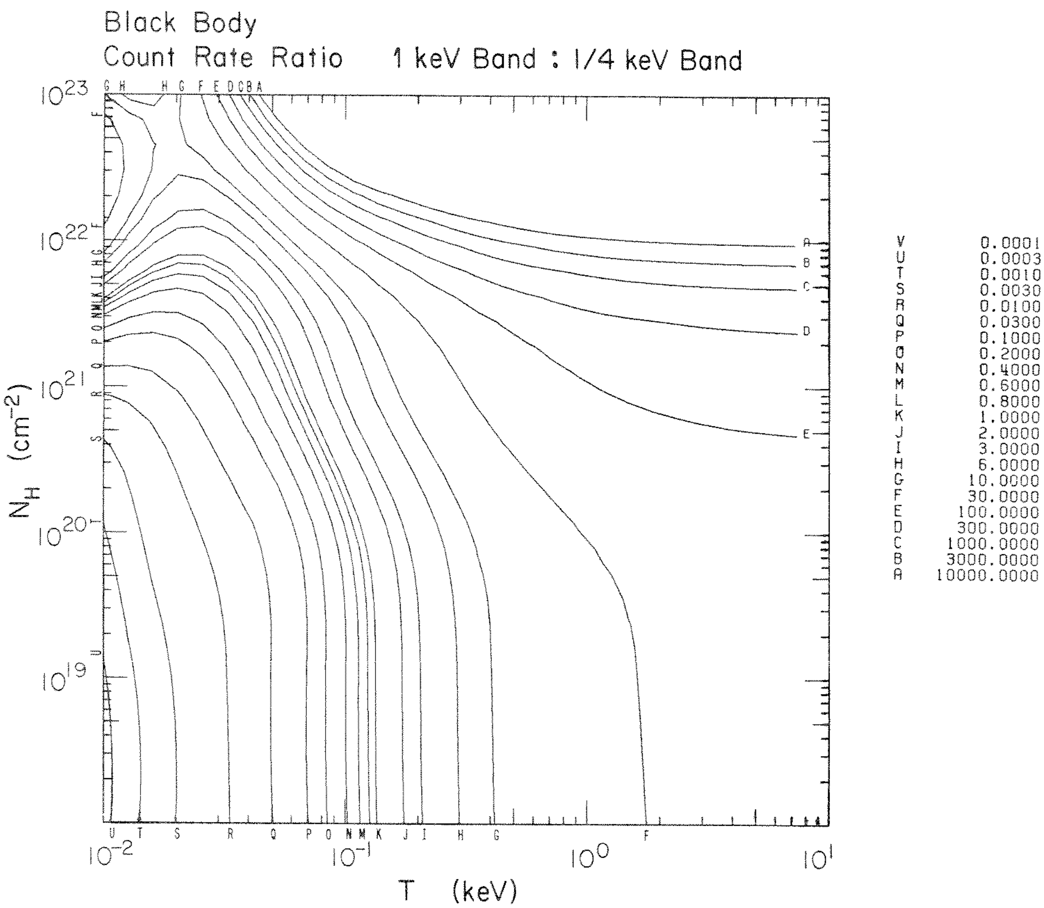

FIG. 7*c*

we can fairly precisely determine N_H to be 2×10^{21} cm^{-2}. Figure 5*a* gives the conversion factor of $\sim3.6\times10^{-11}$ ergs cm^{-2} counts^{-1}, so the Crab Nebula flux at the Earth in the 1 keV band is 2.1×10^{-8} ergs cm^{-2}. From Figure 9*a* we find that without interstellar absorption the source flux is 3.2×10^{-8} ergs cm^{-2}. While detailed pulse-height fitting produces better results, these values are good approximations (see Charles *et al.* 1979).

The observed time varied significantly from place to place on the sky, causing substantial variations in sensitivity to point sources. Figure 11 shows a map of the sensitivity in terms of counts s^{-1} (4 σ upper limits) for the 0.25 keV band (Fig. 11*a*) and the 1 keV band (Fig. 11*b*). The coordinates are galactic, with the galactic center at the middle of the map. The map was calculated for the idealized weak source limit. The weak source approximation for the upper limit breaks down for sky bins containing bright sources such as near the galactic center in the 1 keV band.

VI. DISCUSSION

a) Identifications and Comparisons with Previous X-Ray Catalogs

The following X-ray catalogs have been checked for correspondences between LED sources and previously discovered X-ray sources: 4U catalog (Forman *et al.* 1978); 3A catalog (McHerdy *et al.* 1981); "Positions and Identifications of Galactic X-Ray Sources" (Bradt, Doxsey, and Jernigan 1979); *OSO 7* catalog (Markert *et al.* 1979); "New Hard X-Ray Sources Observed with A-2" (Marshall *et al.* 1979).

b) Nature of Identified Sources

Of the 114 sources contained in this paper, 54 were unreported prior to *HEAO 1*. Despite a number of identifications made by the *HEAO 1* LED team and follow up observations by the *Einstein* satellite, 32 of the

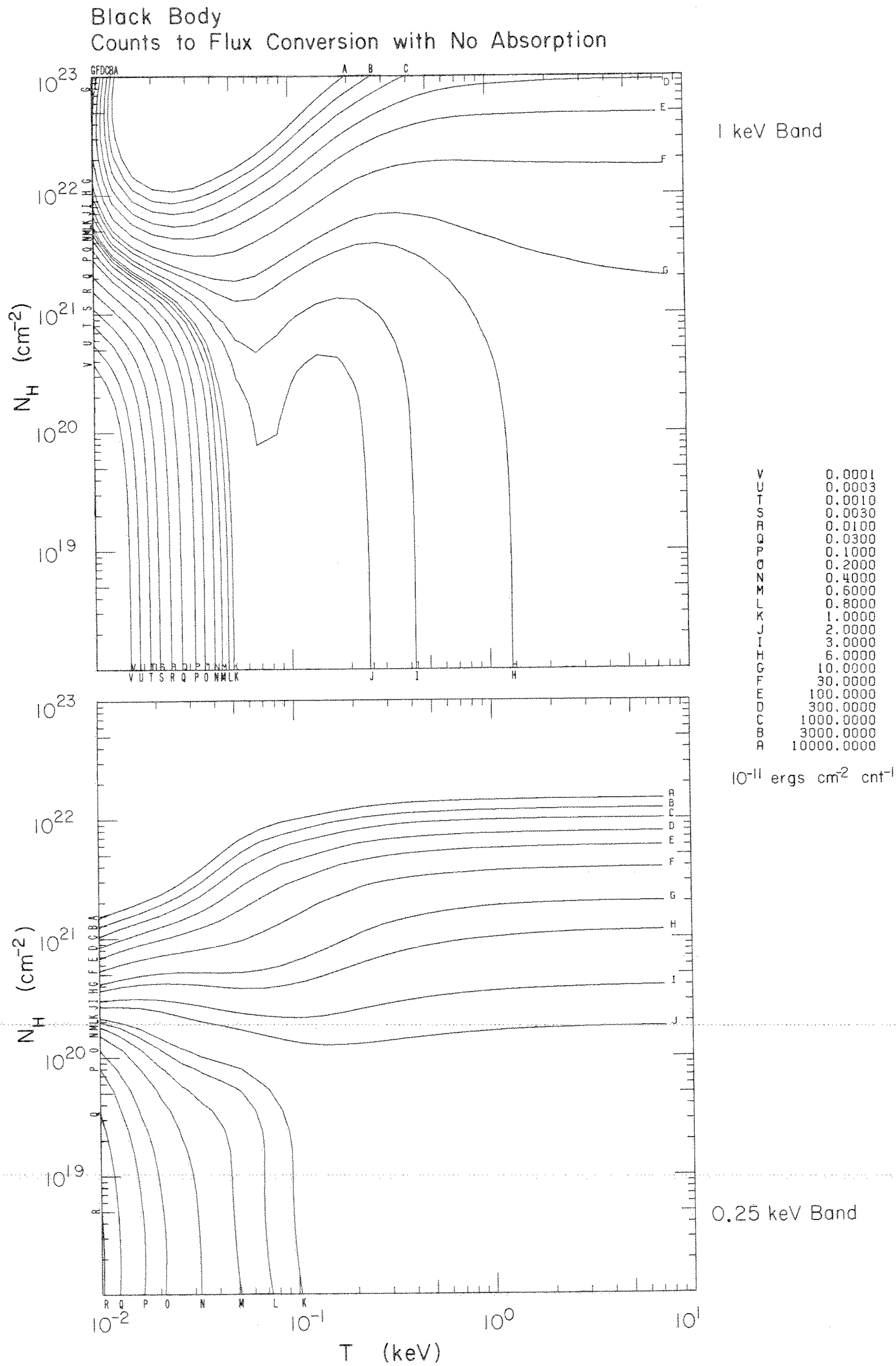

FIG. 10.—Factors to convert counts s^{-1} in the LED detector bands to an energy flux (in units of ergs cm^{-2} s^{-1}). Factors are for a blackbody spectrum and are shown as a function of temperature and interstellar neutral hydrogen column density. These factors give the flux as it would appear if the effects of interstellar absorption were removed. (*a*) (*Top*) is for the 1 keV band; (*b*) (*bottom*) is for the 0.25 keV band.

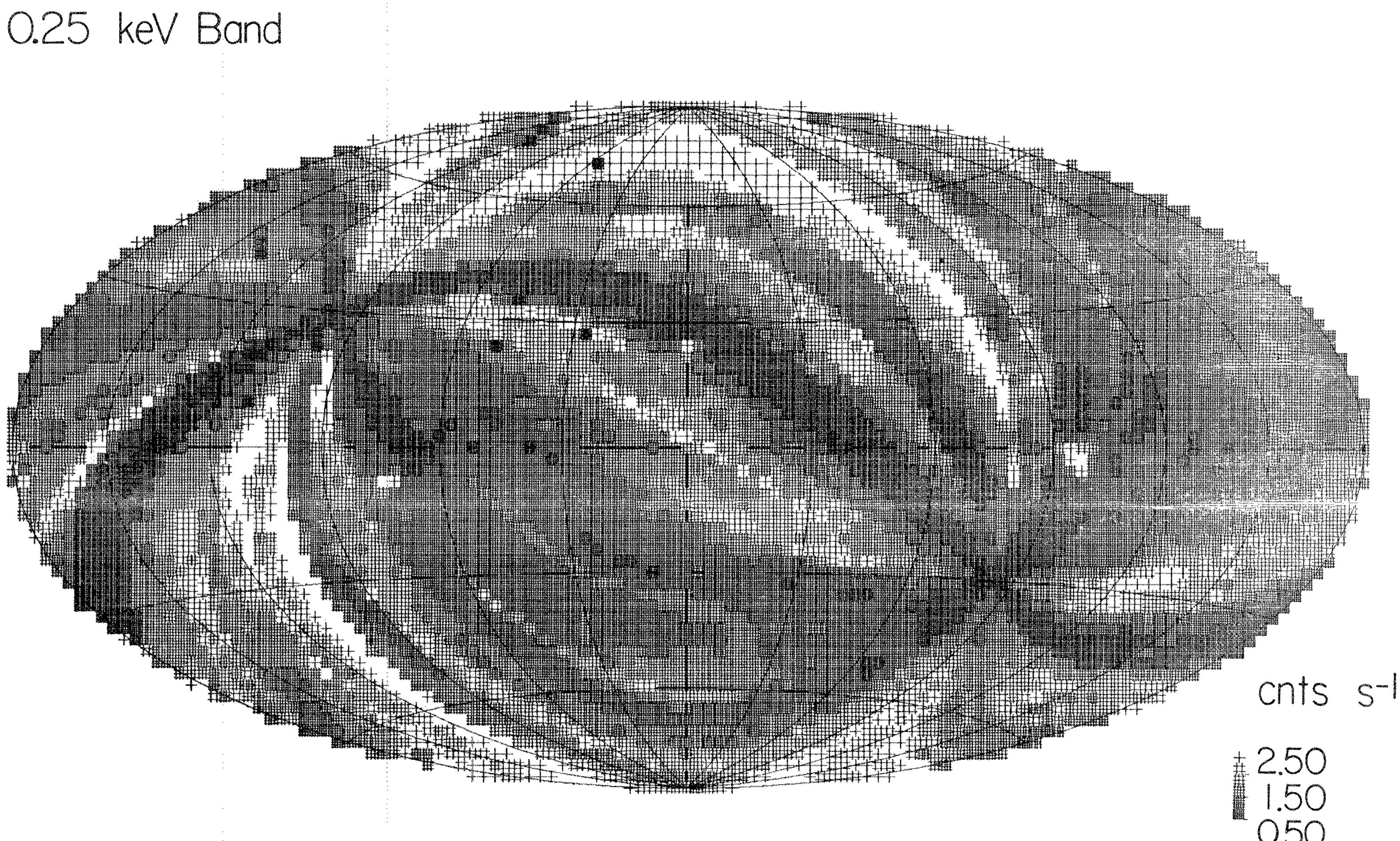

FIG. 11*a*

FIG. 11.—Map of the sensitivity in terms of count s^{-1} (4 σ upper limits) for (*a*) the 0.25 keV band and (*b*) 1 keV band. Coordinates are galactic, with the $l^{II} = 0$ at the center of the map.

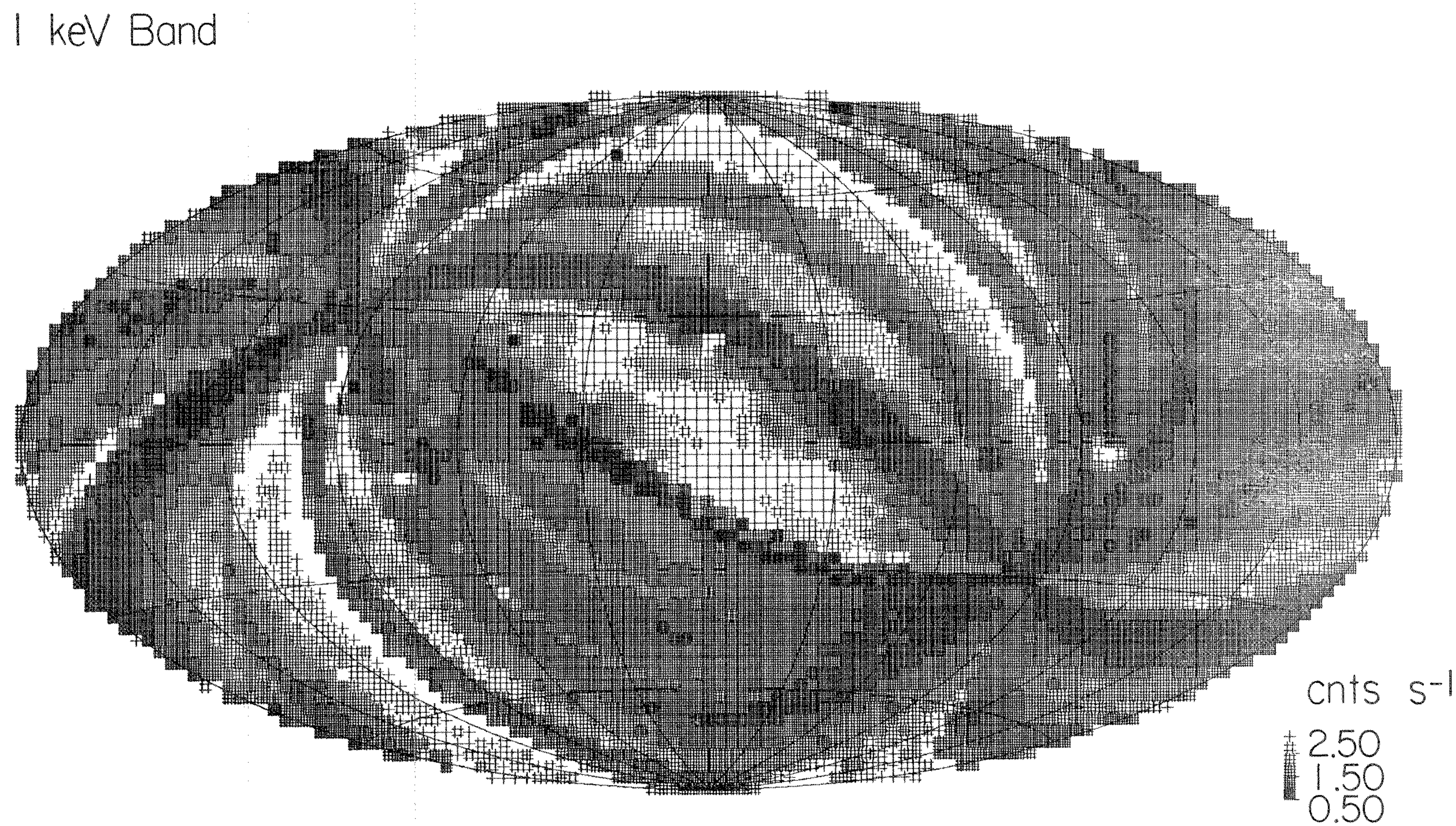

FIG. 11b

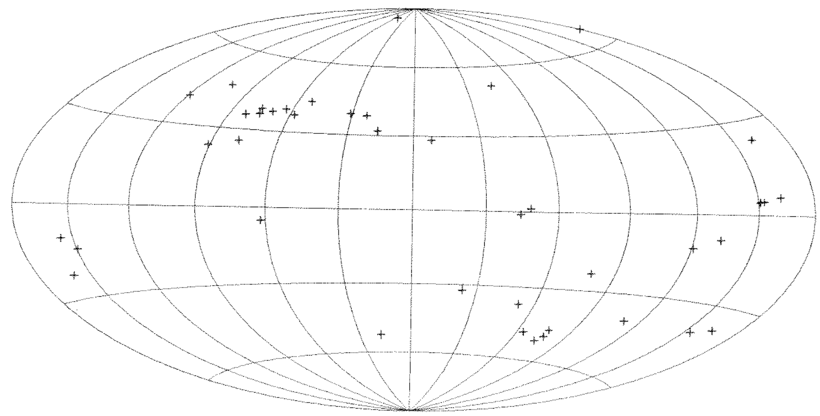

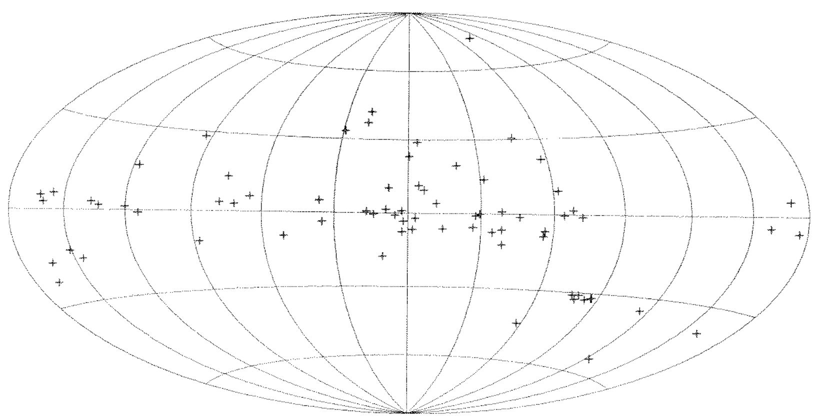

FIG. 12.—Angular distributions of catalog sources are shown. The 0.25 keV sources plotted on top are those catalog sources whose hardness ratio (ratio of the measured intensity in the 1 keV band to measured intensity in the 0.25 keV band) is < 1. The 1 keV sources, which, on the other hand, are sources with hardness ratios ≥ 1, are shown in bottom. Both plots are in galactic coordinates with $l^{\rm II} = 0$ in the center.

sources remain unidentified. The unidentified sources are predominantly 0.25 keV sources, with 10 of 13 sources seen only in the 0.25 keV band lacking identification. Thirty-eight of 45 sources appearing only in the 1 keV band and 29 of 36 seen at both energies have identifications.

The identified sources fall into several categories, primarily dependent on observing energy interval. Sources detected at 1 keV resemble the distribution of previous X-ray catalogs; 20 galactic stellar sources, 19 extragalactic sources, 13 supernova remnants, 11 galactic bulge sources, two globular cluster sources, and two previously reported X-ray sources without optical counterparts. Sources detected at 0.25 keV include a heavier proportion of stellar identifications. Twenty-four out of 43 of these sources identified are galactic stellar objects, followed by 12 extragalactic sources, five supernova remnants, one bulge source, and one globular cluster.

The two most prominent features in the 0.25 keV sky, the Cygnus Loop and Vela supernova remnants, are not included in these statistics because they are too extended to pass the point source inclusion criteria discussed in § III.

c) *Angular Distributions of Catalog Sources*

Figure 12*a* and *b* shows the angular distributions of catalog sources. The 0.25 keV sources plotted in Figure 12*a* are those catalog sources whose hardness ratio (the ratio of the measured intensity in the 1 keV band to the measured intensity in the 0.25 keV band) is < 1. The 1 keV sources, which are sources with hardness ratios ⩾ 1, are shown in Figure 12*b*. Both plots are in galactic coordinates, with $l^{\rm II} = 0$ in the center. One must be careful to include effects due to varying upper limits (see Figs. 11*a* and *b*) when interpreting these figures.

The 1 keV sources show a distribution that predominately lies along the galactic plane with a concentration near the galactic center. This distribution is similar to those observed for sources observed in the 2–10 keV band. The distribution of the 0.25 keV sources appears to be more uniform and shows a departure from that of the 1 keV sources in that there is no disk population. This lack can be accounted for by photoelectric absorption by the interstellar medium. The optical depth at 0.25 keV through the disk is ~100–300 pc. Any galactic component to the 0.25 keV sources would need to be local and hence would produce a distribution more closely resembling uniformity. The existence of an extragalactic component would also be consistent with the observed distribution. Evidence based on identified sources indicates that both components exist.

The authors would like to thank Ian Tuohy, Steve Pravdo, France Cordova, Phil Charles, Prahlad Agrawal, Gail Reichert, Tony Matweecha, Mike Juda, Drew Cushman, and Spencer Klein for ideas and computing assistance. This work was supported by NASA contract NAS 5-25049.

REFERENCES

Agrawal, P. C. and Riegler, G. R. 1979, *Ap. J.* (*Letters*), **231**, L25.
______. 1980, *Ap. J.* (*Letters*), **237**, L33.
Agrawal, P. C., Riegler, G. R., and Garmire, G. P. 1980, *M.N.R.A.S.*, **190**, 853.
Bradt, H. V., Doxsey, R. E., and Jernigan, J. G. 1979, in *Advances in Space Exploration*, Vol. **3**, *X-Ray Astronomy*, ed. W. A. Baity and L. E. Peterson (New York: Pergamon), p. 3.
Brown, R. L., and Gould, R. J. 1970, *Phys. Rev. D*, **1**, 2252.
Cash, W. 1976, *Astr. Ap.*, **52**, 307.
Cash, W., Bowyer, S., Charles, P., A., Lampton, M., Garmire, G., and Riegler, G. 1978, *Ap. J.* (*Letters*), **223**, L21.
Cash, W., Charles, P., Bowyer, S., Walter, F., Ayres, T. R., and Linsky, J. L. 1979, *Ap. J.* (*Letters*), **231**, L137.
Cash, W., Charles, P., Bowyer, S., Walter, F., Garmire, G., and Riegler, G. 1980, *Ap. J.* (*Letters*), **238**, L71.
Charles, P. A., Kahn, S. M., Bowyer, S., Blissett, R. J., Culhane, J. L., Cruise, A. M., and Garmire, G. 1979, *Ap. J.* (*Letters*), **230**, L83.
Charles, P. A., Kahn, S. M., Mason, K. O., and Tuohy, I. R. 1981, *Ap. J.* (*Letters*), **246**, L121.
Charles, P. A., Walter, F., and Cash, W. 1979, in *Advances in Space Exploration*, Vol. **3**, *X-Ray Astronomy*, ed. W. A. Baity and L. E. Peterson (New York: Pergamon), p. 129.
Cordova, F. 1979, in *IAU Colloquium 53*, *White Dwarfs and Variable Degenerate Stars*, ed. H. M. Van Horn and V. Weidemann (Rochester: University of Rochester Press), p. 398.
Cordova, F., Nugent, J. J., Klein, S. R., and Garmire, G. P. 1980, *M.N.R.A.S.*, **190**, 87.
Forman, W., Jones, C., Cominsky, L., Julien, P., Murray, S., Peters, G., Tananbaum, H., and Giacconi, R. 1978, *Ap. J. Suppl.*, **38**, 357.
Galas, C., Tuohy, I. R., and Garmire, G. 1980, *Ap. J.* (*Letters*), **236**, L13.
Galas, C., Venkatesan, B., and Garmire, G. 1981, *Ap. J.*, **250**, 216.
Giacconi, R., Murray, S., Gursky, H., Kellogg, E., Schreier, E., Matilsky, T., Koch, D., and Tananbaum, H. 1974, *Ap. J. Suppl.*, **27**, 237.
Kahn, S. M., Charles, P. A., Bowyer, S., and Blissett, B. J. 1981, *Ap. J.*, **250**, 733.
Lampton, M., Margon, B., and Bowyer, S. 1976, *Ap. J.*, **208**, 177.
Lea, S. M., Mason, K. O., Reichert, G., Charles, P., and Riegler, G. 1979, *Ap. J.* (*Letters*), **227**, L67.
Lea, S., Reichert, G., Mushotzky, R., Baity, W. A., Gruber, D. E., Rothschild, R., and Primini, F. A. 1981, *Ap. J.*, **247**, 803.
Markert, F., *et al.* 1979, *Ap. J. Suppl.*, **39**, 573.
Marshall, F., Boldt, E. A., Holt, S. S., Mushotzky, R. F., Pravdo, S. H., Rothschild, R. E., and Serlimitsos, P. S. 1979, *Ap. J. Suppl.*, **40**, 657.
Mason, K. O., Cordova, F., and Swank, J. 1979, in *Advances in Space Exploration*, Vol. **3**, *X-Ray Astronomy*, ed. W. A. Baity and L. E. Peterson (New York: Pergamon) p. 121.
Mason, K. O., Kahn, S. M., Charles, P. A., Lampton, M. L., and Blissett, R. 1979, *Ap. J.* (*Letters*), **230**, L163.
Mason, K. O., Lampton, M., Charles, P., and Bowyer, S. 1978, *Ap. J.* (*Letters*), **226**, L129.
McHerdy, I. M., Lawrence, A., Pye, J. P., and Pounds, K. A. 1981, *M.N.R.A.S.*, in press.
Middleditch, J., Mason, K. O., Nelson, J. E., and White, N. E. 1981, *Ap. J.*, **244**, 1001.
Nousek, J. A., Cowie, L. L., Hu, E., Lindblad, C. J., and Garmire, G. 1981, *Ap. J.*, **248**, 152.
Nugent, J., and Garmire, G. 1978, *Ap. J.* (*Letters*), **226**, L83.
Pravdo, S., Nugent, J., Nousek, J., Jensen, K., Wilson, A., and Becker, R. 1981, *Ap. J.*, **251**, 501.
Pravdo, S., Smith, B. W., Charles, P. A., and Tuohy, I. R. 1980, *Ap. J.* (*Letters*), **235**, L9.
Primini, F. A., *et al.* 1981, *Ap. J.* (*Letters*), **243**, L13.
Reichert, G., Mason, K. O., Lea, S. M., Charles, P. A., Bowyer, S., and Pravdo, S., 1981, *Ap. J.*, **247**, 803.
Riegler, G. R., Agrawal, P., and Gull, S. F. 1980, *Ap. J.* (*Letters*), **235**, L71.
Rothschild, R. E., *et al.* 1979, *Space Sci. Instr.*, **4**, 269.
Stern, R. A., Agrawal, P. C., and Riegler, G. R. 1981, *Nature*, **290**, 573.
Stern, R. A., Charles, P. A., Walker, A. B. C., Nugent, J. J., and Garmire G. 1980, *Ap. J.* (*Letters*), **238**, L77.
Stern, R. A., Nousek, J. A., Nugent, J. J., Agrawal, P. C., Riegler, G. R., Rosenthal, A., Pravdo, S. H., and Garmire, G. 1981, *Ap. J.* (*Letters*), **251**, L105.
Tuohy, I. R., Clark, D. H., and Garmire, G. P. 1979, *M.N.R.A.S.*, **189**, 59.
Tuohy, I. R., Lamb, F. K., Garmire, G. P., and Mason, K. O. 1978*a*, *Ap. J.* (*Letters*), **226**, L17.
______. 1978*b*, in *Advances in Space Exploration*, Vol. **3**, *X-Ray Astronomy*, ed. W. A. Baity and L. E. Peterson (New York: Pergamon), p. 197.
Tuohy, I. R., Mason, K. O., Clark, D. H., Cordova, F. A., Charles, P. A., Walter, F. M., and Garmire, G. 1979, *Ap. J.* (*Letters*), **230**, L27.
Tuohy, I. R., Mason, K. O., Garmire, G. P., and Lamb, F. 1981, *Ap. J.*, **245**, 183.
Walter, F., Cash, W., Charles, P. A., and Bowyer, C. S. 1980, *Ap. J.*, **236**, 212.
Walter, F., Charles, P., and Bowyer, S. 1978*a*, *Ap. J.* (*Letters*), **225**, L119.
______. 1978, *A.J.*, **83**, 1539.

C. S. Bowyer and K. Mason: Space Science Laboratory, University of California, Berkeley, CA 94702

G. P. Garmire, K. A. Jensen, and J. A. Nousek: Department of Astronomy, 525 Davey Laboratory, Pennsylvania State University, University Park, PA 16802

J. J. Nugent: Downs Laboratory of Physics 320-47, California Institute of Technology, Pasadena, CA 91125

G. Riegler and R. Stern: Jet Propulsion Laboratory, California Institute of Technology, 4800 Oak Grove Dr., Pasadena, CA 91109

From: NCFMRB::OPERATOR 3-MAR-1997 11:49:15.91
To: NCF::ALOPEZ
CC:
Subj:

HEAO A-2 Name	Other Names	Center lII / bII	Center RA (1950) / Dec (1950)	Corners				Box Area	Int/Err	Comments	HEAO A-2 Name
		------------- Overlap Box							1 keV		
		------------- Best Fit Box							1/4 keV		
		120.00	5.48	3.72	6.68	7.30	4.34		8.1	SNR	
		1.17	63.61	63.11	64.39	64.09	62.83	.72	1.0		
H0021+63	TYCHO SNR										H0021+63
									<		
									1.6	Ref. 24 ^	
		302.49	13.53	11.27	14.54	15.59	12.41		3.0	in SMC	
		-44.00	-73.40	-74.22	-72.40	-72.55	-74.39	.72	.5	SMC X-2 ?	
H0054-73											H0054-73
		302.03	14.58	13.70	14.39	15.45	14.77	.16	<		
		-44.60	-72.78	-72.91	-72.49	-72.64	-73.07		1.4		
		296.57	24.15	22.69	21.66	24.27	25.22		<	variable source	
		-48.09	-68.71	-70.15	-69.96	-68.18	-68.35	.80	.8		
H0136-68	3A0143-681										H0136-68
									2.6		
									.5		
		132.75	33.83	35.69	32.21	32.02	35.50		3.0	SNR	
		1.65	62.61	62.94	62.09	62.25	63.11	.33	.3		
H0215+62	HB3										H0215+62
									<		
									.5	Ref. 13 ^	
		285.39	36.44	35.13	37.17	37.69	35.66		<	confused with H0305-65	
		-51.40	-62.57	-63.21	-61.76	-61.92	-63.37	.50	1.0	and H0248-63	
H0225-62											H0225-62
		284.97	36.77	36.19	36.82	37.34	36.71	.16	4.8		
		-51.50	-62.33	-62.48	-62.03	-62.18	-62.64		.7		
		136.24	41.81	44.33	40.08	39.31	43.64		1.4	QSO ?	
		2.84	62.37	62.45	61.53	62.24	63.18	1.76	.3		
H0247+62	3A0241+622										H0247+62
									<		
									1.0		
		145.77	41.87	39.16	44.22	44.60	39.60		3.6	AWM7	
		-16.12	41.20	40.97	42.28	41.36	40.08	3.82	.9	NGC1129 CD group	
H0247+41	3A0251+414										H0247+41
		145.81	41.93	41.10	42.36	42.76	41.51	.95	<		
		-16.08	41.22	41.50	41.83	40.92	40.60		2.7		

HEAO A-2 Name	Other Names	Center lII / bII	Center RA (1950) / Dec (1950)	Corners	Box Area	Int/Err	Comments	HEAO A-2 Name
		------------- Overlap Box		-------------------		1 keV		
		------------- Best Fit Box		-------------------		1/4 keV		

		283.01	42.15	42.16	41.35	42.14	42.93		<	confused with H0305-65	
		-49.15	-63.36	-62.92	-63.60	-63.79	-63.10	.30	1.0	and H0225-62	
H0248-63											H0248-63
									3.1		
									.7		
		283.07	46.30	45.57	46.23	47.02	46.36		<	confused with H0248-63	
		-46.55	-65.24	-65.48	-64.86	-65.00	-65.63	.25	1.8	and H0225-62	
H0305-65											H0305-65
		283.32	46.12	45.37	46.06	46.85	46.17	.25	3.2		
		-46.49	-65.41	-65.65	-65.02	-65.17	-65.80		.6		
		149.33	46.85	48.29	48.39	45.44	45.33			confused with H0316+41	
	ALGOL	-14.55	40.89	41.36	41.10	40.41	40.67	.63			
H0307+40	BETA PER										H0307+40
		149.41	47.00	46.61	46.72	47.40	47.29	.14	2.4	tf=1.20	
		-14.46	40.93	40.98	40.72	40.88	41.13		.3		
		150.62	49.16	49.51	49.52	48.82	48.80		21.9	confused with H0307+40	
	4U0316+41	-13.27	41.30	41.40	41.35	41.20	41.24	.03	.6		
H0316+41	PERSEUS CLUS										H0316+41
										Ref. 26 ^	
		159.66	51.10	52.22	52.29	49.98	49.90		2.4	UV contaminated	
	H0323+28	-22.74	28.62	29.00	28.76	28.23	28.47	.52	.4		
H0324+28	UX ARI										H0324+28
		159.76	51.28	50.95	51.02	51.60	51.53	.13	3.3	tf=1.07	
		-22.61	28.66	28.71	28.47	28.61	28.85		.4	Ref. 37 ^38 ^9 ^ 7 ^	
		237.15	53.35	50.74	55.74	55.91	50.89		5.4	NGC1365 ?	
		-54.27	-35.85	-36.53	-34.80	-35.11	-36.84	1.47	.8		
H0333-35											H0333-35
		237.02	53.55	53.15	53.78	53.95	53.32	.19	<		
		-54.11	-35.78	-35.73	-35.51	-35.83	-36.05		4.7		
		166.89	56.69	58.76	58.89	54.64	54.50		1.1		
		-22.92	24.21	24.92	24.35	23.48	24.04	2.29	.2		
H0346+24	PLEIADES										H0346+24
		166.46	55.94	54.84	54.99	57.03	56.90	1.10	.9		
		-23.50	24.05	24.11	23.55	23.98	24.54		.4	Ref. 3 ^	

HEAD A-2 Name	Other Names	Center lII / bII	Center RA (1950) / Dec(1950)	Overlap Box / Best Fit Box: Corners				Box Area	Int/Err (1 keV / 1/4 keV)	Comments	HEAD A-2 Name
		156.43	57.04	59.57	59.71	54.57	54.38		<	EPS PER?	
		-10.90	39.83	40.54	40.00	39.06	39.60	2.26	1.4		
H0348+39											H0348+39
		156.24	56.64	55.86	56.03	57.42	57.26	.61	1.9		
		-11.15	39.76	39.90	39.36	39.61	40.15		.4		
		163.30	58.35	59.48	59.63	56.17	56.00		1.7	X-ray pulsar	
	CGS0352+309	-17.00	30.86	31.39	30.77	30.11	30.72	1.93	.4		
H0353+30	X PER										H0353+30
		163.25	58.26	57.65	57.81	58.86	58.70	.58	<	tf=1.08	

		-17.07	30.84	31.05	30.43	30.63	31.25		.7		
		195.89	61.85	60.55	63.06	63.15	60.64		<	confused	
H0407-04		-37.37	-4.11	-4.15	-3.63	-4.06	-4.59	1.15	1.0		
		196.65	63.62	62.91	64.24	64.33	63.00	.59	1.7		H0407-04
		-35.67	-3.75	-3.66	-3.40	-3.83	-4.09		.4		
	H0405-08	200.63	62.71	64.73	64.83	60.68	60.58		1.8		
H0410-07	40 ERI	-38.56	-7.94	-7.22	-7.73	-8.60	-8.14	2.18	.4		
		200.31	61.87	61.21	61.31	62.52	62.42	.58	<	tf=1.23	H0410-07
		-39.38	-8.12	-8.02	-8.48	-8.22	-7.76		2.8	Ref. 5 ^	
		206.39	64.03	63.68	64.33	64.38	63.73		<		
		-39.40	-12.31	-12.26	-12.12	-12.36	-12.50	.16	1.2		
H0416-12											H0416-12
									4.3		
									.4		
		248.59	71.88	68.59	74.94	75.11	68.73		<		
		-39.98	-43.76	-44.24	-42.83	-43.19	-44.61	1.85	.4		
H0447-43											
		248.59	71.88	71.62	71.99	72.14	71.78	.11	2.5		H0447-43
		-39.98	-43.76	-43.62	-43.54	-43.91	-43.99		.3		
		155.99	73.18	69.85	76.47	76.52	69.95		7.5		
		5.36	51.66	51.51	52.06	51.72	51.18	1.40	1.3		
H0452+51											
		156.24	73.93	73.73	74.07	74.14	73.80	.07	<		H0452+51
		5.76	51.72	51.88	51.91	51.57	51.54		2.1		

HEAD A-2 Name	Other Names	Center lII bII	Center RA (1950) Dec(1950)	Corners				Box Area	Int/Err	Comments	HEAD A-2 Name
		------------- Overlap Box	------------------						1 keV		
		------------- Best Fit Box	------------------						1/4 keV		
		160.64	74.22	71.31	77.12	77.15	71.37		8.6	SNR	
		2.54	46.28	46.14	46.62	46.34	45.86	1.12	1.3		
H0456+46	HB9										
		160.94	75.05	74.52	75.53	75.57	74.57	.20	<		H0456+46
		3.02	46.34	46.44	46.52	46.24	46.16		2.1	Ref. 35 ^	
		162.65	78.29	82.52	82.54	77.33	77.26		5.5		
		4.56	45.89	46.31	45.83	45.59	46.07	1.75	.9		
H0513+45	CAPELLA										
		162.69	78.41	77.59	77.66	79.22	79.16	.53	4.0	tf=1.01	H0513+45
		4.63	45.90	46.09	45.61	45.71	46.19		.8	Ref. 4 ^ 38 ^ 9 ^ 7 ^	
		244.48	78.44	76.93	79.83	79.94	77.03		4.8	globular cluster	
	CGS0512-401	-34.78	-40.04	-40.02	-39.60	-40.04	-40.45	1.00	1.2	burster	
H0513-40	NGC1851										
		244.48	78.34	77.69	78.87	78.98	77.79	.41	<	tf=1.09	H0513-40
		-34.86	-40.05	-39.91	-39.75	-40.18	-40.35		4.8		
		281.26	81.10	82.33	78.85	79.96	83.44		8.7	near LMC Bar	
		-32.74	-70.49	-71.27	-70.03	-69.69	-70.91	.86	.7	confused with LMC X-1	
H0524-70										and LMC X-2	H0524-70

		280.84	79.90	79.77	78.93	80.03	80.88	.22	2.0		
		-33.21	-70.05	-70.38	-70.06	-69.72	-70.03		.4		
		276.17	83.15	82.56	82.82	83.70	83.50		11.4		
	CGS0532-664	-32.56	-66.26	-67.09	-65.41	-65.43	-67.11	.61	1.5		
H0532-66	LMC X-4										H0532-66
									2.8	tf=1.05	
									.5		
		184.95	83.66	83.67	83.68	82.59	82.58		575.0	SNR	
	CGS0531+219	-5.18	21.98	22.09	21.87	21.82	22.04	.23	6.0		
H0534+21	CRAB = TAU X-1										H0534+21
									24.2	tf=1.33	
									1.7	Ref. 8 ^	
		273.71	84.79	82.18	86.67	87.21	82.74		21.5	1 keV flux may be	
		-32.02	-64.23	-65.30	-62.93	-63.11	-65.50	.95	1.1	contaminated by LMC X-3.	
H0539-64											H0539-64
		275.01	82.73	82.06	82.85	83.41	82.62	.16	3.4		
		-32.82	-65.27	-65.35	-64.98	-65.18	-65.56		.6		

HEAD A-2 Name	Other Names	Center lII / bII	Center RA (1950) / Dec (1950)	Corners (Overlap Box / Best Fit Box)				Box Area	1 keV / 1/4 keV Int/Err	Comments	HEAD A-2 Name
		273.38	84.98	82.26	87.36	87.53	82.43		22.9		
	CGS0538-641	-31.95	-63.95	-64.81	-62.95	-63.04	-64.90	.35	1.4		
H0539-63	LMC X-3										H0539-63
									2.1	tf=1.08	
									.8		
		283.29	85.06	90.69	79.30	79.93	91.09		2.9		
	CGS0521-720	-31.20	-72.42	-73.21	-71.90	-71.49	-72.77	1.65	.6		
H0540-72	LMC X-2										H0540-72
									<	tf=1.65	
									.9		
		280.26	86.41	90.55	82.28	82.42	90.63		10.4		
	CGS0540-697	-31.03	-69.86	-70.21	-69.58	-69.41	-70.04	.52	1.0		
H0545-69	LMC X-1										H0545-69
									<	tf=1.19	
									2.0		
		200.54	92.88	94.90	94.90	92.30	92.30		31.0	burster	
		-3.99	9.15	9.15	9.06	9.12	9.20	.20	1.2		
H0611+09	CGS0614+091										H0611+09
									2.3	tf=1.31	
									.7		
		189.81	95.16	93.42	96.90	96.90	93.42		12.8	SNR	
	IC443	4.31	22.53	22.64	22.52	22.40	22.52	.38	.8		
H0620+22	4U0617+23										H0620+22
									<		
									.7	Ref. 14 ^ 10 ^	
		198.32	100.43	101.41	99.41	99.45	101.46		<	associated with the Monocerous	
		5.53	15.57	15.22	15.36	15.91	15.76	1.07	3.1	Ring	

H0641+15											H0641+15
									5.3		
									1.3	Ref. 22 ^	
		227.28	100.88	101.13	100.61	100.63	101.14		<		
		-8.76	-16.65	-16.75	-16.71	-16.55	-16.60	.08	1.1		
H0643-16	SIRIUS										H0643-16
		227.28	100.88	100.99	100.74	100.76	101.01	.04	9.7	tf=1.05	
		-8.76	-16.65	-16.74	-16.72	-16.56	-16.59		.9		

HEAO A-2 Name	Other Names	Center lII bII	Center RA (1950) Dec (1950)	Corners				Box Area	Int/Err	Comments	HEAO A-2 Name
		Overlap Box							1 keV		
		Best Fit Box							1/4 keV		
		206.92	103.22	104.67	101.71	101.77	104.73		<	confused with H0656+05	
		4.22	7.33	6.92	7.22	7.74	7.44	1.55	2.9		
H0652+07										associated with the	H0652+07
		207.36	104.01	104.25	103.71	103.77	104.31	.28	4.7	Monocerous Ring	
		4.88	7.25	6.96	7.02	7.54	7.48		1.1	Ref. 22 ^	
		239.25	103.23	106.25	106.19	101.27	101.35		<	UV contaminated	
		-11.96	-28.65	-28.79	-29.22	-28.61	-28.17	1.90	.7		
H0652-28	EPS CMA										H0652-28
		239.94	104.60	103.90	103.82	105.31	105.39	.58	2.7	tf=1.06	
		-10.95	-28.84	-28.51	-28.95	-29.16	-28.73		.7		
		209.18	104.06	104.49	103.57	103.63	104.55		<	confused with H0652+07	
		4.01	5.23	4.94	5.04	5.52	5.42	.44	2.2		
H0656+05										associated with the	H0656+05
									5.4	Monocerous Ring	
									1.1	Ref. 22 ^	
		280.91	108.69	110.98	107.10	105.80	109.94		<		
		-23.39	-69.67	-67.19	-72.24	-72.12	-67.09	2.17	.4		
H0714-69											H0714-69
		281.06	108.56	109.19	109.10	107.93	108.02	.04	1.1		
		-23.47	-69.83	-69.84	-69.94	-69.82	-69.72		.4		
		199.50	118.50	115.53	121.48	121.45	115.50		<	variable	
		23.76	22.03	22.61	21.54	21.40	22.46	.85	1.1	New MED source	
H0754+22	U GEM										H0754+22
									48.8	tf=1.18	
									1.4	Ref. 11 ^ 12 ^ 19 ^ 18 ^	
		287.99	161.17	161.50	160.47	160.85	161.88		7.6	ETA CAR	
		-.95	-59.89	-60.27	-59.68	-59.51	-60.10	.20	.9	also near G287.8-0.5(SNR)	
H1044-59	3A1042-595										H1044-59
									<		
									1.0		
		180.24	166.29	162.74	169.87	169.70	162.59		4.8	BL Lac object	
	2A1102+384	65.81	38.07	39.54	36.76	36.51	39.28	1.78	.7		
H1105+38	MRK421										H1105+38
		179.83	164.87	164.53	165.37	165.21	164.37	.20	6.3	tf=1.37	
		64.58	38.62	38.91	38.59	38.33	38.66		.9		

HEAD A-2 Name	Other Names	Center lII / bII	Center RA (1950) / Dec (1950)	Corners				Box Area	Int/Err (Overlap Box: 1 keV; Best Fit Box: 1/4 keV)	Comments	HEAD A-2 Name
		292.14	170.73	171.71	169.60	169.79	171.90		11.5	SNR	
		1.67	-59.10	-59.67	-58.63	-58.53	-59.57	.22	.9		
H1122-59	MSH 11-54										H1122-59
									<		
									.9	Ref. 2 ^	
		295.80	176.75	175.97	177.75	177.55	175.77		9.9	X-ray pulsar	
		-.30	-62.03	-61.58	-62.39	-62.48	-61.67	.15	.5	near G296.1-0.2(SNR)	
H1147-62	CGS1145-619										H1147-62
									<	tf=1.07	
									2.3		
		297.94	183.90	180.13	188.12	187.99	179.99		6.0	SNR	
		9.13	-53.14	-51.35	-54.67	-54.79	-51.46	.82	.4		
H1215-53	PKS 1209-52										H1215-53
		297.70	183.54	183.38	183.84	183.71	183.25	.05	1.5		
		9.25	-52.99	-52.83	-53.03	-53.14	-52.95		.3	Ref. 34 ^	
	M 87 VIRGO	283.13	186.89	178.74	194.85	194.81	178.71		25.6	cluster of galaxies	
H1227+12	3U1228+12	74.45	12.68	16.09	9.10	9.03	16.01	1.44	.9		
		282.33	186.69	186.34	187.07	187.04	186.31	.06	8.1	tf=1.04	H1227+12
		74.47	12.77	12.96	12.64	12.57	12.89		.8	Ref. 17 ^ 16 ^	
		302.61	191.77	190.04	193.64	193.54	189.94		6.3	cluster of galaxies	
		21.85	-40.75	-39.95	-41.37	-41.52	-40.09	.49	.5		
H1247-40	CENTAURUS CLU										H1247-40
									<	tf=1.00	
									.6	Ref. 27 ^	
		303.61	193.96	194.93	192.62	193.03	195.34		7.9		
		-6.69	-69.28	-69.73	-68.98	-68.83	-69.57	.24	.9		
H1255-69	CGS1254-690										H1255-69
		303.43	193.44	193.54	192.93	193.33	193.95	.06	1.9	tf=1.10	
		-6.52	-69.11	-69.29	-69.09	-68.93	-69.14		.7		
		45.01	194.18	195.90	193.40	192.60	194.80		9.5	cluster of galaxies	
	4U1257+28	88.25	27.75	28.30	29.40	27.10	26.20	5.68	.8		
H1256+27	COMA CLU										H1256+27
		41.24	195.23	194.98	195.57	195.48	194.89	.10	<	tf=1.02	
		87.34	27.75	27.96	27.69	27.54	27.81		3.9		

HEAD A-2 Name	Other Names	Center lII / bII	Center RA (1950) / Dec (1950)	Corners				Box Area	Int/Err (Overlap Box: 1 keV; Best Fit Box: 1/4 keV)	Comments	HEAD A-2 Name
		55.17	198.38	196.63	200.16	200.10	196.58		<		
	HZ 43	84.24	29.44	30.26	28.69	28.60	30.17	.35	.3		
H1313+29	MX1313+29										H1313+29
		45.83	199.99	198.21	201.80	201.74	198.16	.35	28.0	tf=1.04	
		83.04	28.73	29.56	27.97	27.88	29.47		1.3		

		314.68	199.63	201.04	200.91	198.22	198.35		<	UV contaminated	
	SPICA	51.42	-10.52	-10.89	-11.20	-10.14	-9.82	.97	2.2		
H1318-10	ALPHA VIR										H1318-10
		315.04	199.88	199.59	199.46	200.17	200.30	.26	5.3	tf=1.43	
		51.27	-10.61	-10.32	-10.63	-10.91	-10.60		.8		
		312.78	202.12	199.73	204.79	204.58	199.50		2.4	cluster of galaxies	
	SC1329-314	30.49	-31.36	-30.19	-32.03	-32.48	-30.62	2.23	.5		
H1328-31	2A1326-311										H1328-31
		313.62	203.06	202.50	203.83	203.62	202.28	.59	1.1		
		30.01	-31.70	-31.24	-31.72	-32.16	-31.68		.5	Ref. 27 ^	
		119.23	204.72	204.78	206.48	204.67	202.50		<		
		40.43	76.60	78.21	75.05	74.99	78.14	1.50	2.2		
H1338+76											H1338+76
		119.98	203.88	204.90	205.18	202.94	202.48	.46	3.2		
		38.87	78.26	78.76	77.80	77.76	78.72		.3		
		311.70	209.94	210.28	209.76	207.08	207.63		<	UV contaminated	
		1.25	-60.16	-59.94	-60.41	-59.64	-59.18	.83	1.3		
H1359-60	BETA CEN										H1359-60
		311.60	209.70	208.41	207.87	211.05	211.55	.97	3.7	tf=1.01	
		1.34	-60.09	-59.42	-59.88	-60.75	-60.28		.8		
		314.36	216.78	213.71	220.05	220.01	213.66		15.2	SNR	
		-1.27	-61.69	-60.89	-62.37	-62.42	-60.93	.16	.4		
H1427-61	MSH14-63										H1427-61
									<		
									1.1		
		315.92	219.56	218.17	221.11	220.98	218.03		<		
		-.99	-60.83	-60.42	-61.08	-61.22	-60.56	.25	.6		
H1438-60	ALPHA CEN										H1438-60
									3.4	tf=1.12	
									.3	Ref. 23 ^	

HEAD A-2 Name	Other Names	Center lII / bII	Center RA (1950) / Dec(1950)	Corners				Box Area	Int/Err (Overlap Box: 1 keV; Best Fit Box: 1/4 keV)	Comments	HEAD A-2 Name
		103.39	226.19	227.97	222.78	224.01	229.02		<		
		46.40	65.51	62.85	67.93	68.14	63.02	2.80	2.2		
H1504+65											H1504+65
		103.65	226.01	227.70	222.72	223.96	228.76	2.65	8.1		
		46.33	65.69	63.17	67.97	68.18	63.34		2.0		
		328.42	226.55	222.73	230.52	230.49	222.69		12.1	SNR	
	SN1006	13.54	-42.21	-41.19	-43.00	-43.09	-41.28	.57	.5		
H1506-42	4U1458-41										H1506-42
									4.8		
									.4		
		321.57	227.60	224.96	230.40	230.34	224.88		8.6	variable	
	CGS1516-569	.82	-56.61	-55.98	-57.06	-57.16	-56.09	.38	.5		
H1510-56	CIR X-1										H1510-56
									<	tf=1.48	

									1.1		
		339.40	233.22	231.57	234.91	234.88	231.54		6.3	SNR ?	
H1532-31		19.41	-31.40	-30.97	-31.69	-31.80	-31.09	.36	.4		
									2.9		H1532-31
									.3	Ref. 28 ^	
	3A1543-624	321.75	235.79	236.78	234.72	234.82	236.87		23.5		
H1543-62	CGS1543-624	-6.27	-62.37	-62.58	-62.28	-62.15	-62.45	.14	1.7		
									1.8	tf=1.02	H1543-62
									.9		
		352.23	236.38	235.45	237.50	237.31	235.25		<		
H1545-16		28.41	-16.92	-16.29	-16.73	-17.54	-17.09	1.66	1.5		
		351.98	235.96	235.60	236.51	236.32	235.41	.73	1.7		H1545-16
		28.76	-16.82	-16.32	-16.52	-17.32	-17.12		.4		
		356.11	238.51	237.01	240.05	240.02	236.97		4.9	possible artifact of SCO X-1	
H1554-14		28.85	-14.17	-13.76	-14.39	-14.57	-13.94	.55	.5		
									<		H1554-14
									.7		

HEAD A-2 Name	Other Names	Center lII bII	Center RA (1950) Dec (1950)	Corners				Box Area	Int/Err	Comments	HEAD A-2 Name
		Overlap Box							1 keV		
		Best Fit Box							1/4 keV		
		18.56	239.27	237.23	241.34	241.30	237.19		3.3	confused with H1614+06	
H1557+08		41.58	8.04	8.59	7.65	7.48	8.42	.76	.5		
		18.61	239.38	239.02	239.78	239.74	238.98	.14	2.2		H1557+08
		41.47	8.01	8.19	8.02	7.84	8.01		.4		
		330.57	241.07	238.02	244.23	244.19	237.96		38.7	nova	
H1604-52	CGS1608-52	-.19	-52.05	-51.51	-52.39	-52.51	-51.63	.49	.9		
									<	tf=1.03	H1604-52
									1.6		
	3A1556-605	325.35	242.83	246.23	239.30	239.55	246.40		6.3		
H1611-60	CGS1556-605	-7.25	-60.77	-61.33	-60.56	-60.12	-60.88	1.59	1.5		
		325.17	242.18	242.88	241.27	241.50	243.09	.37	<	tf=1.24	H1611-60
		-6.98	-60.69	-61.01	-60.82	-60.37	-60.56		1.9		
		19.21	243.64	242.89	244.53	244.39	242.75		2.2	confused with H1557+08	
H1614+06		36.87	6.13	6.63	6.28	5.63	5.98	1.11	.5	Seyfert galaxy	
										E1615+061	H1614+06
									1.7		
									.4	Ref. 25 ^	
		23.02	243.87	243.40	244.41	244.35	243.34		<		
H1615+09		38.26	9.45	9.69	9.49	9.21	9.42	.29	.8		
											H1615+09

									3.8		
									.5		
		332.36	243.90	246.53	241.23	241.32	246.60		11.7	SNR	
		-.85	-51.31	-51.75	-51.08	-50.82	-51.49	.89	1.6		
H1615-51	RCW103										H1615-51
		332.41	244.04	244.68	243.33	243.41	244.76	.23	<		
		-.93	-51.33	-51.54	-51.37	-51.12	-51.28		1.8	Ref. 34 ^	
		321.16	244.08	247.81	240.18	240.53	248.05		11.5	X-ray pulsar	
		-12.22	-67.20	-67.78	-66.95	-66.55	-67.36	1.31	2.8		
H1616-67	CGS1627-673										H1616-67
									<	tf=1.10	
									5.3	Ref. 21 ^	

HEAO A-2 Name	Other Names	Center lII / bII	Center RA (1950) / Dec(1950)	Corners				Box Area	Int/Err	Comments	HEAO A-2 Name
		-------------	Overlap Box	-------------------					1 keV		
		-------------	Best Fit Box	-------------------					1/4 keV		
		359.54	245.18	242.28	248.11	248.09	242.27		1495.5		
	CGS1617-155	22.98	-15.72	-15.20	-16.12	-16.21	-15.29	.55	82.5		
H1620-15	SCO X-1										H1620-15
									53.3	tf=1.00	
									22.2	Ref. 15 ^	
		30.99	246.13	245.64	246.66	246.62	245.60		1.3	Herc cluster ?	
		38.77	15.30	15.50	15.29	15.11	15.31	.19	.5	possible source confusion	
H1624+15										in 1/4 keV Band	H1624+15
									2.4		
									.5		
		53.04	246.64	244.66	248.82	248.59	244.46		<	confused	
		43.09	32.45	33.26	32.25	31.60	32.61	2.47	1.1		
H1626+32											H1626+32
		53.19	245.71	245.09	246.54	246.32	244.87	.86	1.9		
		43.90	32.67	33.17	32.83	32.17	32.51		.4		
		16.37	246.67	245.56	247.84	247.78	245.50		<		
		31.95	1.60	1.97	1.57	1.23	1.63	.80	2.2		
H1626+01											H1626+01
		16.38	246.69	246.13	247.30	247.25	246.07	.40	2.7		
		31.94	1.60	1.86	1.66	1.33	1.53		.5		
		333.19	250.35	253.02	247.66	247.72	253.05		20.5	confused	
		-5.45	-53.86	-54.18	-53.66	-53.48	-54.00	.59	2.1	burster	
H1641-53	CGS1636-536									bulge source	H1641-53
		333.01	249.76	250.29	249.18	249.24	250.34	.12	<	tf=1.07	
		-5.15	-53.80	-53.95	-53.84	-53.66	-53.77		1.9		
		29.22	250.56	247.41	253.76	253.69	247.36		5.4		
		33.41	11.80	12.47	11.47	11.10	12.10	2.35	.9		
H1642+11											H1642+11
		29.13	250.27	249.60	251.00	250.93	249.54	.52	3.8		
		33.69	11.85	12.15	11.92	11.55	11.78		.7		
		355.53	252.31	254.47	250.13	250.16	254.49		9.2	confused with H1650-28	
		11.29	-26.07	-26.41	-25.92	-25.71	-26.19	.84	2.0		

H1649-26			355.26	251.73	252.11	251.33	251.36	252.14	.15	<		H1649-26
			11.73	-26.01	-26.16	-26.07	-25.86	-25.95		5.0		

HEAD A-2 Name	Other Names		Center lII / bII (Overlap Box / Best Fit Box)	Center RA (1950) / Dec (1950)	Corners				Box Area	Int/Err (1 keV / 1/4 keV)	Comments	HEAD A-2 Name
	4U1651+39		63.57	252.49	250.62	254.42	254.33	250.55		2.2	BL Lac object	
		3	39.29	39.86	40.36	39.55	39.33	40.13	.70	.3		
H1649+39	MRK501											H1649+39
	A1653+398		63.52	252.79	252.48	253.17	253.09	252.40	.13	2.4	tf=1.17	
			39.06	39.79	39.98	39.83	39.61	39.76		.4		
			353.38	252.50	254.12	250.85	250.89	254.15		9.1	confused with H1649-26	
			9.39	-28.91	-29.19	-28.84	-28.62	-28.97	.65	1.9	New MED source	
H1650-28												H1650-28
			353.33	252.39	252.95	251.81	251.84	252.98	.23	<		
			9.47	-28.90	-29.07	-28.95	-28.73	-28.85		3.1		
			75.66	253.75	249.52	257.96	257.79	249.39		.7		
			38.69	49.22	50.27	48.29	48.02	49.98	1.77	.3		
H1655+49												H1655+49
										2.9		
										.4		
			348.37	253.88	256.88	250.89	250.90	256.89		49.7	bulge source	
	CGS1702-363		3.93	-36.21	-36.50	-35.94	-35.85	-36.41	.44	2.5		
H1655-36	SCO X-2											H1655-36
										<	tf=1.56	
										2.2		
			58.01	254.44	252.44	256.49	256.43	252.38		5.0		
	CGS1656+354		37.14	35.24	35.66	35.07	34.79	35.38	.94	.7		
H1657+35	HER X-1											H1657+35
										6.9	tf=1.15	
										.9		
			69.64	254.91	254.31	255.66	255.50	254.15		<		
			37.84	44.49	44.82	44.54	44.15	44.43	.41	.6		
H1659+44												H1659+44
			69.69	254.69	254.23	255.31	255.15	254.08	.33	1.8		
			37.99	44.53	44.84	44.61	44.22	44.45		.4		
			75.14	257.13	255.34	259.04	258.89	255.21		<	star HD155638	
H1708+48			36.48	48.81	49.34	48.54	48.26	49.05	.76	1.0	V=8.5	
											RS Cvn/emission reversal	H1708+48
										2.4		
										.3	Ref. 30 ^	

HEAD A-2 Name	Other Names	Center lII / bII (Overlap Box / Best Fit Box)	Center RA (1950) / Dec (1950)	Corners	Box Area	Int/Err (1 keV / 1/4 keV)	Comments	HEAD A-2 Name

		81.98	258.09	255.19	261.10	260.87	254.99		<	binary star (HD154905,06)	
		35.85	54.33	55.20	53.69	53.40	54.90	1.20	.5	V=5.5	H1712+54
H1712+54											
		82.28	257.19	256.73	257.86	257.64	256.52	.23	2.0		
		36.37	54.56	54.84	54.57	54.27	54.55		.3		
		7.90	260.75	257.71	263.80	263.80	257.70		45.7	bulge source	
	CGS1728-169	10.31	-16.75	-16.48	-16.84	-16.97	-16.61	.76	3.2		
H1722-16	GX9+9										H1722-16
									<	tf=1.47	
									4.1		
		345.71	262.73	260.51	264.97	264.96	260.49		37.1	burster	
		-6.28	-44.33	-44.15	-44.32	-44.47	-44.30	.48	2.5	bulge source	
H1730-44	CGS1735-444										H1730-44
		346.26	264.29	264.10	264.49	264.48	264.09	.04	2.9	tf=1.36	
		-7.26	-44.39	-44.31	-44.32	-44.47	-44.45		1.3		
		357.07	265.79	261.77	269.82	269.82	261.76		32.8	confused	
		-1.99	-32.45	-32.22	-32.42	-32.55	-32.35	.88	1.9	transient	
H1743-32	CGS1743-322										H1743-32
									2.1		
									.9		
		2.54	266.14	262.22	270.07	270.07	262.21		12.3	burster	
	CGS1744-265	1.01	-26.22	-25.94	-26.13	-26.39	-26.20	1.84	1.7	bulge source	
H1744-26	GX3+1										H1744-26
									<	tf=1.02	
									3.3		
		5.07	269.34	267.78	270.90	270.90	267.77		17.2	bulge source	
	CGS1758-250	-.84	-24.99	-24.87	-24.88	-25.10	-25.08	.62	2.1		
H1757-24	GX5-1										H1757-24
									<	tf=1.06	
									2.1		
		8.92	269.36	267.85	270.88	270.88	267.85		18.7	bulge source	
	CGS1758-205	1.36	-20.56	-20.45	-20.47	-20.66	-20.64	.55	2.0		
H1757-20	GX9+1										H1757-20
									<	tf=1.10	
									1.9		
		------------- Overlap Box					-------------------		1 keV		
HEAD A-2 Name	Other Names	Center lII / bII	Center RA (1950) / Dec (1950)	Corners				Box Area	Int/Err	Comments	HEAD A-2 Name
		------------- Best Fit Box					-------------------		1/4 keV		
		1.85	269.86	267.69	272.04	272.04	267.68		10.7	confused	
		-3.23	-28.98	-28.77	-28.78	-29.15	-29.14	1.43	1.9	near CGS1743-288	
H1759-28											H1759-28
									<		
									1.6		
		358.21	271.22	267.07	275.36	275.41	267.04		8.9	confused	
		-6.59	-33.78	-33.39	-33.33	-34.02	-34.08	4.78	1.5		
H1804-33	CGS1755-338										H1804-33
		357.49	269.45	268.79	270.11	270.11	268.78	.76	<	tf=3.04	
		-5.30	-33.78	-33.44	-33.44	-34.13	-34.13		1.3		

		93.25	273.50	270.53	275.96	276.66	271.25		1.6	New MED source ?	
H1814+63		28.19	63.74	62.86	64.93	64.55	62.51	1.53	.4	3C 383 ?	
									1.4		H1814+63
									.4		
	CGS1811-171	13.94	273.54	270.79	276.28	276.29	270.80		9.2	bulge source	
H1814-17	GX13+1	-.36	-17.02	-16.91	-16.79	-17.10	-17.22	1.63	1.4		
		13.79	273.23	273.01	273.44	273.44	273.02	.13	<	tf=1.48	H1814-17
		-.10	-17.03	-16.88	-16.87	-17.18	-17.19		2.5		
	CGS1814+498	77.95	274.08	273.40	274.75	274.75	273.41		2.2	variable	
H1816+49	AM HER	25.67	49.88	49.89	49.94	49.87	49.82	.06	.9	binary	
									61.4	tf=1.08	H1816+49
									2.2	Ref. 32 ^ 33 ^ 36 ^	
	CGS1813-140	16.81	274.17	272.16	276.18	276.19	272.17		16.5	bulge source	
H1816-14	GX17+2	.51	-14.09	-13.99	-13.89	-14.18	-14.28	1.10	1.5		
		16.36	273.25	272.84	273.66	273.66	272.85	.22	<	tf=1.21	H1816-14
		1.29	-14.11	-13.98	-13.96	-14.25	-14.26		1.7		
	CGS1820-303	2.54	274.48	272.37	276.59	276.59	272.37		79.1	confused	
H1817-30	NGC6624	-7.42	-30.38	-30.39	-30.28	-30.32	-30.44	.19	1.8	burster	
										globular cluster	H1817-30
									2.7	tf=1.23	
									.8		

HEAD A-2 Name	Other Names	Center lII bII	Center RA (1950) Dec (1950)	Corners				Box Area	Int/Err	Comments	HEAD A-2 Name
		Overlap Box							1 keV		
		Best Fit Box							1/4 keV		
	CGS1837+049	36.09	279.28	278.59	279.97	279.98	278.59		32.7	burster	
H1837+05	SER X-1	4.93	5.01	4.99	5.10	5.02	4.91	.11	1.5		
									<	tf=1.03	H1837+05
									2.0		
		90.79	283.24	287.73	288.16	279.46	279.00		<	transient	
H1852+60		23.18	60.66	62.50	62.21	58.78	59.04	1.92	2.2	binary star HD173739,40 ?	
									4.6		H1852+60
									.8	Ref. 31 ^	
		34.92	286.25	285.58	286.88	286.93	285.63		4.7	burster	
H1905+00	CGS1905+000	-3.51	.09	.20	.37	-.03	-.19	.52	.9	near AQL X-1	
		34.88	286.18	285.80	286.52	286.57	285.85	.29	<	tf=1.08	H1905+00
		-3.46	.08	.23	.32	-.07	-.16		1.6		
		10.46	288.71	287.04	290.31	290.37	287.09		6.1	confused	
H1914-27		-17.56	-27.60	-27.59	-27.21	-27.59	-27.97	1.12	1.1		
									<		H1914-27

									1.5		
		75.42	289.69	286.25	293.00	293.19	286.49		3.1	cluster of galaxies	
	A2319	13.55	43.63	43.01	44.62	44.15	42.54	2.57	.6		
H1918+43	4U1919+44										H1918+43
									1.7	Ref. 27 ^	
									.6		
		64.96	292.30	291.72	292.83	292.88	291.77		8.4	SNR	
		6.00	31.03	30.99	31.23	31.06	30.82	.17	.9	near Cygnus Superbubble	
H1929+31	G65.2+5.7										H1929+31
									5.9		
									.6	Ref. 20 ^^6 ^	
		51.34	299.32	297.81	300.79	300.83	297.85		14.9		
		-9.38	11.57	11.31	12.00	11.82	11.13	.55	1.3		
H1957+11	4U1956+11										H1957+11
									2.1	tf=1.02	
									.8		

HEAD A-2 Name	Other Names	Center lII / bII	Center RA (1950) / Dec (1950)	Overlap Box / Best Fit Box Corners				Box Area	Int/Err (1 keV / 1/4 keV)	Comments	HEAD A-2 Name
		71.48	299.35	299.06	299.62	299.64	299.08		45.9		
	CGS1956+350	2.94	35.12	35.07	35.22	35.18	35.03	.02	1.3		
H1957+35	CYG X-1										H1957+35
									<	tf=1.07	
									1.7		
		336.61	300.28	299.71	300.65	300.86	299.91		<	extented region in Delphinus	
		-32.40	-60.56	-60.46	-60.32	-60.67	-60.80	.18	1.5	SNR?	
H2001-60											H2001-60
		336.76	301.27	300.73	301.60	301.81	300.94	.16	3.2		
		-32.89	-60.42	-60.31	-60.18	-60.53	-60.66		.6	Ref. 29 ^	
		62.13	301.33	299.37	303.18	303.31	299.51		<		
		-5.03	22.97	22.68	23.68	23.23	22.24	1.67	1.9		
H2005+22											H2005+22
		62.14	301.34	300.90	301.66	301.79	301.03	.33	3.8		
		-5.04	22.97	23.09	23.29	22.85	22.65		.7		
		77.78	303.08	304.74	304.89	301.45	301.29		9.8	part of Cygnus A extended	
		3.49	40.71	41.42	41.15	39.97	40.23	.82	1.3	region?	
H2012+40										Cygnus Superbubble?	H2012+40
									<		
									1.6	Ref. 6 ^	
		87.45	325.81	325.05	326.53	326.58	325.11		78.5		
	CGS2142+380	-11.37	38.12	37.81	38.50	38.43	37.74	.11	3.6		
H2143+38	CYG X-2										H2143+38
									4.0	tf=1.04	
									1.4		
		17.49	328.68	328.12	328.06	329.22	329.29		10.5	BL Lac object	
		-51.99	-30.58	-30.85	-30.69	-30.31	-30.46	.17	.9	New MED source	
H2154-30	PKS 2155-304										H2154-30

									14.1	tf=1.11	
									1.1	Ref. 1 ^	
		117.73	347.90	350.11	347.62	345.97	348.23		1.1		
		16.05	77.64	78.49	76.68	76.78	78.60	.74	.2		
H2311+77											H2311+77
		118.19	348.85	350.24	349.32	347.51	348.34	.24	<		
		16.61	78.33	78.57	77.97	78.08	78.68		.8		

HEAD A-2 Name	Other Names	Center lII / bII	Center RA (1950) / Dec(1950)	Corners				Box Area	Int/Err (1 keV / 1/4 keV)	Comments	HEAD A-2 Name
		-------------	Overlap Box	-------------------					1 keV		
		-------------	Best Fit Box	-------------------					1/4 keV		
		307.69	350.92	344.12	354.45	356.07	346.09		.8		
		-36.96	-79.65	-81.05	-77.98	-78.15	-81.26	1.32	.4		
H2323-79											H2323-79
									3.9		
									.5		
		113.94	353.59	348.96	358.14	358.81	349.64		4.4	SNR	
		-.76	60.52	58.46	62.78	62.41	58.13	3.03	.9		
H2334+60	CAS A										H2334+60
		114.32	354.23	352.24	355.61	356.30	352.92	1.09	<		
		-.56	60.82	60.19	61.78	61.42	59.85		1.9		

REQ. AGENT	RAND NO.	ACQ. AGENT
RLR		SJK

HEAO-3

HEAVY NUCLEI REDUCED DATA - GOLD

79-082A-03A SPIS-00003

This data set catalog consists of 21 tapes. The tapes are 6250 bpi, 9-track, multifiled, binary, created on the IBM 360. The tapes are in a chapter verse format described in the format. The D and C numbers, time spans, and number of files are as follows:

D#	C#	FILES	TIME SPANS
D-76215	C-29107	01	01/12/79 - 01/18/79
D-76216	C-29108	01	01/18/79 - 02/18/79
D-76217	C-29109	01	02/18/79 - 03/20/79
D-76218	C-29110	01	03/20/79 - 03/22/79
D-76219	C-29111	01	01/01/80 - 02/01/80
D-76220	C-29112	01	02/01/80 - 03/01/80
D-76221	C-29113	01	03/01/80 - 03/31/80
D-76222	C-29114	01	04/01/80 - 05/01/80
D-76223	C-29115	01	05/01/80 - 06/01/80
D-76224	C-29116	01	06/01/80 - 07/01/80
D-76225	C-29117	01	07/01/80 - 08/04/80
D-76226	C-29118 ← Bad	01	08/05/80 - 09/01/80
D-76227	C-29119	01	09/01/80 - 01/19/80 ?
D-76228	C-29120	01	01/19/80 - 02/19/80
D-76229	C-29121	01	02/19/80 - 03/19/80
D-76230	C-29122	01	03/20/80 - 04/10/80
D-76231	C-29123	01	01/05/81 - 03/21/81
D-76232	C-29124	01	02/01/81 - 03/01/81
D-76233	C-29125	01	02/29/80 - 04/01/81
D-76234	C-29126	01	05/01/81 - 05/15/81
D-76235	C-29127	01	04/01/81 - 05/01/81

* Ending timespans are very difficult to locate and therefore are probably unreliable

FULL DATASET LISTING OF 79-082A-03A
HEAO 3 HEAVY NUCLEI REDUCED DATA-GOLD

SYSTEM: MEDIA #	COPY #	RECEIVED	DENS	TR	FILES	LOCATION	MODE: TIME SPAN	
DD076215	DC029107	09/18/1987		9	1	060B28	01/12/1979	01/18/1979
DD076216	DC029108	09/18/1987		9	1	060B29	01/18/1979	02/18/1979
DD076217	DC029109	09/18/1987		9	1	060B30	02/18/1979	03/20/1979
DD076218	DC029110	09/18/1987		9	1	060B31	03/20/1979	03/22/1979
DD076219	DC029111	09/18/1987		9	1	060B32	01/01/1980	02/01/1980
DD076220	DC029112	09/18/1987		9	1	060B33	02/01/1980	03/01/1980
DD076221	DC029113	09/18/1987		9	1	060B34	03/01/1980	03/31/1980
DD076222	DC029114	09/18/1987		9	1	060B35	04/01/1980	05/01/1980
DD076223	DC029115	09/18/1987		9	1	060B36	05/01/1980	06/01/1980
DD076224	DC029116	09/18/1987		9	1	060B37	06/01/1980	07/01/1980
DD076225	DC029117	09/18/1987		9	1	060B38	07/01/1980	08/04/1980
DD076226	DC029118	09/18/1987		9	1	060B39	08/05/1980	09/01/1980
DD076227	DC029119	09/18/1987		9	1	060B40	09/01/1980	
DD076228	DC029120	09/18/1987		9	1	060B41	01/19/1980	02/19/1980
DD076229	DC029121	09/18/1987		9	1	060B42	02/19/1980	03/19/1980
DD076230	DC029122	09/18/1987		9	1	060B43	03/20/1980	04/10/1980
DD076231	DC029123	09/18/1987		9	1	060B44	01/05/1981	03/21/1981
DD076232	DC029124	09/18/1987		9	1	060C01	02/01/1981	03/01/1981
DD076233	DC029125	09/18/1987		9	1	060C02	02/28/1981	04/01/1981
DD076234	DC029126	09/18/1987		9	1	060C03	05/01/1981	05/15/1981
DD076235	DC029127	09/18/1987		9	1	060C04	04/01/1981	05/01/1981
DC029107	DD076215	04/27/1992	38000	18	1	107/033	01/12/1979	01/18/1979
DC029108	DD076216	04/27/1992	38000	18	1	107/034	01/18/1979	02/18/1979
DC029109	DD076217	04/27/1992	38000	18	1	107/035	02/18/1979	03/20/1979
DC029110	DD076218	04/27/1992	38000	18	1	107/036	03/20/1979	03/22/1979
DC029111	DD076219	04/27/1992	38000	18	1	107/037	01/01/1980	02/01/1980
DC029112	DD076220	04/27/1992	38000	18	1	107/038	02/01/1980	03/01/1980
DC029113	DD076221	04/27/1992	38000	18	1	107/039	03/01/1980	03/31/1980
DC029114	DD076222	04/27/1992	38000	18	1	107/040	04/01/1980	05/01/1980
DC029115	DD076223	04/27/1992	38000	18	1	107/041	05/01/1980	06/01/1980
DC029116	DD076224	04/27/1992	38000	18	1	107/042	06/01/1980	07/01/1980
DC029117	DD076225	04/27/1992	38000	18	1	107/043	07/01/1980	08/04/1980
DC029118	DD076226	04/27/1992	38000	18	1	107/044	08/05/1980	09/01/1980
DC029119	DD076227	04/27/1992	38000	18	1	107/045	09/01/1980	
DC029120	DD076228	04/27/1992	38000	18	1	107/046	01/19/1980	02/19/1980
DC029121	DD076229	04/27/1992	38000	18	1	107/047	02/19/1980	03/19/1980
DC029122	DD076230	04/27/1992	38000	18	1	107/048	03/20/1980	04/10/1980
DC029123	DD076231	04/27/1992	38000	18	1	107/049	01/05/1981	03/21/1981
DC029124	DD076232	04/27/1992	38000	18	1	107/050	02/01/1981	03/01/1981
DC029125	DD076233	04/27/1992	38000	18	1	107/051	02/28/1981	04/01/1981
DC029126	DD076234	04/27/1992	38000	18	1	107/052	05/01/1981	05/15/1981
DC029127	DD076235	04/27/1992	38000	18	1	107/053	04/01/1981	05/01/1981

FULL DATASET LISTING OF 79-082A-03B
HEAO 3 HEAVY NUCLEI REDUCED DATA-COBALT

SYSTEM: MEDIA #	COPY #	RECEIVED	DENS	TR	FILES	LOCATION	MODE: TIME SPAN	
DD076236	DC029128	09/18/1987		9	1	031B18	01/12/1979	10/01/1980
DD076237	DC029129	09/18/1987		9	1	031B19	01/18/1979	02/18/1979
DD076238	DC029130	09/18/1987		9	1	031B20	02/18/1979	03/20/1979
DD076239	DC029131	09/18/1987		9	1	031B21	03/20/1979	04/19/1979
DD076240	DC029132	09/18/1987		9	1	031B22	01/01/1980	02/01/1980
DD076241	DC029133	09/18/1987		9	1	031B23	02/01/1980	03/01/1980

DD076242	DC029134	09/18/1987		9	1	031B24	03/01/1980	04/01/1980
DD076243	DC029135	09/18/1987		9	1	031B25	04/01/1980	05/01/1980
DD076244	DC029136	09/18/1987		9	1	031B26	05/01/1980	06/01/1980
DD076245	DC029137	09/18/1987		9	1	031B27	06/01/1980	07/01/1980
DD076246	DC029138	09/18/1987		9	1	031B28	07/01/1980	08/04/1980
DC029128	DD076236	04/27/1992	38000	18	1	107/054	01/12/1979	10/01/1980
DC029129	DD076237	04/27/1992	38000	18	1	107/055	01/18/1979	02/18/1979
DC029130	DD076238	04/27/1992	38000	18	1	107/056	02/18/1979	03/20/1979
DC029131	DD076239	04/27/1992	38000	18	1	107/057	03/20/1979	04/19/1979
DC029132	DD076240	04/27/1992	38000	18	1	107/058	01/01/1980	02/01/1980
DC029133	DD076241	04/27/1992	38000	18	1	104/068	02/01/1980	03/01/1980
DC029134	DD076242	04/27/1992	38000	18	1	104/069	03/01/1980	04/01/1980
DC029135	DD076243	04/27/1992	38000	18	1	104/070	04/01/1980	05/01/1980
DC029136	DD076244	04/27/1992	38000	18	1	104/071	05/01/1980	06/01/1980
DC029137	DD076245	04/27/1992	38000	18	1	104/072	06/01/1980	07/01/1980
DC029138	DD076246	04/27/1992	38000	18	1	104/073	07/01/1980	08/04/1980

FULL DATASET LISTING OF 79-082A-03C
HEAO 3 HEAO C-3 VERIFY PROGRAM

SYSTEM:

MODE:

MEDIA #	COPY #	RECEIVED	DENS	TR	FILES	LOCATION	TIME SPAN
DD076250	DC029139	09/23/1987		9	8	026E36	
DC029139	DD076250	04/27/1992	6250	9	8	104/074	

FULL DATASET LISTING OF 79-082A-03D
HEAO-3 HNE LIBRARY ON TAPE

SYSTEM: XDS

MODE: BIN

MEDIA #	COPY #	RECEIVED	DENS	TR	FILES	LOCATION	TIME SPAN
DD100521		07/16/1993	6250	9	0	FRC	
DD100522		07/16/1993	6250	9	0	FRC	
DD100523		07/16/1993	6250	9	0	FRC	
DD100524		07/16/1993	6250	9	0	FRC	
DD100525		07/16/1993	6250	9	0	FRC	

FULL DATASET LISTING OF 79-082A-03E
HEAO 3 C-3 Software Library

SYSTEM: Vax

MODE: ASC

SYSTEM: XDS

MODE: BIN

MEDIA #	COPY #	RECEIVED	DENS	TR	FILES	LOCATION	TIME SPAN
DD108876		07/28/1997		88	0	108/326	

REQ. AGENT	RAND NO.	ACQ. AGENT
RLR		SJK

HEAO-3

FIRST 28 FROM HEAO-3

79-082A-01A ASGA-00023

This data set catalog consists of 3 tapes. The tapes are 6250 bpi, 9-track, multifiled, binary, created on the IBM-3081. The D and C numbers, time spans, and number of files are as follows:

#D	#C	FILES	TIME SPANS
D-80374	C-27837	10	09/23/79 - 10/02/79
D-80375	C-27838	09	10/03/79 - 10/11/79
D-80376	C-27839	09	10/12/79 - 10/20/79

REQ. AGENT	RAND NO.	ACQ. AGENT
RLR		SJK

HEAO-3

HEAO3-A COMPRESSED DATA BASE

79-082A-01B ASGA-00029

This data set catalog consists of 25 tapes. The tapes are 1600 bpi, 9-track, multifiled, binary,and created on the IBM-3081. The D and C numbers, time spans, and number of files are as follows

D	C	FILES	TIME SPANS
D-82485	C-29163	09	10/21/79 - 10/29/79
D-82486	C-29164	09	10/30/79 - 11/07/79
D-82487	C-29165	09	11/08/79 - 11/16/79
D-82488	C-29166	09	11/17/79 - 11/25/79
D-82489	C-29167	09	11/26/79 - 12/04/79
D-82490	C-29168	09	12/05/79 - 12/13/79
D-82491	C-29169	09	12/14/79 - 12/22/79
D-82492	C-29170	09	12/23/79 - 12/31/79
D-82493	C-29171	09	01/01/80 - 01/09/80
D-82494	C-29172	09	01/10/80 - 01/18/80
D-82495	C-29173	08	01/19/80 - 01/26/80
D-82496	C-29174	09	01/28/80 - 02/05/80
D-82497	C-29175	09	02/06/80 - 02/14/80
D-82498	C-29176	09	02/15/80 - 02/23/80
D-82499	C-29177	09	02/24/80 - 03/03/80
D-82500	C-29178	09	03/04/80 - 03/12/80
D-82501	C-29179	09	03/13/80 - 03/21/80
D-82502	C-29180	09	03/22/80 - 03/30/80
D-82503	C-29181	09	03/31/80 - 04/08/80
D-82504	C-29182	09	04/09/80 - 04/17/80

D	C	FILES	TIME SPANS
D-82505	C-29183	09	04/18/80 - 04/26/80
D-82506	C-29184	09	04/27/80 - 05/05/80
D-82507	C-29185	09	05/06/80 - 05/14/80
D-82508	C-29186	09	05/15/80 - 05/23/80
D-82509	C-29187	10	05/24/80 - 06/02/80

Jet Propulsion Laboratory
California Institute of Technology

4800 Oak Grove Drive
Pasadena, California 91109

(818) 354-4321

JPL

Mail Code 169-327

September 15, 1989

Dr. Sang J. Kim
Goddard Space Flight Center
National Space Science Data Center
Code 633
Greenbelt, Maryland 20771

Dear Dr. Kim:

I am writing to follow up on our recent telephone conversation and to outline our present plans for submitting data from the HEAO C-1 experiment to you for archival. As I mentioned, we are in the process of reformatting all the HEAO 3 data for transfer to a SUN workstation which we are now setting up. The resulting data will be in a more standard format.

The HEAO 3 data are presently contained in two standard data bases. The first consists of the raw data received from GSFC, presently one 1600 bpi tape for each day of the mission (618 tapes). The second is a slightly compressed data base covering the 254-day period when the germanium detectors (our prime sensors) were fully operational. This data base currently consists of 51 1600 bpi tapes.

We are now reformatting and compressing both data bases for use on the SUN workstation, beginning with the second one described above. The necessary software is nearly complete and we expect to start production within a few days. The size of the resulting data base will be approximately 1 gigabyte. We expect to have this new data base completed within two months, at which time we will submit a copy to you on magnetic tape together with all relevant documentation.

Reformatting of the raw data base should be complete within about six months. The output will be about 75 6250 bpi tapes which we will submit to you upon completion.

Additional submissions are less well defined, but should include the analysis software and possibly source catalogs. We will keep you advised on our plans as they become clearer during the next year.

I hope the plan outlined above is acceptable to you. If not, please let me know and we will work with you to revise it.

Sincerely,

W. A. Mahoney

William A. Mahoney

Jet Propulsion Laboratory
California Institute of Technology

4800 Oak Grove Drive
Pasadena, California 91109

(818) 354-4321

JPL

Mail Code 169-327

29 March 1990

Dr. Sang J. Kim
Goddard Space Flight Center
National Space Science Data Center
Code 633
Greenbelt, Maryland 20771

Dear Dr. Kim:

Enclosed are three 1600 bpi tapes containing data from the first 28 days of the HEAO 3 mission. The data have been organized into 20.48 second time bins (half of a spacecraft major frame) with the format defined in the attached document.

I had expected to send these data tapes to you earlier, but the computer operator who had been working on the project was unable to continue. We will have a new operator starting in June, so we will have the rest of this compressed database to you by the end of the summer. We also expect to supply you with a copy of the raw database by the end of the summer.

If you have any questions, please call me at FTS 792-6606. For any technical discussions on the format and data content, you should call Bob Radocinski at FTS 792-5672.

Sincerely,

W. A. Mahoney

William A. Mahoney

Enclosures

F1

HEAO-C1 Scan Tape Format
September 21, 1989

Each file of the HEAO-C1 scan tapes contains one day of data. Each day is stored as a collection of logical records known as bin records that are of 20.48 second duration. The time associated with the bin record is the time at the center of the bin. Each parameter in the bin record is either sampled at the center time (or interpolated to the center time) or is accumulated over the entire duration of the bin.

Each physical record on the HEAO-C1 scan tapes is 2000 words (8000 bytes) in length with the exception of the last record in the file. Each bin record which is stored in the physical record is preceded by three words. The first is the hexadecimal pattern '89ABCDEF', the second is the record number, and the third is the number of words which the bin record occupies. Each bin record begins on a word boundary. It should also be noted that bin records may span physical records.

Bin Record Description

Word	Type	Description
1.	I4	Absolute major frame number
2.	I4	First or second half of major frame
3.	I4	Year
4.	I4	Day
5.	I4	Seconds of day
6.	I4	Microseconds
7.	I4	Time since SAA exit(seconds)
8.	I4	Time since command status change(seconds)
9.	I4	Time since GeD HVPS change(seconds)
10.	I4	Command Status
11.	I4	GeD 1 High Voltage(millivolts)
12.	I4	GeD 2 High Voltage(millivolts)
13.	I4	GeD 3 High Voltage(millivolts)
14.	I4	GeD 4 High Voltage(millivolts)
15.	I4	GeD 1 leakage current(femtoamp)
16.	I4	GeD 2 leakage current(femtoamp)
17.	I4	GeD 3 leakage current(femtoamp)
18.	I4	GeD 4 leakage current(femtoamp)
19.	I4	Orbit longitude(microradians)
20.	I4	Orbit angle(microradians)
21.	I4	Geocentric longitude(microradians)
22.	I4	Geocentric latitude(microradians)
23.	I4	Spacecraft's height above spheroid(meters)
24.	I4	X-component of spacecraft's position(meters)
25.	I4	Y-component of spacecraft's position(meters)
26.	I4	Z-component of spacecraft's position(meters)
27.	I4	X-component of spacecraft's velocity(meters/sec)
28.	I4	Y-component of spacecraft's velocity(meters/sec)
29.	I4	Z-component of spacecraft's velocity(meters/sec)
30.	I4	Right Ascension of Y-axis(microradians)
31.	I4	Declination of Y-axis(microradians)
32.	I4	Right Ascension of Z-axis(microradians)
33.	I4	Declination of Z-axis(microradians)
34.	I4	Scan angle(microradians)
35.	I4	Zenith angle of Y-axis(microradians)
36.	I4	Magnetic field angle to Y-axis(microradians)
37.	I4	Magnitude of magnetic field(microgauss)
38.	I4	X-component of magnetic field vector(1/1000000)
39.	I4	Y-component of magnetic field vector(1/1000000)
40.	I4	Z-component of magnetic field vector(1/1000000)
41.	I4	McIlwain L parameter(earth radii/1000000)
42.	I4	Solar time(microradians)
43.	I4	X-component of lunar position(meters)
44.	I4	Y-component of lunar position(meters)
45.	I4	Z-component of lunar position(meters)
46.	I4	GeD 1 live time(microseconds)
47.	I4	GeD 2 live time(microseconds)
48.	I4	GeD 3 live time(microseconds)

F3

49.	I4	GeD 4 live time(microseconds)
50.	I4	GeD 1 LLD(counts)
51.	I4	GeD 2 LLD(counts)
52.	I4	GeD 3 LLD(counts)
53.	I4	GeD 4 LLD(counts)
54.	I4	GeD 1 ULD(counts)
55.	I4	GeD 2 ULD(counts)
56.	I4	GeD 3 ULD(counts)
57.	I4	GeD 4 ULD(counts)
58.	I4	Shield 1 LLD(counts)
59.	I4	Shield 2 LLD(counts)
60.	I4	Shield 3 LLD(counts)
61.	I4	Shield 4 LLD(counts)
62.	I4	Collimator LLD(counts)
63.	I4	Or'd LLD(counts)
64.	I4	CPD LLD(counts)
65.	I4	Shield 1 ULD(counts)
66.	I4	Shield 2 ULD(counts)
67.	I4	Shield 3 ULD(counts)
68.	I4	Shield 4 ULD(counts)
69.	I4	Collimator ULD(counts)
70.	I4	Or'd ULD(counts)
71.	I4	CPD ULD(counts)
72.	I4	Shield 1 window(counts)
73.	I4	Shield 2 window(counts)
74.	I4	Shield 3 window(counts)
75.	I4	Shield 4 window(counts)
76.	I4	Collimator window(counts)
77.	I4	Number of bytes in GeD 1 event sub-record
78.	I4	Number of bytes in GeD 2 event sub-record
79.	I4	Number of bytes in GeD 3 event sub-record
80.	I4	Number of bytes in GeD 4 event sub-record
81.	I4	Number of bytes in simultaneous event sub-record
		GeD 1 event sub-record
		GeD 2 event sub-record
		GeD 3 event sub-record
		GeD 4 event sub-record
		Simultaneous event sub-record

Note: I4 is a 32-bit (4 byte) integer. Negative values are stored in two's complement form.

GeD Event Sub-record Format

Each GeD event sub-record covers a period of 20.48 seconds for a single detector. The vast majority of GeD events are seen by only one detector (S=1) and do not have any window flags (W=0) or veto flags (V=0) set. Furthermore, a majority of the GeD events occur in the lower channels. The basic storage scheme tries to take advantage of these facts.

The storage algorithm uses only non-simultaneous GeD events (S=1). Any simultaneous event (S≠1) is only noted and is stored outside GeD sub-record. GeD events which do not have either the window flag or veto flag set will be referred to as non-flagged GeD events, the remaining events will be called flagged GeD events.

For the non-flagged GeD events, the algorithm accumulates a spectrum for channels 0-255 and maintains lists for events in the ranges 256-511, 512-767, 768-1023, 1024-1279, 1280-1535, and 1536-8191. Each range except for the last range contains exactly 256 channels. Therefore, the channel number of any event in the lower five ranges can be stored using one byte. GeD events in the last range are stored in two bytes where the lower thirteen bits contain the raw channel number and the upper three bits are zero. The spectrum for channels 0-255 contains a few channels in which the number of events is greater than four. These channels are stored in two bytes. The first byte contains the channel number and the second byte contains the number of events. The remaining channels are stored in lists of channels with four events, three events, two events, and one event. The list of one event channels is not a true list but a 256-bit map. The i^{th} bit is one if the channel contains exactly one event and is zero otherwise.

Finally, the flagged GeD events are stored in a list. Each event is stored in two bytes. The most significant bit is used to store the veto flag, the next two bits are used to store the window flag, and the least significant 13 bits are used to store the channel number.

Byte	Description
1	Number of channels with more than four (S=1,W=0,V=0) events
2	Number of channels with four (S=1,W=0,V=0) events
3	Number of channels with three (S=1,W=0,V=0) events
4	Number of channels with two (S=1,W=0,V=0) events
5	Number of (S=1,W=0,V=0) events in channels 256-511
6	Number of (S=1,W=0,V=0) events in channels 512-767
7	Number of (S=1,W=0,V=0) events in channels 768-1023
8	Number of (S=1,W=0,V=0) events in channels 1024-1279
9	Number of (S=1,W=0,V=0) events in channels 1280-1535
10	Number of (S=1,W=0,V=0) events in channels 1536-8191
11	Number of (S=1,W≠0 or V≠0) events
12	Number of (S≠1) events
13-44	Map of one (S=1,W=0,V=0) event channels (1 bit/channel)
	Channels with more than four (S=1,W=0,V=0) events (2 bytes/chan.)
	Channels with four (S=1,W=0,V=0) events (1 byte/channel)
	Channels with three (S=1,W=0,V=0) events (1 byte/channel)
	Channels with two events (S=1,W=0,V=0) (1 byte/channel)

(S=1,W=0,V=0) events in channels 256-511 (1 byte/event)
(S=1,W=0,V=0) events in channels 511-767 (1 byte/event)
(S=1,W=0,V=0) events in channels 768-1023 (1 byte/event)
(S=1,W=0,V=0) events in channels 1024-1279 (1 byte/event)
(S=1,W=0,V=0) events in channels 1280-1535 (1 byte/event)
(S=1,W=0,V=0) events in channels 1536-8191 (2 bytes/event)
(S=1,W≠0 or V≠0) events (2 bytes/event)

Simultaneous Event Sub-record Format

Each simultaneous event is stored as a string of 3 to 9 bytes. The first byte of each simultaneous events is the flag byte. The bits in this byte are interpreted in the following manner:

bit 0 - Missing detector flag,
bit 1 - Veto flag,
bits 2-3 - Window flag,
bit 4 - Event present in GeD 1,
bit 5 - Event present in GeD 2,
bit 6 - Event present in GeD 3,
bit 7 - Event present in GeD 4.

Following the flag byte of each simultaneous event is a list of channels for each detector in which the event is present. Each channel value occupies two bytes.

The missing detector flag is zero whenever the number of detectors indicated by the simultaneous flag field of the event is equal to the number of detectors in which the event is found; otherwise, it is set to one.

DUMP OF D-82485

Start date: 10/21/79 STOP date: 10/29/79

(Record 1 File 9)

DUMP OF TAPE RR0001

NPUT TAPE RR0001 ON HT1

DATA INPUT F9 NF=9 SR=1=1=1 SR=9=1=1

1979 YR   294 DOY

FILE 1 RECORD 1 LENGTH 3" / 8000 BYTES

(0)	89ABCDEF	00000001	00000137	00010146	00000002	000007BB	00000126	00000068	00095350	0000001F
(4)	0000001F	0000001F	0000FDFC	001B2011	003B4611	002A31E1	0031BAC9	00028FC1	000696DB	0003A9D8
(8)	000A111D	0007FDB6	005A963D	00041470	FFFC6569	0007AC40	00485BFC	004798C1	FFE76F3F	FFFFF3C0
(12)	00001300	0001348	005 F9D1	FFF4CC3D	0036738A	FFFD3653	005A1746	001797DF	001D06E3	0003D6B4
(16)	FFFE377C	FFFBC8A1	FFF1B3E7	0013BA73	0027B849	EAAA0A05	F5DE9090	FD56D55C	00D688A8	00ECCA49
(20)	00E8D828	00E64C4D	00000BE1	00000C2B	00000B69	00000B56	000001B7	000001D1	00000174	0000017D
(24)	000 9F66	000AEFF	000 A2AC	000CA2E7	00016462	0002D39C	00002F44	000012DF	000014C2	00001336
(28)	00001178	00001E2C	000039DE	00000174	00000D13	00000DD0	00000CA7	00000AF9	0000231D	000000A3
(32)	000000AC	000000B9	000000CC	000000C2	0102010B	1D060B06	01041511	1A000009	00064043	C8A16100
(36)	CC514608	84CC401E	400C0448	24200084	10110004	35083249	36253C34	37505D70	8A969798	D16C5794
(40)	9575A252	46C8E3C2	92A30948	2F63E13A	6A1270 6E	18931FFE	251A2537	B2A7E993	29186476	08C24408
(44)	D2911F5F	5DED0907	9675C15	E2062807	CD221921	9F411880	9E20BC24	F7345621	5F208120	A0241E20
(48)	F72CD20	8C223C24	A3448621	30218B20	A8209403	0102091E	14080501	02151310	000001C4	D10199A9
(52)	54261504	01C8200	1A 22906	50000220	180A0000	00440034	0535C54A	05A03336	232A3A46	484F8486
(56)	95850E29	CD228291	AD4F5A6A	47FA83BE	91606131	9AEB8AB1	58B323A1	76236620	2C10962F	0EFF600B
(60)	CE2080AD	4CC50B81	AA20298A	6772F809	6F3E67A9	CD47A689	7507BB09	39230221	ED21A121	03432021
(64)	A14E9020	60241720	1A239123	D6248A20	BE213923	6845F32C	75211220	58213D00	03011526	0A080301
(68)	05171600	00C00400	00041361	88C08F08	020C1700	01843824	2401C480	10040010	06800249	A0A34A18
(72)	1930C143	4445464B	4D4F5A5B	656B7C83	85A4ACC2	36E4CD50	205D4AB2	E66955B5	CF27E48E	429B5746
(76)	04347667	AF2B66E3	38DFA726	9809352D	192B66BB	3F197F3A	390A68AE	C49C9F5E	1EA4AA2A	0404F450
(80)	088E134F	070E07A9	08BF2052	208E2149	2191212D	41DE23EA	3AA72125	20B040D7	21A2232F	212021D6
(84)	21E2228F	22B7217A	22EA4703	249B2601	0202C40A	1F0DC9C2	01162410	00000000	020442A7	21226084
(88)	012800A3	A7410E02	48821 1	F0C11080	08100000	4055F05	5EAC494C	79883P41	484F5B60	74B5B6F4
(92)	FBB68EEA	66B9447B	9C644139	6A8C7FF3	755EBD28	E2097A33	F5516392	78845338	383725B7	F2DC0125
(96)	3883E735	EAE9976B	15F3FD52	272C69A2	06AC0773	0A4E065D	0A5B0813	2186407F	21B7230D	20592207
(100)	20B621A6	3FFF4095	25 72268	210D2351	206A20F3	2454258F	269F31D8	413A2071	20BB4078	221C2698
(104)	21B64040	212020D9	281A207D	207B2429	20464144	9403CE23	013801B6	09011704	55090360	00728201
(108)	3F910075	0C030300	E8060034	017B9100	57060157	00C282C3	7188C6B8	8805FC0A	009200B2	88009B81
(112)	02E68200	D2030060	01811901	4B02870 6	060D0CA6	840C4809	0429C094	03004C04	A40603FC	00AB0301
(116)	7904C792	01EA0902	AF 108 C	065E039C	9401FD16	03550278	0A014504	73190295	00821C00	60004584
(120)	00711C0F	F3009381	02671600	A4020F1C	01150486	82009706	067500E0	13028701	308200A1	94023406
(124)	0550 0095	0300D000	5700C045	03C30000	89ABCDEF	00000002	0000013A	00010147	00000001	000007BB —YR
(128)	00000126	0000007D	00016410	00000033	00000033	00000033	0000FDFC	001B2011	003B4611	002A31E1
(132)	0031BAC9	00023213	000695DB	0003102B	000A111D	0007F7C7	005AEF9F	00045273	FFFCA0A1	00079EFC
(136)	00479BAF	0049179C	FFE8FC0E	FFFFF349	00001289	00001372	005075AB	FFF670F9	0036713B	FFFD3579
(140)	005BC852	0018D1C6	001D4E21	0003DA37	FFFD64A8	FFFAC57B	FFF1E9FE	0013780B	0027E955	EAAA2F00
(144)	F5DE4EA	FD56BDB	00DC0513	00E321C1	00DFCCD5	00E3F628	00000CA1	00000C18	00000ED3	00000B85
(148)	000001B0	000001DD	00000187	00000198	00009F00	0000AE1F	0000993B	0000A0FA	00014C55	0002B829
(152)	00002096	00001263	0000145D	0000127D	00001176	00001DA5	00003883	0000017B	00000CC5	00000D24
(156)	0000 0C76	0000 0A92	00 12109	000000AF	000000B9	000000BD	000000BF	000000BF	0100041C	1B0C0904
(160)	01011B13	6BC00000	02E811 1	A72A02C0	8A8041C4	82050001	00800800	000A050	80100420	35053134
(164)	49812528	2E363B3E	434B4F52	6E757A82	94A0555B	BCFFF02F	040A8C7D	9F8495A1	396B54F9	56470749
(168)	3FA62F04	AE7D76D3	55B8490	A943C144	02503C96	80363891	BB48ADAC	A8AD5CCD	20235421	05203B21
(172)	A120C424	C241C320	6E22C122	C0226924	3E20A52C	D521EB21	7A20E523	122D7B27	6A229020	A420D622
(176)	C123082A	2921EC01	00051323	18060101	00181000	00008040	15A63145	00C4641A	049070AA	10022112
(180)	20040011	10460020	84400434	061F2627	33540728	292A2E38	3D494A4B	4C618A91	9597A0DF	E39E75FD
(184)	679985F8	66E12256	2D9EBC65	E4970785	A06C8C6E	A100D66AB	B86342EC	1D8D20F5	3997C1D6	E5F9AFCE
(188)	213AFF20	B3201221	91 B77A9	A5513AAF	BBE7C03C	08C45F5B	219F2065	4115219F	22E921A1	208E21AB
(192)	20A1233A	21244772	22A922A9	20AF4065	26892076	202E2075	2A3F2263	2798206F	0101060D	1E0E0803
(196)	00071B17	03C00210	0000400A0	25197844	100132EC	00D9270C	70108C21	C0590100	21200013	5B053F3B
(200)	43495A7B	A4183C40	4144484A	4E555C64	6DCD3BDF	32E035F4	7045DB93	402C4D1E	9D10E47A	2B219847
(204)	30205B04	C11D3079	4A52CC2E	79705072	FA080866	977718C3	174F7CD4	592D4302	020A971A	3608E006
(208)	520779 0E	08076921	D8225922	2422C440	F6205B20	FC204921	4B22E942	0A20E222	A244DF25	71231D20
(212)	6F243A21	7A225A41	6F203D24	7020AE24	2C20A020	61010201	10211505	0502021C	0F000000	000000E9
(216)	27098020	21035000	0A 09A	03650024	00000868	0028084 0	404A0640	41953545	46494E4C	53595E60
(220)	588789B3	B6E32AEA	4624B498	7BEA1C0B	5B0144F3	5A2B886F	3A1D5B24	5745004E	78337F77	9426045E
(224)	EC68EB8D	60D23724	22A936C8	024F98FA	8138BD9B	7355AF7B	7FC739C0	46C2D9B7	0829086A	20AE23AF
(228)	20B22047	26B8276A	2041233B	21DB2370	20E1222C	435D2242	206A411F	4111415F	44E32133	20FA2A25

(2320)	21A620A0	2120221A	20482489	06122000	F9880088	84024F98	00381306	A80108CA	C25A006D	19006203
(2360)	A5820076	920422DC	05510069	92014A1A	036F004C	05007A04	250901A1	01B20601	2600EEDC	00CE01A7
(2400)	1500EC01	0A0C0046	004B0300	A400892A	16FF00D3	0300E201	00940CDA	8202BF09	0300007A	03017F01
(2440)	B709006A	02198200	E410023C	03579803	37840297	0E02D400	71030CD3	0E0C1A01	9D01AF91	01179202
(2480)	E4060248	014C0901	0E042206	060B00E5	8800F592	00948101	9D0A00C1	01439801	0F26028A	00650501
(2520)	E8003E00	89ABCDEF	00000003	0000014A	00010147	00000002	0000C7BB	00000126	00000091	0008B710
(2560)	00000048	00000048	00000048	000CFDFC	001E2011	003B4611	002A31E1	0031BAC9	000176B8	000667FF
(2600)	0003D8BC	0019E242	0007F10D	005B47AC	00048F74	FFFCDC20	00079DBD	00468F40	C04A8AEF	FFEABCD3
(2640)	FFFFF205	0000125E	00001396	005004AB	FFF817A2	0036710B	FFFD375B	005D797B	001A089B	001D6AD0
(2680)	0003DD79	FFFC6F96	FFFAAA85	FFF22F95	00133793	0027B61E	EAAA5400	F5DE0CB0	FD56A600	00DF2D2E
(2720)	00DBFA16	00E1A4E5	00E2F2C1	0000C8B7	0000CB98	0000CB58	0000CAF8	0000C1EE	0000C1CE	00000170
(2760)	00000180	000098AC	0000A628	0000956C	00009A2A	0001446A	0002A761	0000160D	000011BC	00001327
(2800)	0000117F	000011CA	00001C3F	00003653	0000014C	00000C85	00000D08	00000C4C	00000A78	000021D9
(2840)	000009B0	000000D1	000000C0	000000D0	000000D0	0101040E	200D0364	03071517	08000001	00002003
(2880)	034C1814	01213915	06204284	28006001	50121010	00000808	4A053620	35A3FE05	27282F34	39414348
(2920)	4E55A1DA	F85BA809	168AF101	1026085B	50E1C75A	3F72B198	A2884997	1CCB2EC2	90884A66	08337322
(2960)	2278220C	28B71439	14DA93BE	C5E46848	15EC0A06	085D0915	0AE1061C	0BAC06DF	0633410C	264E20B1
(3000)	2029283E	22A1402E	21A0203F	2093244D	20372CCA	21A0216B	208A25E8	3068205A	24452074	0000030E
(3040)	231B0901	02091C15	00800000	022A0422	11504178	0422C500	5011E28C	24A00103	2001140C	0000001C
(3080)	33346F1F	2B2F373C	46484A50	5372767C	9B2E471B	86D265E7	67F64DA1	0005BCE0	E1BF8225	5786672F
(3120)	7BF1C344	192656A0	AAE76925	75299B65	20226C0C	20271F59	1AC5804B	20712018	7BC51D20	2100CD3B
(3160)	A6B97378	68237B05	4A517709	6A064307	4E082214	8E09F719	B8065A06	CA20AC20	76261822	DE272222
(3200)	B022B342	74219C20	6B209620	AF202020	4F21A120	8C220422	A920B321	A1209921	1F230820	EB41D824
(3240)	E12D0B21	28020104	14240806	0201031E	13008000	3A000002	3900C456	8AA20014	03004008	0110A020
(3280)	0708809C	0102005E	0049064A	06405A5B	5D9C1619	39414243	4E576E71	727B7C7D	848A8D95	A1B33419
(3320)	7AE5CAE4	16517E1A	5E306E0C	46294EAC	0E4A1A43	1DFB3283	5CF61A06	203D05E4	2F0DA6ED	8BD6085F
(3360)	78C60220	6F47E278	4A02890F	9406A307	DE216320	79247F20	8A2E5E21	F6226D20	5D40B422	52233F20
(3400)	D920B725	00217924	70214120	7320D125	FB269822	40209A20	C520DB20	CA25E221	4A20E023	03020103
(3440)	0F210006	06000721	12010000	00000103	82300A50	14000002	00005008	40000003	10000422	00444000
(3480)	C04A0860	055E3348	A5404547	494B5F61	6A6D6E84	87A4B4C2	1550DCB4	208C5C23	6B025D65	EAE9234C
(3520)	696EDB11	65A3F2F2	1B1540D7	B79543B7	BE2EC84E	AC368EDF	4A39BCEE	31369550	C70693A9	A8A9A765
(3560)	C3352F38	3509F107	8006B706	4806A00D	7308B922	FC21B645	A521E420	42224722	4921E520	B5209F21
(3600)	A023E448	85244722	B924DD20	B42F2F21	2120A141	1421B722	4E20F520	7F205620	3C21F822	EA20C122
(3640)	F8223F20	859801DB	06003E00	95130256	05EE0903	D1009F0C	008D0057	06007F00	BC0E002B	00C20C00
(3680)	98006319	02CD01D7	05002D02	441600F7	01FA8802	2416010D	02348202	CE0A002D	009D0C00	F1008681
(3720)	00CD1502	0D00D91C	016A001D	0C00AF01	17920253	1A003402	879101A2	C8012F81	01A7090C	A301B30C
(3760)	03640074	09009700	49130179	02520C01	4C009F05	0098015A	0A00B805	340C008D	01B30302	2601D915
(3800)	054D00C7	06007400	511902F7	00E61902	3001EA82	03F89200	7A8800F2	0600EC01	1D0304A0	00790900
(3840)	6E022E06	00BA0146	0C005C01	05000010	89ABCDEF	00000004	00000134	00010148	00000001	000007BB
(3880)	00000126	000000A6	0000C7D1	0000005C	0000005C	0000005C	0000FDFC	001E2011	003B4611	002A31E1
(3920)	0031BAC9	000176B8	00054EDB	0003A9D8	0009848B	0007EBEE	005BA0E7	0004CC75	FFFD17DE	00079C80
(3960)	004578A1	004BF66E	FFEC1FA7	FFFFF261	00001192	000013B8	004FA19E	FFF9BFD7	0036707D	FFFD3775
(4000)	005F2AD4	001B3724	001D5D6B	0003E095	FFFB6F2C	FFFAB721	FFF274A4	0012F869	0027B03E	EAAA7900
(4040)	F5DDCAD0	FD568E50	00E1A7F2	00EE4F15	00E9EAD0	00E30204	00000E03	00000E0D	00000E1F	00000A79
(4080)	00000191	000001AF	00000165	00000189	00009364	0000A171	00009399	000095A5	00013C24	00029C04
(4120)	000013AC	00001125	000012AD	000010DA	0000101F	00001BE2	00003510	00001163	0000CCDF	00000CD6
(4160)	0000CC51	00000A41	0000208F	000000B9	000000BA	000000A2	000000BB	000000EC	5101030C	230B0506
(4200)	02051911	05000001	038E21CA	801234E2	110062C2	2006100D	10000408	28180800	C0400842	35054A2A
(4240)	339A2930	3643494F	528B96A0	A1C7224C	9518CCB5	F066869B	31CC397F	3C401B44	E5E81EC6	728DDE21
(4280)	3DEB4D13	4FBD65D5	A0236CAE	D895C222	F7964015	19F791BF	5A92F2EB	8CDE16CF	ACD8628D	E617350C
(4320)	D01C6E7A	8A0F7621	45247423	9E21BA20	6C20DC20	43205C20	37229D21	F421A140	89202C21	E7203422
(4360)	EC21AF20	9A210632	CD202020	4A238F20	1B010102	00240606	06000122	12000000	036A6852	9F54173C
(4400)	041000A8	71102040	0803020A	08431100	80108600	00340548	A0FA252B	35373947	49515759	8F979FFF
(4440)	C3D27A48	DC476200	62A0DAB2	4F8415A0	4242FAC8	9E983824	5AC25E58	9C85D12A	95570C39	AF203681
(4480)	0214FEE6	454D0261	94897387	2C065920	6D203220	9820CA22	DB2A0B21	CC216121	83219642	AF430E21
(4520)	6720B424	8F226820	77207A25	60232140	2820F527	FB206A20	25221D22	54202320	5D44DE21	9E207E20
(4560)	9620DF04	02060A23	06050301	01141200	20110000	0014085A	0A088895	8A89640B	12402818	9040982A
(4600)	00C10882	98800149	054A055A	075B0619	48183840	5D7EA21D	42454D4F	50628D9B	C3D6667A	D2EBB87B
(4640)	1770C3B6	BE2A15A9	F22F3763	B244E32D	D0764179	285C5E65	90806202	74269344	789E629D	FEB5321C
(4680)	2A039108	6A216520	F0266824	BB213123	7120D220	F8208221	2720A822	B6206F21	F5204326	0020A320
(4720)	BE20B720	79000104	0C1A100A	05030120	13000000	00000016	94F2A619	8070089C	6101748C	91190625
(4760)	01101815	68882800	004B444F	5F603237	393E3F45	49525B67	81B62E6F	459A11A5	1EB7E4A3	1200A671
(4800)	33FC9D4F	12B1C210	5E25CE01	6A36A0BF	E9C43751	C87F4AD3	BEB5E31E	F9A4CC9D	4DA31B0C	46BB4FAB
(4840)	C3AF834C	83BA0741	20E52395	20EA20D5	20E2210A	22112171	20CB4201	45CE2119	20CB29FF	20372123
(4880)	24F54458	2A51404D	20D4433A	21E720C1	21782CC6	40BC2054	41F22135	216A25C7	0C05EF04	BA0C007D
(4920)	002D1502	F7008119	01000647	84005316	009B0CC2	0A065400	8B060084	0F41820A	ED036137	01EC0C05

(7280)	[illegible]5A 292B	[illegible]5343A49	4A545859	6F737993	B2CBA78E	17[illegible]BFE10	BF8C4C26	01C41F72	609DEB2C	FF84EC7B
(7320)	AAE18E61	C86812AC	9F557741	7FC5A3D3	1B7E1C62	68838F65	4137B366	154F39C0	361EB420	79608488
(7360)	EB1F6247	3C1434A0	A92CB27A	A71E9063	0FA5255E	295F6A2C	A6B4CCEF	28089A06	C407BD07	DC06C607
(7400)	35[illegible]613[illegible]9	3D238D46	2020BE20	8F236C23	A822D140	BE445B25	1A220725	C5214723	4F24DE24	DD261B27
(7440)	F12[illegible]B429	D3219D41	AE[illegible]3421	C7254520	C9249121	4E202B20	CF20E222	48239021	07404020	AE24E120
(7480)	8D20FD23	41207621	A2220920	5B229326	AF219D25	89242320	C9237822	48238120	21002208	0D32170E
(7520)	03010628	18000000	E4000000	0A81170C	82108085	28040030	D9991411	10100C10	00001004	40485A42
(7560)	4449595B	62717D0A	3F464A4C	50768889	919DA6DD	15BC271C	071A7580	45D368B8	EBE5D35C	0A207131
(7600)	4FE529DF	791[illegible]7A28	88A5F[illegible]38	ED872341	F7616B31	577AF9A7	7[illegible]2[illegible]8FAD	1CE33A56	88C0EAB8	7703ACCE
(7640)	3E5BC0D3	3FB54485	5C981D98	442A1E43	75033432	B24D2A8A	6184A756	011F3607	2707CB09	0D03A606
(7680)	7708BB25	17208C21	4220E620	EF20DA20	9D265A22	E5217620	8621EB22	AE201B23	36229621	7A40B822
(7720)	D0217C22	E6258D20	AD245134	0E211C21	08225821	2541A520	B1205A21	7A21B020	6F239520	97226220
(7760)	F8246900	[illegible]0040F25	1913[illegible]5[illegible]4	072D1E04	00000000	4[illegible]10862	8986C068	02060104	40010800	543326C4
(7800)	99080004	5411023E	4A4B7235	363F4345	47495E5F	6F7387AE	F1F6C80B	88E83628	92AC5064	399F847C
(7840)	205D8A88	F337DC6C	83FB1B[illegible]4	2EBBF225	BD2E06F2	0A5BAEEE	25B280B7	E3397ED2	36764A68	4F620C23
(7880)	D355C729	54350429	A66A35A9	FCF7BF6D	5D8FDDCD	F2[illegible]E2D64	BBC1A768	8158C261	3A140CCF	08E30617
(7920)	08E10810	053F1FFF	07C420C1	240F21B6	25FB2185	20602152	2060207B	252C211E	213A2194	20D020BC
(7960)	20C82510	202B44C8	26B52066	21452A04	20FF21B4	205C2051	20A72216	204F246B	22EE210D	20EA2365

FILE	INPUT RECS.	DATA RECORDS INPUT	MAX. SIZE	READ ERROR SUMMARY PERM	ZERO B	SHORT	UNDEF.	INPUT RETRIES # RECS.	TOTAL#
9	529	529	8000	0	0	0	0	2	2

IOJ DUMP STOPPED AFTER FILE 9 # OF PERMANENT READ ERRORS 0

START TIME 05/14/92 09:27:44 STOP TIME 05/14/92 09:32:26

REQ. AGENT	RAND NO.	ACQ. AGENT
RLR		SJK

HEAO-3

HEAVY NUCLEI REDUCED DATA - COBALT

79-082A-03B SPIS-00013

This data set catalog consists of 11 tapes. The tapes are 6250 bpi, 9-track, multifiled, binary, created on the IBM 360. The tapes are in a chapter verse format described in the format. The D and C numbers, time spans, and number of files are as follows:

D#	C#	FILES	TIME SPANS
D-76236	C-29128	01	01/12/79 - 10/01/80
D-76237	C-29129	01	01/18/79 - 02/18/79
D-76238	C-29130	01	02/18/79 - 03/20/79
D-76239	C-29131	01	03/20/79 - 04/19/79
D-76240	C-29132	01	01/01/80 - 02/01/80
D-76241	C-29133	01	02/01/80 - 03/01/80
D-76242	C-29134	01	03/01/80 - 04/01/80
D-76243	C-29135	01	04/01/80 - 05/01/80
D-76244	C-29136	01	05/01/80 - 06/01/80
D-76245	C-29137	01	06/01/80 - 07/01/80
D-76246	C-29138	01	07/01/80 - 08/04/80

CALIFORNIA INSTITUTE OF TECHNOLOGY

GEORGE W. DOWNS LABORATORY OF PHYSICS
PASADENA, CALIFORNIA 91125

May 4, 1987

Dr. Sang Kim
NASA/Goddard Space Flight
Center
Code 633
Greenblet, MD 20771

Dear Dr. Kim:

The HEAO C3 Internal Report TLG-22 documents the difference between the *gold* data set which we have already sent you and the *cobalt* data set which I am now sending. Report 22 is in the packet of documentation which you have already gotten from Washington University in St. Louis. I will summarize it for you here:

> The basic data set consists of 600 *library* tapes which contain all HEAO C-3 data. These tapes have been *crushed* into two small data sets -- *gold* which contains all data for nuclei with atomic number above 30 and *cobalt* which contains all data for nuclei which pass thru the center of the instrument at small angles of incidence (and thus have good resolution). These two crushed data sets support greater than ~2/3 of our work. I am now suggesting that we furnish the large *library* data set to the NSSDC for completeness.

Yours,

Tom Garrard

Tom Garrard

SPACE RADIATION LABORATORY

CALIFORNIA INSTITUTE OF TECHNOLOGY

TO J. Klarmann **DATE** September 19, 1986

FROM Tom Garrard **EXTENSION** 6635 **MAIL CODE** 220-47

SUBJECT HEAO C-3 Archival Data

Enclosed are the documents which describe our data set for you to submit to to the archival program. These documents are described below and should be read in the order listed.

The instrument paper, Binns et al., NIM 185, 415-426, 1981, for obvious reasons. One should read this paper for understanding of the instrument and of the data which comes from the instrument.

The HEAO C-3 Production Tape Format, SRL Tech Rept 79-3, specifies the data which we receive from GSFC. This includes such things as position, attitude, and data quality, as well as the instrument data stream.

The HNE Data Processing Plan, SRL Tech Rept 78-1, gives an overview of how we handle the data. This report introduces such concepts as library and "crush" tapes, and how they are formatted into chapters and verses.

The SRL Chapter/Verse Format, SRL Internal Rept 86, 1981, describes in more detail the techniques of using chapter/verse format and descibes the program library used at CIT, WU, and UM to handle data formatted in this fashion. This program library depends heavily on pointers and hence is written in C, not FORTRAN. It would not be particularly difficult to rewrite it in FORTRAN but a large penalty in execution time would be expected.

The HNE Library Generator, SRL Tech Rept 78-3, describes the program which generates the library tapes and the data which is on the library tapes.

The HNE Data Crusher, SRL Tech Rept 79-1, describes in general terms how the library tapes are "crushed" to produce small data sets on crush tapes.

The New "gold" and "cobalt" programs, HEAO C-3 Internal Rept TLG-22, describes the particular crush programs and corresponding data sets that are most likely to be of use to foreign users.

Finally, the Data Chapter Formats database printout specifies the formats of all the chapters/verses used by the C-3 team. Heavy use of acronyms is made in this document, but it is intelligible to anyone who has read all the preceding documents.

Clearly, this is a large hunk of documentation to digest, but it has been adequate for new grad students and is presumably adequate for visiting scientists. I do agree with your statement that some CIT residence time is necessary.

cc: E. C. Stone, M. H. Israel, C. J. Waddington
without enclosure

Nuclear Instruments and Methods 185 (1981) 415–426
North-Holland Publishing Company

THE UH-NUCLEI COSMIC RAY DETECTOR ON THE THIRD HIGH ENERGY ASTRONOMY OBSERVATORY

W.R. BINNS, [1] M.H. ISRAEL, [2] J. KLARMANN, [2] W.R. SCARLETT, [3]* E.C. STONE [4]
and C.J. WADDINGTON [3]

[1] *McDonnell Douglas Research Laboratories, St. Louis, MO 63166, U.S.A. (present address: 2).*
[2] *Department of Physics and the McDonnell Center for the Space Sciences, Washington University, St. Louis, MO 63130, U.S.A.*
[3] *School of Physics and Astronomy, University of Minnesota, Minneapolis, MN 55455, U.S.A.*
[4] *Downs Laboratory of Physics, California Institute of Technology, Pasadena, CA 91125, U.S.A.*

Received 20 November 1980

The third High Energy Astronomy Observatory satellite (HEAO-3) carries a particle telescope for the detection of highly charged cosmic ray nuclei. These nuclei, which have $Z \gtrsim 28$, are much rarer than the lower charged nuclei in the cosmic radiation. As a consequence, this particle telescope was required to have a large collecting area as well as an ability to resolve individual elements. This paper describes the telescope, composed of large area parallel plate ionization chambers, multiwire ion chamber hodoscopes and a Cherenkov radiation detector. The resulting telescope has a total geometry factor of 59 000 cm^2 sr and is capable of measuring the charges of nuclei in the range $14 \lesssim Z \lesssim 120$.

1. Introduction

This paper describes the design and function of a detector of UH or ultra-heavy cosmic ray nuclei, which was flown on the HEAO-3 spacecraft launched into near-earth orbit on September 20, 1979. This instrument was designed to make observations with good charge resolution and high statistical weight on the elemental abundances of those cosmic ray nuclei that have atomic numbers, Z, significantly greater than that of iron, $Z = 26$. These UH-nuclei are relatively rare in the cosmic radiation, having abundances four to six orders of magnitude less than those of the nuclei in the iron charge region. Consequently, it has been difficult to accumulate a statistically adequate sample of UH-nuclei and those samples that have been obtained have suffered from rather poor experimental charge resolution, inadequate to distinguish individual elements [1,2]. The astrophysical significance of observations on the UH-nuclei has been reviewed by Israel et al. [3], but in every case must be greatly improved by measurements with a capability of resolving individual elements. These nuclei represent a sample of matter that has had a unique history, and a knowledge of their abundances should allow us to examine both the nucleosynthesis processes that are responsible for the creation of these heavy elements, and the acceleration mechanisms that produce the cosmic radiation. Similarly, the propagation of cosmic ray nuclei in the interstellar medium will be most sensitively probed by examining these heavy elements.

Our current knowledge of the abundances of these nuclei has been summarized by various groups [1,4], but there is still considerable uncertainty regarding even the gross features of the abundance distribution. For example, Meyer [5] has recently suggested that the abundances of the actinides, those elements with $89 \leqslant Z \leqslant 103$, may be as much as a factor of three less than previously claimed, which would seriously affect the interpretation of these abundances in terms of theories of nucleosynthesis. Similar uncertainties affect our understanding of the origin and significance of the intermediate charged nuclei.

It has been clear for a long time that these uncertainties would be significantly reduced by a long duration space exposure of a large detector capable of resolving the individual elements. In about 1970 we made various proposals to NASA for such exposures on the High Energy Astronomy Observatory series of

* Present address: Los Alamos Scientific Lab, NM 87545, U.S.A.

satellite missions. The resulting detector array described in this paper is an amalgamation of our several proposals that has been optimized to the configuration of the HEAO-3 spacecraft.

In our design of this detector, we have had two major requirements. Firstly, as an overriding factor, we have required that the detector system should be capable, in principle, of resolving individual elements over the range $17 \leq Z \leq 100$, and, secondly, that the collecting power or geometry factor, the area-solid-angle product, be as large as physically possible. These two requirements have affected the design at every stage of development, from the initial selection of the basic detector types, to the selection of details such as the wire spacing of the hodoscopes.

In order to meet the charge resolution requirement, it was necessary to select detector elements that we could reasonably expect to produce signals that were linearly related to the energy loss, even in a charge region in which there was little or no prior experimental data. Thus, while some types of detectors, such as plastic or crystalline scintillators, produce signals that are nonlinear with increasing energy loss even at charges as low as $Z \approx 26$, we required detectors that would have a good probability of a linear, or at least smoothly increasing, response up to $Z \gtrsim 100$. A further consideration in any selection of a detector type came from the wide range of the particles that any space mission would encounter, so that both Z and the reduced velocity β ($\beta = v/c$) have to be determined for each particle, which in general requires at least two different measurements. Conventionally, high energy cosmic ray detector arrays have used a measure of ionization energy loss, dE/dx, which varies as $Z^2/\beta^2 \cdot f(\beta)$, combined with a measure of Cherenkov energy loss, which varies as $Z^2(1 - 1/\beta^2 n^2)$, where n is the refractive index. Such a combination is generally, though not always, sufficient to define both Z and β uniquely. At low latitudes, where the geomagnetic field cutoff ensures that all the incident nuclei have $\beta \cong 1$, measurements of dE/dx and C provide essentially independent measurements of Z.

These considerations led to a detector array in which we measure the ionization energy loss by using a parallel plate gas-filled ionization chamber of a type similar to those developed by Epstein et al. [6] for use in balloon flights. Such chambers have the advantages of introducing very little matter into the trajectory of the particles, which therefore have only a small probability of suffering a nuclear interaction while they traverse the detector; of having a nearly linear response to energy loss even for ionization densities larger than those expected from the highest charged cosmic ray nuclei; and of not requiring accurately controlled bias voltages. Their principal disadvantage is the relativistic rise of the signal as the energy increases above several GeV/nucleon, which is a larger effect in a gas than in a solid medium. As a result, for many of the detected nuclei Z is a double-valued function of the instrument response. In addition, there is the practical disadvantage that a pressure vessel is required to maintain the gas at a pressure of about one atmosphere. The Cherenkov energy loss is determined using plastic radiators mounted in a light diffusion box viewed by photomultiplier tubes (PMT) which measured the integrated light intensity produced in the radiators by the passage of nuclei. These charge measuring detectors, when combined with multiwire ionization chamber hodoscopes to define particle trajectories, make up the HEAO-3 detector array.

The HEAO-3 spacecraft was launched into a circular orbit with initial altitude 496 km and inclination 43.6°. During the first 9 months of operation the spacecraft spun about its Z axis with a 20 min period. Our instrument is oriented with its principal viewing directions along the spacecraft's Y axis. Since the spin axis is oriented toward the Sun (or toward some other celestial point within 30° of the Sun), the instrument does not have a fixed orientation with respect to the Earth; however, star sensors on the spacecraft provide post-facto attitude determination to better than 0.5°.

2. Physical description

A schematic of the detector array (fig. 1) shows that the array is composed of two modules which when combined make a system symmetric about the X–Z plane that responds to particles entering from either side of this plane. A particle penetrating the entire array from "above" will encounter successively a hodoscope, H1, which gives two coordinates; three ion chambers, each with separate pulse height analyzers (PHA); another hodoscope, H2; two layers of Cherenkov radiator, the combined light from which is viewed by eight photomultiplier tubes, each of which has a separate PHA; a hodoscope, H3; three ion chambers; and a final hodoscope, H4. Such events, designated as H1 · H4 events, have a geometry factor of

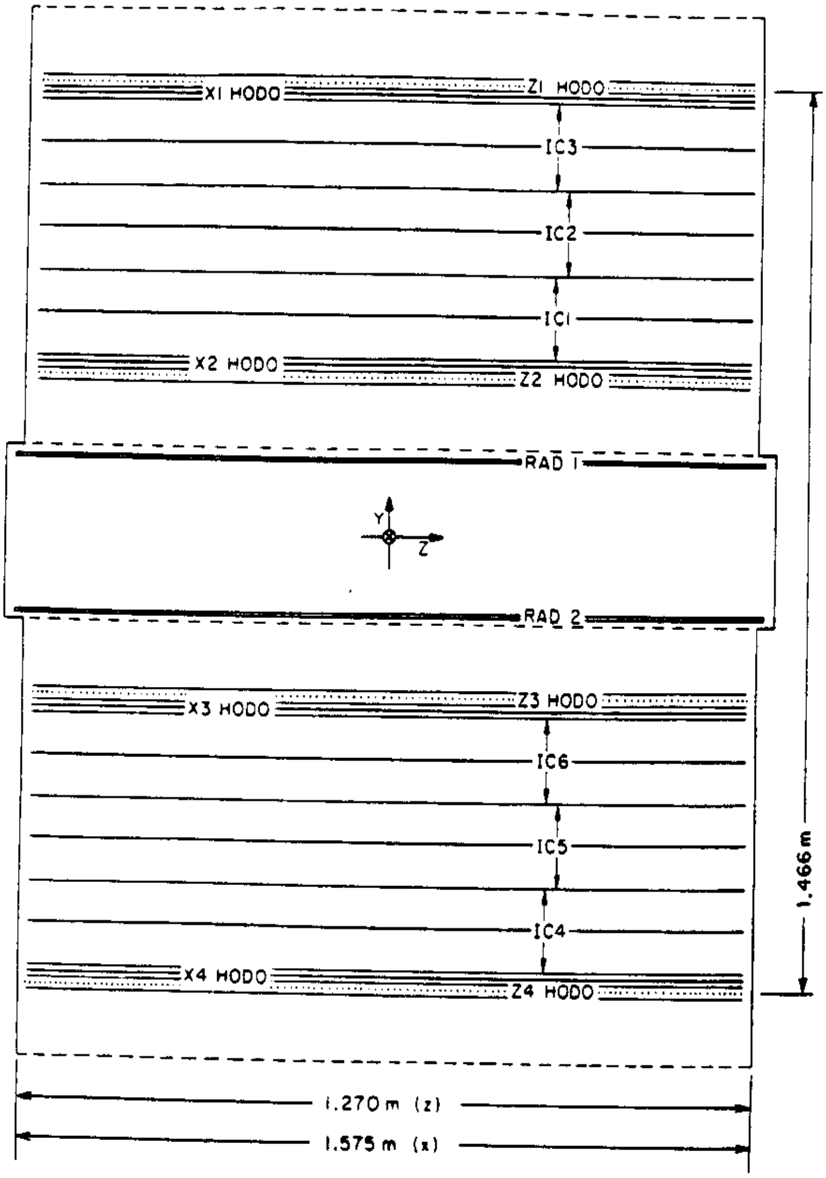

Fig. 1. A schematic view of the particle telescope. From the top this diagram shows hodoscope H1, ion chambers, IC3, IC2 and IC1, H2, Cherenkov radiators 1 and 2, H3, IC6, IC5, IC4 and H4.

1.12 m^2 sr and are clearly those with the highest obtainable charge resolution.

In operation, the requirement for an event was not nearly as restrictive, but instead was generally that the particle trigger at least two of the seven charge measuring detectors and at least two of the four hodoscopes (see sect. 3.4 for variations in this basic trigger requirement). The resulting total geometry factor is 5.9 m^2 sr, made up of the various different classes of events. The different integral and differential geometry factors, expressed as a function of the angle with respect to the instrument axis, are shown in figs. 2a and b, where these factors are calculated from a numerical integration and confirmed with totals calculated from the analytical expressions of Sillivan [7]. Not all of the total geometry factor is useful at all times. For example, 32% of the $H1 \cdot H2 \cdot \overline{H3}$ or $H4 \cdot H3 \cdot \overline{H2}$ particle trajectories miss both Cherenkov radiators. It is possible to assign a charge to such particles only if the geomagnetic cutoff is greater than about 5 GV, which is the case for some 70% of all those observed, and even then only with reduced confidence.

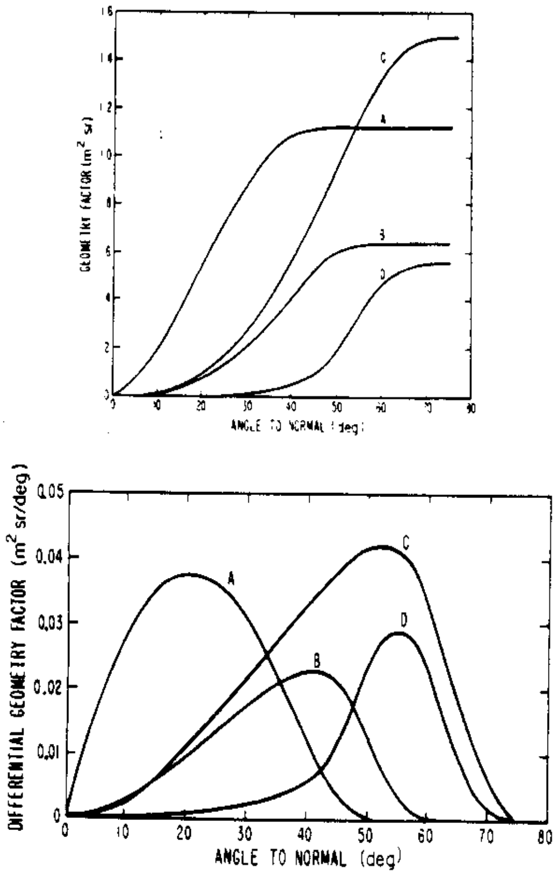

Fig. 2. Geometry factors resulting from four different selection modes. A, H1 : H4 mode; B, H1 : H3 : $\overline{H4}$ and H4 : H2 : $\overline{H1}$; C, H1 : H2 : $\overline{H3}$ and H4 : H3 : $\overline{H2}$; D, $\overline{H1}$: H2 : H3 : $\overline{H4}$. (a) Integral factors in $m^2 \cdot sr$, (b) differential in $m^2 \cdot sr$ for 2° intervals.

2.1. Gas detectors

The two rectangular pressure vessels each contain two hodoscopes and three ionization chambers. Each dual-gap ionization chamber consists of a central anode mounted midway betweeen two cathodes, with anode to cathode spacing of 6.9 cm. These electrodes are aluminum screen-wire stretched in a frame of aluminum channels, and look rather like standard window screens. The electrodes are basically rectangular, 155.6 cm × 125.1 cm. Aluminum frames take the outermost 2.5 cm of this rectangle, and the remainder is unsupported screens woven of 0.025 cm diameter aluminum wires, spaced 6.3 per cm. The mean areal density of each screen is 0.02 g/cm². The screens are attached to the frames under sufficient tension to bow the frames inward about 1 cm at the center of each side, thus ensuring that the screens remain flat. Fourteen insulated stainless steel posts spaced along the perimeter support all the electrodes and maintain their spacing.

Each hodoscope consists of two layers, giving X- and Z-coordinates. Each layer has an anode plane composed of discrete parallel wires (0.025 cm diameter stainless steel) spaced 1 cm apart; the anode plane is midway between two screen-wire cathodes, identical to the ionization chamber electrodes. The anode–cathode spacing in the hodoscope is 1.0 cm. The theory and operation of a similar multiwire ionization hodoscope has been described by Love et al. [8].

Each pressure vessel has top and bottom windows made of aluminum honeycomb 8.9 cm deep, with mean areal density of 1.2 g/cm². The side walls are 0.32 cm thick aluminum with 5.1 cm deep ribs on the outside. Electronic packages are mounted on the sides between the ribs. The cosmic ray nuclei that enter through a side wall (45% of the total 5.9 m² sr geometry) penetrate various amounts of material, typically 2–3 g/cm². While these side-entering events are thus of lower quality than window-entering events, they are essential for maximizing our geometry. Similarly, a rectangular shape for the pressure vessel was chosen to maximize the geometry within the constraints imposed by spacecraft despite the fact that it required thicker windows than would a cylindrical design.

The gas inside the pressure vessels in 90% argon, 10% methane (P-10). A trace (~0.5%) of helium was added to facilitate leak checking; this helium had no significant effect on the ionization characteristics. The gas pressure is slightly greater than one atmosphere absolute (838 Torr at 20°C). These vessels are sealed and have no make-up gas supply in the spacecraft. The resulting requirement that the gas maintain the necessary purity for several years required careful selection of materials and cleaning procedures which are discussed in the next section.

2.2. Gas quality tests

The inherent difficulties of providing an onboard gas supply capable of refilling or flushing the ion chamber/hodoscope detectors in case of gas degradation made it desirable to develop sealed ion chambers that could operate for a long time without showing significant changes in characteristics. For this reason, it was necessary to ensure that thermal or radiation induced outgassing of the materials used in the construction of the ion chambers would not degrade the detector performance over a period at least equal to the maximum expected HEAO-3 lifetime. A small test ion chamber similar to the flight chamber was constructed in order to test the various materials used. This chamber was a dual gap chamber with screen electrodes of the same type and with the same spacing as those in the flight instrument. A ^{252}Cf source was mounted in the chamber to act as a source of constant amplitude signals to monitor the ionization-chamber response to charged particles. Materials used in the flight chamber construction were initially selected on the basis of their low outgassing properties, and those judged likely to outgas any electronegative contaminates were particularly avoided.

Table 1 lists all the materials tested including some materials not used in flight chamber constructions. The chamber was irradiated four different times with various combinations of materials included for each test. Two of these tests used 25 MeV electrons (Washington University Clinac 35 electron accelerator) at a dose of 5×10^4 rad; and two utilized 600 MeV protons (Space Radiation Effects Laboratory proton cyclotron) at a dose of 10^4 rad. The calculated in-flight dose received by materials inside the HNE ion chambers is ~450 rad, primarily due to exposure to protons in the South Atlantic Anomaly (SAA). Since electrons are only about 1% as effective in producing damage in solids as protons (for the above energies), the effective test electron dose is about equal to, and the test proton dose a factor of 20 greater, than that expected in orbit. After each irradiation, the chamber was monitored for a period of a year or longer. The results of these tests were that no significant degradation (>1%) in signal was observed to occur for any of the listed materials (table 1) and they could therefore be used in ion chamber construction. Flight data has confirmed these test results, since the chambers were sealed in February 1978, launched September 30, 1979, and have performed with no observable changes.

2.3. Ionization chamber operation parameters

The ionization chamber operating pressure was chosen so that ionization statistics would be sufficient for the combination of three ionization chamber measurements to give an overall charge resolution of $\sigma = 0.3$ charge units for minimum ionizing iron nuclei.

The operating voltage for the ionization chambers is −1000 V with electrode spacing 6.9 cm. The operating voltage was chosen on the basis of two considerations. The first was that the electron drift velocity be on the drift velocity plateau so that small changes in pressure or voltage would not significantly alter the chamber electron collection characteristics. The broad peak in the drift velocity curve for P-10 gas taken from English and Hanna [9] is at $E/p = 120$ V/(m · kPa) and is plotted as a dashed line in fig. 3. The operating E/p is 128 V/(m · kPa), providing an adequate margin for small pressure or voltage changes.

The second consideration in the choice of operat-

Table 1

A. *Flight instrument materials*
1. Aluminum (various alloys)
2. Stainless steel (various alloys)
3. Vespel polyimide (SP-1)
4. Mylar (type A) polyester
5. PR-1660 polyurethane adhesive
6. Glass
7. Copper
8. Gold
9. Platinum
10. Californium

B. *Other materials tested*
1. Mycalex 410
2. FM 96U adhesive
3. Epon 828-TETA adhesive
4. Epon 828-versamid 125

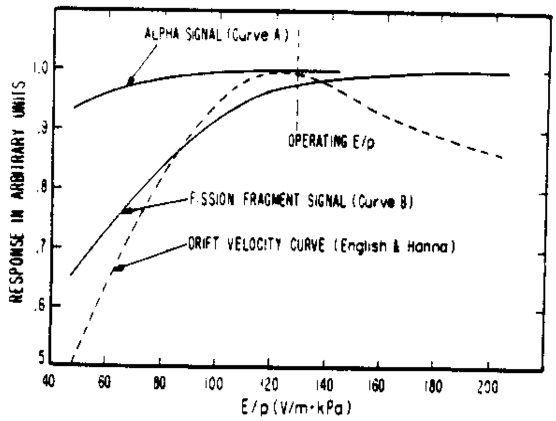

Fig. 3. Voltage and pressure dependence of the ion chamber charge signal for 6.1 MeV alpha particles and ~100 MeV fission fragments from ^{252}Cf. The expected dependence of the electron drift velocity is also shown.

ing voltage was the requirement that electron collection losses must be small for even the most densely ionizing nuclei expected in this experiment. To determine the voltage necessary to satisfy this requirement, a laboratory experiment was performed utilizing a three electrode, gridded (Frisch) ion chamber with fission fragments and alpha particles from a ^{252}Cf radioactive source as the ionization source. Curves A and B in fig. 3 show the peak signals of the alpha distribution (E_α = 6.1 MeV) and the most energetic fission fragment distribution [10] (E_F = 102 MeV) for a P-10 gas pressure of 107 kPa (800 Torr). At the operating E/p, the alpha curve exhibits essentially no electron loss (dE/dx of the alphas is approximately equivalent to a 300 MeV/amu, Z = 17 nucleus) but the fission fragment curve indicates electron losses of ~3%. The fact that electron losses are more severe for large dE/dx indicates that nonlinear effects in dE/dx are operative. A simple model assuming electron-ion recombination (quadratic in dE/dx) as the primary loss mechanism results in qualitative agreement with these experimental results. Actual electron losses for relativistic cosmic rays should be less than 3% however, since the average dE/dx for ^{252}Cf fission fragments is ≈3 times that of a 300 MeV/amu, Z = 100 nucleus. In addition, the fission fragment volumetric ionization density is even greater because the maximum energy it can transfer to a secondary electron is small (≈1 keV) compared to that of a 300 MeV/n nucleus (≈800 keV). A linear scaling of the α and fission fragment results according to dE/dx would indicate ≈1% losses, whereas a quadratic scaling gives ≅0.3%. Thus it is expected that electron collection losses for 300 MeV/amu, Z = 100 nuclei will be ≤1%.

2.4. Cherenkov chamber

The top and bottom of the Cherenkov chamber are formed by the outsides of the adjacent ion chamber pressure vessel covers. The Cherenkov chamber side walls are an extension of one of the pressure vessel covers and mate with a flange on the other pressure vessel to form a light-tight chamber when the two pressure vessels are mounted in the spacecraft. The radiators, one mounted on each of the pressure chambers, are 24.7 cm apart. A photomultiplier assembly (PMA) containing two EMI 9791NA 5″ photomultiplier tubes, high voltage power supplies, preamplifiers and precision pulse generators for calibration, are mounted in each corner. In order to accommodate these PMAs within the envelope of the array without reducing the dimensions of the gas detectors, it was necessary to remove the corners of the Cherenkov radiators, which therefore have a total area that is 11% less than that of the hodoscopes. Each 0.47 cm thick radiator of Pilot 425 was sandblasted in order to improve the uniformity of response, and its back, like the walls of the chamber, painted with Kodak white paint No. 6080 and supported by a 5 mm sheet of Dorvan. The response of this Cherenkov chamber to sea level muons (Z = 1) was measured before flight and was found to correspond to 3–4 photoelectrons. The response of small samples of radiator to iron nuclei accelerated at the Bevalac showed a simple secant θ dependence out to 45° to better than 1% and a typical low level scintillation component. The uniformity of response obtained in flight is discussed in sec. 4.

3. Electronics description

Fig. 4 is a simplified overall block diagram of the electronics. Each of the six ionization chambers and each of the eight photomultipliers has its own signal processing electronics that consists of an amplifier with charge-sensitive input stage, pulse height analyzer (PHA) with pseudo-logarithmic transfer function, and discriminators. Each of the 1120 hodoscope wires is attached to an amplifier and a discriminator; encoding logic records the location of wires with signals above the discriminator level. Outputs of the PHAs and hodoscope encoding logic are stored in a set of output buffers which transfer data to the spacecraft telemetry system in a single pre-determined format. The various discriminator outputs and the status of the data buffers are used by the event control logic (sec. 3.5) to decide when to initiate event analysis.

3.1. Ion chamber electronics

The chambers are operated in orbit with a fixed −1000 V dc on the cathodes. For test purposes on the ground only, the high voltage was externally adjustable to lower values because previous experience had demonstrated that at lower voltages the chamber is more sensitive to trace contaminants in the gas. During ground testing we routinely monitored the chamber response to the internal calibration sources for operating voltages over the range −400 V to −1000 V but saw no degradation from the time the chambers were first sealed through the last prelaunch check.

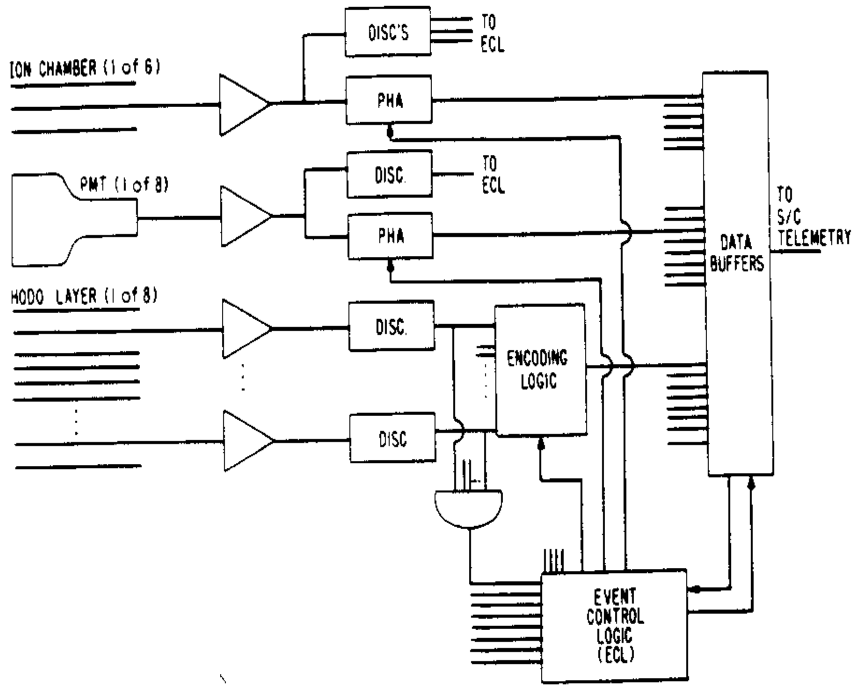

Fig 4. Overall block diagram of the electronics. Each signal is coupled to an amplifier through a charge sensitive preamplifier. Pulse height analyzer (PHA) and discriminators (DISC) provide the digital input to the control logic and data buffers.

The amplifiers shape their input signal with two integrations and two differentiations, all with 2 μs time-constant. This shaping permits effective response to the electron component of the ionization, which is fully collected at the anode in 1.2 μs, but the positive ions, with drift velocity several thousand times slower, make negligible contribution to the analyzed signal. The resulting charge signal on the input of the amplifier is $\frac{1}{2}Ne$ coulombs (C) for collection of N electons, each of charge e, uniformly produced along the path of a cosmic ray nucleus traversing the chamber [6]. The input signal to the preamplifier for a vertically incident iron nucleus ($Z = 26$) of about 2 GeV/amu is 76 fC. Since the energy-loss of such a nucleus in the gas of one chamber is calculated to be 25.2 MeV, this signal implies that the mean energy required to produce each electron is 26.6 eV, consistent with earlier published values [11].

The input of the charge-sensitive preamplifier is a low-noise FET, 2N6453. The root-mean-square (rms) noise referred to input for the full linear system is 0.7 fC, derived from the Gaussian shape of the pulse-height distribution produced by the precision test pulses accumulated in orbit. For a single ionization chamber this noise contributes an rms error of 0.12 charge units to the signal of a minimum ionizing iron nucleus ($Z = 26$) with a trajectory perpendicular to the plates. For the mean of n chambers the rms charge error is reduced by $1/\sqrt{n}$, with n typically 3–6. For other nuclei the rms charge error varies as $1/Z$ and hence is negligible for UH-nuclei.

Each chamber has three discriminators set for signals at the preamplifier input of 29 fC, 125 fC, and 215 fC. The lowest of these three discriminators (designated LLD) is used in the basic event trigger logic. Its threshold is the signal expected of a minimum-ionizing sulfur nucleus ($Z = 16$) penetrating perpendicular to the electrodes. The intermediate and high level discriminators designated ILD and HLD, respectively) have corresponding thresholds at $Z = 33$ and 44, and are used by the event control logic to identify events which are recorded on a priority basis (see sec. 3.4).

The pulse height analyzers (PHA) have a pseudo-logarithmic response, characterized by the function

$$N = A \ln\left(\frac{Q}{B} + 1\right) + C$$

where Q = charge at preamplifier input, N = output channel number (maximum 4095). Typical values of the three parameters are:

$A = 1215$, $B = 230$ fC , $C = 55$.

For small signals ($Q \ll B$) the analyzer response is approximately linear at 0.2 fC/channel, while for large signals ($Q \gg B$) the response is approximately logarithmic at 0.1%/channel. Full scale, approximately 6.2 pC, is approximately the signal expected from a nucleus of charge 126 and energy about 250 MeV/amu penetrating at 60° to the perpendicular. The ability to handle such high signals insures analysis of the highest-charged known elements, as well as any in the theoretically suggested islands of nuclear stability near $Z = 114$ and $Z = 126$. The constants of the pseudo-logarithmic function were selected to give channel widths that were approximately uniform with charge over the full range of interest. The channel width, expressed in terms of the nuclear charge of a minimum-ionizing nucleus penetrating perpendicular to the electrodes, is a minimum of 0.04 charge units for $Z \approx 50$ and rises slowly for lower or higher Z, reaching 0.06 charge units at $Z = 18$ and $Z = 126$. The analyzer response has proven to be very stable, with temperature coefficients less than 0.2 channels/°C, a negligible effect since the temperature variations encountered by the pulse-height analyzers has been only 8°C.

To verify the stability of the linear electronics, a calibration pulser is built into the front end of each preamplifier. Precision pulses with eight different amplitudes are switched in turn onto a precision test input capacitor. This calibration sequence runs at a low rate (0.19/s) continuously pulsing all linear systems throughout the flight. For ground tests, the pulser voltage was externally controlled to permit calibration at many more pulse levels and at higher rates.

3.2. Cherenkov electronics

Each of the eight PMTs has an independent high voltage supply which can be commanded to any one of thirty-one levels between about 1200 V and 1400 V. Each voltage step corresponds to a PMT gain change of approximately 8%. The operating voltages were selected to give nearly equal response from all eight PMTs to cosmic ray nuclei penetrating near the center of the Cherenkov counter, and to give the desired absolute signal on the preamplifier input. Care was taken to verify that the complete system was linear over the entire voltage range, with no measurable saturation effects [12].

The signal at the pulse-height analyzer input for a nucleus of charge 26, $\beta = 1$, perpendicular to the radiators, is 20 pC at the PMT anode. Since such a cosmic ray nucleus causes the generation of approximately 250 photoelectrons from the cathode of each PMT, the PMT gain is approximately 5×10^5.

The Cherenkov signals are shaped in the same manner as the ion chamber signals using time constants of 1.9 μs. While the response time of the Cherenkov counter is very substantially shorter than this value, the slower response of the ionization chambers sets the instrument speed and there is no value to a higher Cherenkov electronics bandwidth, which would have resulted in increased noise. In fact, the Cherenkov electronic noise is negligible, 0.1 pC rms, contributing a rms error of 0.025 charge units at $Z = 26$ ($\beta = 1$, perpendicular) when the mean of eight PMTs is used to determine charge.

The discriminator on each PMT is set at 3.2 pC, approximately 16% of the signal of a perpendicular, $\beta = 1$, $Z = 26$, nucleus (or to the full signal of a corresponding nucleus of $Z \approx 10$). This discriminator is used in conjunction with the ionization chamber LLDs in the event-trigger logic and with the ILDs in determining priority events. This level is high enough to avoid signals from iron nuclei below the Cherenkov threshold which give signals due to scintillation and knock-on electrons at about 6% of the signal corresponding to $\beta = 1$. (The event logic actually uses a signal called C2, which is generated by coincidence of Cherenkov discriminators on two PMTs not in the same corner of the instrument.)

The Cherenkov pulse height analyzers have a pseudo-logarithmic transfer function similar to those of the ionization chambers. Typical values of the constants are $A = 1390$, $B = 61$ pC, and $C = 105$. These values produce a dynamic range and nuclear digitization comparable to those of the ionization chambers with channel widths of 0.034 charge units at $Z \approx 46$, rising to 0.047 charge units at $Z \approx 20$ and 110 and a full scale at 870 pC when $\beta = 1$, $Z = 26$ gives 20 pC. A twelve-level in-flight calibration, carried out in conjunction with the ionization chamber calibration, has demonstrated slow gain drifts, with a typical range of variations of less than 0.3%.

3.3. Hodoscope electronics

The hodoscope cathodes share the −1000 V high-voltage supply of the ionization chambers. With the

0.025 cm anode wire diameter the electric field strength is still low enough that the hodoscope works in the ionization mode, without gas gain.

Each anode wire is connected to the input of a charge-sensitive preamplifier. This preamplifier, a post-amplifier, and a discriminator comprise a hybrid circuit. The discriminator thresholds are set between 2.4 and 3.0 fC (referred to preamplifier input). The 3 fC threshold corresponds to the anode signal for $Z = 16.2$ in 1 cm of hodoscope gas. It should be noted that for the typical trajectory the path contributing to one anode is about 2 cm for which 3 fC corresponds to $Z \simeq 11.5$, but in the worst case, a nearly vertical trajectory midway between two anodes, the path contributing to each signal is indeed only 1 cm. Note also that for the electric field configuration of the hodoscope, the charge collection efficiency is 0.7 rather than the 0.5 value characteristic of plane parallel electrodes [8]. The electronic noise width of the discriminator thresholds is measured to be typically between 0.2 and 0.3 fC rms. This low noise is achieved by using 10 μs shaping time constants.

The locations of hodoscope wires which fired (i.e., gave signals above the discriminator threshold) are encoded in the following manner. There are eight layers of wires; four layers of 156 wires each, giving X-coordinates and four of 124 wires each giving Z-coordinates. A typical cosmic ray nucleus traversing a layer should fire from one to eight adjacent wires, depending upon the angle of the trajectory. For each layer the instrument records the address (1–124 or 1–156) of the first (lowest address) fired wire and a seven-bit "pattern" representing the firing or non-firing of each of the next seven wires. Two such address/pattern combinations are recorded for each layer. For a normal event, only one address/pattern per layer would be required to describe it, but by recording two we ensure not only that a single discriminator malfunctioning in the "on" state does not block the recording of higher number wires, but also that if the effects of δ-rays produced by very high charge nuclei exceed the capacity of one address we still can record the entire pattern. In addition, an overflow for each layer indicates if more wires fired than could be encoded in the two address/patterns.

Test inputs on each hodoscope preamplifier permit in-orbit testing at a single pulse level, as part of the normal electronic calibrate sequence. During ground test these levels were externally adjustable to test the discriminator levels and noise width..

3.4. Event control logic

The event control logic (ECL) utilizes inputs from discriminators on the various detectors to determine when an "event" has occured, i.e., when a cosmic ray nucleus has traversed the detector within its acceptance geometry, and to determine whether an event is to be recorded as "normal" or "priority". If a data buffer (see sec. 3.5) is available for recording this event, then the ECL issues signals to the pulse height analyzers and to the hodoscope encoding logic causing all fourteen PHAs to record pulse heights and all eight hodoscope layers to encode address/patterns. The standard event requirement is discriminator signals from at least two of the seven "charge detectors" and from two of the four hodoscopes. (The seven "charge detector" discriminators are the six ionization chamber LLDs, sec. 3.1, and the Cherenkov C2, sec. 3.2.) A hodoscope discriminator output occurs if at least one wire fires in both the X and Z layers. The standard event requirement means that an event is analyzed whenever there is adequate information to determine a trajectory and to make two estimates of the nuclear charge, independent of whether the assumed cosmic ray nucleus entered the detector through the front or back window or through a side wall.

Several alternatives to the standard event requirements are available by command. In the "source mode" the ECL recognizes either a standard event or an event due to an alpha particle or fission fragment from the internal radioactive calibration sources located in ion chambers 2 and 5. Events due to an internal source are characterized by an LLD from chamber 2 in anticoincidence with the LLD of chambers 1 and 3, or by LLD5 in anti-coincidence with LLD4 and LLD6. The "source mode" was used extensively during ground testing before launch, and in flight this mode is activated by command for about 1 orbit every two weeks. The fission fragments give the only simple test of the stability of the ionization chamber's response to ionization levels well above those produced by cosmic ray iron nuclei. The upper fission peak gives a signal approximately equal to that of a minimum-ionizing cosmic ray nucleus of charge 60 traversing perpendicular to the electrodes.

By command the requirement for two-of-seven "charge detectors" can be changed to one-of-seven. The spacecraft's stored-command processor is used to implement this one-of-seven mode regularly at low event rate parts of the orbit, when the vertical geomagnetic cutoff is above about 12 GV. Since the nuclear charge threshold of the Cherenkov discriminator is significantly below that of the ionization chamber LLD, the effect is to lower the instrument's charge threshold from $Z \simeq 17$ to $Z \simeq 12$ for vertically incident $\beta = 1$ particles.

Several other commands are available, chiefly for the purpose of overriding malfunctioning inputs to the ECL. These permit disabling inputs from any of the charge detectors or enabling inputs from individual X or Z hodoscope layers.

Events, other than those from the fission source, are labeled as "priority" if at least one HLD is triggered, or if at least one ILD and the C2 are triggered. The ILD · C2 insures priority for all events with $Z > 33$ and energy above about 350 MeV/amu, while the HLD insures priority for all events with $Z > 44$ regardless of energy. In fact, most of the priority events are iron ($Z = 26$) or nickel ($Z = 28$) nuclei which triggered an ILD or HDL by virtue of having moderately low energy and/or large angle with respect to the instrument axis. The ILD and HLD threshold were set so that the rate of priority events is low enough to permit telemetry of these events with nearly 100% efficiency throughout the orbit.

The coincidence resolving time of the ECL for normal events is 26 μs, dictated principally by the time constants of the hodoscope amplifier-discriminators. For priority events the hodoscope signals are necessarily far above threshold and the resulting faster trigger permits a shorter resolving time of approximately 10 μs.

3.5. Data readout

For each event 464 bits are recorded in a primary buffer including fourteen 12-bit pulse heights, eight 32-bit hodoscope address/patterns, 27 bits indicating discriminator inputs to the ECL, a priority bit, a parity bit, a bit indicating a pulser-calibration event, 6 bits reserved for a calibration pulse code, two bits indicating one or more repeated transmissions of the same event, and a bit indicating the output buffer. In the absence of priority events, normal events are handled in the following manner. An event is held in the primary buffer until one of two output buffers is available, at which time it is transferred to that output buffer and the primary buffer is reset, thus becoming available to accept another event. The spacecraft reads the output buffers in turn, emptying one output buffer during each spacecraft minor frame, at a rate of one minor frame every 0.32 s. As each event is transferred serially out to the spacecraft, it is fed back into the output buffer. After being read out once, the buffer is "available" to accept a new event, but if no new event appears in the primary buffer before the next spacecraft readout of that output buffer, the same event is re-transmitted.

For priority events the buffer system operates in nearly the same manner as for normal events except that normal events stored in buffers are ignored by priority events. Thus the primary buffer is "available" for accepting a priority event unless it is holding another priority event. An output buffer is "available" for accepting a priority event unless that buffer is in the process of shifting data to the spacecraft or it is holding another priority event that has not been transmitted; a normal event in an output buffer can be written over by a priority event. An output buffer holding a priority event is "available" to a normal event only after the priority event has been transmitted twice. The result of this system is that nearly all priority events are transmitted at least once, and most of them are transmitted at least twice.

The recording efficiencies (or live times) for normal events and for priority events during any time interval are determined by comparing the number of transmitted events of each kind with the total. The total numbers of each type are registered in two rate scalers, one which scales every event that occurs regardless of the state of the data buffers, and another which similarly records every priority event. These rate scalers are read out and reset at a fixed time in each major frame (i.e., every 128 minor frames or 40.96 s).

The event rates and the recording efficiency for normal events vary strongly with location of the spacecraft due to the geomagnetic cutoff, and vary weakly with the orientation of the spacecraft relative to the local zenith. At the highest geomagnetic cutoffs, where the total event rate is typically 1.4/s and the priority rate is 0.15/s, the normal event recording efficiency is typically 91% while the priority events are recorded with essentially 100% efficiency. At the lowest cutoffs, where the total event rate is typically 13/s and the priority event rate is 1.3/s, the normal event efficiency is typically only 10%, while the efficiency for priority events is 97%. In the central part of the South Atlantic Anomaly, where most events are accidental coincidences, the total event rates reach levels as high as 50/s.

3.6. Housekeeping

In addition to the event rates described above, a number of other rates are scaled in each major frame: radioactive source rate in each module (i.e., rate of LLD2 in anti-coincidence with LLD1 and LLD3; the hodoscope discriminator rates in each module; the two LLD rates not in the source-chamber in each module (e.g., LLD1 or LLD3); singles rate in each PMT; the rate of two-fold (C2 signals) and four-fold coincident PMT signals.

Analog housekeeping monitors transmitted in each major frame include temperatures on all sides of the ionization chamber modules, at each PMT, and at key points in the electronics, and temperature differences across the ionization chamber modules. In orbit the typical detector temperatures have ranged between 13° and 21°C. The insulation and thermal mass are such that no variation (<0.2°C) occurs during an orbit. The most rapid changes observed are about 0.6°C/day but typically the changes have been much slower. The temperature variations have been dominated by changes in the proportion of an orbit spent in sunlight (due to variations in the angle between the Earth-Sun line and the plane of the spacecraft's orbit). Variations in the temperature difference between the opposite sides of either ionization chamber module have not exceeded 0.2°C.

Analog monitors of the gas pressure in each ionization chamber module have displayed good correlation with the temperature, indicating no detectable change in the gas density to within 0.2%.

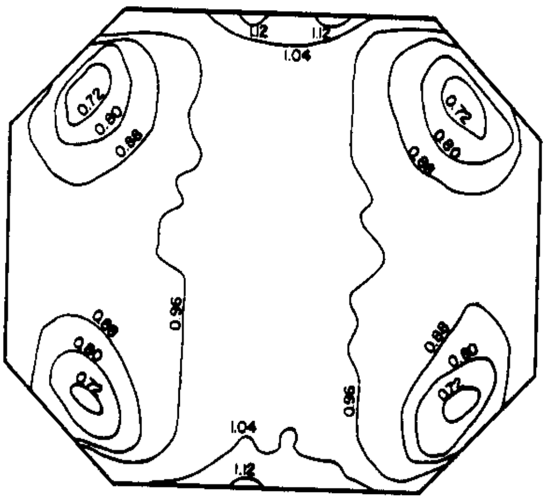

Fig. 5. Map of correction factors for the sum of the responses of the eight Cherenkov photomultiplier tubes, two of which are located in each of the four corners. The map is circumscribed by the outline of the Cherenkov radiator and is normalized to unity at the center.

4. Performance

The typical response in orbit of the ionization chambers to iron nuclei has been essentially constant with time, exhibiting maximum variations of signal amplitude less than 0.2%. The Cherenkov counter response has exhibited measurable temporal variations, with the mean of the eight PMT signals varying over a range of 5% and variations in the gain of the individual PMTs ranging from about 3% to 7%. The variations are well correlated with temperature changes, although showing small hysteresis effects, and can be explained as thermal effects on PMT gains ranging from ≈0.5%/°C to 1%/°C. These gain changes are slow, as are the temperature changes; the fastest observed change on any tube to data has been about 0.5%/day. The response to iron nuclei can be determined to better than 0.15% with data from just one day, so the gain variations can easily be removed in the data analysis.

The areal response of each of the six ionization chambers is quite flat. No non-uniformity (≥0.1%) is detected over a rectangular region 40 cm × 70 cm at the center (i.e., >44 cm from the walls). Outside this region the response falls approximately linearly to 98% of the central response at 8 cm from the walls, with larger variations near the walls.

The areal response of the Cherenkov counter is

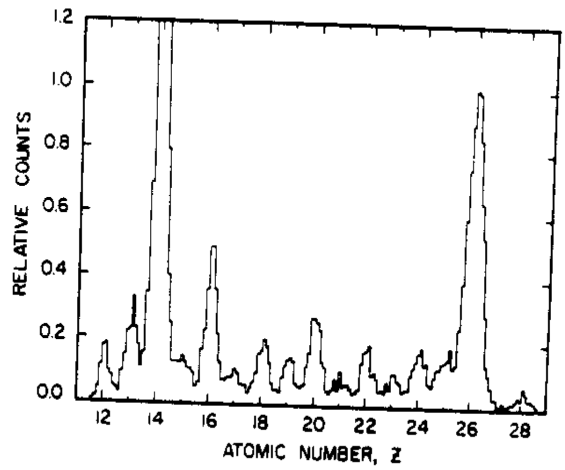

Fig. 6. A charge spectrum for the abundant lower charged nuclei. This spectrum comes from a selected set of data obtained early in the mission and is uncorrected for any systematic biases.

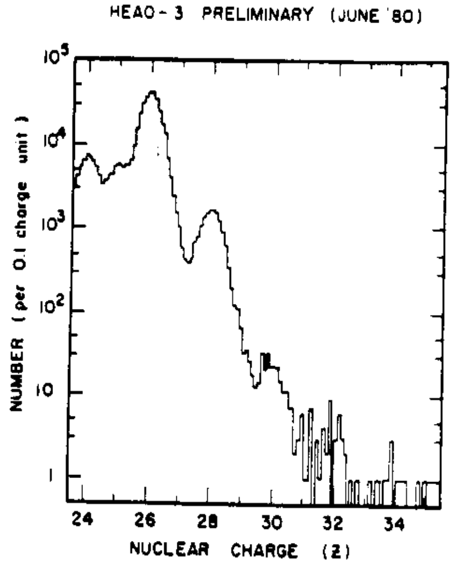

Fig. 7. A charge spectrum of the elements just heavier than iron. Note the logarithmic abundance scale. The same cautions as in fig. 6 are applicable.

much less uniform, exhibiting strong peaks in the light collection efficiency near each PMT (fig. 5). The mean of the eight PMTs is reasonably uniform over the central third of the area; this region, which is more than 25 cm from any PMT, shows variations of about 10% with typical gradients of about 0.2%/cm. The peaks in the response, about 10 cm in front of each pair of PMT, are a factor of about 1.4 above the central region, and near these peaks the gradient reaches about 1.5%/cm; however, by appropriate weighting of the responses of the individual PMTs these gradients can be reduced by a factor of at least three. By accumulating data over three to four month periods so as to get adequate statistics in small areas, we can determine areal response corrections good to 0.5%.

That the telescope can resolve individual charges during flight is illustrated in figs. 6 and 7 which show charge spectra obtained for nuclei in the $_{14}Si-_{28}Ni$ range and for the $_{26}Fe-_{30}Zn$ range from data that has not been fully corrected. Clearly individual elements can be resolved even in this case except when there is an extreme disparity between neighboring abundances. In each figure, the iron peak is characterized by a standard deviation of about 0.34 charge units, a figure of merit that should improve as further corrections are applied.

The design, fabrication and testing of an instrument such as this is the product of the dedicated efforts of a large number of people, only some of whom can be recognized by name. However, we must thank for engineering assistance, V.M. Noble, W.A. Gneiser, H.A. Chameroy and C. Springer of BASD, J.W. Epstein of WU, W.G. Blodgett of CIT and W. Erickson, G. Peterson and R. Howard of UM. Management of this program was under NASA Marshall Space Flight Center and we acknowledge with thanks the continued assistance of personnel at that Center. The excellent performance of the HEAO spacecraft owes much to the personnel of TRW to whom we are deeply indebted. Funding for this instrument was supported in part by NASA under Contracts NAS8-27976, 7, 8 and grants NGR 05-002-160, 24-005-050 and 26-008-001.

References

[1] E.K. Shirk and P.B. Price, Astrophys. J. 220 (1978) 719.
[2] P.H. Fowler, C. Alexander, W.M. Clapham, D.L. Henshaw, D. O'Sullivan and A. Thompson, 15th Int. Cosmic ray Conf. Plovdiv (1977) vol. 11, p. 165.
[3] M.H. Israel, P.B. Price and C.J. Waddington, Phys. Today 28 (1975) 23.
[4] P.H. Fowler, W.M. Clapham, D.L. Henshaw, A. Thompson and D. O'Sullivan, 16th Int. Cosmic ray Conf. Kyoto (1979) vol. 1, p. 370.
[5] J.P. Meyer, ibid., p. 374.
[6] J.W. Epstein, J.I. Fernandez, M.H. Israel, J. Klarmann, R.A. Mewaldt and W.R. Binns, Nucl. Instr. and Meth. 95 (1971) 77.
[7] J.D. Sullivan, Nucl. Instr. and Meth. 95 (1971) 5; ibid. 98 (1972) 187.
[8] P.L. Love, J. Tueller, J.W. Epstein, M.H. Israel and J. Klarmann, Nucl. Instr. and Meth. 140 (1977) 569.
[9] W.N. English and G.C. Hanna, Can. J. Phys. 31 (1953) 768.
[10] E.K. Hyde, The nuclear properties of the heavy elements, vol. 3 (Prentice-Hall, New Jersey, 1964).
[11] R. Brandt, S.G. Thompson, R.C. Gotti and L. Phillips, Phys. Rev. 131 (1963) 2617.
[12] W.R. Scarlett, Ph.D. Thesis (University of Minnesota, 1977).

HEAO C-3 Production Tape Format

SRL Technical Report

79-3

Tom Garrard

California Institute of Technology
Pasadena, CA 91125

5/6/79

Revised: 7/4/79

The C-3 tapes will contain experiment data, ephemeris (orbit) data, and attitude data in a format similar to HEAO A. In general these tapes:

- will normally contain only playback data.
- will contain spacecraft data as required.
- will contain one file per dump of the spacecraft tape recorder.
- will contain roughly one day's data, beginning and ending near midnight.
- will be 9-track, 1600 b.p.i.
- will be numbered by year and day number.
- will be terminated by a double end-of-file.

Each file will contain, in order:

- a label record (data type 1).
- an orbit record (data type 2).
- major frame data blocks (data types 3 & 4).
- an end-of-file.

Tape files will be time ordered with no duplication of data. Major frames will not be split between different files.

Each major frame data block will contain two records. Record 1 will contain header and attitude data (see Table I) and record 2 will contain experiment data (see Table II). Much of the major frame data is made up of repeated minor frame data; this is documented in Tables III to V.

Floating point data will be in IBM-360 format.

All orbit data in GEI coordinates except specific geodetic items (as on HEAO-A).

Record lengths are multiples of 9 bytes due to IPD computer word structure. Note that all table indices start at 0 in this document.

TABLE I

Major Frame Record 1

Index (byte)	Length (byte)	Type	Name	Description
0	1	I	XNM	Experiment number (3)
1	1	I	DTYP	Data Type indicator (3)
2	2	I	RECNM	Record number in file
4	2	I	YEAR	Calender year - 1900 (79,80,...)
6	2	I	DOY	Day count of year (1-366)
8	4	I	MOD	Millisecond of day (precision time from major frame header).
12	4	I	SCCK	Spacecraft clock
16	1	I	NFF	Number of fill frames
17	1	I	NSNE	Number of frames with sync error
18	14	-	-	Spare
32	32	mixed	MJAT	Major frame attitude data (IVa).
64	32	I	AFF	Attitude flag field for 8 minor frames 0,16,32,...,112
96	8	I	SB120	Data from subcom word 120. (IIIb).
104	24	I	SCSB	Spacecraft subcom data. (IIIc).
128	128	I	SB119	Data from subcom word 119. (IIIa).
256	128	I	DFF	Data flag field for all 128 minor frames.
384	512	F	MNAT	Minor frame attitude data (see IVb.) for 8 minor frames 0,16,...,112.
896	128	I	C1RT	C1 rate data. (See Table IVc.)
1024	384	I	FAILMD	MF(109,j), MF(110,j), MF(111,j), where 0<=j<=127 is the minor frame number.
1408	5	-		spare
1413				

TABLE II

Major Frame Record 2

Index	Length	Type	Name	Description
0	1	I	XNM	Experiment number (3)
1	1	I	DTYP	Data type indicator (4)
2	2	I	RECNM	Record number in file.
4	60	I		Data from minor frame 0. (V).
64	60	I		Data from minor frame 1. (V).
.	.	.		.
.	.	.		.
7624	60	I		Data from minor frame 127. (V).
7684	2	-		spare
7686				

TABLE IIIa

Minor frame word 119 should be supplied for minor frames 0 through 127.

TABLE IIIb

Minor frame word 120 should be supplied for minor frames 112 through 119. (Numbers run from 0 to 127).

TABLE IIIc

Index	Minor frame word	Minor frame #
0	220	0
1	252	0
2	81	19
3	81	20
4	17	22
5	81	22
6	81	23
7	17	25
8	17	27
9	81	27
10	81	28
11	81	29
12	17	30
13	81	30
14	17	32
15	17	36
16	17	48
17	17	113
18	17	117
19	81	120
20	81	125
21	spare	
22	spare	
23	spare	

TABLE IVa

Attitude Major-frame Format

Index (byte)	Length (byte)	Type	Description	
0	4	-	Spare	
4	4	-	Spare	
8	4	F	Angle theta	Center of earth in
12	4	F	Angle phi	spacecraft coordinates.
16	16	-	Spare	
32				

TABLE IVb

Attitude Minor-frame Format

Index (byte)	Length (byte)	Type	Description
0	4	F	Zenith angle of spin (Z) axis.
4	4	F	Azimuth angle of spin (Z) axis.
8	4	F	Zenith angle of Y axis.
12	4	F	Azimuth angle of Y axis.
16	4	F	Magnetic-field vector S/C coordinate, Xb
20	4	F	Magnetic-field vector S/C coordinate, Yb
24	4	F	Magnetic-field vector S/C coordinate, Zb
28	4	F	Geocentric longitude
32	4	F	Geocentric latitude
36	4	F	Geocentric radial distance
40	24	-	Spare
64			

All angles should be in radians.
Reference direction for zenith is radial outward
from center of earth (geocentric radial).
Reference direction for azimuth is east (negotiable).

179-3 p.6

TABLE IVc

C1 Rate Data

Index	Minor frame word	Minor frame #	Name	Timebase, T (sec)
0	238	25	PLLD	10.24
1	239	25		
2	238	26	XULD	10.24
3	239	26		
4	238	27	PULD	10.24
5	239	27		
6	238	57	PLLD	10.24
7	239	57		
8	238	58	XULD	10.24
9	239	58		
10	238	59	PULD	10.24
11	239	59		
12	238	89	PLLD	10.24
13	239	89		
14	238	90	XULD	10.24
15	239	90		
16	238	91	PULD	10.24
17	239	91		
18	238	121	PLLD	10.24
19	239	121		
20	238	122	XULD	10.24
21	239	122		
22	238	123	PULD	10.24
23	239	123		
24	254	2	XLLD	1.28
25	222	3		
26	254	6	XLLD	1.28
27	222	7		
28	254	10	XLLD	1.28
29	222	11		
.	.	.		
2n+24	254	4n+2	XLLD	1.28
2n+25	222	4n+3		
.	.	.		
84	254	122	XLLD	1.28
85	222	123		
86	254	126	XLLD	1.28
87	222	127		
88-127	spare			

0<=n<=31
Rate (cps), R, is given by:

```
IF (N<32768)
        R = N/T
ELSE
        R = (1073741824)/(T(65536-N))
```

79-3 p.7

TABLE V

The 60-byte minor frame data blocks referenced in Table II consist of the 58 minor frame words allocated to C3, one spacecraft word, and one spare as listed below.

7	12	13	15
16	18	19	20
21	22	23	24
25	26	27	28
29	31	39	44
45	47	48	49
50	51	52	53
54	55	56	57
58	59	60	61
63	71	76	77
78	79	80	82
83	84	85	86
87	88	89	90
91	93	94	95
103	108	156	spare

79-3 p 8

Decom Label Record Description

Index (byte)	Length	Type	Contents	
0	1	I	Experiment number	
1	1	I	Data type indicator, 1=label	
2	2	I	Record number in file	
4	4	I	Year of data	
8	4	I	Start day count of data (I-366)	
12	4	I	Start time of data (milliseconds of day)	
16	4	I	Stop day count of data (I-366)	
20	4	I	Stop time of data (milliseconds of day)	
24	4	I	STDN station number	
28	4	A2	Satellite ID, fieldata, right justified, zero fill	
32	4	A1	PDF, fieldata, right justified, zero fill	
36	12	A16	Pre-edit file name - fieldata, left justified	
48	8	I	Spare	
56	4	I	Decom number	
60	4	I	Decom reel number	
64	4	I	Number of major frames in file	
68	4	I	Number of minor frames with bit errors in frame synch word	
72	4	I	Number of minor frames with fill data	
76	4	I	Spare	
80	4	F	Year, month, day	Epoch of elements
84	4	F	Day count of year	
88	4	F	Seconds of day	
92	4	F	Semi-major axis, a, (km)	
96	4	F	Eccentricity, e	
100	4	F	Inclination, I (deg)	
104	4	F	Mean anomaly, M (deg)	
108	4	F	Mean motion eta (deg)	
112	4	F	Right ascension of ascending node, omega (deg)	
116	4	F	Rate of change of right ascension of ascending node, omega (deg/day)	
120	4	F	Argument of perigee, (deg)	
124	4	F	Rate of change of perigee (deg/day)	
128	4	F	Period, P (min)	
132	4	F	Rate of change of period, P (min/day)	
136	4	F	True anomaly, gamma (deg)	
140	4	F	Eccentric anomaly, E (deg)	
144	4	F	Year, month, day	Time reference for pos. coordinate system
148	4	F	Day count of year	
152	4	F	Apparent sideral time (rad)	
	156		Length of this description	

Total length of the record is 1413 bytes.

79-3 p.9

Orbit Data Block Description

Index (byte)	Length	Description	
0	1	Experiment number	
1	1	Orbit record	
2	2	Record number in file	
4	4	Type of data	
		1 = Regular spacecraft data item	
		2 = Ascending node crossing	
		3 = North point data item	
		4 = Descending node crossing	
		5 = South point data item	
		6 = Sunlight entrance	
		7 = Sunlight exit	
		10 = SAA entrance Area A	
		11 = SAA exit Area A	
		12 = SAA entrance Area B	
		13 = SAA exit Area B	
8	4	Day count of year, time of data	
12	4	Seconds of day, time of data	
16	4	Orbit number	
20	4	Spacecraft position vector X (km)	
24	4	Spacecraft position vector Y (km)	Geocentric
28	4	Spacecraft position vector Z (km)	
32	4	Spacecraft velocity vector X (km/s)	
36	4	Spacecraft velocity vector Y (km/s)	
40	4	Spacecraft velocity vector Z (km/s)	
44	4	Longitude (deg)	
48	4	Latitude (deg)	
52	4	Height above spheroid (km)	
56	4	Inertial unit Sun vector S(x)	
60	4	Inertial unit Sun vector S(y)	
64	4	Inertial unit Sun vector S(z)	
68	4	Inertial lunar position vector X (km)	
72	4	Inertial lunar position vector Y (km)	
76	4	Inertial lunar position vector Z (km)	
80	4	McIllwain L. parameter L (Earth radii)	
84	4	Magnetic field strength B (gauss)	
88	4	B (r)	Geocentric spherical
92	4	B (theta)	components, unit
96	4	B (phi)	vectors
100	4	Magnetic field right ascension (rad)	
104	4	Magnetic field declination (rad)	
108	4	Solar time (Sun, Earth, satellite angle, deg)	
112	4	Flag for shadow condition	
		0 = Satellite in shadow	
		1 = Satellite in Sun	
116	4	Angle between subsatellite point and Earth horizon	
120	4	Spare	
	124	Length of this data block	

1) Repeat bytes 4-123 until record is full. Fill with 8888888 after last orbit item to end of record.
2) Total length of record is 7686 bytes. Up to 4 records per acquisition will be needed.
3) Note that all of bytes 4-123 are floating point words, even type and flag.

SRL TECHNICAL REPORT 78-1
HNE DATA PROCESSING PLAN

Tom Garrard

September 1, 1978

Revised 1/10/79

TABLE OF CONTENTS

1. INTRODUCTION

This plan describes a means of processing HEAD HNE data on the Caltech SRL time-sharing system. Major data products are SL (science library) tapes intended to be used primarily at Caltech and CR (crushed) tapes intended for use by individual members of the team at any location, including Caltech. The programs described here supply the means of doing science, but contain essentially no science as such. It is up to the HNE team to provide this science input, as soon as possible.

2. CIT SRL DATA SYSTEM

A. Introduction

The SRL data system is a time-sharing system intended to support three major tasks; tape crunching, graphics, and program development. Tape crunching is, of course, typically i-o bound. The HNE library generator (LIBGEN) will use significant CPU time as well. The graphics and program development are normally done in an interactive fashion and require very little CPU time per clock hour. It is therefore cost effective to time-share the CPU.

B. Hardware

The SRL data system is composed of the hardware listed in Table 2B-1 and illustrated in Figure 2B-1. It is a time-sharing system intended for tape crunching, graphics, and program development. A typical job mix might be LIBGEN (2 tape drives, LA 36, ≥ 32K core), 2 graphics users (HP2648A's, 1 drive, ≥ 20K each), and one programmer (VT52, no tape, 32K).

Graphic displays are normally generated on the CRT screen and then copied onto the printer-plotter via the 210-8 hardware. Graphics can be generated directly from the CPU via the 121 interface, but at a considerable cost in CPU time.

Each of the double-density disk drivers looks like 2 RK05's to the software. They are not media compatible with DEC. The RX02 floppies will be used for individual program storage and as a back-up to the RK disks.

Table 2B-1

Manufacturer	Model Number	DEC Equivalent	Quantity	Description
DEC	11/34A			CPU
DEC	FP11A			Floating-point arithmetic hardware
DEC	MS11JP		128K	Memory (64K in hand)
DEC	KW11L			Generates 60-Hertz interrupts
Digital Pathways	TCU100	None		Calendar and time-of-day clock, 2048-Hertz timer
DEC	DL11W			Serial interface for LA3
ACT	Quad/B	4DL11's		Serial interface for CRT
DEC	LA36			DEC writer terminal
DEC	VT52			DEC scope CRT terminal
HP	2648A	None	2	Graphics CRT terminal (1 in hand)
Versatec	210-8	None		CRT hard copy interface (210 in hand)
Versatec	121	~LPi/f		Printer-plotter interface
Versatec	1200A	~LP		Printer-plotter, 11" wide 200 dots/inch
Datum	5191	TM11	2	Mag tape interface (1 in hand)
Kennedy	9100	~ TU10	5	9-track, 800/1600 bpi, 75 ips drives (3 in hand
Datum	4091	RK11		Disk interface
Pertec	10MB	~ RK05	2	Double density disk drive one fixed, one cartridge
AED	2500	None		Floppy system (borrowed)
DEC	RX02		2-drive	Floppy system (0 in hand)

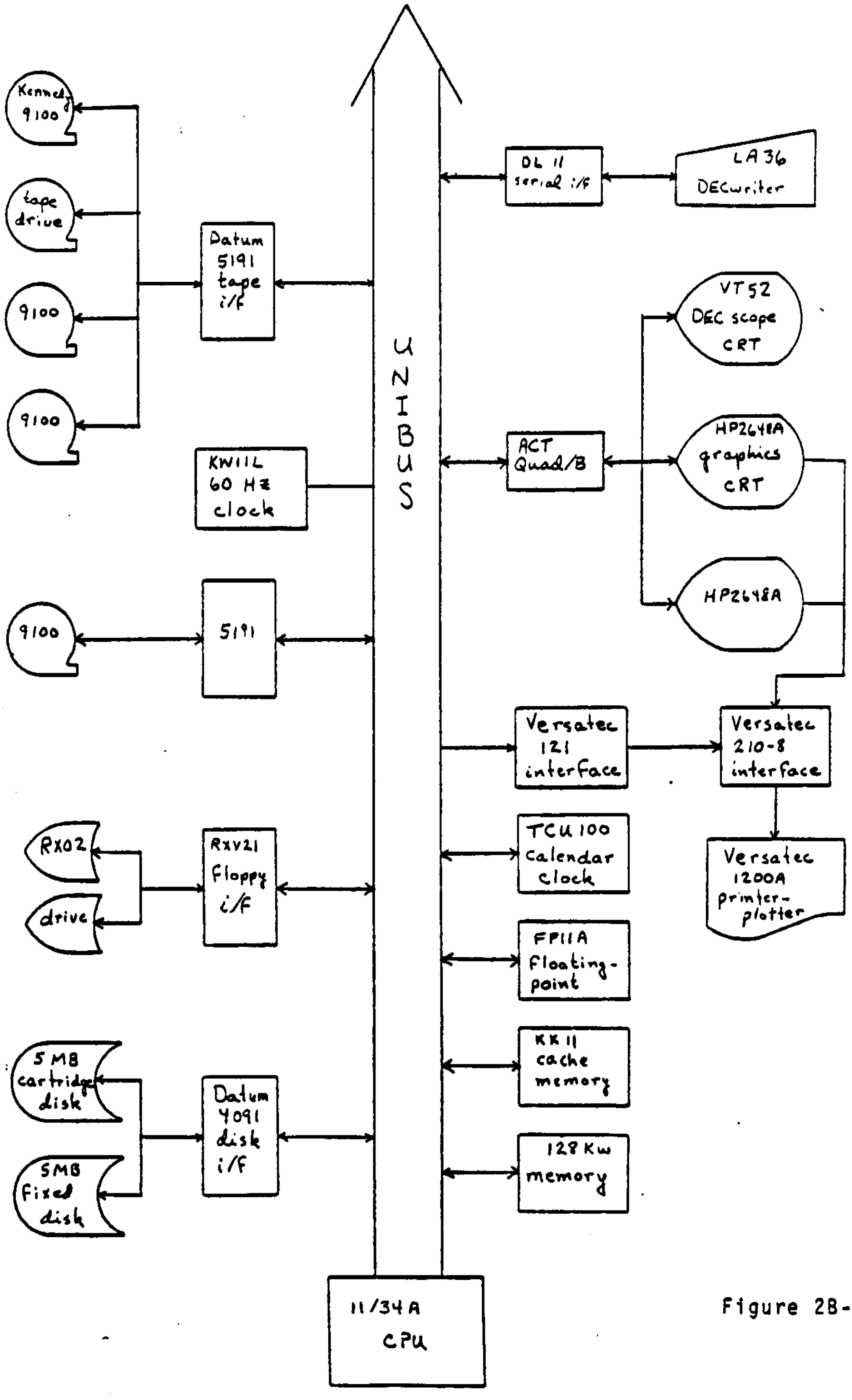
Kennedy 9100
tape drive
9100
9100
Datum 5191 tape i/f
KW11L 60 Hz clock
9100
5191
RX02
drive
RXV21 floppy i/f
5MB cartridge disk
5MB fixed disk
Datum 4091 disk i/f
UNIBUS
11/34A CPU
DL 11 serial i/f
LA36 DECwriter
VT52 DEC scope CRT
ACT Quad/B
HP2648A graphics CRT
HP2648A
Versatec 121 interface
Versatec 210-8 interface
Versatec 1200A printer-plotter
TCU100 calendar clock
FP11A floating-point
KK11 cache memory
128 Kw memory

Figure 2B-1

C. Software

The data system will use the Unix operating system available from Bell Labs for large PDP-11's. Unix is a time-sharing system with a host of features for program development. It is not intended for real-time instrument control applications. It includes and is written in a very high-level language called C. The SRL system will also include FORTRAN, MORTRAN, and FORTH.

MORTRAN is a structured version of FORTRAN available on any computer which runs FORTRAN. FORTH is a language well suited to interactive applications and will be used for graphics programs. Most programming will be done in C, which looks similar to MORTRAN to the programmer but executes much faster than FORTRAN.

The complete system should include the features in Table 2C-1.

Table 2C-1

	Component	Comments
Standard System	Op Sys	Written in C, hence modifiable
	C	looks like MORTRAN
	FORTRAN IV	Relatively slow
	ed	Text editor, better than TECO
	roff, nroff	Formatters
	MACRO-11	Assembler
	-	Desk Calculator
Optional	FORTRAN IV +	$3300, not worth it
Added by SRL	FORTH	Interactive, convenient
	MORTRAN	Translates to FORTRAN, looks like C
	BASIC	Slow but familiar
	PASCAL	Another "new" language
	VERSAPLOT	Graphics package

3. A. Introduction

HNE data processing will be done as indicated on Figure 3A-1. Four processes are indicated:

QLP - the quick look processor
LIBGEN - the library tape generator
CRSH - the data crusher (s)
DSPLY - the display program

The QLP will be used to check quick look data for instrument health and to check parameters (gain, etc.) used by LIBGEN. The LIBGEN formats the telemetry data, decodes pulse heights, unfolds hodoscope address, integrates orbit and attitude data, etc. The CRSH selects and compresses data from SL (library) tapes to create a CR (crushed) tape appropriate to a particular physics problem. The DSPLY program is a general purpose program for printing and plotting the data on CR (or SL) tapes.

These processors and the data tapes used are described in the following sections.

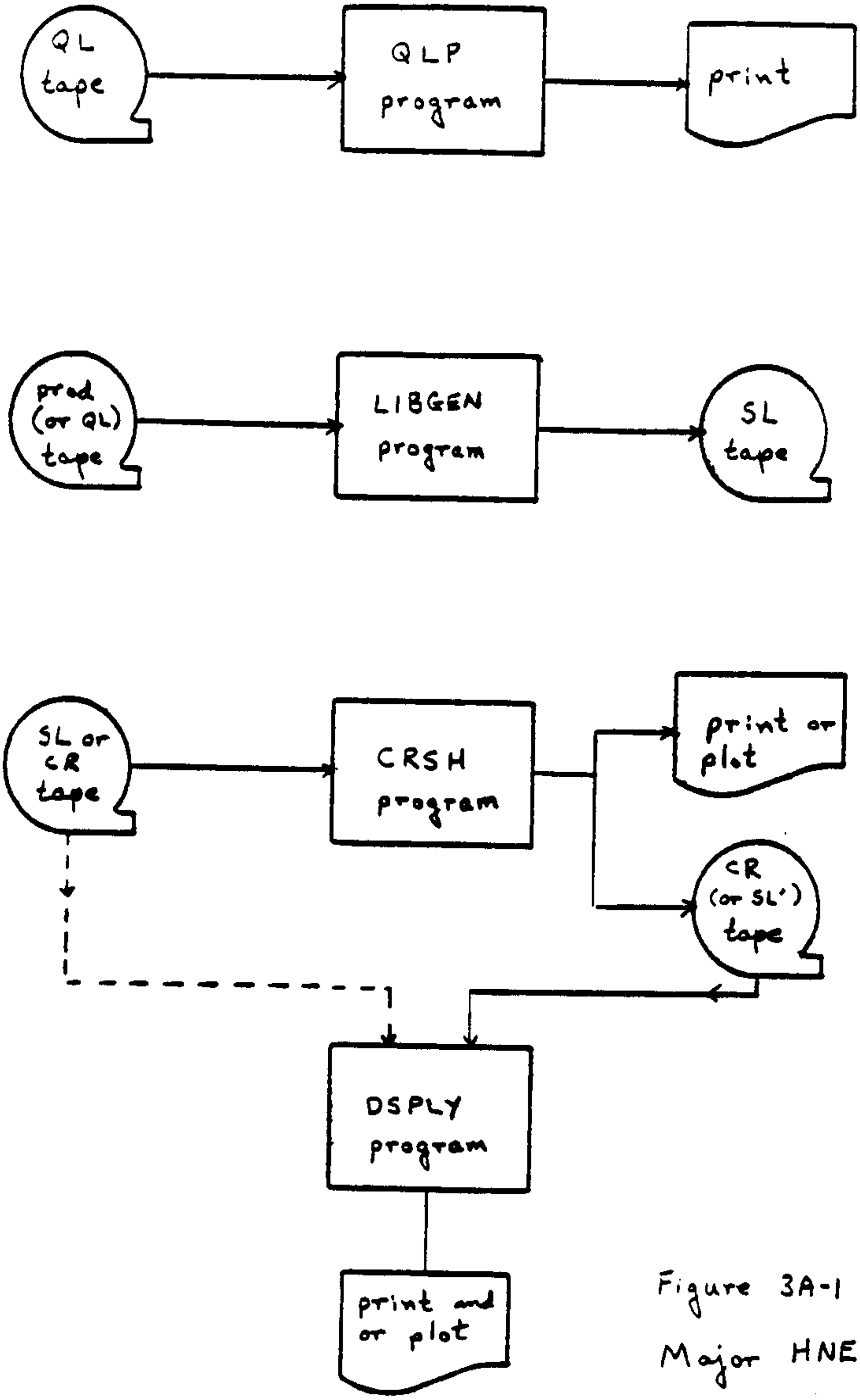

Figure 3A-1

Major HNE programs

B. Production Tapes

These tapes are produced at GSFC and shipped to CIT. They contain all science, attitude, and orbit data available. One tape per day is generated.

The format of these tapes is controlled by DRF #H-C4017. This format is also described in SRL Technical Report #78-2.The tapes have orbit data at the beginning of the tape. For each major frame one record with attitude and subcom data and one record with event data are generated.

C. Quick Look Tapes

These tapes may come from either of two sources - shipped to CIT by GSFC or transmitted to JPL by GSFC via NASCOM. Tapes coming directly from GSFC will have the production tape format. Transmission via NASCOM and regeneration at JPL will probably result in a changed format.

We expect to have 4 orbits (6 hours) per day of QL data during early mission, 1 orbit/day thereafter.

D. EBTE Tapes

These tapes contain event data, some subcom data, and comments generated during testing at BASD and TRW. The format is documented in Ball Document "Instrument Test Program Operators Guide (Program IDP1)", revision 1, 25 July 1978, by Steve Gill.

E. QLP

The quick look processor will read quick look tapes and perform the following tasks:

<u>Status Check</u> - Verification and display of analog and digital status data including event logic, rates, command status, temperatures, etc.

<u>Calibration Check</u> - Verify that the internal calibrator signal analysis has not changed.

<u>Discriminator Histograms</u> - Pulse height distributions for each of the 18 ion chamber discriminators.

<u>Hodoscope Histograms</u> - Distribution of event addresses for each of the 8 hodoscope planes for all events.

<u>I and C Histograms</u> - Distributions of raw pulse heights for each of the 14 analyzers and for various radiator areas for the 8 Cerenkov analyzers.

The following tasks are optionally performed by QLP:

<u>Alpha Histogram</u> - Pulse height histograms for ionization chambers 2 and 5 for alpha events. Done only when source made command is sent.

<u>Event Dump</u> - A formatted dump of raw event data.

The QLP programs will have the capability of reading either production tapes, quick-look tapes in the production format, or quick-look tapes in a TBD format used for NASCOM transmission.

See the QLP write-up SRL Technical Report #78-2, for more details.

F. LIBGEN

The library generator reads production tapes and generates SL tapes. All data is maintained on the SL tapes, but in a format which is much more useful than the production format. The library data are formatted into chapters, which are logical units of data. Examples of a chapter are normal events, $Z \geq 31$ events, time of major frame, etc.

Depending on record size selected, an SL tape should hold $\geq$ 30 hours data at 1600 bpi and $\geq$ 20 hours at 800 bpi. Normal procedure will be to put 24 hours data per SL tape at 1600 bps.

G. CRSH

This program will test chapters and output data for successful tests. The output data will be grouped by chapters in a fashion very similar to the SL data. Thus any program which reads SL tapes can be easily modified to read CR tapes (including CRSH itself). The output format can, if desired, be essentially identical to the SL format so that CRSH can be used to correct or map SL tapes into new SL tapes.

The intent is to produce a data set of manageable size which contains all the data relevant to a particular problem. Test and output subroutines are user supplied. One obvious example would be a CRSH which tests for cutoff rigidity above 8 GV/nuc and estimated charge between 24 and 28. One might output all Cerenkov and hodoscope data for such events.

H. DSPLY

DSPLY reads the relatively small data sets produced by CRSH and plots one function of the data for one event versus another function of the data for that event. "Event" here is a generalized word which includes any organized data set (chapter or tape record). One use of such a program is C versus I plots. Another might be rate versus time. See the attached example, Figure 3H-1. DSPLY will also have the capability of reading SL tapes but runs too slowly to process any large portion of the data.

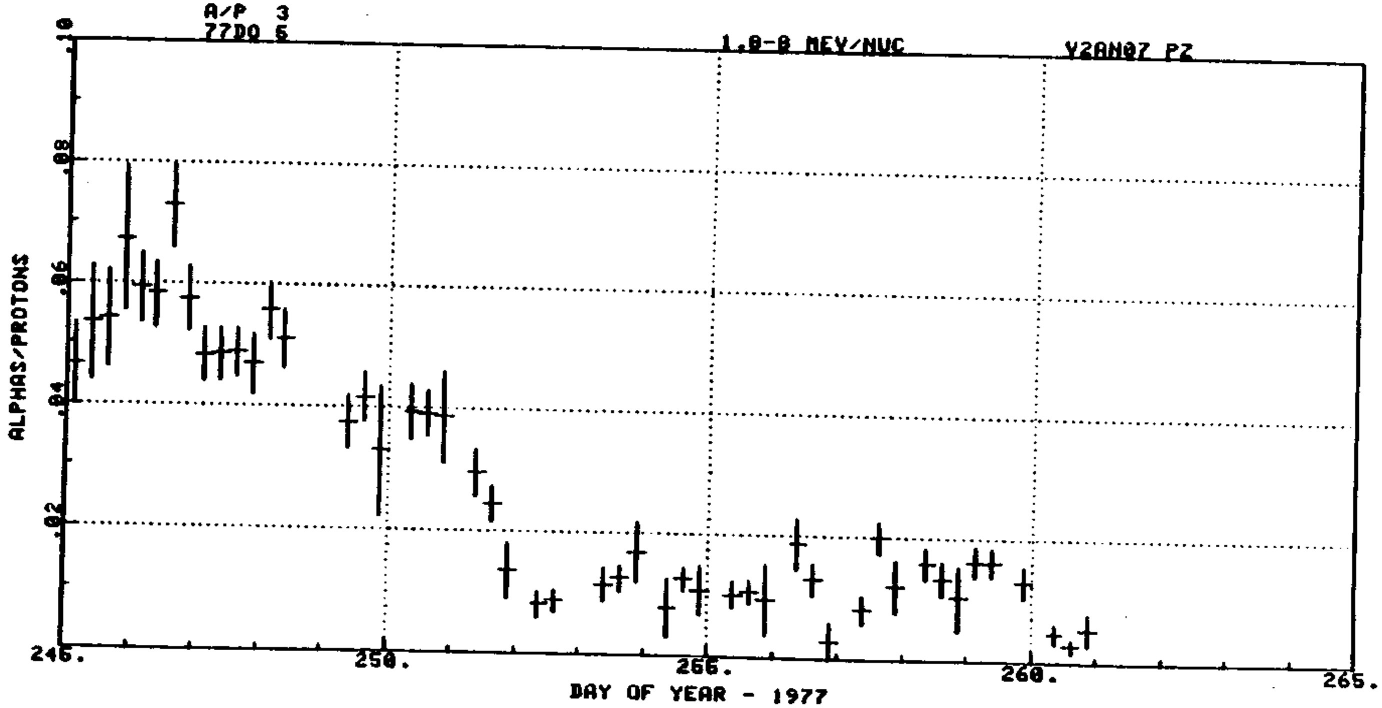

VOYAGER DSPLY PLOT

Figure 3H-1

INTERNAL REPORT #86

SRL Chapter/Verse Format

by

T. L. Garrard

N. S. Collins

Space Radiation Laboratory

California Institute of Technology

Pasadena, California

9/21/81
(revised 10/8/81)

SRL Chapter/Verse Format

1. Description

In order to maximize flexibility and minimize tape length, tapes should be formatted with lots of small logical blocks squeezed together into long physical records. The blocking technique described below was worked out for the HEAO C-3 data analysis but is clearly adaptable to other projects. It should be treated as a SRL standard and utilized whenever possible. A substantial library of programs exists already for handling data in this format and more are being written.

The blocking technique is reminiscent of IBM System 370 VB or VBS blocking, but is much more visible to the user, much less demanding on the system, and much less prone to catastrophic data loss to tape errors. Data is organized into logical blocks called chapters. Chapters are placed in a buffer as they are generated, and when chapter input threatens to overflow the buffer, the buffer is flushed to tape. This process is handled by a library routine called putchap. Normally only the data is written, not the trailing, empty portion of the buffer. Thus records are of variable length, but always contain an integral number of chapters. Each chapter begins with a 2-byte "key" integer which specifies the type of chapter. All chapters of this type have identical lengths. When reading tape, chapters are retrieved from the input buffer by a library routine called getchap. Getchap finds chapters using a table of chapter lengths which is indexed by the chapter key. This table is written on each tape in the first record on the tape, in a special chapter with key = 0. Chapter 0 has fixed a format, known to getchap.

An embellishment of the scheme allows chapters to be broken down into verses. Offsets of the verses within a chapter are also specified in Chapter 0.

The decision of what constitutes a "logical block", i.e., a chapter or verse is up to the user but some guidelines are clear. Since the key imposes a 2-byte overhead on each chapter, very short chapters are inefficient in their tape usage. Since a physical record length of ~4K to 8K bytes is appropriate to PDP-11 applications with 1600 bpi tapes, very long chapters do not fit into the output buffer efficiently. Thus chapters should be between ~20 bytes and ~400 bytes long. Any point in a logical format which seems a likely candidate for insertion of additional items at some future time, is a good point for a chapter or verse break. Example:

current format

variable	verse	word
r	1	0
theta	1	1
X	2	0
Y	2	1
Z	2	2

new format

variable	verse	word
r	1	0
theta	1	1
phi	1	2
X	2	0
Y	2	1
Z	2	2

Note that since X (& Y & Z) is in a separate verse it is still addressed as word 0 of verse 2 in either format. Thus no program changes are required in programs which read this data when the new format is introduced.

A list of chapters is maintained by Tom Garrard, and selection of chapter numbers should be done in consultation with him. Documentation for existing chapters is on /usr/tlg/dpgeneral/chap.dc. Note that some special chapters should be used by all users for consistency:

Chapter 0	specifies format
Chapter 101	specifies end-of-record
Chapter 102	specifies end-of-interval
Chapter 103	specifies end-of-tape
Chapter 105	specifies end-of-single-file
Chapter 206	specifies end-of-plot

In addition, a number of existing chapters can be used by other users. Chapter 1 specifies time for both HEAO C-3 and Voyager. Chapters 202-204 are Voyager display points, and can quite likely be used as they are by other projects.

2. Programming

Although the previous section applies only to tapes, the following routines work on both disk and tape for compatibility. Disk records must always be the same length (currently 2K bytes) so for disk applications, very large chapters will waste disk space.

To make a tape in chapter/verse format, this is the general idea:

1) Get a unique set of chapter numbers from Tom G.
2) Include (with a *#include* statement) <chap.h> in your program.
3) For each different chapter format, define a global array of 14 integers. i.e:

   int chpA[14] = { length, v1, v2, v3, ... , v12, numverses };

   where length is the total number of bytes in the chapter (including the 2-byte key), v1, etc. is the (byte) offset from the start of the chapter to the beginning of the verse. The first data byte in a chapter has an offset of 2. The last entry is the number of verses actually used. Unused verses still need to be given an offset (usually 0).

4) Inside the program, before *putchp()* is called the first time, for each chapter used, the internal chapter array needs to be initialized:

    chapter[*key*] = chpA;

   where chpA is the name of the corresponding array for chapter *key*. (The chapter array is declared in <chap.h>, and is otherwise unused in the user program).

5) Call *putchp(key)*. It returns a pointer to a space large enough to hold data for a chapter of type *key*.

6) Fill the buffer space by assigning and incrementing the pointer. See the C manual for the "++" operator and pointer usage. If the data is already in an array, see *movechp()* below.

7) Repeat 5) and 6) until done. The routines will take care of output names and whether the output medium is filled. No bookkeeping needs to be done in the program.

8) When done, call *putchp(C_EOT)*.

To read a tape in chapter/verse format:

1) Include <chap.h>
2) Call *getchp()*. It returns the key number of the next chapter.
3) Call *getvrs(N)*. It returns a pointer to verse *N*.
4) A key of *C_EOT* (103) means end of input.

When running programs using chapter/verse format, when a name is required, it prompts on the terminal for input or output file. If a tape is being used, enter the unit number. If a disk file is being used, enter the name of the file. Disk file names cannot begin with numbers. They can contain numbers, but the first character must be alphabetic.

When the end of an input file is reached, it asks for the next input. Thus it is easy to add files or tapes together. When the last input is reached, enter "-1" for input and the program will quit. When the end of an output tape is reached (disk files should never have this problem) it prompts for the next output tape, so both input and output can be continued over many different tapes and files.

3. Chapter Routines

The routines will someday be installed in the default library, so they will be automatically included with your program. For now, they are in their own library and are included by " -lchap " when compiling.

Predefined Values

C_EOF and *C_EOP* are defined as 103 and 206 respectivly, for end-of-file and end-of-plot.

getchp()

returns the key number of the next chapter on the input file.

*char *getvrs(N)*
must be called after ***getchp()***. Returns a pointer to verse *N* of the current chapter (the one returned by the last ***getchp()***).

*char *putchp(key)*
returns a pointer to an area large enough for a chapter of type ***key***.

copychp(key)
assumes ***key*** to be the number of the last chapter read by ***getchp()***, and copies it to the output file. Can be used to copy a whole file like this:

```
copychp(getchp());
```

movechp(key,pointer)
called instead of ***putchp(key)***, it allocates space for a chapter ***key***, and copies the data starting at ***pointer*** into it.

rewchp()
rewinds the input unit. If it's a disk file, it seeks to the beginning of the file.

4. Multiple Units

There are also routines for handling multiple input and output units. Generally speaking, they are the same as the above, with the letter "m" prepended and an extra argument for the unit number. Unit numbers can be 0 or 1. If there are two input tapes, any chapters on both tapes that are going to be used must have the same format.

mgetchp(U)
*char *mgetvrs(U,N)*
*char *mputchp(U,key)*
mrewchp(U)
same as above, but *U* is the input or output unit number (0 or 1).

mcopychp(Ufrom,Uto,key)
assumes the last chapter read on unit *Ufrom* was of type ***key***, and copies it onto unit *Uto*.

mmovechp(U,key,pointer)
used instead of ***mputchp(U,key)***, it writes a chapter of type ***key*** on unit *U* using the data starting at ***pointer***.

SRL TECHNICAL REPORT 78-3

HNE LIBRARY GENERATOR

Tom Garrard

May 6, 1979
updated to
December 17, 1979

78-3

TABLE OF CONTENTS

78-3 p. 1

I. Introduction

The HNE data will be supplied to CIT by GSFC in the form of "production" tapes. These tapes will be processed by a library generator program (LIBGEN) which will create science library (SL) tapes. These SL tapes will form the basic data set for all scientific analysis. Since all subsequent analysis depends on this library it must be complete, but the size of the data set forces us to economize as much as possible with the format. The compromise proposed here is to use variable format.

Section II describes the library generator program and section IV describes the tape format; section III has notes on specific problems.

II. Program Description

The program description is primarily in terms of flow charts and notes. The structure of the program is fairly simple. All the difficulty lies in the dirty details — what to do with events with poorly defined trajectories, events which differ when repeated, etc. I have tried to postpone these decisions beyond the library generation stage. The design philosophy is that provision for failures should be made when the failure is identified. Details of the flow charts are described in the algorithm notes (III).

LAYCAL
6/1/79

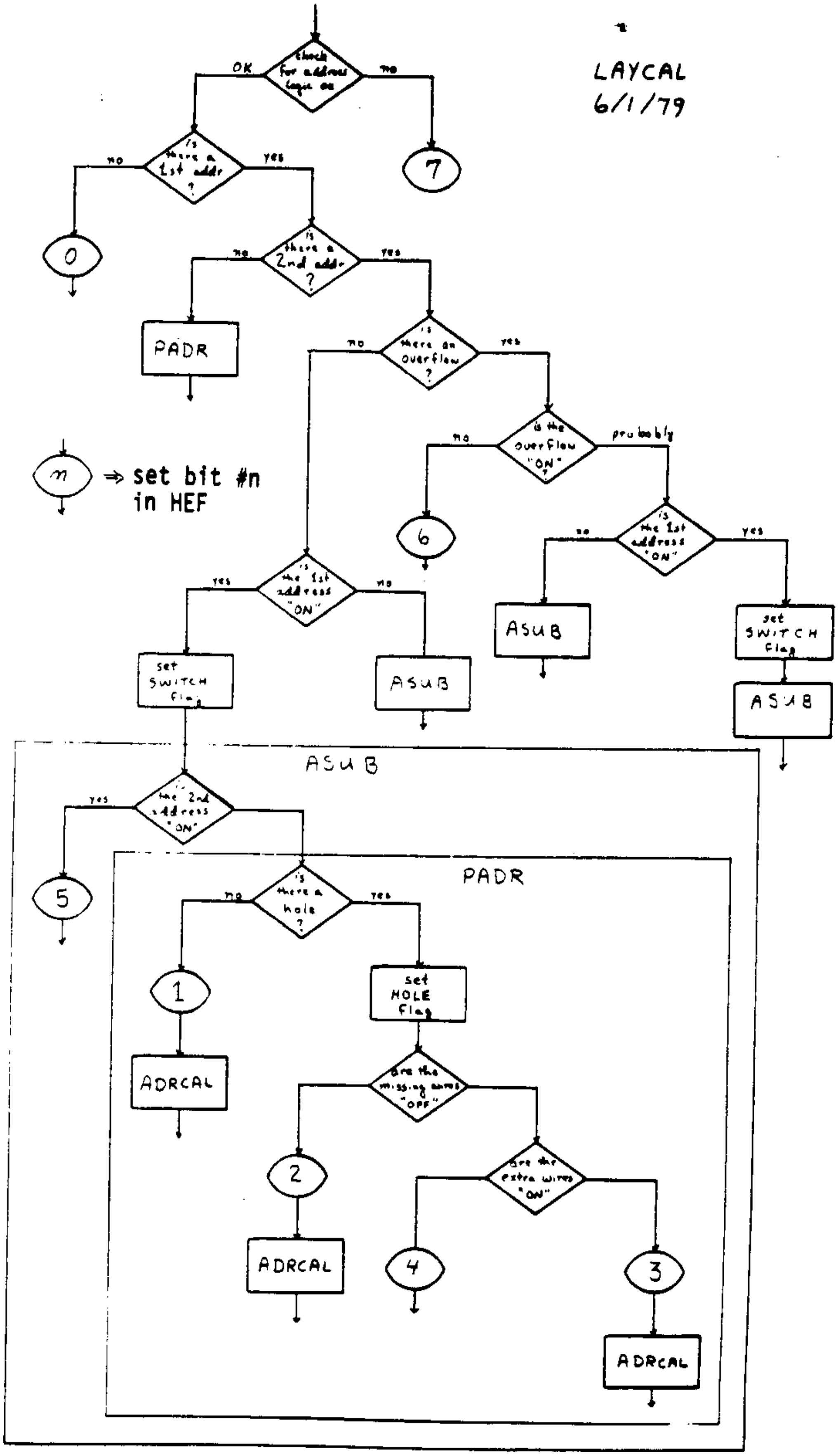
check for address logic on
OK
no
7
is there a 1st addr ?
no
yes
0
is there a 2nd addr ?
no
yes
PADR
is there an overflow ?
no
yes
is the overflow "ON" ?
no
probably
6
is the 1st address "ON"
no
yes
ASUB
set SWITCH flag
ASUB
n ⇒ set bit #n in HEF
is the 1st address "ON"
yes
no
set SWITCH flag
ASUB
ASUB
is the 2nd address "ON"
yes
5
PADR
is there a hole ?
no
yes
1
ADRCAL
set HOLE flag
are the missing wires "OFF"
2
ADRCAL
are the extra wires "ON"
4
3
ADRCAL

78-3 p.3

LIBGEN
5/6/79

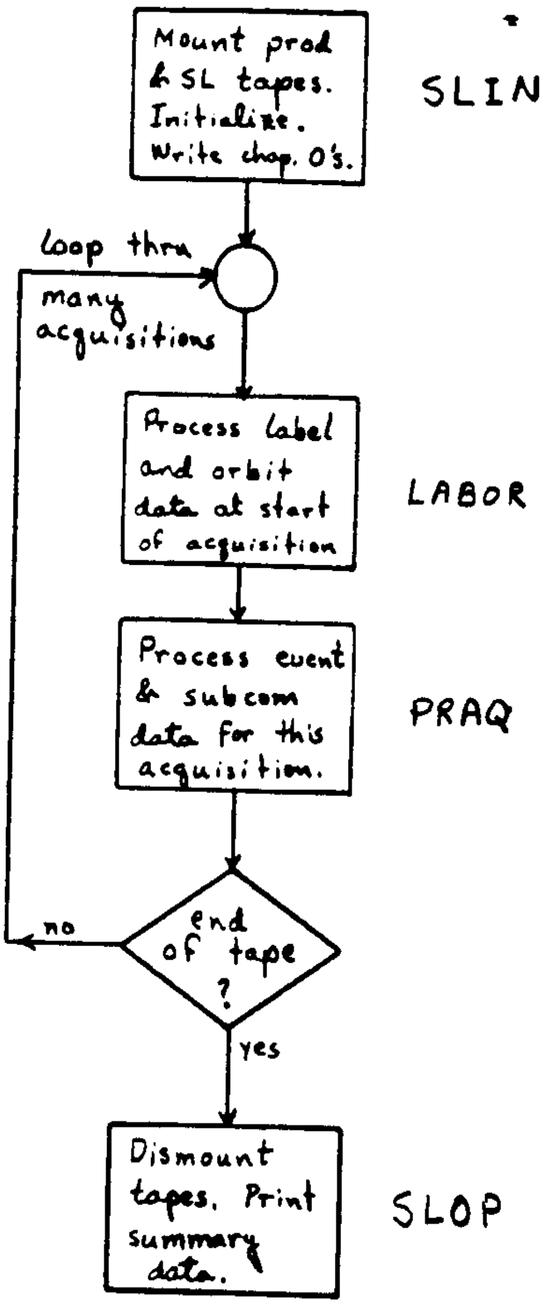

78-3 p.4

PRAQ
5/6/79

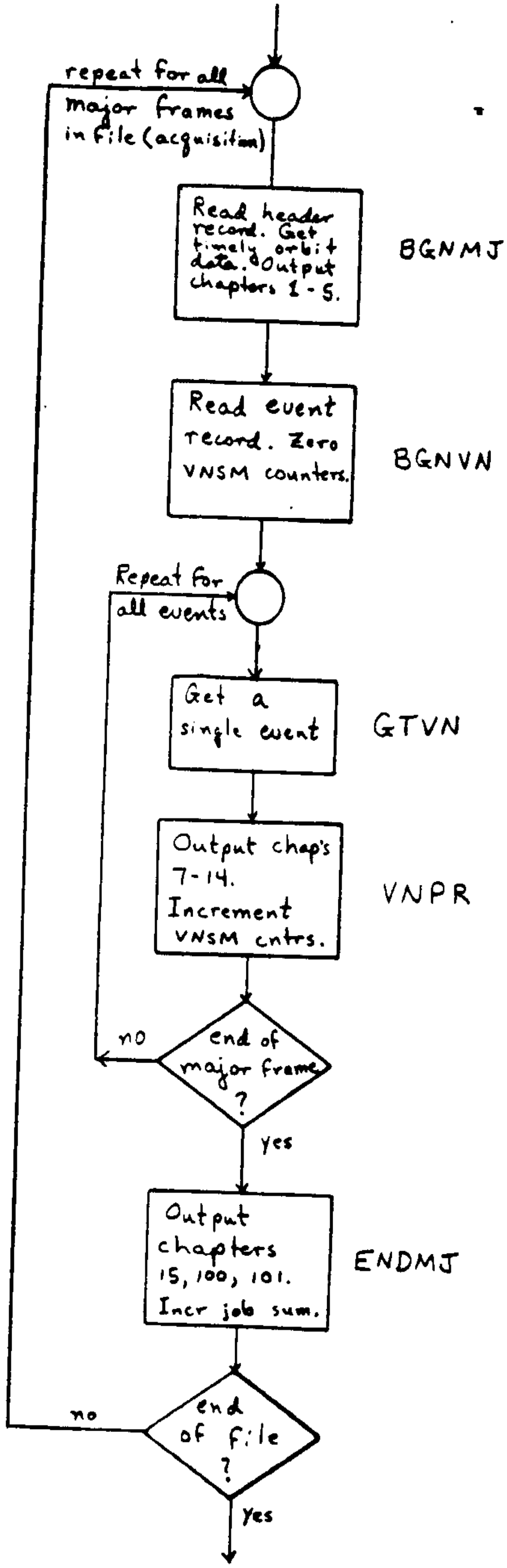

78-3 p.5

VNPR
5/6/79*

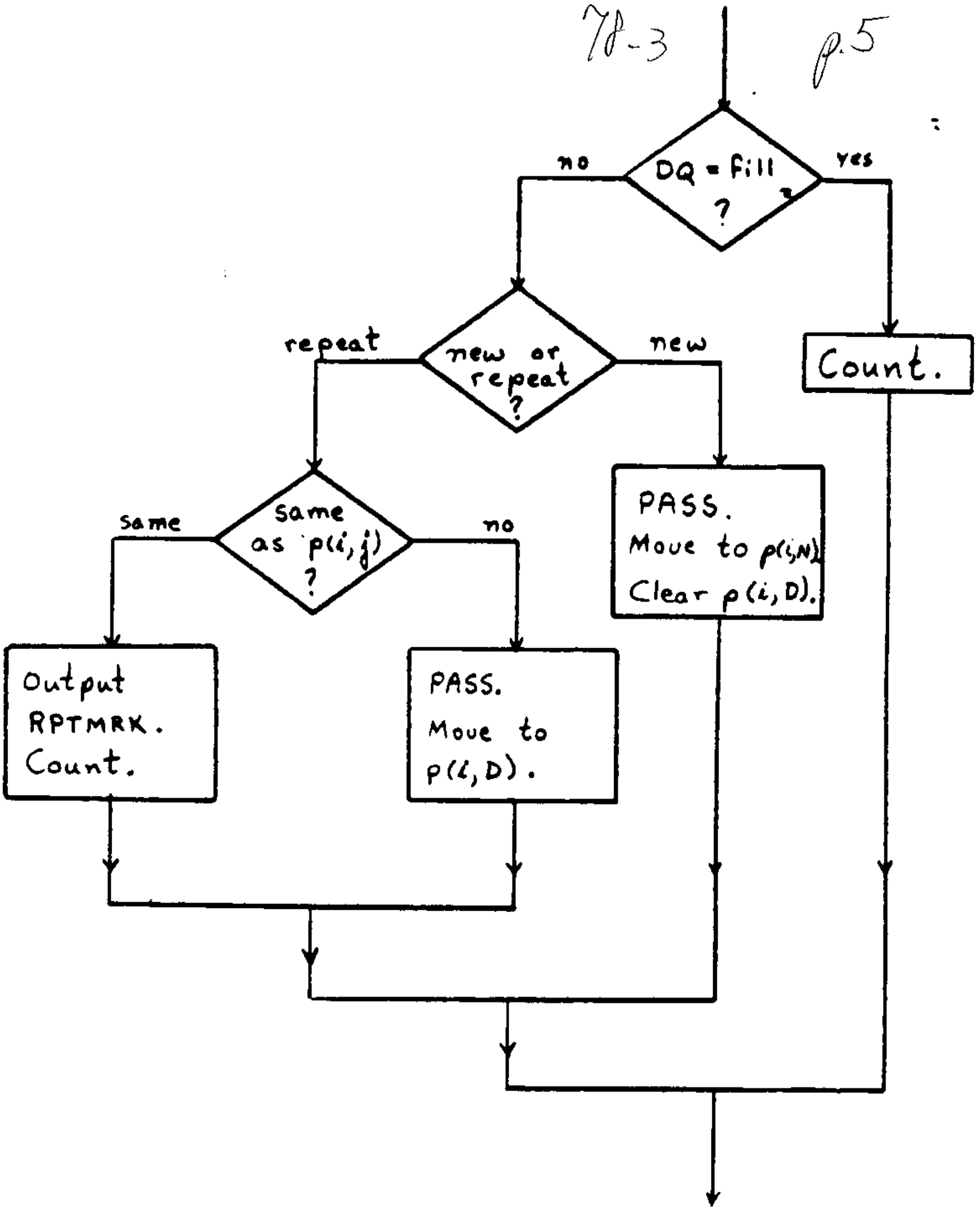

i = A, B buffer
j = N, D for "new" or "different"

78-3 p.6

PASS
6/1/79

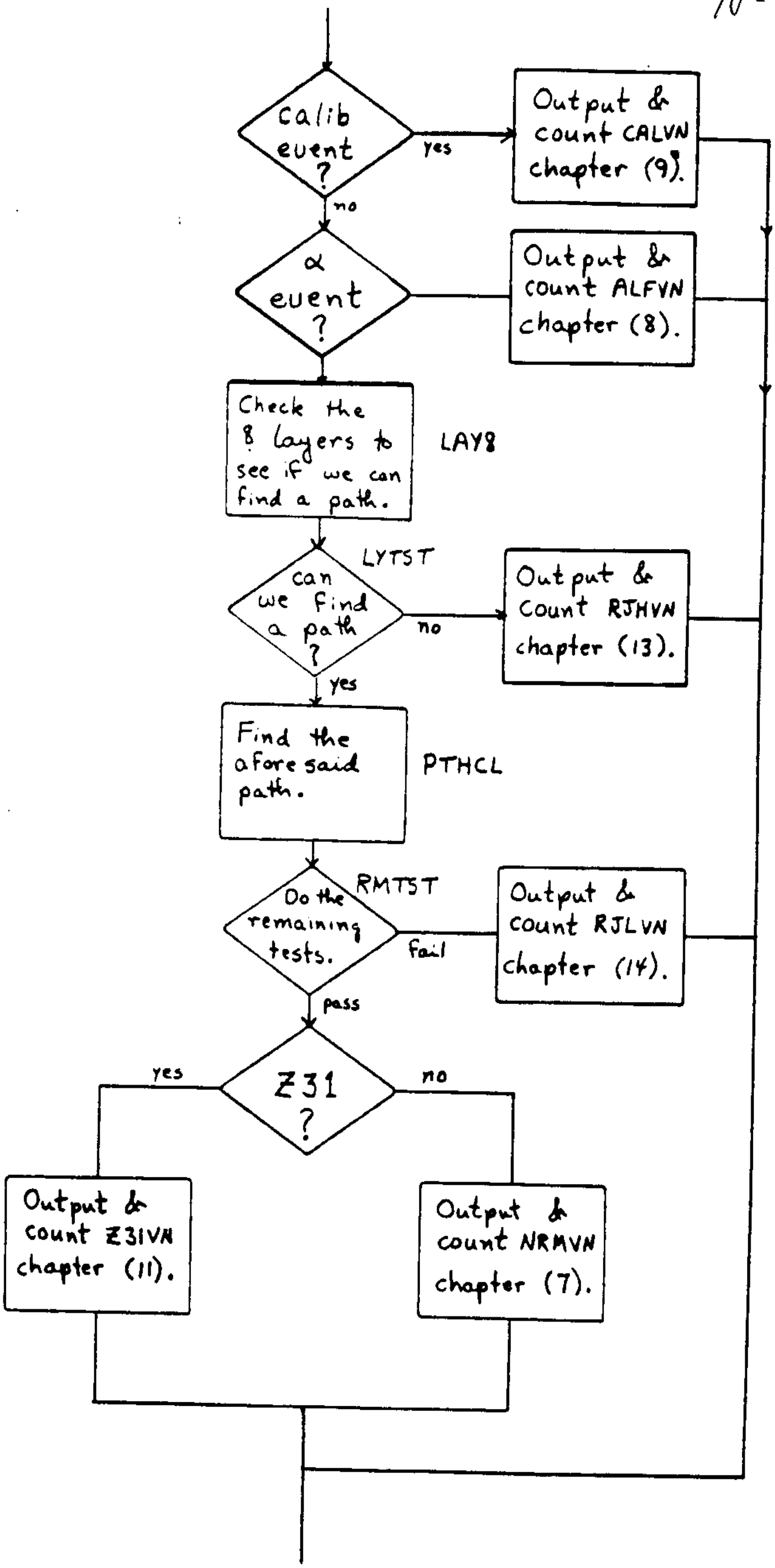

Z31 ⇒
either ZCI
>30.5

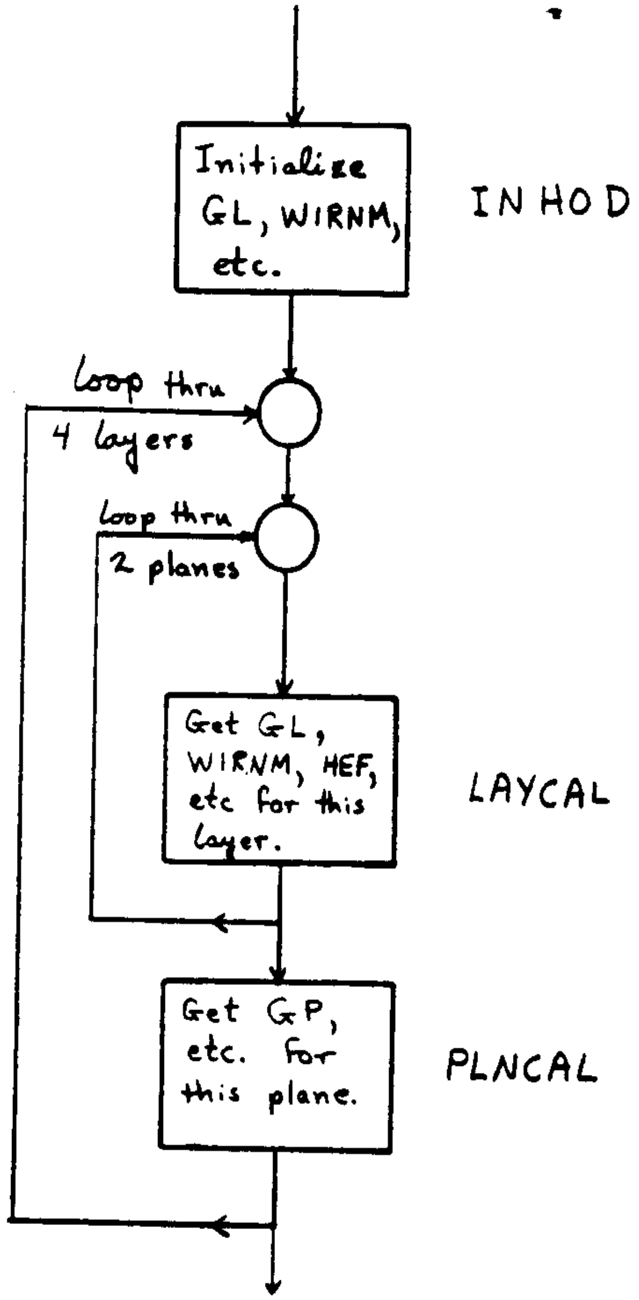
Initialize GL, WIRNM, etc.
INHOD
Loop thru 4 layers
Loop thru 2 planes
Get GL, WIRNM, HEF, etc for this layer.
LAYCAL
Get GP, etc. for this plane.
PLNCAL

78-3 p.8

PTHCL
6/1/79

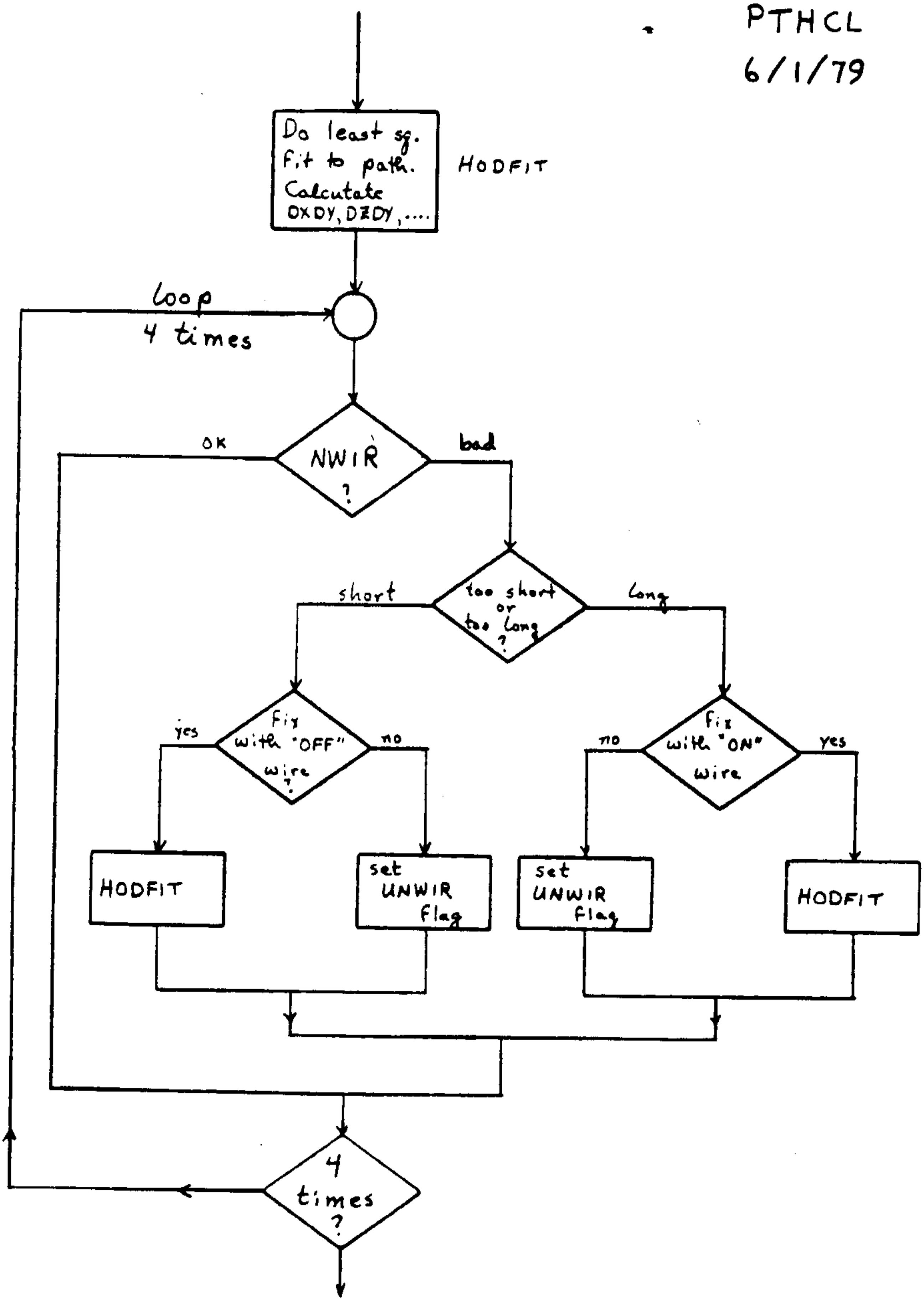

III. Algorithm Notes

Hodo path notes

Good Layer is defined as 1 address with no unfixable holes.

Good Plane defined as plane with two good layers.

Good Path defined as path with two or more food planes. -

By my notes this is still subject to debate. Another possible requirement is path with at least 2 good X layers and 2 good Z layers.

"on" List is a list of wires which are failed in the "on" state.
"ON" means"on the "on" list".

"off" List is a list of wires which have failed in the "off" state.
"OFF" means "on the "off" list".

Any inconsistency in the address data causes a chapter 13, e.g., second address bit on with second address = 200.

RMTST notes

Events go into RJLVN if any bit of the word RJTG is set. See the format description. Note that RALF is set for any of:

overflow	&	(! valid 2nd addr)
First pattern	&	(! first addr)
2nd pattern	&	(! 2nd addr)
2nd addr	XOR	valid 2nd addr
2nd addr	&	(! first addr)
first addr + 7	≥	2nd addr

HODFIT notes

For 3 & 4 plane events, do least squares fit to get $X(y)$ and χ^2_x

I.e., assume $X = ay + b$ and

we have N measurements X_i, y_i.

We calculate and minimize

$$\chi^2_x = \sum (X_i - ay_i - b)^2 .$$

We get

$$a = \frac{N \cdot \sum X_i y_i - (\sum X_i)(\sum y_i)}{D}$$

$$b = \frac{(\sum X_i)(\sum y_i^2) - (\sum y_i)(\sum X_i y_i)}{D}$$

where $$D = N \cdot \sum y_i^2 - (\sum y_i)^2$$

we take advantage of the fact that the y_i's are constant to speed execution. Note also that $y_2 = -y_3$ & $y_1 = -y_4$.

For a 4-plane event, define a list of constants k_j:

$$k_1 = \frac{4y_1 - \Sigma y_i}{D}$$

$$= \frac{4 \cdot 71.294 - 0}{4\left[2(71.294^2 + 27.766^2)\right] - 0} = 6.08956 \times 10^{-3}$$

$$k_2 = \frac{4y_2 - \Sigma y_i}{D} = 2.37163 \times 10^{-3}$$

$$k_3 = -k_2 \qquad k_4 = -k_1$$

$$a = k_1(X_1 - X_4) + k_2(X_2 - X_3)$$

$$k_5 = \frac{\Sigma y_i^2 - y_i \Sigma y_i}{D} = \frac{1}{4} = k_6 = k_7 = k_8$$

$$b = \frac{X_1 + X_2 + X_3 + X_4}{4}$$

$$\chi_x^2 = \frac{(X_1 - ay_1 - b)^2 + (X_2 - ay_2 - b)^2 + \cdots}{4}$$

Consider a 3-plane event with plane 1 missing:

$$D = 3(y_2^2 + y_3^2 + y_4^2) - (y_2 + y_3 + y_4)^2$$
$$= 6y_2^2 + 2y_1^2 = 14\,791.3734 \text{ cm}^2$$

k_1 irrelevant

$$k_2 = \frac{3y_2 - (y_2 + y_3 + y_4)}{D} = \frac{3y_2 - y_4}{D} = \frac{3y_2 + y_1}{D}$$
$$= 1/(95.6801 \text{ cm})$$

$$k_3 = \frac{3y_3 - (y_2 + y_3 + y_4)}{D} = \frac{3y_3 - y_4}{D} = \frac{-3y_2 + y_1}{D}$$
$$= -1/(1232.2037 \text{ cm})$$

$$k_4 = \frac{3y_4 - (y_2 + y_3 + y_4)}{D} = \frac{2y_4}{D} = \frac{-2y_1}{D}$$
$$= -1/(103.7351 \text{ cm})$$

k_5 irrelevant

$$k_6 = \frac{(y_2^2 + y_3^2 + y_4^2) - (y_2 + y_3 + y_4)(y_2)}{D}$$
$$= \frac{2y_2^2 + y_1^2 + y_1 y_2}{D} = 0.581709684$$

$$k_1 = \frac{2y_2^2 + y_1^2 - y_1 y_2}{D} = .314047$$

$$k_2 = \frac{2y_2^2}{D} = .104243$$

$$a = \frac{X_2}{207.2482\ \text{cm}} + \frac{X_3}{2669.023\ \text{cm}} + \frac{X_4}{224.6957\ \text{cm}}$$

$$b = .268557 X_2 + .144986 X_3 + .048126 X_4$$

$$\chi_x^2 = \frac{(X_2 - ay_2 - b)^2 + (X_3 + ay_2 - b)^2 + (X_4 + ay_1 - b)^2}{3}$$

For 2 plane events, least square fit is not possible.

$$a = \frac{X_i - X_j}{Y_i - Y_j}$$

$$b = X_i - a Y_i$$

$$\chi_x^2 = 0$$

Given a_x, b_x & a_z, b_z we can get ϕ & $\cos\theta$ &c.

Unit vector for particle is

$$\hat{p} = \frac{a_x \mathbf{e}_x + \mathbf{e}_y + a_z \mathbf{e}_z}{(a_x^2 + 1 + a_z^2)^{1/2}}$$

Angle with y axis is θ

$$\cos\theta = \hat{p} \cdot \mathbf{e}_y = \frac{1}{(a_x^2 + 1 + a_z^2)^{1/2}}$$

Azimuthal angle around y, +ve from Z towards X is ϕ

$$\phi = \tan^{-1}\left\{\frac{\hat{p}\cdot\mathbf{e}_x}{\hat{p}\cdot\mathbf{e}_z}\right\} = \tan^{-1}(a_x/a_z)$$

Notes on ORBT verse

Given:

Zenith & azimuth angles of Z & Y axes of spacecraft in earth referenced system (see Table IVb of production tape) once each 16 minor frames.

and

Slopes of particle trajectory in spacecraft coordinate system (see HODO verse & HODFIT notes).

Find:

Polar and azimuthal angles in earth referenced system of particle trajectory for a particular event (or particular minor frame).

Technique:

Get Euler angles of rotation transform matrix at two time near of bracketing the desired time.

Interpolate to get Euler angles at time of event.

Calculate matrix & apply to vector. Calculate angles from vector components.

Name in notes	Description	Documentation Reference
znz	zenith angle of z	Production tape, table IV b.
azz	azimuth " " "	
zny	zenith " " y	
azy	azimuth " " "	
a_{ij}	XYZ to ENV transform	
eath	Euler angle theta	1st, 2nd, 3rd Euler angles, ch 3, v 2-9.
eaf	Euler angle phi	
eaps	Euler angle psi	
a_x	X-projected slope	DXDY/8K, ch 11, v2.
a_y	Y-projected slope	DZDY/8K, ch 11, v2.
θ	polar angle of particle	THTA, ch 11, v3.
ϕ	azimuthal " " "	PHI, ch 11 v3.

The S/C system unit vectors are

$$e_z = \cos(znz)\, e_v + \sin(znz)\cos(azz)\, e_E + \sin(znz)\sin(azz)\, e_N$$

$$e_y = \cos(zny)\, e_v + \sin(zny)\cos(azy)\, e_E + \sin(zny)\sin(azy)\, e_N$$

hence

$$a_{33} = \cos(znz)$$
$$a_{23} = \sin(znz)\sin(azz)$$
$$a_{13} = \sin(znz)\cos(azz)$$

$$a_{32} = \cos(zny)$$
$$a_{22} = \sin(zny)\sin(azy)$$
$$a_{12} = \sin(zny)\cos(azy)$$

$$a_{31} = a_{12}\, a_{23} - a_{22}\, a_{13}$$

Then,

$$eath = \cos^{-1}(a_{33}) = znz$$

$$eaf = \tan^{-1}\left(a_{31}/(-a_{32})\right)$$

$$= \tan^{-1}\left\{ \frac{\sin(zny)\sin(znz)\left[\cos(azy)\sin(azz) - \sin(azy)\cos(azz)\right]}{-\cos(zny)} \right\}$$

$$eaps = \tan^{-1}(a_{13}/a_{23})$$
$$= \tan^{-1}\left(\cos(azz)/\sin(azz)\right)$$
$$= \pi/2 - azz$$

Linear interpolation of Euler angles is straightforward:

$$eaf(t) = eaf(t_1)\left\{1 - \frac{t-t_1}{t_2-t_1}\right\} + eaf(t_2)\left\{\frac{t-t_1}{t_2-t_1}\right\}, \text{etc}$$

Given the appropriate Euler angles, the transform matrix is easily constructed:

$$a_{11} = \cos(eops)\cos(eaf) - \cos(eath)\sin(eaps)\sin(eaf)$$
$$\vdots$$
$$a_{33} = \cos(eath)$$

The particle trajectory is described by a unit vector $\hat{p}$ which has XYZ components

$$\hat{p} = \begin{pmatrix} a_x/pmag \\ 1/pmag \\ a_z/pmag \end{pmatrix} \quad \text{where} \quad pmag = (1 + a_x^2 + a_z^2)^{1/2}$$

and ENV components

$$\hat{p}\cdot pmag = \begin{pmatrix} a_{11}a_x + a_{12} + a_{13}a_z \\ a_{21}a_x + a_{22} + a_{23}a_z \\ a_{31}a_x + a_{23} + a_{33}a_z \end{pmatrix}$$

Thus

$$\theta = \cos^{-1}(\hat{p}\cdot e_v)$$
$$= \cos^{-1}\left\{\frac{a_{31}a_x + a_{23} + a_{33}a_z}{pmag}\right\}$$
$$= \cos^{-1}\left\{\frac{\sin(eath)\sin(eap)a_x + \cos(eaps)\sin(eath) + \cos(eath)}{pmag}\right.$$

$$\phi = \tan^{-1}\left\{\frac{a_{21}a_x + a_{22} + a_{23}a_z}{a_{11}a_x + a_{12} + a_{13}a_z}\right\}$$

$$\phi = \tan^{-1}\left\{\frac{(-\sin(eaps)\cos(eaf) - \cos(eath)\sin(eaf)\cos(eaps))a_x}{(\cos(eaps)\cos(eaf) - \cos(eath)\sin(eaf)\sin(eaps))a_x}\right.$$

$$\frac{+(-\sin(eaps)\sin(eaf) + \cos(eath)\cos(eaf)\cos(eaps))}{+(\cos(eaps)\sin(eaf) + \cos(eath)\cos(eaf)\sin(eapt))}$$

$$\left.\frac{+\cos(eaps)\sin(eath)a_z}{+\sin(eops)\sin(eath)a_z}\right\}$$

let

$$q_1 = \cos(eath)\sin(eaf) \qquad q_3 = a_x\cos(eaf) + \sin(ea$$

$$q_2 = \cos(eath)\cos(eaf) \qquad q_4 = a_x q_1 - a_z\sin(eath)$$

then

$$\phi = \tan^{-1}\left\{\frac{-a_x(\sin(eops)\cos(eaf) + q_1\cos(eaps)) - \sin(eaps)\sin(eaf)}{a_x(\cos(eaps)\cos(eaf) - q_1\sin(eaps)) + \cos(eaps)\sin(eaf)}\right.$$

$$\left.\frac{+q_2\cos(eaps) + a_z\cos(eops)\sin(eath)}{+q_2\cos(eaps) + a_z\sin(eaps)\sin(eath)}\right\}$$

$$\phi = \tan^{-1}\left\{\frac{\cos(eaps)(q_2 - q_4) - \sin(eaps)q_3}{\cos(eaps)(q_2 + q_3) - \sin(eaps)q_4}\right\}$$

Note that the a_{ij} themselves need not be calculated, only the sine's and cosine's of the Euler angles.

V. Library Tape Format

A. General Description

In order to maximize flexibility and minimize tape length, the SL tape will be formatted with lots of small logical blocks squeezed together into long physical records ($\leq$ 8K words). The logical blocks are called chapters. Each chapter begins with an identifier key. In some cases the chapter is broken up into verses. Pointers for the verses and chapter lengths are specified in one or more control chapters. The control chapters are always the first chapters on the tape.

With the chapter and verse structure and the pointers, a change in format affects only the changed verse or chapter. Other verses and chapters are not affected if the pointers have been treated as variables. No spare words are necessary for future expansion. Details of the ~ 30 different types of chapters are given in a separate report.

The collection of chapters into records will be done in such a manner that records contain integral numbers of chapters and such that major frames contain integral numbers of records (usually 1 or 2). This will prevent loss of synchronism from propagating from record to record.

Note that chapters with identifier keys larger than 99 are fixed-format, 4-byte markers, hence require no pointers.

SRL TECHNICAL REPORT 79-1

HNE DATA CRUSHER

by

Tom Garrard

January 28, 1979

California Institute of Technology
Pasadena, California

Table of Contents

I. Introduction

The data crusher (CRSH) program will be used primarily to produce data sets containing selected data from the science library (SL) tapes relevant to a particular science problem. The intention is to produce as small a data set as possible so that it can be intensively worked at a small cost.

The CRSH program does not require a small output set, so it can also be used to produce modified SL tapes. Thus if corrections or mappings need to be incorporated into the SL tapes, these modifications can be done with CRSH rather than re-running a corrected library generator.

The structure of CRSH is quite general and it is expected to have dozens of versions. Some obvious possibilities are:

daily-average or orbit-average rate plots

collection of histogram data for construction of maps

application of maps

collection of charge histograms

Examples of necessary programming to create new versions are given in Section III.

79-1

II. Program Description

The CRSH program, in all its many versions, has the overall structure shown in the CRSH flow chart. A SL tape chapter is read and processed, then this is repeated until one of the processes sets the end-of-job flag (EOJFLG). Although it is not shown explicitly, many of the chapter processes will create output chapters which are accumulated and flushed to the output tape when the buffer is full.

In the initialization block tasks such as zeroing of histogram arrays and reading and storage of verse pointers are performed. The ABORT routine will output an EOT chapter, a double end-of-file, and a printed "error" message.

Two subroutines are used to hide the "dirty details" from the user. One, which can be called GTCHP, is seen explicitly in the flow chart. It gets chapters from the input tape. The other, FLUSH, is contained within the process subroutines and does not show up on the flow chart. FLUSH is used to output chapters to the output tape (or printer, etc.). Note that the longest SL chapter is only 284 bytes. Core limitations of PDP-11's make it convenient to keep chapter length small (< 500-1000 bytes).

GTCHP returns the index (PNTR) within the common or global array INBF of the KEY of the next available chapter. INBF contains one tape record which is made up of several chapters. After a call to GTCHP the chapter KEY is obtained (in FORTRAN) by

KEY = INBF(PNTR)

and an item in that chapter is obtained by

ITEM = INBF(PNTR + OFFSET(KEY, VERSE) + ITMOF)

where OFFSET(KEY, VERSE) is the relative address within the chapter of verse number VERSE and ITMOF is the relative offset within the verse of ITEM. Offsets are specified in bytes; division by 2 or 4 may be necessary to address words.

Global (or common) variables WNTKEY and NROV and array SKIP are used to allow additional control to the user. If WNTKEY is n, then the subroutine GTCHP will not return to the user until chapter type n is located. A negative value for WNTKEY means the user is not using this feature. If the

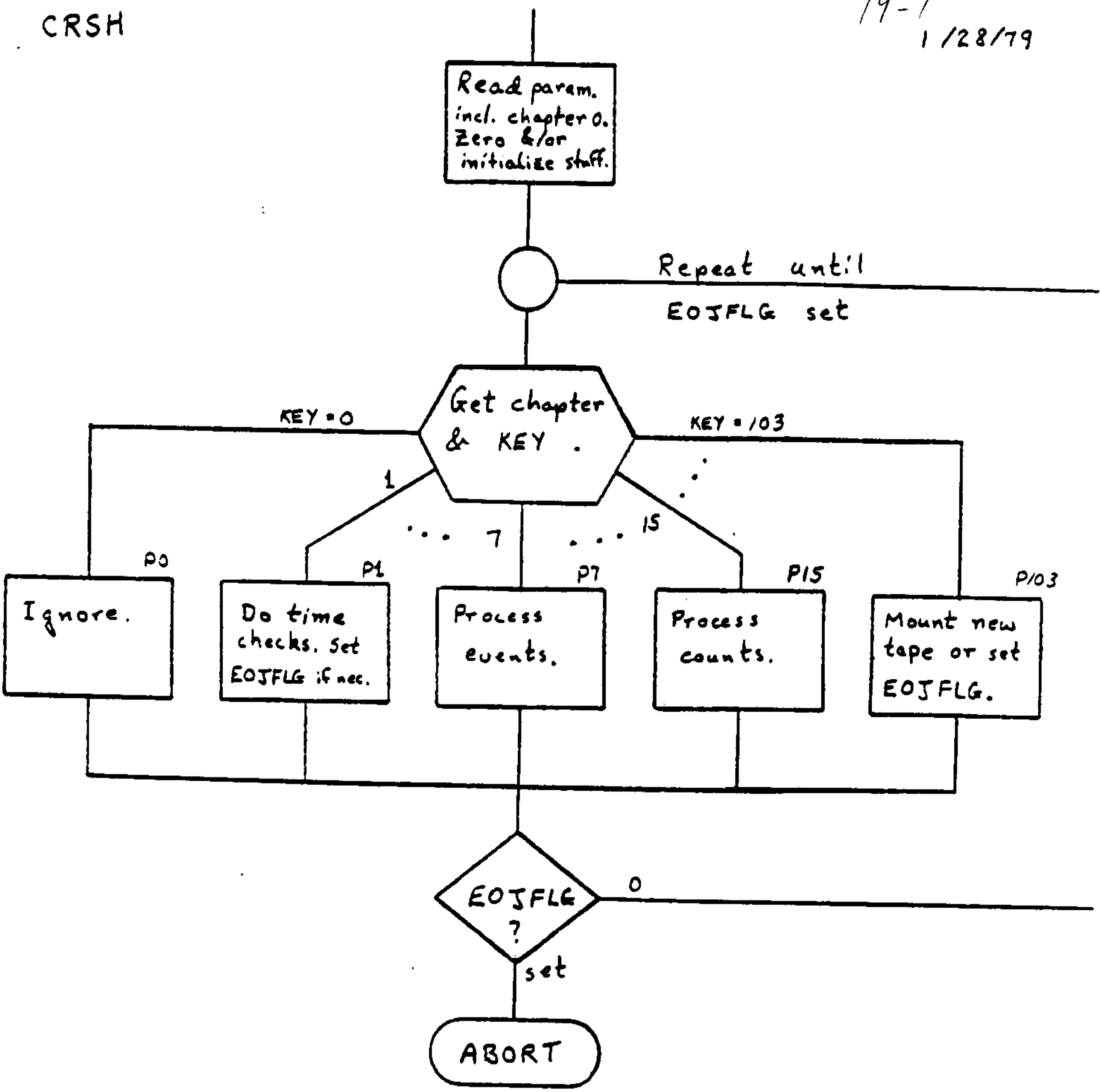
Read param. incl. chapter 0. Zero &/or initialize stuff.
Repeat until EOJFLG set
Get chapter & KEY.
KEY = 0
1
. . . 7
. . . 15
KEY = /03
P0
Ignore.
P1
Do time checks. Set EOJFLG if nec.
P7
Process events.
P15
Process counts.
P/03
Mount new tape or set EOJFLG.
EOJFLG ?
0
set
ABORT

79-1

ith element of SKIP is set then GTCHP will not return any chapter type i to the user (unless WNTKEY = i). For chapter 101, GTCHP will set an internal flag that causes it to read a new record and reset PNTR before answering the next call, unless NROV is set. If NROV is set then the user is responsible for reading the next records and resetting PNTR. For chapter 103, a flag (EOTF) is set which will cause an Abort on the next call to GTCHP. If the user process 103 causes a new tape to be mounted then the user should clear EOTF.

FLUSH is called with a user-supplied argument (KEYLOC) which is the address of the KEY of the chapter to be output. FLUSH moves this chapter into an output buffer (OBF) with an offset OBPNT. OBPNT is then incremented by the chapter length. If, after incrementing,

$$\text{OBPNT} - \text{OBF} > \text{OBLN} - \text{MXCH} - 4$$

where OBLN is the length of the output buffer and MXCH is the length of the longest chapter to be output, then FLUSH will add a chapter 101 to the output buffer and write it out. It will also reset OBPNT to OBF.

If KEY is 100 FLUSH supplies the record number, puts chapters 100 and 101 in the output buffer, writes the buffer out, and resets OBPNT. If KEY is 101, FLUSH supplies record number, puts chapter 101 in output buffer, writes it out and resets OBPNT. If KEY is 102 FLUSH moves chapter 102 to output buffer, adds a chapter 101, writes it out, and resets OBPNT. If KEY is 103 no chapter 101 is necessary. FLUSH puts a chapter 103 in the buffer, writes it out, and resets OBPNT. It then writes a double end-of-file and rewinds.

79-1

III. Examples

A. Daily-Average Rate Plots

This CRSH will read an SL and output a tape with the data necessary for creating rate plots. This output data will be organized into chapters like the SL. Only one type of chapter is needed, which we shall call AVRAT and number 16. Some detail for this chapter is given in table III-A-1. The chapter will contain accumulation time, accumulated rate scaler counts, and accumulated event counts for a particular day.

The "user-supplied" processes of interest are P1, which does the time checking to separate output chapters by day, and P4 and P15, which accumulate rate scales counts and event counts. Chapters 2,3, 5-11, and 13 are ignored. A flow chart for P1 is presented. TBGN and TEND are begin and end time of current day (in seconds since 1-1-79 to agree with TSEC): TSTP is the end time for the job. P4 increments rate accumulators by the contents of the rate scales for that major frame, provided that the data quality is OK. No such check is necessary in P15. Note that the time interval length (INTVL) is a variable, even though we have been discussing daily averages. We could equally well do hourly, weekly, etc. A trivial program change would allow checking orbit number (RBNO) instead of TSEC.

79-1

Chapter Number 16
Chapter Name AVRAT

Verse Name	Verse No.	Item Name	Item Length	Relative Index	Comments
		KEY	2	0	Key = 16
		Spare	2	2	
RTTM	1		48	4	Begin & end of interval, etc.
RTSM	2		120	52	Accumulated rates.
VNCNT	3			172	Accumulated event counts.
AVRVR	4				Program version info.

Verse Number 1 of Chapter 16
Verse Name RTTM

Item Name	Item Length	Relative Index	Comments
TBGN	4	0	Begin and end times
TEND	4	4	of interval.
FRSTM	18	8	Copy chapter 1, verse 1 for
LSTM	18	26	first and last major frame in interval.
INTVL	2	44	Interval length.
MFCNT	2	46	Major frame count for interval.
		48	

Verse Number 2 of Chapter 16
Verse Name RTSM

Item Name	Item Length	Relative Index	Comments
RTSUM	20 x 4	0	Accumulated rate counts.
NRO	20 x 2	80	Number of valid readouts.
		120	

79-1

Verse Number 3 of Chapter 16

Verse Name VNCNT

Item Name	Item Length	Relative Index	Comments
VNCOU	11 x 2	0	Accumulated counts.
Spare	2	22	
		24	

Verse Number 4 of Chapter 16

Verse Name AVRVR

Item Name	Item Length	Relative Index	Comments
PNAM	8	0	Program name.
PVRS	8	8	Program version date.
EXDT	8	16	Execution date.
		24	

79-1

P1
Repeated interv
version

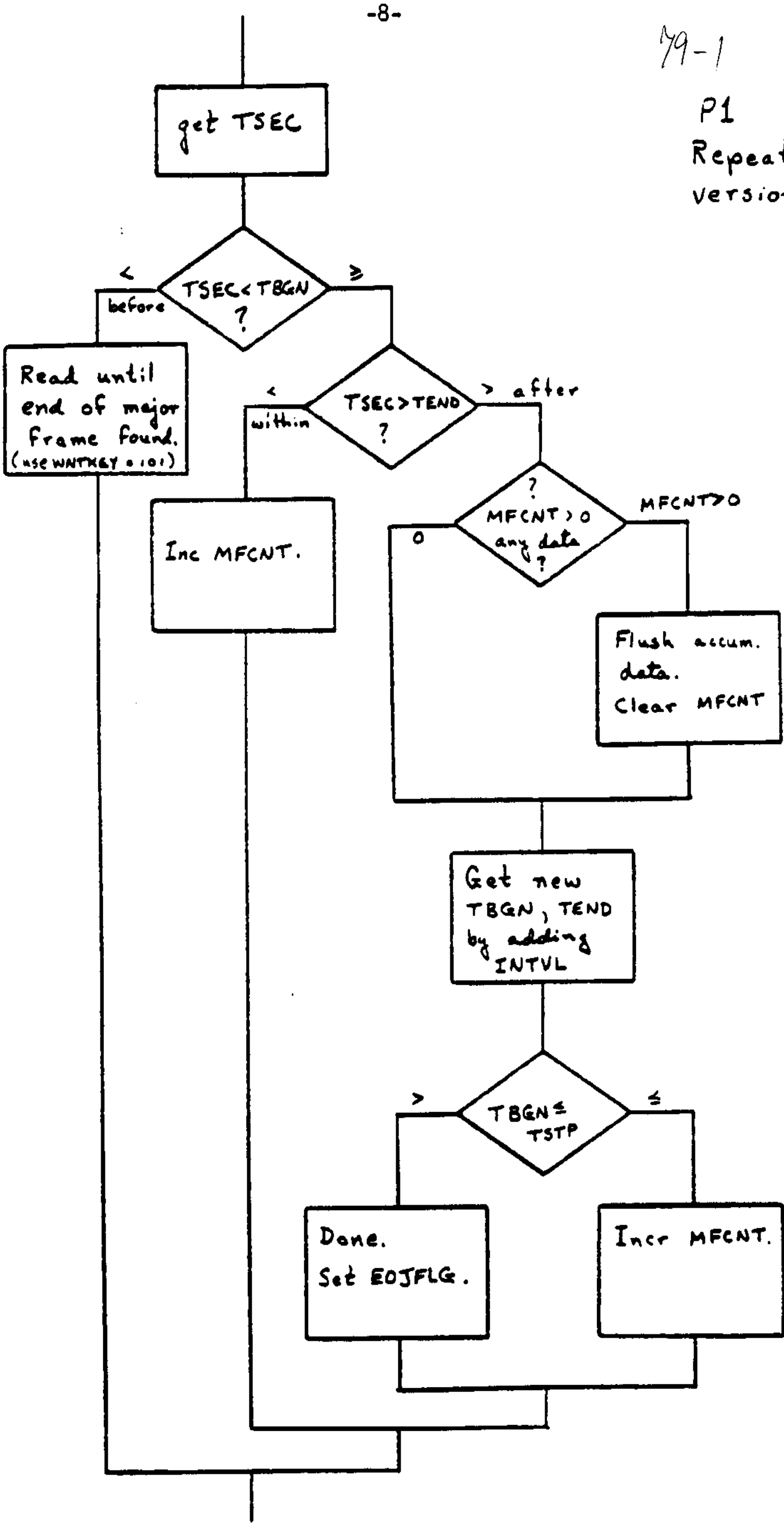

79-1

III. Examples

B. Collection of Histogram Data

Histograms will presumably be the basis of the mapping effort and are thus quite important. They also have the potential to be difficult because of the temptation to accumulate histograms with very many channels. One might, for instance, want to accumulate a Cerenkov map histogram with 100 X channels by 100 Y channels by 100 pulse height channels. This histogram requires 1000000 words of memory and is essentially impossible on a PDP-11/34 and is non-trivial on an IBM 370. Because of the importance of the problem I will discuss several alternatives for handling this problem.

Alternative I: Use an IBM 370 or a CDC 7600 or the like. With these computers mega-word arrays can be handled. Major costs of this solution are money and loss of interactive capabilities of the 11/34 time-sharing system.

Alternative 2: Use the ever-popular technique of reduction of scope. One might accumulate average and sigma of pulse height distribution for 100 X by 100 Y channels. These two histograms require 20000 words of memory, which is trivial on an IBM 370 and possible on the 11/34.

Alternative 3: Break the problem into pieces. One might, with 100 CRSH runs, accumulate 100 10000-word arrays. If the input data set has been pre-crushed somehow so that less than one hour per run is required, this is quite feasible on the 11/34 (but very expensive on the CIT IBM 370).

Note also that these large arrays violate the suggestion that data chapters be held to a few hundred words. One obvious possibility is to break up

79-1

each array into many chapters. Each X,Y pair might be represented by a chapter containing the 100 word pulse height histogram. Another possibility is to modify FLUSH so that it handles chapters up to ~ 10000 words. Note that 11/34's & 370's have a hardware maximum mag tape record size of about 30000 <u>bytes</u> (370's and PDP-11's can have standard word lengths of 1,2,4, or 8 bytes).

For this example, we shall accumulate average and sigma for each of a few hundred 6cm x 6cm bins. The data set is restricted to roughly normal incidence iron by requiring same bin number in each radiator and 24 < ZEST < 28. We also require McIlwain L value LMCI, greater than a specified LCUT and Stoermer cutoff, STRM, larger than SCUT (both cutoffs > SCUT. The job will run from a start time to a stop time and then quit. The interval between start and stop will be ~ 30 days so that many input SL tapes are required. Output will be one single chapter of type 17 (plus one EOT chapter). "User-supplied" processes are:

P∅ : Chapter ∅ of the first tape is processed in the first block of the CRSH flow chart by a non-user routine. Succeeding chapter ∅'s (of succeeding tapes) are ignored on the assumption that they are all identical.

P1 : Checks start and stop time. Upon finding stop time, flushes chapter and sets EOJFLG. See flow chart.

P2, 3,4 : Ignore these chapters. Use SKIP array.

P5 : Check LMCI. If LMCI < LCUT then skip to next major frame by using WNTKEY = 101. If LMCI ≥ LCUT do nothing. Checking LMCI on a minute-by-minute basis in this fashion is somewhat crude but much faster than checking each individual event.

P6 : Ignore this chapter.

79-1

P1

one interval version

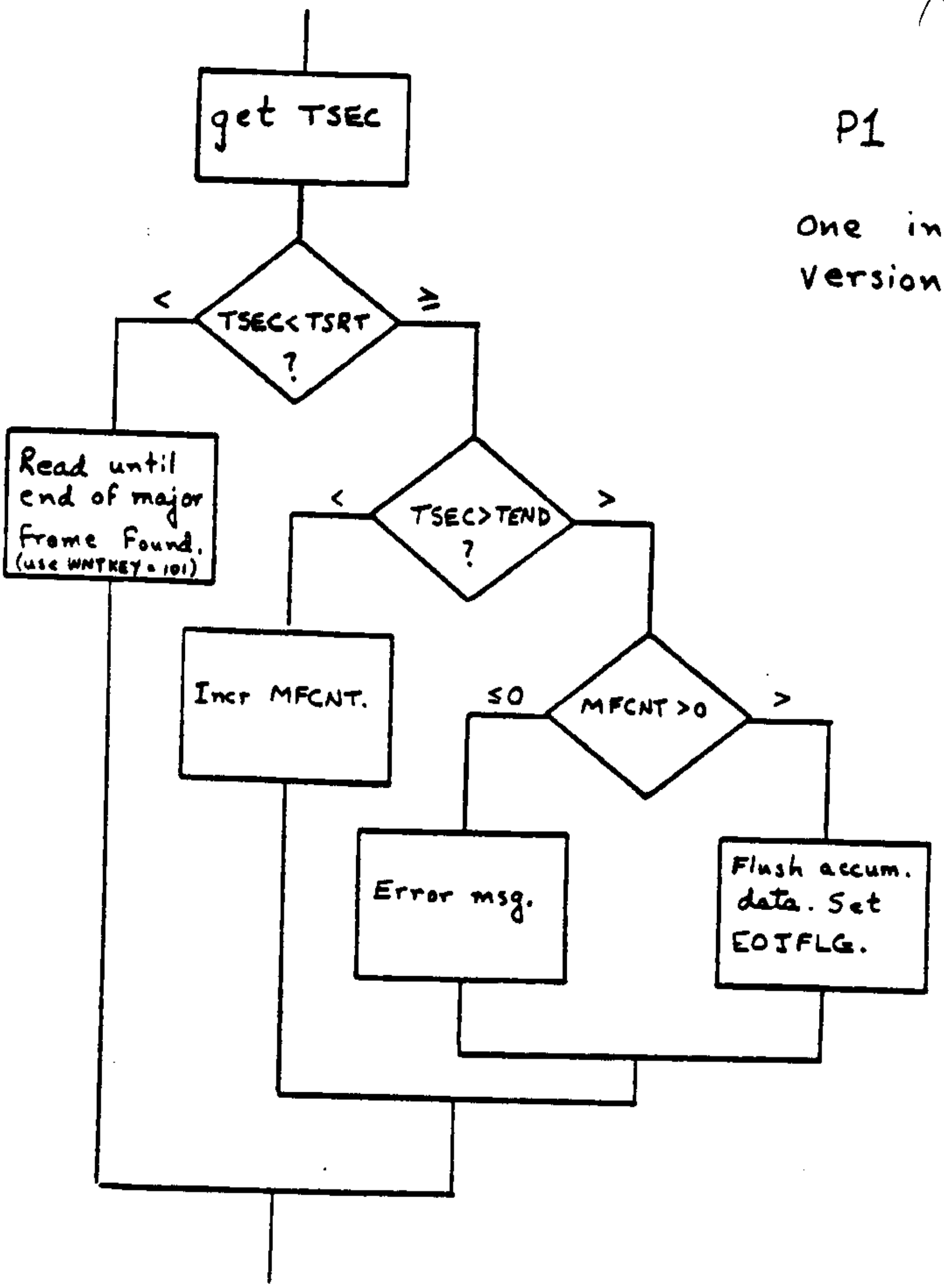

79-1

P7 : If 24 x 64 < ZEST < 28 x 64 and

if STRM (1) > SCUT and

if STRM (2) > SCUT and

if NC $\frac{(1 \to X,\ 1 = \text{rad no.})}{6} = \frac{NC(1,2)}{6}$ and

if $\frac{NC\ (2 \to Z,\ 1)}{6} = \frac{NC(2,2)}{6}$ and

if tag bits are OK and

if at least 5 of the 8 Cerenkov meet some consistency criteria then

calculate NCX = NC(1,1)/6 and
NCZ = NC(2,1)/6 and
CKV = mean of good tubes and

increment CKVCNT(NCX,NCZ) by 1 and
CKVSUM(NCX,NCZ) by CKV and
CSQSUM(NCX,NCZ) by CKV**2.

P8,9,10,11,13,15 : Ignore these chapters.

P100: Ignore

P101: Ignore. NROV must be not set

P102: Ignore

P103: Request new tape. If available continue.
If not available, flush data and set EOJFLG.

79-1

III. Examples

C. Application of Map

This job will run from BOT to EOT. Input in chapters 0-15 and 100-103. All except 0,7, and 11 are output without modification. Chapters 7 and 11 have one verse added to contain mapped pulse heights. Chapter 0 is modified to specify new chapter lengths and new verse pointers. Thus the processes are:

P0:	Modify and flush.
P7,P11:	Calculate and add new verse, then flush.
P1,P2 :	Flush
P103 :	Set EOJFLG and flush.

C-3 -1

HEAO C-3 INTERNAL REPORT

No. TLG - 22
Date 4/01/83
By Tom G
Page 1 of

Re: New "gold" & "cobalt" programs

Abstract, Introduction, Etc: Descriptions for programs shown in this flow chart.

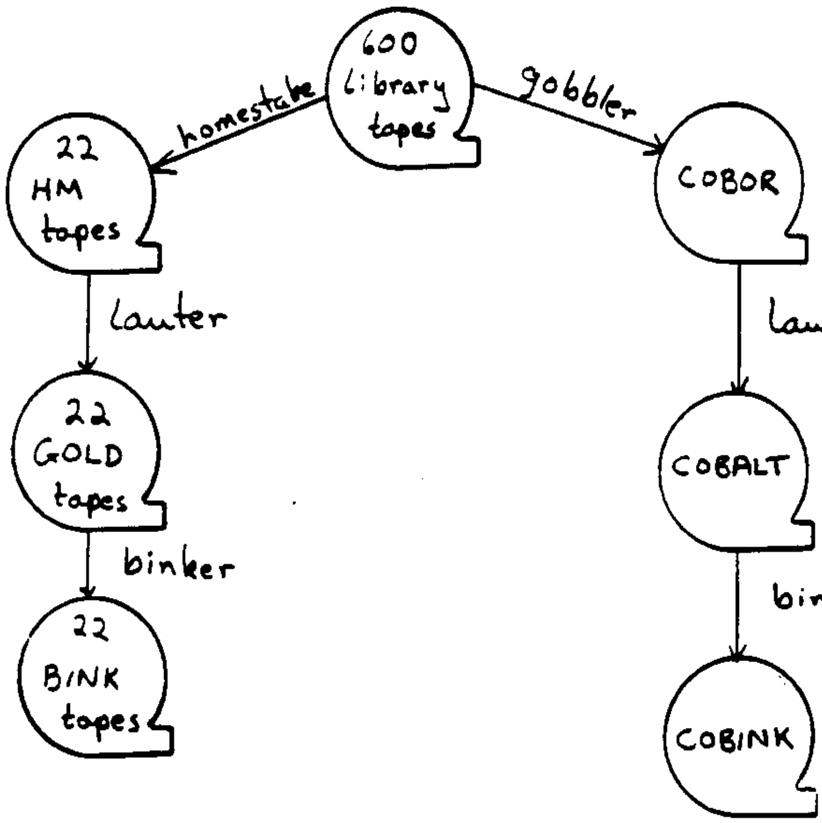

Distribution:

CIT
- E. C. Stone
- ✓ T. L. [redacted]
- ✓ B. W. Gauld
- K. E. Krombel
- ✓ N. S. Collins
- ✓ S. E. Mjolsness
- ✓ B. Newport

WU/MDRL
- ✓ J. Klarmann
- ✓ M. D. Jones
- ✓ W. R. Binns
- ✓ D. Grossman
- ✓ M. H. Israel

UM
- ✓ C. J. Waddington
- R. K. Fickle

- N. R. Brewster

C3-2

HOMESTAKE; a new, improved GOLDMINE
revised 11/23/81
revised 3/9/82
revised 7/29/82

Purpose: Save all events with any chance of being high Z, i.e., above about 30 Also, save a known fraction of the iron for normalization purposes. Do this in a manner which does not depend on chapter number, i.e., 7, 11, 12, 13, or 14.

Input: Library tapes, M version only.

Selections: Reject data quality and SAA problems. Reject Z < 20 and most Z < 30.

Processing: Careful charge estimates in the selections. Create improved chapter 12's and condense 2's, 4's, and 15's into 20's.

Output: Gold ore tapes, called gore tapes. HM

Program Outline:

get a chapter
do that chapter process
loop until operator says quit
output a chapter 99
quit

chapter processes:

1... --time chapter
Output chapter 1 as read
if (dqf or SAA or readerr) {clear svrf(a);
clear svrf(b);}

clear dqf, readerr, SAA, srcflg --output all chapter 1's so we can keep track of sample time
calculate SAA from lat and lon

2... --data quality
calculate dqf
(NFF>10 or NSNE>20)
save NFF, NSNE for chapter 20

3...
save data for use in convert subroutine.
Output nothing.

4...
save ISNG, DSNG, VNRT from RATE verse and entire STAT verse for chapter 20.
calculate the status funny flag.

5...
Note -- there will almost always be more than one chapter 5 per major frame.
Output the chapter 5

6...
Output the chapter 6

--acquisition label

15...
Save NRMCN, NRMRT, HICN, HIRT, ALCN, FILLCN for use in chapter 20.
Set dqf if FILLCN > 10.
Calculate srcflg.
Output chapter 20.

7,11,14...
```
increment rejcnt(1)
if (SAA) reject(5)
if (dqf) reject(9)
fixckv
if (high Z) outhi
if (low Z and lucky) outlow
if (svrf(a/b)) outlow
else
  reject(13-15), if zflg= 13-15 from high Z test
  else reject(11)
```
Note -- All the if branches above end with breaks, hence only one branch will be executed.

8...
```
if (svrf(a/b)) {output chapter 8;
                clear svrf(a/b); }
```

9,10...
break

C3-4

```
12...
increment rejcnt(1)
if (SAA) reject(5)
if (dqf) reject(9)
fixckv
if (high Z) {if not(convert) out12; else outhi;}
if (low Z and lucky) {if not(convert) out12; else outlow;}
if (svrf(a/b)) {if not(convert) out12; else outlow;}
else
  reject(13-15), if zflg= 13-15 from high Z test
  else reject(11)


13...
increment rejcnt(1)
if (SAA) reject(5)
if (dqf) reject(9)
if (not[prehiz or lucky# or svrf(a/b)]) reject(11)
if (not[convert]) out13
if (high Z) outhi
if (low Z and lucky#) outlow
if (svrf(a/b)) outlow
else
  outlow, with chp 21 gflg 200 set
  reject(13-15), if zflg= 13-15 from high Z test
  else reject(11)

Note# -- The second lucky equals the first, it is not a new call.


98,99...
break


100...                                          -- end of major frame
if (SAA or dqf or readerr or srcflg)
        {clear svrf(a); clear svrf(b)}
clear SAA, dqf, readerr, srcflg
output chapter 100 as read from input tape.


103 or 0...
output a chapter 98


other chapter numbers...
break
```

C3-5

subroutine notes:

convert -
take vnro and calculate a chapter 12 as in libgen or goldmine except with updates on tag bits.
Return true if conversion possible, false if conversion impossible.
See additional notes below.

outhi -
set svrf(a/b)
output 7,11,12,14
calculate lucky
output flag chapter (21) with high Z and lucky flag
for chapter 12's, output a chapter 28
increment rejcnt(50)
increment rejcnt(51)
break

--svrf declares that we want to save repeats or possible repeats of this event.

outlow -
output 7,11,12,14
output flag chapter (21) with lucky, low Z, and svrf flags
for chapter 12's, output a chapter 28
clear svrf(a/b)
increment rejcnt(50)
break

out13 -
output chapter 13
output flag (21) chapter with prehiz, svrf, lucky flags
break

reject -
increment reject counter at index
break

dqf -
set if (FILLCN > 10 or NFF > 10 or NSME > 20)

readerr -
set if a record on the input tape has a hard error. No data is processed from that record. All further data from this major frame is flagged in chapter 21's and 20's.

prehiz -
event must have (large ion signal and high cutoff) or (large ion and moderate cerenkov) or (large cerenkov) to pass this test. Large ion means at least 2 pulse heights above 600 or an hld. Moderate cerenkov means at least 2 pulse heights above 200. Large cerenkov means at least 2 above 500 or at least 1 above 1000.

status funny -
Status if funny if HV is off or other things tbd. HV off is determined from chapter 4 status and analog data shown below.

```
ICDM    current v3, byte 25  iccr
        voltage v3, byte 26  icv
        status  v1, byte 15&010  ibias
DDM     current v3, byte 57  dccr
        voltage v3, byte 62  dcv
        status  v1, byte 15&04  dbias
Ckv     status  v1, byte 15&03  ckbias
if(dbias!=0 or 2 < dcv < 0220 or 2 < dccr < 060) set ddmhvflag
if(ibias!=0 or 2 < icv < 0220 or 2 < iccr < 060) set icdmhvflag
if(ckbias!=0) set ckvhvflag
```

srcflg -
This flag is set if any of the alpha counts in chapter 15 (IALCF, IALCB, DALCF, DALCB) is non-zero. It flags contamination by alpha or source mode.

SAA -

```
If (lat<=-345 and 5250<=lon<=5920)
        { if(lat<=-505 or [(lat-5585)/335]**2+[(lon+505)/160]**2 < 1) set SAA }
```

lucky -
For any event being considered, use ranf to generate a random floating point number in the interval 0.0 to 1.0. If ranf < 0.02 the event is lucky.

high Z, low Z -
See picture.

```
if ((zc>30.5 & !tubehit) or zi>50) set zflg= 1
elseif (strm>4GV) {
        if (zi>30.5 or [(11zi+6zc)>500]) set zflg= 1  (high Z)
        elseif (zi>19.5 or [(13zi+6zc)>364])set zflg= 0  (low Z)
        else set zflg = 13
                    }
elseif (strm<2GV and zc<2)      {
        if (zi>50) set zflg = 1
        elseif (zi>19.5) set zflg =0
        else zflg = 14
                                }
else    {
        if (11zi+6zc>500) set zflg = 1
        elseif (13zi+6zc)>364) set zflg = 0
        else zflg = 15
        }
```

where zi = 11.1sqrt(larger of 2 i's) and zc = 57.17sqrt(c)
and i and c are mapped using best available map
and strm is the higher of the 2 strm's even if trkn.

∡ = ZC

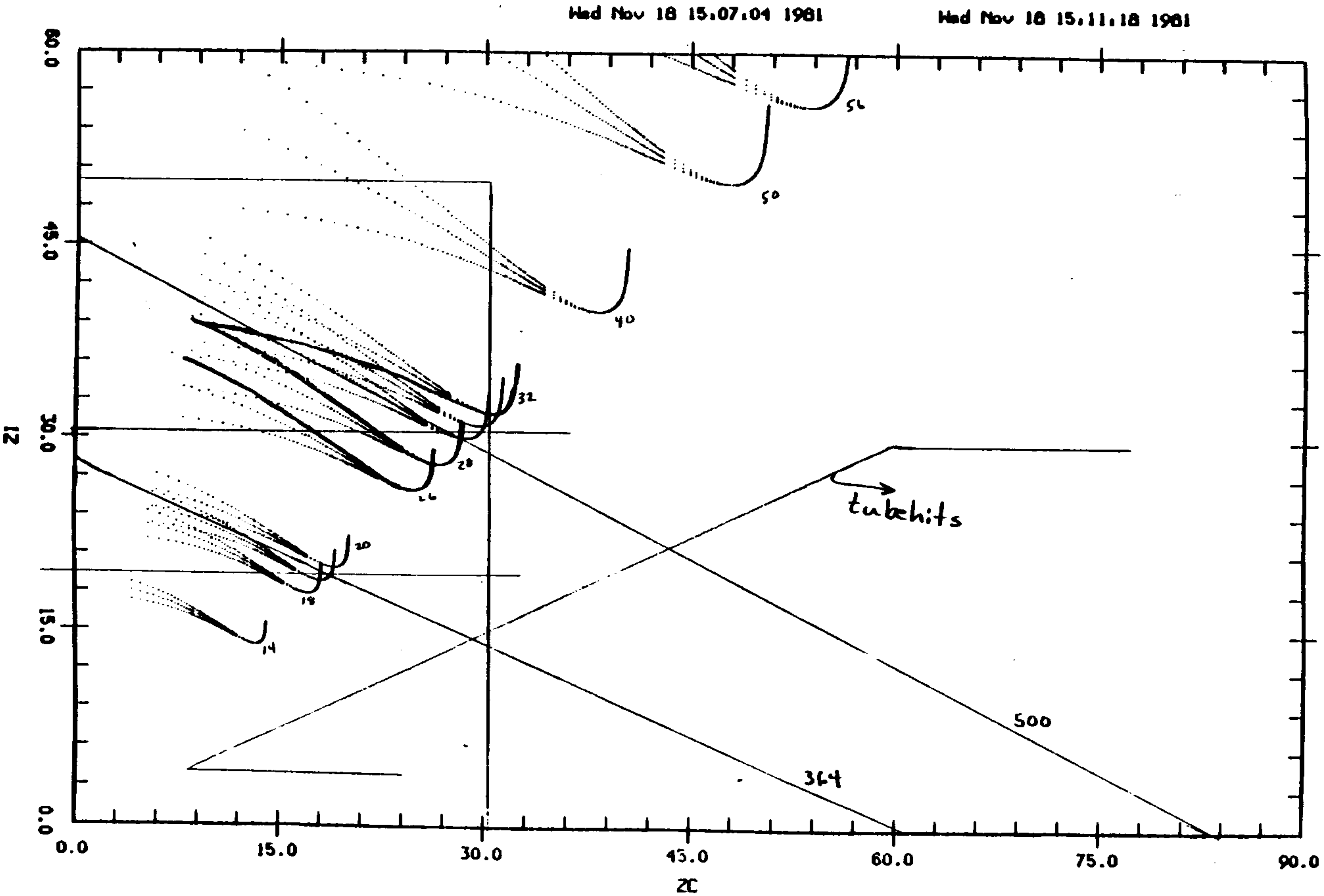

Wed Nov 18 15:07:04 1981
Wed Nov 18 15:11:18 1981
IZ
ZC
0.0
15.0
30.0
45.0
60.0
75.0
90.0
56
50
40
32
28
26
20
18
14
tubehits
500
364

C3-7

C3-8

chapter 20 -
This chapter describes the major frame. It includes data from chapters 2 and 4, dqf, srcflg, readerr, SAA, and status funny flags. It specifies time intervals since the last SAA or status funny and reserves a place for a time interval until the next ditto.

chapter 21 -
This chapter is appended to each 7, 11, 12, 13, or 14. It includes mfn, svrf, lucky, high and low Z, readerr, and prehiz.

chapter 28 -
Appended only to chapter 12's. Contains data from the convert subroutine.

convert -
Additional notes.
Check for ALF on the x-planes. If (ALF) return (failure).
Count how many first addresses. If (<2x or <2z) return (failure).
Label all layers with ALF or without first address as level 6.
Label existing libgen good layers as level 0 and leave them alone.
Check each libgen bad layer for OVFLO, ALF, NFAD, POVF.
    If (ok) label this layer as good, but level 1.
Check each good (i.e., level 0 or 1) layer -- its x or z partner must exist,
    i.e., have a first address. Else, change it to bad (flag level 2).
Count good (i.e., level 0 or 1) layers. If (<2x or <2z) {add in level 2 layers.
    If still (<2x or <2z) return (failure).
    Else set NCFAD and change level 2 layers to good.}
Check each good layer for a 2nd address near the first (6 < difference < 11).
    If (found) set flag level 3 and use all wires in and between the 2 groups to calculate the center of the group. If (larger difference (>=11) and SWTCH) exchange 1st and 2nd addresses and patterns & set flag level 4. If (smaller difference (<7)) set flag level 5)
For each good layer calculate cenw and numw.
Call hodfit, signal, orbitvrs, etc. to polish off this event.
Calculate the chapter 28 data.

fixckv -
Set bit 8 in btag to show that this subroutine has been invoked.
if (at least one cerenkov pulse height is > 1000, but one or more are 0 or 1) then {the signal for the ones at 0 or 1 should be calculated as if they were 4096. Set bit 9 of btag.}

next time -
A test should be included which rejects chapter 14's (and 12's ?) which have one of the funny status bits set in RJTG -- PARP, QBMP, ...

C3-9

BINKER; a new, improved goldhist
4/07/82

revised 4/01/82

Purpose: Calculate a event branch and twig (jbin) for all non-garbage events using a goldhist style tree. Does not assign "the" charge and does not plot histograms -- that should be done in a separate step. For events in the appropriate twigs, KK charge is calculated.

Input: Refinery tapes with chapter 16's.

Selections: None. In particular rejection for fdz, larger SAA, uncertain trajectory, etc., are left for later.

Processing: Calculate jbin using the tree. Calculate KK charge.

Output: Refinery tapes with new chapter 16's. Called gorfin, norfin, ... depending on what ore was input.

Program Outline:

get a chapter
do that chapter process
loop until operator says quit
quit

chapter processes:

1,2,3,4,5,6...
Output as read

7,8,11,12,13,14,15...
Output as read unless it is a 12 or 14 with funny status in RJTG, in which case reject this event including its 16, 21, 28, etc.

16...
Modify by inserting branch and twig, or jbin, (verse 1, index 10) and KK charges (verse 3) or MI charges.
Flag the replacement of trkn by ntn by setting lkn and hkn to 0 (all in htag).

20,21,28...
Copy as read.

98...
Replace with new 98.

99,100...
Copy as read.

other chapter numbers...
Ignore.

C3-10

BINKER; a new, improved goldhist
4/07/82

revised 4/01/82

Purpose: Calculate a event branch and twig (jbin) for all non-garbage events using a goldhist style tree. Does not assign "the" charge and does not plot histograms -- that should be done in a separate step. For events in the appropriate twigs, KK charge is calculated.

Input: Refinery tapes with chapter 16's.

Selections: None. In particular rejection for fdz, larger SAA, uncertain trajectory, etc., are left for later.

Processing: Calculate jbin using the tree. Calculate KK charge.

Output: Refinery tapes with new chapter 16's. Called gorfin, norfin, ... depending on what ore was input.

Program Outline:

get a chapter
do that chapter process
loop until operator says quit
quit

chapter processes:

1,2,3,4,5,6...
Output as read

7,8,11,12,13,14,15...
Output as read unless it is a 12 or 14 with funny status in RJTG, in which case reject this event including its 16, 21, 28, etc.

16...
Modify by inserting branch and twig, or jbin, (verse 1, index 10) and KK charges (verse 3) or MI charges.
Flag the replacement of trkn by ntn by setting lkn and hkn to 0 (all in htag).

20,21,28...
Copy as read.

98...
Replace with new 98.

99,100...
Copy as read.

other chapter numbers...
Ignore.

C3-11

Tree notes:

A jbin type consists of a letter and a number. The letters specify gross type; the numbers specify detailed type withing the letter. (Letters = branches and numbers = twigs if you wish.) The structure of the branches and twigs are specified in attached flow charts and/or in the following tables.

a twigs	test b>700	comments
1	y	resolution is probably OK
0	n	very poor resolution

c twigs	test b>400	test sumitg >1	comments
3	y	y	resolution is probably OK
2	y	n	Dangerously little info.
1	n	y	very poor resolution
0	n	n	garbage

f twigs	test zc"zi	test zc>zi	test th<35	test c first	comments
8	y	-	-	-	zkk unnecessary at high strm
7	n	y	y	-	good, use zc
6	n	y	y	y	interacted, use zc
4	n	y	n	n	garbage
3	n	n	y	-	ugly mixture of 6 & 7
2	n	n	y	y	extreme rel rise
0	n	n	n	n	interacted, use zi or extreme rel rise, use zc.
				-	garbage mixture of 2 & 3

h twig	comments
4	good. calculate zkk but probably use zc
3	interacted, use zc. No zkk.
2	garbage
0	Ugly mixture of 2 & 3.

C3-12

m twigs	test trkn	test E>0.75	comments
2	y	-	use KK knowing fore and aft
1	n	y	fore-aft spreading not too bad. Need zkk's.
0	n	n	fore-aft spreading is quite bad. Need zkk's.

n twigs	comments All twigs need zkk.
7	interaction
6	garbage
4	good
2	Probably an interaction. Take larger i as fore and pre-interaction.
1	Mostly OK. Fore-aft spreading not too bad.
0	Mostly OK. Let rdz => fore chamber.

rdz:
Stands for "relative delta z". Functional equivalent of twdelz. Array of 2 values indexed by direction of travel, i.e., first value calculated assuming pmy is true; second value assuming pmy false. Floating point. Not saved on output tape. In branches h and k rdz is based on change in zi; in n rdz is based on change in zkk. Large rdz means > 6%.

zc~zi:
This comparison requires that .9 < zc/zi < 1.02, using mean i.
0.9 translates to c/i = 0.03053. 1.02 to 0.03922.

zc~fore, aft, between:
This test separates g 12, 14, and 15 and k 0, 2, and 3. If rdz is < 10%, (i.e., in the 6 - 10% range), then zc~fore or zc~aft, whichever is nearer. If rdz > 10%, then ~ requires within 5%, else zc is between fore and aft.

tree

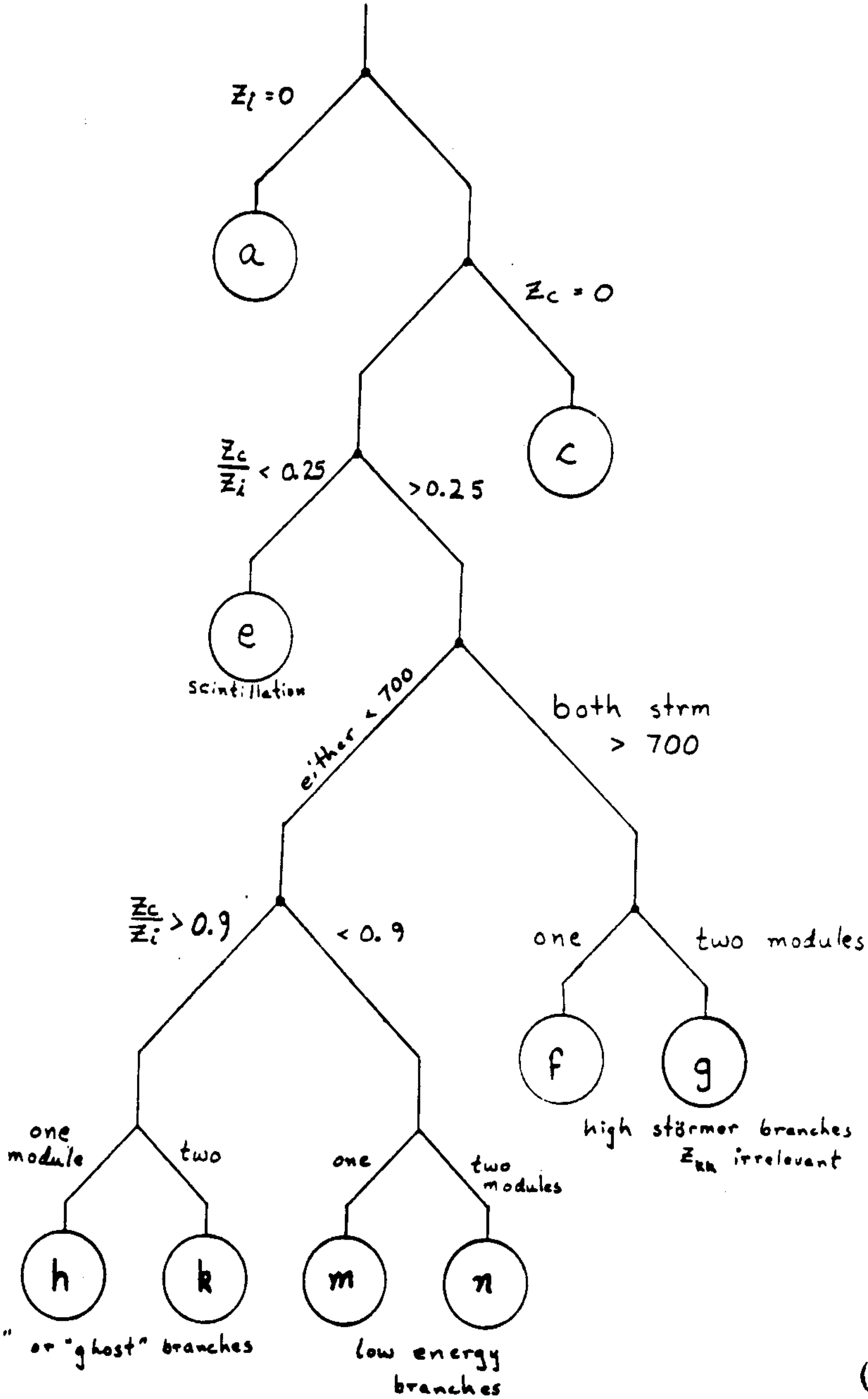
$Z_l = 0$
a
$Z_c = 0$
c
$\frac{Z_c}{Z_i} < 0.25$
> 0.25
e
scintillation
either < 700
both strm > 700
$\frac{Z_c}{Z_i} > 0.9$
< 0.9
one
two modules
f
g
high störmer branches
Z_{kk} irrelevant
one module
two
one
two modules
h
k
m
n
"J" or "ghost" branches
low energy branches

C3-14

branch e

Scintillation region

$Z_c/Z_i < 0.25$

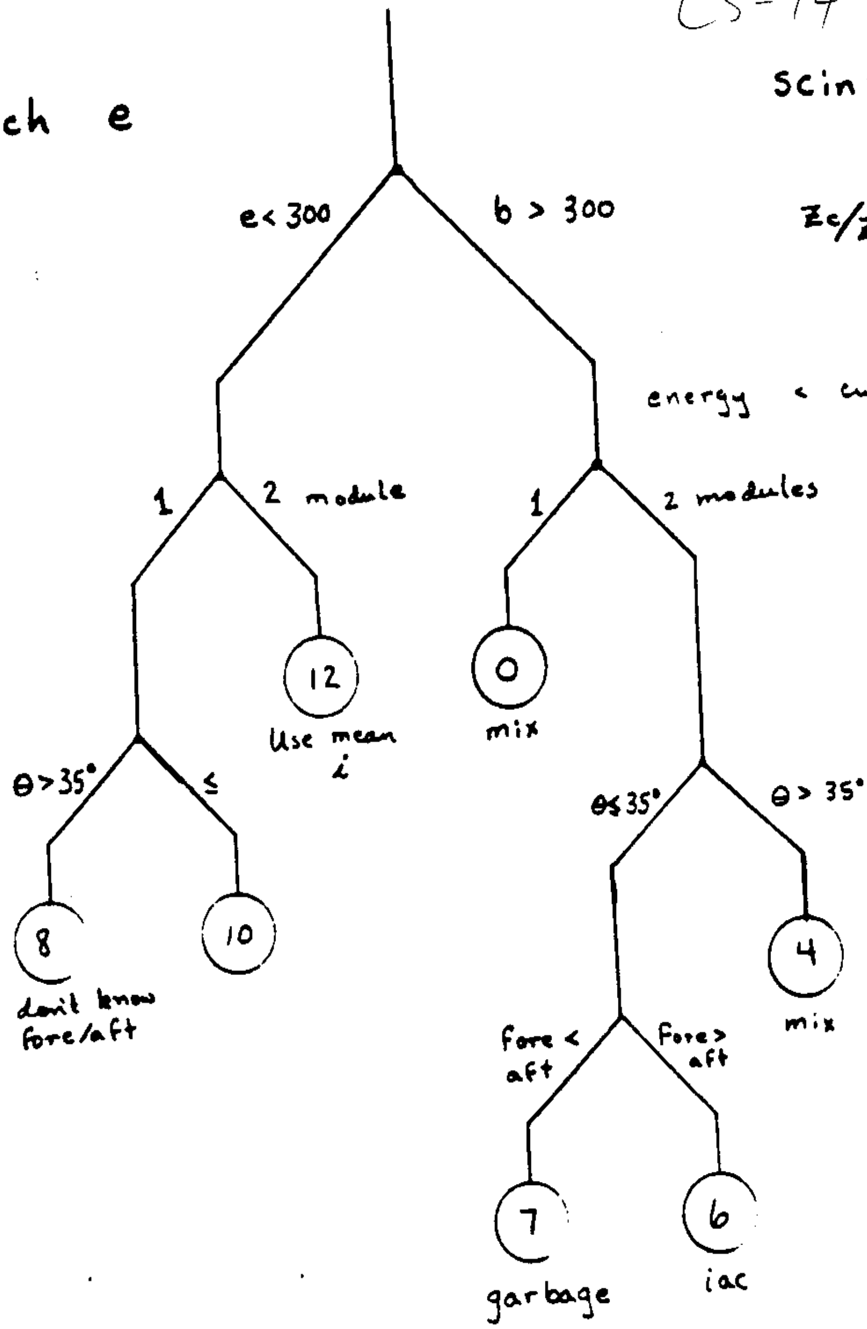

C3-15

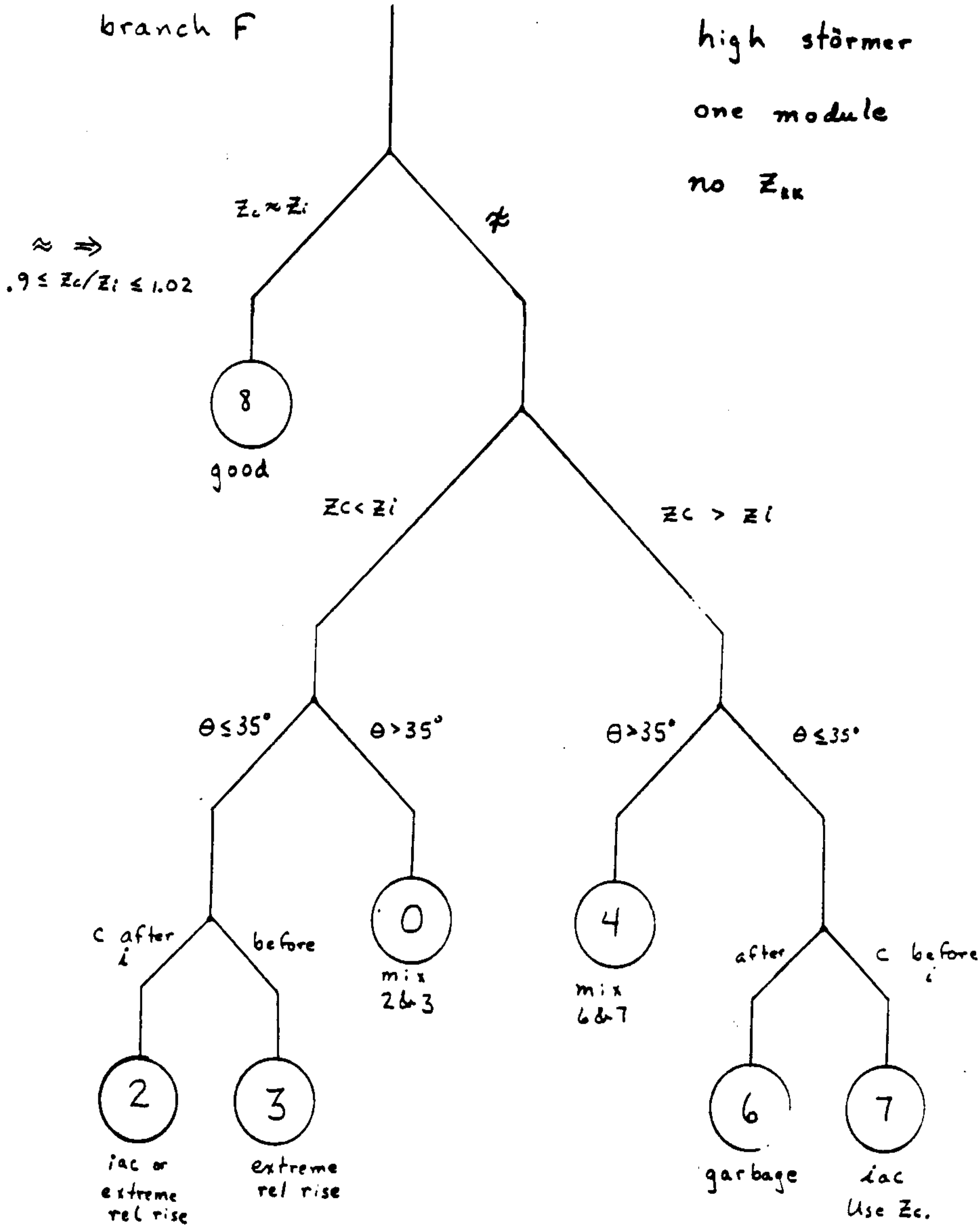
branch F
high störmer
one module
no Z_{xx}
$Z_c \approx Z_i$
$\not\approx$
$\approx \Rightarrow$
$.9 \le Z_c/Z_i \le 1.02$
8
good
$Z_c < Z_i$
$Z_c > Z_i$
$\theta \le 35°$
$\theta > 35°$
$\theta > 35°$
$\theta \le 35°$
c after i
before
0
mix 2&3
4
mix 6&7
after
c before i
2
iac or extreme rel rise
3
extreme rel rise
6
garbage
7
iac
Use Z_c.

g
branch

C3-16

high störmer
two module
no Zxx

≈ ⇒
.9 to 1.02

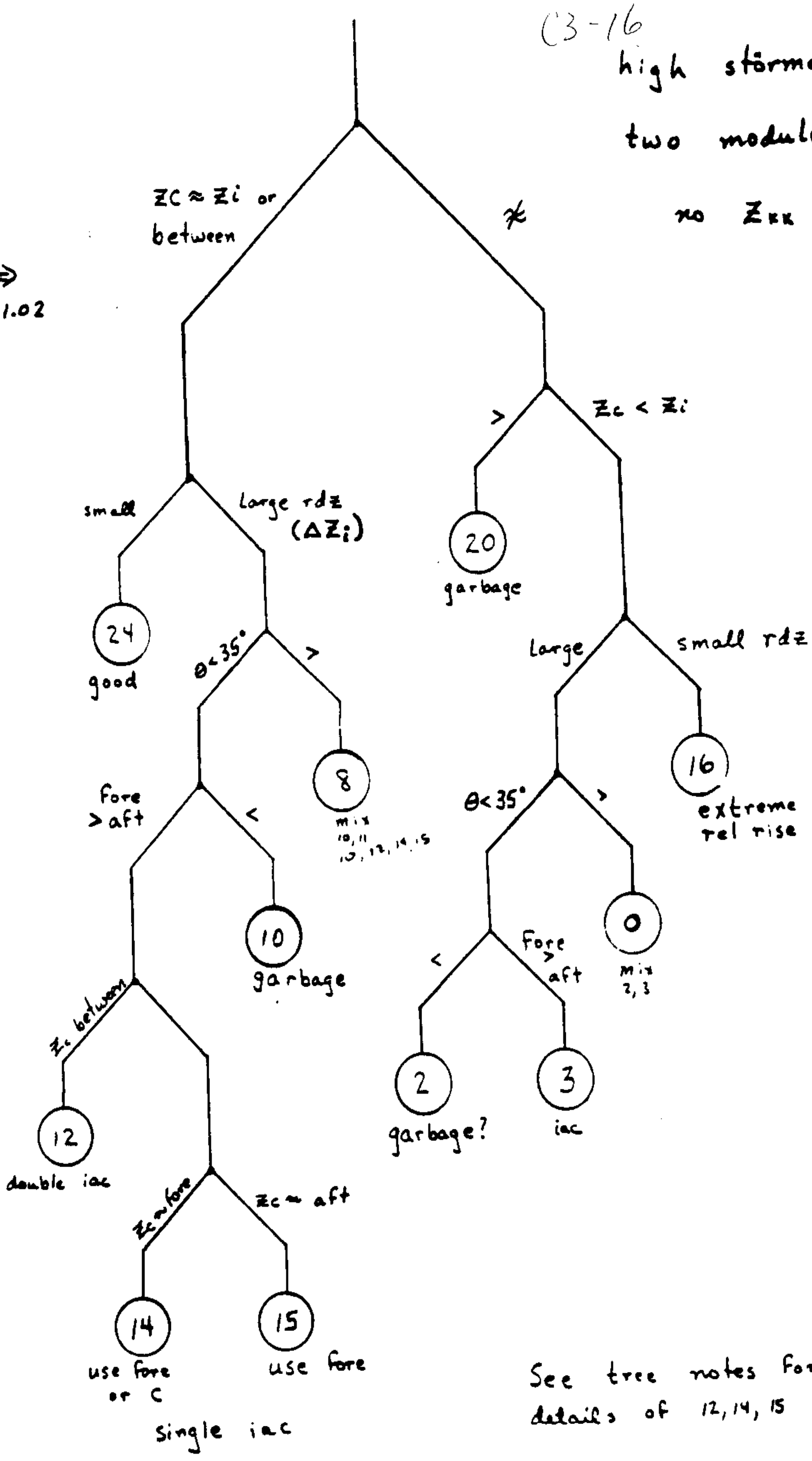

See tree notes for details of 12, 14, 15 choice.

C3-17

branch h

"ghost" region

$Z_c/Z_i > 0.9$ (

one module

$\approx \Rightarrow$
.9 - 1.02

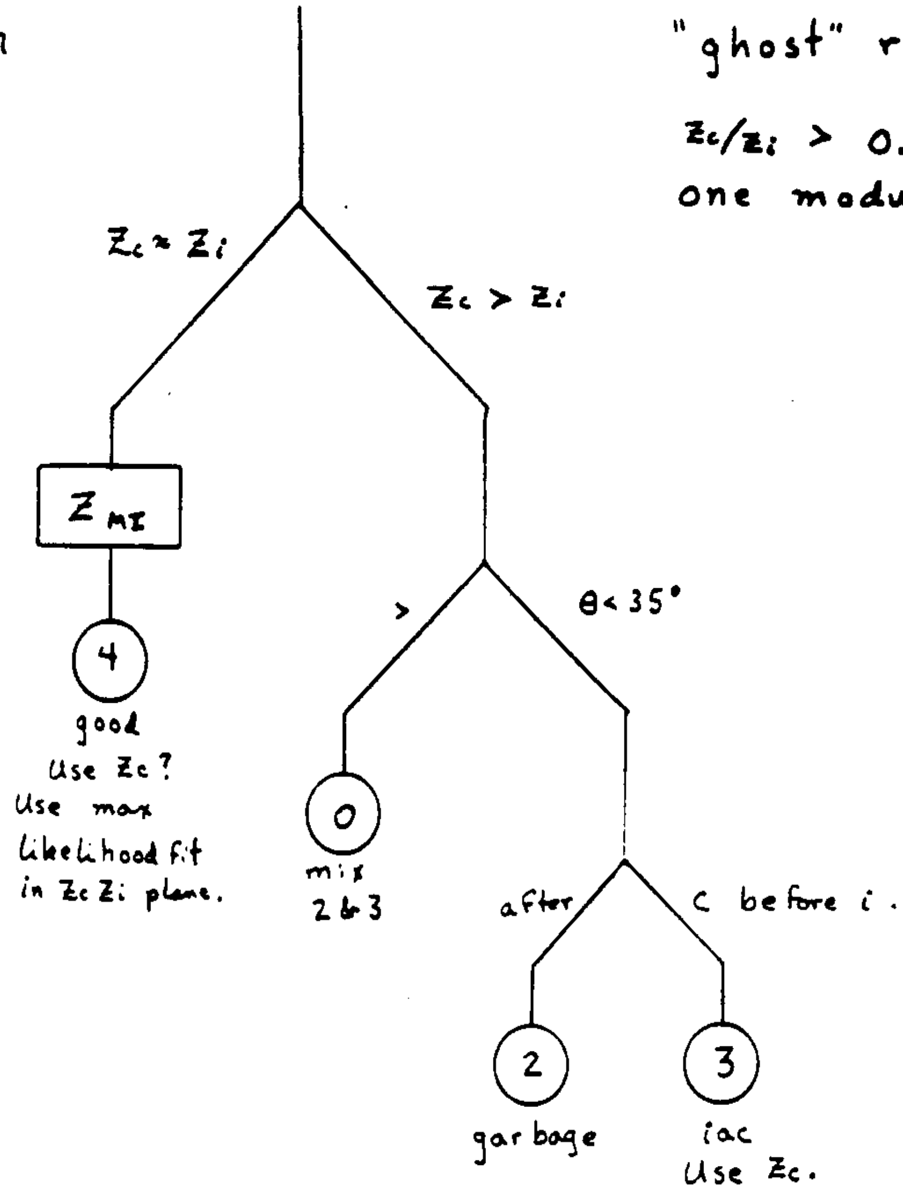

C3-18

branch k

"ghost" region
$Z_c/Z_i > 0.9$
two module

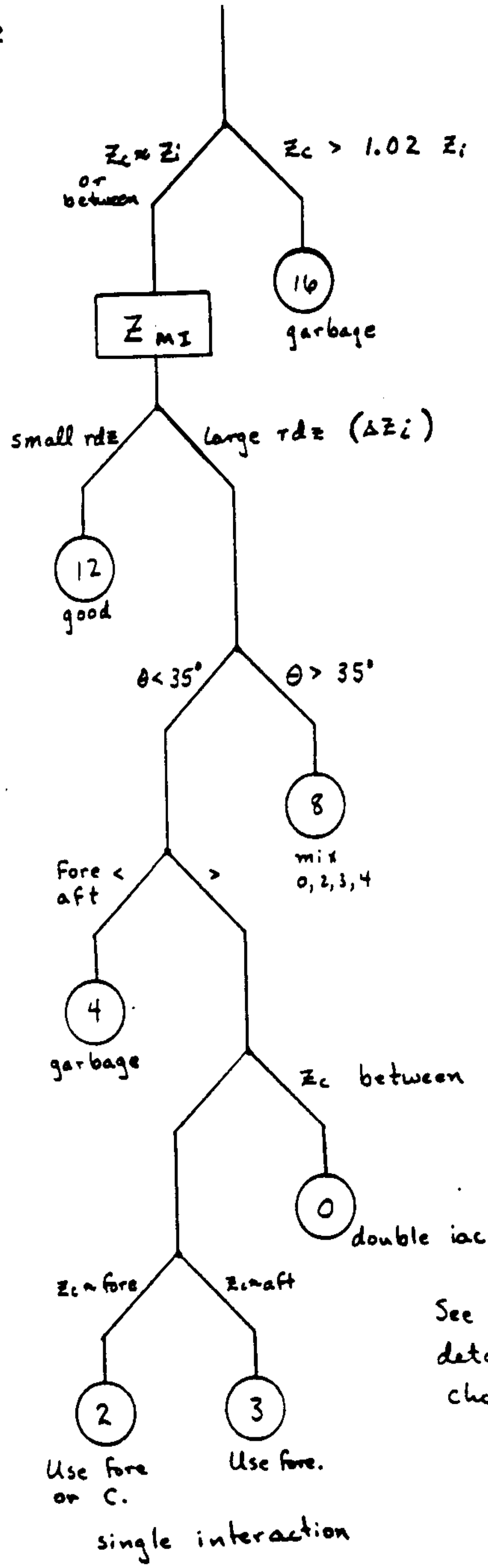

See tree notes for details of 0, 2, 3 choice.

C3-19

branch n

$0.25 \le Z_c/Z_i \le 0.9$
two module

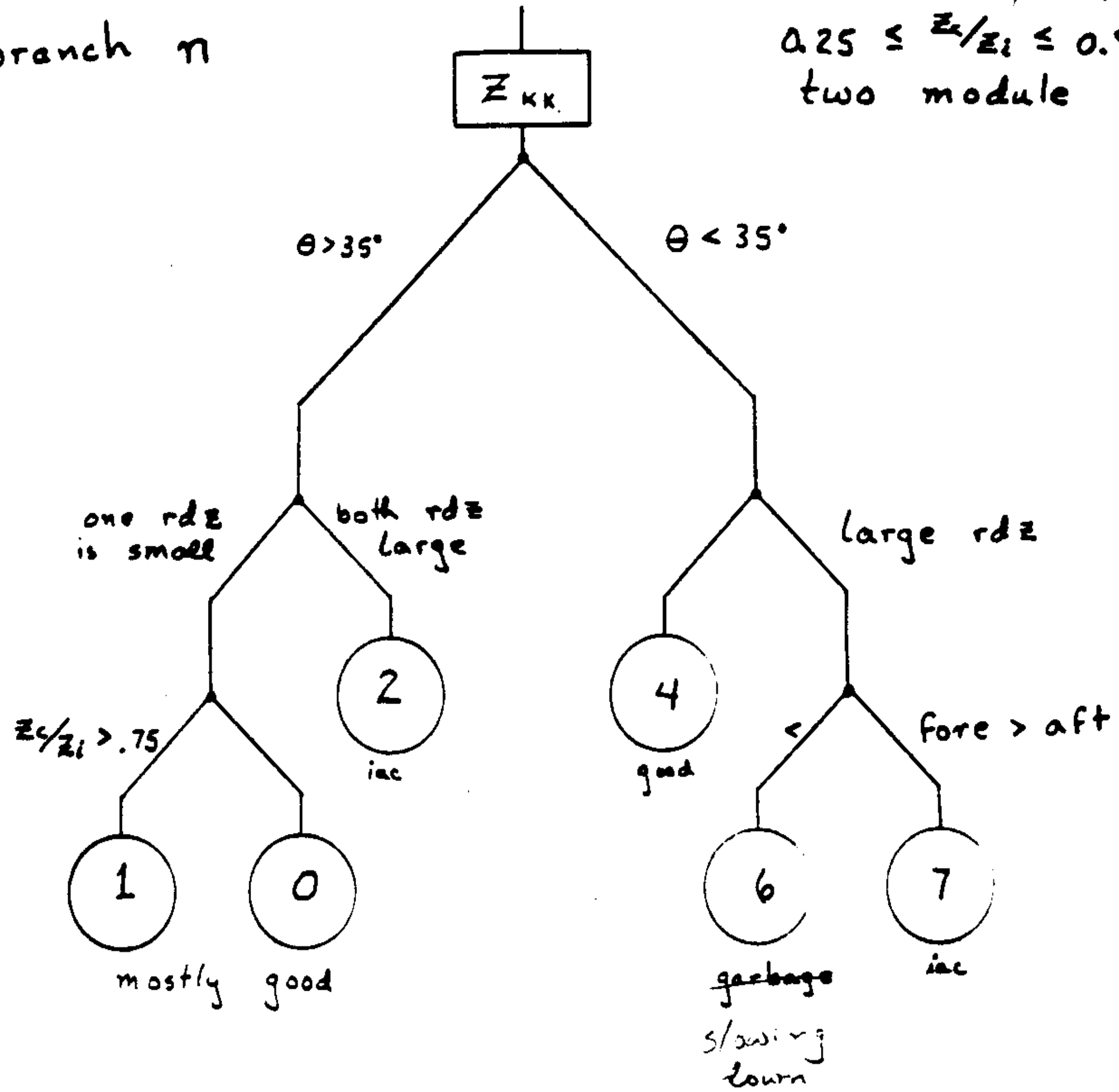

$rdz = \Delta Z_{KK} / Z_{KK}^{mean}$

C3-20

LAUTER; a new, improved refinery
3/9/82
revised 4/01/83

Purpose: Calculate best possible C and I for all non-garbage events.

Input: Normally ore tapes, but library tapes can be used. M version.

Selections: Reject data quality problems, SAA, ... just as in the mining crushers. Do nothing to introduce charge bias.

Processing: Calculate best possible C and I. Include map21, interpolation on map, RKF's low signal correction, WRB ion chamber map, ...

Output: Refinery tapes, with chapter 16's. Called gorfin, norfin, ... depending on what ore was input.

Program Outline:

get a chapter
do that chapter process
loop until operator says quit
output a chapter 99
quit

chapter processes:

1... --time chapter
Output chapter 1 as read --output all chapter 1's so we can keep track of sample time
clear dqf, readerr, SAA, sroflg
calculate SAA from lat and lon

2... --data quality
calculate dqf

3...
break

```
4...
Output the chapter 4.

5...
break

6...
Output the chapter 6.                        --acquisition label

15...
Calculate dqf from FILLCN and "or" with dqf calculated
from chapter 2.
Calculate srcflg.
Output the chapter 15.

7,11,12,14...
clear svtg
increment rejcnt(1)
if (SAA) reject(5)
if (dqf) reject(9)
if (srcflg) reject(10)
if (calibrate event) reject(13)
get best c and i
Calculate relct
Output a chapter 16.
If any z > 40 or if this is a 12 or 14 output the 7, 11, 12, 14.
Set the svtg flag to get 21's and 28's for this event.
Except, throw away "accidental" 12's

8...
Output the chapter 8.

9,10,13...
break
```

C3-22

20...
Output the chapter 20.

21...
if (svtg) output the 21

28...
if (svtg) output the 28
clear svtg

98,99...
break

100...
clear SAA, dqf, readerr, arcflg --end of major frame
output chapter 100 as read from input tape.

103 or 0...
output a chapter 98

other chapter numbers...
Output as read.

C3-23

subroutine notes:

reject -
increment reject counter at index
break

dqf, SAA, readerr, srcflg...
See homestake writeup.

relct -
Calculate as per writeup.

calibrate events -
if dxdy = 0 and dzdy = 0 and NLYR = 8, reject this event.

C3-24

GOBBLER; a new, improved COMINE
2/17/82
revised 1/5/83

Purpose: Select a set of data which has good charge resolution. Do the selection in a fashion which allows normalization to homestake data.

Input: Library tapes, M version only.

Selections: Reject SAA, data quality problems, and source mode. Reject Z < 17.5 and reject scintillating iron.

Processing: Careful charge estimates in the selections. Create improved chapter 12's and condense 2's, 4's, and 15's into 20's.

Output: Cobalt ore tapes, called cobor tapes.

Program Outline:

get a chapter
do that chapter process
loop until operator says quit
output a chapter 99
quit

chapter processes:

1... --time chapter
Output chapter 1 as read
clear dqf, readerr, SAA, srcflg
calculate SAA from lat and lon
--output all chapter 1's so we can keep track of sample time

2... --data quality
calculate dqf
save NFF, NSNE for chapter 20

3...
break

C3-25

4...
save ISNG, DSNG, VNRT from RATE verse and entire STAT verse for chapter 20.
calculate the status funny flag.

5...
Note -- there will almost always be more than one chapter 5 per major frame.
Output the chapter 5

6...
Output the chapter 6 —acquisition label

15...
Save NRMCN, NRMRT, HICN, HIRT, ALCN, FILLCN for use in chapter 20.
Calculate dqf from FILLCN and "or" with dqf calculated from chapter 2.
Calculate srcflg.
Output chapter 20.

7,11,14...
```
increment rejcnt(1)
if (SAA) reject(5)
if (dqf) reject(9)
if (srcflg) reject(10)
if (readerr) reject(31)
if (geomcrit=failure) reject(17)
if (zci<15.0 or zc<5.0) reject(19)
get best c and i
if (zci<17.5 or zc<7.0) reject(21)
output 7,11,14
```
Note -- All the if branches above end with breaks, hence only one branch will be executed.

8...
break

9,10...
break

subroutine notes:

geomcrit -
The geometry criterion is ok if the event is inside the specified boundary at the top, center, and bottom of the instrument. Otherwise return failure.
if (abs(xcn) > 65 cm or abs(zcn) > 50 cm or lckv1 = 0 or lckv2 = 0) return(failure)
xtop = abs(xcn + dxdy*75cm); ztop = similar
if (xtop > 70 cm or ztop > 55 cm) return(failure)
xbot = abs(xcn - dxdy*75cm); zbot = similar
if (xbot > 70 cm or zbot > 55 cm) return(failure)
return(ok)

convert -
take vnro and calculate a chapter 12 as in libgen or goldmine except with updates on tag bits.
Return true if conversion possible, false if conversion impossible.
See additional notes in homestake writeup.

reject -
increment reject counter at index
break

dqf, sroflg, SAA, readerr, status funny -
See the homestake writeup.

chapter 20 --
format for this chapter is specified in the homestake writeup.

```
12...
increment rejcnt(1)
if (SAA) reject(5)
if (dqf) reject(9)
if (srcflg) reject(10)
if (readerr) reject(31)
count chambers using pulse heights
if (<5) reject(23)
convert
if (geomcrit=failure) reject(17)
if (zci<15.0 or zc<5.0) reject(19)
get best c and i
if (zci<17.5 or zc <7.0) reject(21)
output a chapter 12
output a chapter 28


13...
increment rejcnt(1)
if (SAA) reject(5)
if (dqf) reject(9)
if (srcflg) reject(10)
if (readerr) reject(31)
if (not(convert)) reject(27)
if (geomcrit=failure) reject(17)
if (zci<15.0 or zc<5.0) reject(19)
get best c and i
if (zci<17.5 or zc <7.0) reject(21)
output a chapter 12 and a 28.


98,99...
break


100...
clear SAA, dqf, readerr, srcflg          --end of major frame
output chapter 100 as read from input tape.


103 or 0...
output a chapter 98


other chapter numbers...
break
```

DATA CHAPTER FORMATS

revised 12/06/79
revised 12/18/79
revised 06/18/80
revised for M version library generator 07/25/80
revised for other projects 03/01/81
revised 07/26/82
revised 04/14/83

List of Chapters

Chapter	Chapter	Comments
CNTRL	0	Specifies format of chapters 1-99. Has fixed format. One set of these per tape.
MJTIM	1	Time of major frame.
	1	Time of Voyager volume.
DQUAL	2	Data quality flags.
MJAT	3	Attitude data.
SBCM	4	Subcom data.
MJRB	5	Orbit data.
FLBL	6	Decom file label. Once per acquisition.
NRMVN	7	Normal event.
RPTMRK	8	Marker for repeat event.
CALVN	9	Calibration event.
ALFVN	10	Alpha event.
PLSDAT	10	PLS data for merging onto Voyager tapes.
Z31VN	11	Z31 event.
ANRVN	12	Analyzed reject event.
RJHVN	13	Reject event with hodoscope failure.
RJLVN	14	Reject event with logic or other failure.
VNSM	15	Event counts. Once per major frame.
MAGDAT	15	MAG data for merging onto Voyager tapes.
RFKK	16	HNE Refined gold chapter.
ALLZ	17	Extended event analysis.
AVRAT	19	Daily rate and count sums.
MJFSTAT	20	HNE Major frame status chapter.
GLDFLG	21	HNE Goldflag chapter.
IONVN	22	Ion crush event chapter.
IONRS	23	Ion crush rate and sum chapter.
IONRBT	24	Ion crush orbit/SAA data.
ICEDGE	25	Ion chamber edge data.
CNVFLG	28	HNE Chapter 12 conversion flags.
CNTRL1	30	HIST Control chapter for before failure.
CNTRL2	31	HIST Control chapter for after failure.
ISTAT	32	HIST Istrument status chapter.
EVNT	33	HIST Event chapter.
FSTAT1	34	HIST Final status chapter for before failure.

FSTAT2	35	HIST Final status chapter for after failure.
HISTDC	36	HIST Data center tape chapter.
	45	
	46	
	47	
	48	
	49	
	50	
CKSTAT	51	Cerenkov crush status data.
CKMAJ	52	Cerenkov crush major frame data.
CKVNT	53	Cerenkov crush event data.
CKMAP	55	Single element of map.
	60	IMP
	61	IMP
	62	IMP
	68	
	69	
PARAMS	70	IMP Strip. Program input parameters.
PEVNT	71	IMP Strip. Event specifications.
ISTAT	72	IMP Strip. Initial status.
EVNT	73	IMP Strip. Event chapter.
RATE	74	IMP Strip. Rate count chapter.
FSTAT	75	IMP Strip. Final status chapter.
	76	
	77	
	78	
	85	
	92	Comments
APRM	97	Aniso parameters.
INHIST	98	Input history.
RJCN	99	Summary of reject count.
EOMJ	100	End of major frame.
EOR	101	End of record.
EOI	102	End of interval.
EOT	103	End of tape.
EOSF	105	End of single file, but not end of tape.
DSMJ	106	Disposition of major frame.
HIST0	120	Histogram program parameters
HIST1	121	Histogram run data
HIST2	122	Histogram arrays

Chapter number: 0
Chapter name: CNTRL

Verse Name	Verse No.	Item Name	Item Length	Relative Index	Comments
		KEY	2	0	Identifier key = 0.
		spare	2	2	
VRSN	1		28	4	Program version data.
PNTR	2		32	32	Pointer and length data.
				64	

1) Each tape will begin with as many of these chapters as necessary to describe that tape.
2) There is no PNTR verse describing chapter 0; it has a fixed format as specified here.

Verse number: 1 of Chapter 0
Verse name: VRSN

Item Name	Item Length	Relative Index	Comments
PVRS	8	0	Program version date.
EXDT	8	8	Execution date.
TPNM	8	16	Tape Name.
spare	4	24	
		28	

Verse number: 2 of Chapter 0
Verse name: VRSN

Item Name	Item Length	Relative Index	Comments
CHNO	2	0	Number of chapter described by these pointers.
CHLN	2	2	Length of chapter number CHNO.
VPNT	12x2	4	Relative indices, up to 12 verses in CHNO.
VRCN	2	28	Number of verses in chapter CHNO.
spare	2	30	
		32	

Chapter number: 1
Chapter name: MJTIM

Verse Name	Verse No.	Item Name	Item Length	Relative Index	Comments
		KEY	2	0	Key=1
MJTIM	1		26	2	Time of major frame.
				28	

Verse number: 1 of Chapter 1
Verse name: MJTIM

Item Name	Item Length	Relative Index	Comments
RBNO	2	0	Orbit number.
YR	2	2	Year (e.g., 79, 80, 81)
DOY	2	4	Day of year (1-366)
MOD	4	6	Millisecond of day.
SCCK	4	10	Spacecraft clock.
TMSC	4	14	Time in 32-msec. units since 1-Jan-79.
LAT	2	18	Latitude -- M versions only
LON	2	20	Longitude -- M versions only
LMCI	2	22	McIlwain L value in kilometers. -- M versions only
spare	2	24	
		26	

Chapter number: 2
Chapter name: DQUAL

Verse Name	Verse No.	Item Name	Item Length	Relative Index	Comments
		KEY	2	0	Key=2
MJFF	1		2	2	Major frame flags.
DFF	2		128	4	Data flag field.
				132	

Verse number: 1 of Chapter 2
Verse name: MJFF

Item Name	Item Length	Relative Index	Comments
NFF	1	0	Number of fill frames.
NSNE	1	1	Number of frames with sync error.
		2	

Verse number: 2 of Chapter 2
Verse name: DFF

Item Name	Item Length	Relative Index	Comments
DFF	128x1	0	Minor frame data flag field.
		128	

Word Index: 2 of Chapter 2
Word name: DFF

Bit No.	Bit Name	Comments
7	FILL	1 --> Fill data
6		
5		
4	NBE	
3	NBE	Number of bit errors in
2	NBE	minor frame sync word.
1	NBE	
0	NBE	

Chapter number: 3
Chapter name: MJAT

Verse Name	Verse No.	Item Name	Item Length	Relative Index	Comments
		KEY	2	0	Key=3
		spare	2	2	
ECEN	1		4	4	Center of Earth.
ATDT	2		24	8	Data, minor frame 0.
ATDT	3		24	32	Data, minor frame 16.
.	.		.	.	.
.	.		.	.	.
.	.		.	.	.
ATDT	8		24	152	Data, minor frame 96.
ATDT	9		24	176	Data, minor frame 112.
				200	

Verse number: 1 of Chapter 3
Verse name: ECEN

Item Name	Item Length	Relative Index	Comments
THTE	2	0	Theta (the azimuthal angle).
PHIE	2	2	Phi (the polar angle).
		4	

Direction of center of earth in spacecraft coordinates.
All angles in milliradians.

Verse number: 2-9 of Chapter 3
Verse name: ATDT

Item Name	Item Length	Relative Index	Comments
MNN	2	0	Minor frame number.
AFF	2	2	Attitude flag field.
EANG	3x2	4	Euler angles of S/C to Z-A transform.
LAT	2	10	Latitude.
LON	2	12	Longitude.
RAD	2	14	Radial distance (km).
BANG	2x2	16	Polar and azimuthal angles of B field.
ZENY	2	20	Zenith angle of s/c Y axis.
AZY	2	22	Azimuth angle of s/c Y axis.
		24	

All angles in milliradians.

Chapter number: 4
Chapter name: SBCM

Verse Name	Verse No.	Item Name	Item Length	Relative Index	Comments
		KEY	2	0	Key=4
		spare	2	2	
STAT	1		16	4	Status.
RATE	2		40	20	C3 rates.
ANSD	3		80	60	Analog subcom data.
C1RT	4		16	140	C1 rates.
SCAN	5		24	156	Spacecraft analog data.
				180	

Verse number: 1 of Chapter 4
Verse name: STAT

Item Name	Item Length	Relative Index	Comments
	1	0	SCS 80, left PM A,B gain.
	1	1	SCS 81, left PM B,C gain.
	1	2	SCS 82, left D gain, etc.
	1	3	SCS 83, left ramp select, etc.
	1	4	SCS 96, right PM A,B gain.
	1	5	SCS 97, right PM B,C gain.
	1	6	SCS 98, right D gain, etc.
	1	7	SCS 99, right ramp select, etc.
	1	8	SCS 120, LLD disable.
	1	9	SCS 121, Hodo 1-3 disable, etc.
	1	10	SCS 122, ILD 1-3 disable, etc.
	1	11	SCS 123, HLD 1-5 disable, etc.
	1	12	SCS 124, X4, Z4, hodo 4, etc.
	1	13	SCS 125, TMOD, etc.
	1	14	SCS 126, ignore x4, etc.
	1	15	SCS 127, cal sys, ckov power, etc.
		16	

Command status data. Set to 0 for poor data quality.
SCS = subcom state. See separate subcom document.

Verse number: 2 of Chapter 4
Verse name: RATE

Item Name	Item Length	Relative Index	Comments
ISNG	2	0	ICDM singles rate. Prescaled by 4.
DSNG	2	2	DDM singles. Prescaled by 4.
IHOD	2	4	ICDM hodo. Prescaled by 8.
DHOD	2	6	DDM hodo. Prescaled by 8.
VNRT	2	8	Event rate.
HZRT	2	10	HIZ rate.
IALF	2	12	ICDM alpha rate. Prescaled by 8.
DALF	2	14	DDM alpha rate. Prescaled by 8.
LFC4	2	16	Left C4.
LFC2	2	18	Left C2.
LFC1D	2	20	Left C1D.
LFC1C	2	22	Left C1C.
LFC1B	2	24	Left C1B.
LFC1A	2	26	Left C1A.
RTC4	2	28	Right C4.
RTC2	2	30	Right C2.
RTC1D	2	32	Right C1D.
RTC1C	2	34	Right C1C.
RTC1B	2	36	Right C1B.
RTC1A	2	38	Right C1A.
		40	

Note: If data quality is poor, rate will be set to 0.

Verse number: 3 of Chapter 4
Verse name: ANSD

Item Name	Item Length	Relative Index	Comments
ANLG	80	0	Data from SCS 0-79. See separate subcom doc.
		80	

Verse number: 4 of Chapter 4
Verse name: ClRT

Item Name	Item Length	Relative Index	Comments
PLLD	4	0	Plastic low-level discriminator.
XULD	4	4	Crystal upper-level discriminator.
PULD	4	8	Plastic upper-level discriminator.
XLLD	4	12	Crystal low-level discriminator.
		16	

Floating point counts/second. Only small part of total data is saved.
Negative number indicates poor data quality.

Verse number: 5 of Chapter 4
Verse name: SCAN

Item Name	Item Length	Relative Index	Comments
SCNLG	22	0	Data from production tape table IIIc. See seperate subcom documentation.
BUSV	2	22	Bus voltage from minor frame word 156, SCS 1 (Production tape table V).
		24	

Chapter number: 5
Chapter name: MJRB

Verse Name	Verse No.	Item Name	Item Length	Relative Index	Comments
		KEY	2	0	Key=5
		spare	2	2	
MJRB	1		36	4	Orbit data for times in major frame.
				40	

Verse number: 1 of Chapter 5
Verse name: MJRB

Item Name	Item Length	Relative Index	Comments
TMSC	4	0	Time in 32-msec. units since 1-Jan-79.
RBNO	2	4	Orbit number.
TYPE	1	6	Type of data (regular, asc. node, SAA, etc.).
SHFL	1	7	Shadow flag.
SESA	2	8	Sun-earth-satellite angle.
HRZA	2	10	Horizon angle.
RCMP	3x2	12	Components of position vector (km).
VCMP	3x2	18	Components of velocity vector (m/sec).
BMAG	4	24	Magnitude of B field (gamma).
BCMP	3x2	28	Unit vector components of B (x16k).
LMCI	2	34	McIlwain L value (km).
		36	

All angles in milliradians.

Chapter number: 6
Chapter name: FLBL

Verse Name	Verse No.	Item Name	Item Length	Relative Index	Comments
		KEY	2	0	Key=6
DECOM	1		126	2	From GSFC decom label record.
				128	

Verse number: 1 of Chapter 6
Verse name: DECOM

Item Name	Item Length	Relative Index	Comments
DOYB	2	0	Begin day of data.
MODB	4	2	Millisecond of day - begin.
MODE	4	6	Millisecond of day - end.
DOYE	2	10	End day of data.
PDF	2	12	Leave in EBCDIC.
STDN	4	14	Station number.
FNM	16	18	Pre-edit file Name, EBCDIC.
DCNM	4	34	Decom number.
RLNM	4	38	Decom reel number.
NMJ	2	42	Number of major frames in file.
NBE	2	44	Number of sync word bit errors.
NFL	2	46	Number of filled minor frames.
YR	2	48	Year of data - 1900.
RBPRM	76	50	19 Floating point numbers from decom label beginning at offset = 80.
		126	

Chapter number: 7
Chapter name: NRMVN

Verse Name	Verse No.	Item Name	Item Length	Relative Index	Comments
		KEY	2	0	Key = 7
		spare	2	2	
TAG	1		18	4	Event tag bits, etc.
HODO	2		12	22	Path through instrument.
ORBT	3		20	34	Location & path re earth.
SGNL	4		66	54	PHA's & similar data.
				120	

Note: See chapter 11 (Z31VN) for descriptions of the verses in this chapter.

Chapter number: 8
Chapter name: RPTMRK

Verse Name	Verse No.	Item Name	Item Length	Relative Index	Comments
		KEY	2	0	Key = 8
FN	1		2	2	Frame numbers.
				4	

Verse number: 1 of Chapter 8
Verse name: FN

Item Name	Item Length	Relative Index	Comments
CFN	1	0	Current minor frame number.
PFN	1	1	Initial minor frame number.
		2	Most Significant Bit indicates A/B buffer.

Chapter number: 9
Chapter name: CALVN

Verse Name	Verse No.	Item Name	Item Length	Relative Index	Comments
		Key	2	0	Key = 9
		spare	2	2	
VNRO	1		60	4	Event readout.
				64	

Note: See chapter 11 (Z31VN) for description of the VNRO verse.

Chapter number: 10
Chapter name: ALFVN

Verse Name	Verse No.	Item Name	Item Length	Relative Index	Comments
		KEY	2	0	Key = 10
ALFDT	1		26	2	Useful data from event.
				28	

Verse number: 1 of Chapter 10
Verse name: ALFDT

Item Name	Item No.	Relative Index	Comments
CDSP2	2	0	Channel number from chamber 2.
CDSP5	2	2	Channel number from chamber 5.
Z1AP1	2	4	Z1 first address and pattern.
Z2AP1	2	6	Z2 first address and pattern.
Z3AP1	2	8	Z3 first address and pattern.
Z4AP1	2	10	Z4 first address and pattern.
X1AP1	2	12	X1 first address and pattern.
X2AP1	2	14	X2 first address and pattern.
X3AP1	2	16	X3 first address and pattern.
X4AP1	2	18	X4 first address and pattern.
DISC	1	20	LLD's and COR.
ILD	1	21	ILD's.
HLD	1	22	HLD's.
XZD	1	23	Hodo discriminators.
ETC	1	24	HIZ, RMOR, RONE, BMP, and ABF.
MFN	1	25	Minor frame number.
		26	

Chapter number: 11
Chapter name: Z31VN

Verse Name	Verse No.	Item Name	Item Length	Relative Index	Comments
		KEY	2	0	Key = 11
		spare	2	2	
TAG	1		18	4	Event tag bits, etc.
HODO	2		12	22	Path through instrument.
ORBT	3		20	34	Location & path re earth.
SGNL	4		66	54	PHA's & similar data.
VNRO	5		60	120	Event readout.
				180	

Verse number: 1 of Chapter 11
Verse name: TAG

Item Name	Item Length	Relative Index	Comments
BTAG	2	0	Event tag bits.
HTAG	2	2	Hodoscope tag bits.
DISC	2	4	LLD, COR, and GL (i=1,8).
ZEST	4x2	6	Estimated charge (x64). ZC, ZCI, ZCI1-3, ZCI4-6.
CHISQ	2x2	14	Reduced chi squared of least squares fit to X and Z data (x64).
		18	

Word Index: 0 of Verse 1 of Chapter 11
Word name: BTAG

Bit No.	Bit Name	Comments
15	HIZ	From VNRO data. Repeat events are output only if they differ from previous readouts in some unexpected fashion.
14	RONE	
13	RMOR	
12	HZB	
11	ABF	
10	DGAP	Time or DQ gap in data (M versions only)
9		
8		
7		
6	MFN	
5	MFN	
4	MFN	Minor frame number.
3	MFN	
2	MFN	

1	MFN
0	MFN

Word Index: 2 of Verse 1 of Chapter 11
Word name: HTAG

Bit No.	Bit Name	Comments
15	RMLT	One or more V2A's (second addresses).
14	RHOL	One or more patterns with holes.
13	REDG	One or more patterns at edge of hodo.
12	RNWR	One or more NWIR problems.
11	FXHL	One or more holes was fixed.
10	LKN	Trajectory known for low energy particles.
9	HKN	Trajectory known for high energy particles.
8	CPOS	Position of Cerenkov system could cause problem (edge, hole).
7	TRKN	Sense of trajectory known.
6	EXIT	Particle exitted through sidewall.
5	ENTR	Particle entered through sidewall.
4	PMY	Set if flip necessary to get THTA < pi/2.
3		
2	NLYR	
1	NLYR	Number of layers with pattern
0	NLYR	error (MULT, HOLE, EDGE, NWIR).

Word Index: 4 of Verse 1 of Chapter 11
Word name: DISC

Bit No.	Bit Name	Comments
15	COR	Cerenkov "OR".
14		
13	LLD6	Low level disc's.
12	LLD5	
11	LLD4	
10	LLD3	
9	LLD2	
8	LLD1	
7	GLZ4	Good layer bits.
6	GLZ3	
5	GLZ2	
4	GLZ1	
3	GLX4	
2	GLX3	
1	GLX2	
0	GLX1	

Verse number: 2 of Chapter 11
Verse name: HODO

Item Name	Item Length	Relative Index	Comments
XCN	2	0	Intercept (mm) and slope
ZCN	2	2	(x8K) of particle trajectory
DXDY	2	4	in spacecraft coordinates.
DZDY	2	6	
SCAZ	2	8	Azimuth angle of above from z toward x.
SCEL	2	10	Cosine (x16K) of polar angle from y.
		12	

L5 and M versions only.

Verse number: 3 of Chapter 11
Verse name: ORBT

Item Name	Item Length	Relative Index	Comments
LAT	2	0	Latitude.
LON	2	2	Longtitude.
ALT	2	4	Altitude (km).
THTA	2	6	Polar angle with vertical.
PHI	2	8	Azimuthal angle from east.
LMCI	2	10	McIlwain L value (km).
STRM	2x2	12	Stoermer cutoff (10 MV).
BMAG	4	16	Field strength (gamma), sign bit from radial compone
		20	

Verse number: 4 of Chapter 11
Verse name: SGNL

Item Name	Item Length	Relative Index	Comments
CKOV	8x4	0	Cerenkov signal in volts.
ION	6x4	32	Ion chamber signal in femto-coulombs/cm..
EPRM	4	56	Mean CKOV/Mean ION.
LCKV	2x2	60	CKOV path length in the 2 radiators (microns).
IHLD	2	64	ILD (low byte), HLD (high byte) (M versions only).
		66	

1) Negative signal is flag for ion chamber edge problem, or missed chamber, or miss
2) Pulse heights are deramped and floating point representations.
3) No Cerenkov collection mapping is done.

Verse number: 5 of Chapter 11
Verse name: VNRO

Item Name	Item Length	Relative Index	Comments
MFN	1	0	Minor frame number

DFF	1	1	Data flag field.
EVNT	58	2	Event data.
		60	

Chapter number: 12
Chapter name: ANRVN

Verse Name	Verse No.	Item Name	Item Length	Relative Index	Comments
		KEY	2	0	
		spare	2	2	
TAG	1		18	4	
HODO	2		12	22	
ORBT	3		20	34	
SGNL	4		66	54	
TAGF	5		20	120	
VNRO	6		60	140	
				200	

All verses are described in chapter 13 or 11.

Chapter number: 13
Chapter name: RJHVN

Verse Name	Verse No.	Item Name	Item Length	Relative Index	Comments
		KEY	2	0	
		spare	2	2	
TAGF	1		20	4	
VNRO	2		60	24	See ch. 11
				84	

Verse number: 1 of Chapter 13
Verse name: TAGF

Item Name	Item Length	Relative Index	Comments
RJTG	2	0	Cause of rejection.
NGP	1	2	Number of good planes.
GL	1	3	Good layer flags.
FLX1	2	4	
FLX2	2	6	
FLX3	2	8	
FLX4	2	10	Failure tags for each
FLZ1	2	12	of eight hodo's.
FLZ2	2	14	
FLZ3	2	16	
FLZ4	2	18	
		20	

Word Index: 0 of Verse 1 of Chapter 13
Word name: RJTG

Bit No.	Bit Name	Comments
15	DQFL	Data Quality not perfect.
14	PARP	Parity problem.
13	QBMP	HIZBUMP but not HIZ.
12	RPFL	RMOR but not RONE.
11	UNHI	HIZ but not appropriate HLD, ILD, etc.
10	RALF	Various address logic failures. See LIBGEN doc.
9	SNGP	Small NGP (< 2).
8		
7		
6		
5		
4	XTPH	Not used.
3	GAP	Chamber on path has channel number < 90.

2	LHEF	Large HEF on more than one layer. Large means (HEF > 3) o
1	LUNW	Large number of UNWIR flags (> 1).
0	LCHI	Large chisq (> 99% level).

Word Index: 4 of Verse 1 of Chapter 13
Word name: FLZ1

Bit No.	Bit Name	Comments
15	V2A	Second address bit.
14	OVFLO	Address overflow bit.
13	NWIR	Problem with NUMW, the number of wires fired.
12	BNDRY	Boundary of pattern is edge or "ON" or "OFF".
11	HOLE	Pattern has hole in it.
10	SWITCH	Used second address.
9	ALF	Address logic failure.
8	UNWIR	Unfixable NWIR problem.
7		
6		
5		
4	HEF	Hodoscope error flag assigned by LAYCAL.
3		
2		
1		
0		

Chapter number: 14
Chapter name: RJLVN

Verse Name	Verse No.	Item Name	Item Length	Relative Index	Comments
		KEY	2	0	
		spare	2	2	
TAG	1		18	4	
HODO	2		12	22	
ORBT	3		20	34	
SGNL	4		66	54	
TAGF	5		20	120	
VNRO	6		60	140	
				200	

All verses are described in chapter 13 or 11.

Chapter number: 15
Chapter name: VNSM

Verse Name	Verse No.	Item Name	Item Length	Relative Index	Comments
		KEY	2	0	Key-15
VNSM	1		50	2	Event counts.
				52	

Verse number: 1 of Chapter 15
Verse name: VNSM

Item Name	Item Length	Relative Index	Comments
			Count of ...
Z31CN	2	0	Z31's (chapter 11)
VNCF	2	2	Front events (chapter's 7, 11, 13, 14).
VNCB	2	4	Back events.
HZCF	2	6	Front HIZ events.
HZCB	2	8	Back HIZ events.
IALCF	2	10	Front ICDM events.
IALCB	2	12	Back ICDM events.
DALCF	2	14	Front DDM alpha's.
DALCB	2	16	Back DDM alpha's.
CLCF	2	18	Front calibration (HIZ or not).
CLCB	2	20	Back calibration (SCS > 116) .
HCLCF	2	22	HIZ front calibration events.
HCLCB	2	24	HIZ back calibration events.
RJHCN	2	26	Reject hodo events (chapter 13).
RJLCN	2	28	Reject logic events (chapter 14).
FILLCN	2	30	Fill.
HZMR	2	32	Mandatory repeats (HIZ, RONE, RMORE).
HZBM	2	34	HIZ BUMP events.
RPCNT	2	36	Repeat marks (chapter 8).
CS117	2	38	Calib status in minor frame 117.
NRMCN	2	40	Number of normal CR events read out between rate readouts.
NRMRT	2	42	Number of normal CR events scaled in rate scalers.
HICN	2	44	High priority events read out.
HIRT	2	46	High priority events scaled.
ANRCN	2	48	Analyzed reject events (Chapter 12).
		50	

Chapter number: 16
Chapter name: RFKK

Verse Name	Verse No.	Item Name	Item Length	Relative Index	Comments
		KEY	2	0	Key-16
RKTG	1		12	2	
RKSG	2		28	14	
RKZ	3		22	42	
				64	

Verse number: 1 of Chapter 16
Verse name: RKTG

Item Name	Item Length	Relative Index	Comments
BRANCH	1	0	Calculated in binker.
TWIG	1	1	Calculated in binker.
CHPTG	1	2	7, 11, 12, 13, 14.
RELCT	1	3	Relative C tag from ratio maps.
CITAG	1	4	msb-rad 2, lsb-ion chamber 1.
SMITG	1	5	1-6, Number of chambers.
DZ123	1	6	Relative delta i.
DZ456	1	7	Relative delta i.
BTAG	2	8	From input.
HTAG	2	10	From input.
		12	

Verse number: 2 of Chapter 16
Verse name: RKSG

Item Name	Item Length	Relative Index	Comments
MI123	4	0	mean i, mapped.
MI456	4	4	
ZC	4	8	57.17 root mean C, mapped.
XCN	2	12	
ZCN	2	14	
SCAZ	2	16	
SCEL	2	18	
STRM1	2	20	
STRM2	2	22	
THTA	2	24	Chapter 11, verse 3
PHI	2	26	" "
		28	

Verse number: 3 of Chapter 16
Verse name: RKZ

Item Name	Item Length	Relative Index	Comments
ZM	4	0	Mean.
ZF	4	4	Fore-according to PMY.
ZA	4	8	Aft-according to PMY.
ZFO	4	12	Fore-going the other way.
ZAO	4	16	Aft-going the other way.
ECENT	2	20	Energy at center-MeV, <= 0 flags that chp. 16
		22	charge values were used instead of the zkk algorith

Chapter number: 17
Chapter name: ALLZ

Verse Name	Verse No.	Item Name	Item Length	Relative Index	Comments
		KEY	2	0	Key=17
AZTG	1		6	2	Tags
AZDAT	2		40	8	Words
				48	

Verse number: 1 of Chapter 17
Verse name: AZTG

Item Name	Item Length	Relative Index	Comments
HTAG	2	0	
BITAG	1	2	HIZ, HZB, itag.
SUMITG	1	3	fdz[0], sumitg.
FDZ	1	4	ctag, fdz[1].
TWDELZ1	1	5	2*(difference of charge estimates)
		6	

Verse number: 2 of Chapter 17
Verse name: AZDAT

Item Name	Item Length	Relative Index	Comments
MI123	4	0	Mean I in IC 1,2, & 3.
MI456	4	4	Mean I in IC 4,5, & 6.
SQRTMC	4	8	Root mean C.
ZCI123	4	12	Z based on MI123.
ZCI456	4	16	Z based on MI456.
ZCI	4	20	Z based on mean of 123456.
XCN	2	24	Intercept coordinate.
ZCN	2	26	Intercept coordinate.
SCAZ	2	28	Angle coordinate.
SCEL	2	30	Angle coordinate.
STRM1	2	32	Stormer cutoff.
STRM2	2	34	Stormer cutoff.
TWDELZ2	1	36	2*(difference of charge estimates)
GTAG	1	37	0-Chap. 7,11; 1-Chap. 12; 2-Chap. 14.
CFTAG	2	38	Flag for 6/8 tube Cerenkov maps.
		40	

Chapter number: 19
Chapter name: AVRAT

Verse Name	Verse No.	Item Name	Item Length	Relative Index	Comments
		Key	2	0	Key=19
		spare	2	2	
RTDSCR	1		64	4	Chapter descriptor.
CNSM	2		96	68	Summed VNSM counts.
RTSM	3		80	164	Summed rates.
RTSQ	4		80	244	Summed (rate)*(rate).
				324	

Verse number: 1 of Chapter 19
Verse name: RTDSCR

Item Name	Item Length	Relative Index	Comments
LOLAT	2	0	Limits of search box.
HILAT	2	2	
LOLON	2	4	
HILON	2	6	
MJFCN	2	8	Number of major frames in box.
spare	2	10	
ERCN	20x2	12	Rates rejected for data quality.
START	6	52	Time.
END	6	58	Time.
		64	

Chapter number: 20
Chapter name: MJFSTAT

Verse Name	Verse No.	Item Name	Item Length	Relative Index	Comments
		KEY	2	0	
CRNT	1		20	2	
STAT	2		16	22	Hardware status-ch4, vl.
DELT	3		4	38	Delta t.
				42	

Verse number: 1 of Chapter 20
Verse name: CRNT

Item Name	Item Length	Relative Index	Comments
NFF	1	0	-see chapters 2, 4, 15.
NSNE	1	1	
ISNG	2	2	
DSNG	2	4	
VNRT	2	6	
NRMCN	2	8	
NRMRT	2	10	
HICN	2	12	
HIRT	2	14	
ALCN	2	16	Sum of four alpha counts.
FILLCN	2	18	
CRFL	2	20	Current flag bits.
		22	

Word Index: 20 of Verse 1 of Chapter 20
Word name: CRFL

Bit No.	Bit Name	Comments
15		
14		
13		
12		
11		
10		Ckv HV flag.
9		DDM HV flag.
8		ICDM HV flag.
7		
6		

5	
4	
3	srcflg.
2	readerr.
1	dqf.
0	SAA.

Verse number: 3 of Chapter 20
Verse name: DELT

Item Name	Item Length	Relative Index	Comments
PSA	1	0	Since previous SAA.
NSA	1	1	Until next SAA.
PSF	1	2	Since previous status funny.
NSF	1	3	Until next status funny.

Units of delta t are major frames.
If > 200, set to 200. If unknown,
set to 250. Note that SCCK (chapter 1)
counts minor frames (128 per major frame).

Chapter number: 21
Chapter name: GLDFLG

Verse Name	Verse No.	Item Name	Item Length	Relative Index	Comments
		KEY	2	0	Key=21.
GLDF	1		2	2	
				4	

Verse number: 1 of Chapter 21
Verse name: GLDF

Item Name	Item Length	Relative Index	Comments
MFN	1	0	Minor frame number, a/b flag.
GFLG	1	1	
		2	

Word Index: 1 of Verse 1 of Chapter 21
Word name: GFLG

Bit No.	Bit Name	Comments
7		Accidental "13".
6		readerr.
5		prehiz.
4		low z.
3		high z.
2		lucky.
1		svrf (b).
0		svrf (a).

Chapter number: 22
Chapter name: IONVN

Verse Name	Verse No.	Item Name	Item Length	Relative Index	Comments
		KEY	2	0	Key=22.
TAG	1		18	2	Copy from library tape.
HDION	2		36	20	Hodo, orbit data.
SGION	3		36	56	Signal data.
				92	

Verse number: 2 of Chapter 22
Verse name: HDION

Item Name	Item Length	Relative Index	Comments
XCN	2	0	
ZCN	2	2	
DXDY	2	4	
DZDY	2	6	
SCAZ	2	8	
SCEL	2	10	
NION	12x1	12	Position index in centimeters.
EPSIND	6x1	24	Epsilon indicator.
LMCI	2	30	
STRM	2x2	32	
		36	

Verse number: 3 of Chapter 22
Verse name: SGION

Item Name	Item Length	Relative Index	Comments
ION	6x4	0	
EPRM	4	24	
IBAR	4	28	Average of good ION's.
NGD	2	32	Number of good ION's.
TWDELZ	1	34	2 x delta Z from ICDM to DDM.
TWORST	1	35	2 x worst delta Z of all NGD ION's.
		36	

Chapter number: 23
Chapter name: IONRS

Verse Name	Verse No.	Item Name	Item Length	Relative Index	Comments
		KEY	2	0	Key=23
RS4	1		10	2	Data from chap. 4.
RS15	2		12	12	Data from chap. 15.
				24	

Verse number: 1 of Chapter 23
Verse name: RS4

Item Name	Item Length	Relative Index	Comments
SMDET	2	0	Subcom word 119, states 120 & 121.
ISNG	2	2	ICDM singles rate.
DSNG	2	4	DDM singles rate.
VNRT	2	6	Event rate.
HZRT	2	8	High Z rate.
		10	

Verse number: 2 of Chapter 23
Verse name: RS15

Item

tem Name	Relative Length	Index	Comments
VNCF	2	0	
VNCB	2	2	
HZCF	2	4	
HZCB	2	6	
RJCN	2	8	RJHCN + RJLCN.
HZBM	2	10	
		12	

Chapter number: 24
Chapter name: IONRBT

Verse Name	Verse No.	Item Name	Item Length	Relative Index	Comments
		KEY	2	0	Key=24
SAAFL	1		10	2	Output for SAA enter/exit.
				12	

Verse number: 1 of Chapter 24
Verse name: SAAFL

Item Name	Item Length	Relative Index	Comments
IRBNO	2	0	
ITMSC	4	2	
ITYPE	1	6	Only if TYPE= 10, 11, 12, 13.
ISHFL	1	7	
ISESA	2	8	
		10	

All from Chapter 5.

Chapter number: 25
Chapter name: ICEDGE

Verse Name	Verse No.	Item Name	Item Length	Relative Index	Comments
		KEY	2	0	Key = 25.
ICETG	1		4	2	
ICEHD	2		16	6	
ICESG	3		16	22	
				38	

Verse Number: 1 of Chapter 25
Verse Name: ICETG

Item Name	Item Length	Relative Index	Comments
BTAG	2	0	
HTAG	2	2	

Verse Number 2 of Chapter 25
Verse Name: ICEHD

Item Name	Item Length	Relative Index	Comments
XCN	2	0	
ZCN	2	2	
DXDY	2	4	
DZDY	2	6	
NION	2x1	8	One chamber only.
LMCI	2	10	
STRM	2x2	12	
		16	

Verse Number: 3 of Chapter 25
Verse Name: ICESG

Item Name	Item Length	Relative Index	Comments
ION	4	0	Only one, indicated by NIC.
EPRM	4	4	
IBAR	4	8	
NIC	1	12	Chamber number for this chapter.
NGD	1	13	Number of chambers in IBAR.
TWDELZ	1	14	
TWORST	1	15	
		16	

Chapter number: 28
Chapter name: CNVFLG

Verse Name	Verse No.	Item Name	Item Length	Relative Index	Comments
		KEY	2	0	Key=28.
CNV	1		14	2	
				16	

Verse number: 1 of Chapter 28
Verse name: CNV

Item Name	Item Length	Relative Index	Comments
MFN	1	0	Minor frame number, A/B flag.
NCFAD	1	1	Used level 2.
SHUD	2	2	Should have hit.
DID	2	4	Did hit.
XZ1LV	2	6	Level flags.
XZ2LV	2	8	" "
XZ3LV	2	10	" "
XZ4LV	2	12	" "
		14	

Word Index: 2 of Verse 1 of Chapter 28
Word name: SHUD

Bit No.	Bit Name	Comment
15	C	Should have hit the indicated detector according to "best-fit" trajectory.
14	I6	
13	I5	
12	I4	
11	I3	
10	I2	
9	I1	
8		
7	Z4	
6	X4	
5	Z3	
4	X3	
3	Z2	
2	X2	
1	Z1	
0	X1	

Word Index: 4 of Verse 1 of Chapter 28
Word name: DID

Bit No.	Bit Name	Comments
15	C	Did hit the indicated detector according to pulse height or wire number.
14	I6	
13	I5	
12	I4	
11	I3	
10	I2	
9	I1	
8		
7	Z4	
6	X4	
5	Z3	
4	X3	
3	Z2	
2	X2	
1	Z1	
0	X1	

Word Index: 6 of Verse 1 of Chapter 28
Word name: XZ1LV

Bit No.	Bit Name	Comments
15		
14		X1 level 6 - ALF or NFAD.
13		X1 level 5 - 1st & 2nd too close.
12		X1 level 4 - switched.
11		X1 level 3 - adjacent groups.
10		X1 level 2 - missing partner.
9		X1 level 1
8		X1 level 0 - libgen "good".
7		
6		Z1 level 6
5		Z1 level 5
4		Z1 level 4
3		Z1 level 3
2		Z1 level 2
1		Z1 level 1
0		Z1 level 0

Chapter number: 30
Chapter name: CNTRL1

Verse Name	Verse No.	Item Name	Item Length	Relative Index	Comments
		Key	2	0	Key=30
		spare	2	2	
GEN	1		128	4	Time & general status.
EVSP	2		1702	132	Event specifications.
COMM	3		192	1834	Comments, version, etc.
				2026	

Verse number: 1 of Chapter 30
Verse name: GEN

Item Name	Item Length	Relative Index	Comments
BTIME	4	0	Begin time, time format*.
ETIME	4	4	End time. time format*
ITIME	2	8	Interval time in minutes.
spare	2	10	
ADGP	2	12	Analog data general parameters.
CSGP	2	14	Command status general parameters.
spare	4	16	
CMDNRM	32	20	Normal command status.
CMDCM	32	52	Irrelevant command status.
CMDPRM	16	84	Skip if not irrelevant & different from normal.
ADPRM	4	100	Skip if analog unusaual.
spare	24	104	
		128	

* time format- time in two words 1000(yr-70)+dy and (min in day)

Verse number: 2 of Chapter 30
Verse name: EVSP

Item Name	Item Length	Relative Index	Comments
NES	2	0	Number of events specified.
TANMF	1	2	T mask ANMF. ----begin block
FANMF	1	3	F mask ANMF.
ttag	1	4	Tag mask.
FTAG	1	5	Tag mask.
TPHST	1	6	PHST mask.
FPHST	1	7	PHST mask.
RMIN	1	8	RNG minimum.
RMAX	1	9	RNG maximum.
SECT	1	10	Bits for sectors to reject.
CVSF	1	11	Counted only, or counted & copied to output.
spare	1	12	
INOUT	1	13	In or out of selection area.
XYCRN	12	14	X1,X2,Y1,Y2,Y3,Y4 (corner of selection area).
I1	1	26	PHA # for x axis of 2D plot.
I2	1	27	PHA # for y axis of 2D plot.
THDST	2	28	HDST mask.
FHDST	2	30	HDST mask.
CSMIN	2	32	Minimum of CSTH.
CSMAX	2	34	Maximum of CSTH. ----end of block.
	1666	36	49 repeats of block.
		1702	

Verse number: 3 of chapter 30
Verse name: COMM

Item Name	Item Length	Relative Index	Comments
CMNT	160	0	Space for comments.
SVRSN	8	160	Version number.
EXDT	8	168	Execution date.
CBNM	16	176	Control block file name.
		192	

Chapter number: 31
Chapter name: CNTRL2

Verse Name	Verse No.	Item Name	Item Length	Relative Index	Comments
		KEY	2	0	Key=31
		spare	2	2	
GEN	1		128	4	Time & general status. time format.
DUM	2		2	132	Zero in HIST2.
COMM	3		192	134	Comments, version, etc.
				326	

Verse number: 1 of Chapter 31
Verse name: GEN

Item Name	Item Length	Relative Index	Comments
BTIME	4	0	Begin time. time format.
ETIME	4	4	End time.
ITIME	2	8	Interval time in minutes.
spare	2	10	
ADGP	2	12	Analog data general parameters.
CSGP	2	14	Command status general parameter.
spare	4	16	
CMDNRM	32	20	Normal command status.
CMDDCM	32	52	Irrelevant command status.
CMDPRM	16	84	Skip if nor irrelevant & different from normal.
ADPRM	4	100	Skip if analog unusual.
spare	24	104	
		128	

Verse number: 2 of Chapter 31
Verse name: DUM

Item Name	Item Length	Relative Index	Comments
	2	0	Value is zero. Verse is place holder to provide consistency between chapters 30 & 31.

Verse number: 3 of Chapter 31
Verse name: COMM

Item Name	Item Length	Relative Index	Comments

CMNT	160	0	Space for comments.
SVRSN	8	160	Version number.
EXDT	8	168	Execution date.
CBNM	16	176	Control block file name.
		192	

Chapter number: 32
Chapter name: ISTAT

Verse Name	Verse No.	Item Name	Item Length	Relative Index	Comments
		KEY	2	0	Key=32
		spare	2	2	
STAT	60	4		Status bits.	
				64	

Verse number: 1 of Chapter 32
Verse name: STAT

Item Name	Item Length	Relative Index	Comments
BOI	4	0	Begin of interval. Time format.
EOI	4	4	End of interval. " "
FTIME	4	8	Time of first data record in interval.
STS	32	12	Command status.
ETMP	2	44	Electronic temperature (0.1 deg. C).
TTMP	2	46	Telescope termperature ("").
SP	2	48	Spin period.
BRT	1	50	Bit rate.
spare	1	51	
XGSE	2	52	Position in units of 100 km.
YGSE	2	54	""
ZGSE	2	56	""
spare	2	58	
		60	

Chapter number: 33
Chapter name: EVNT

Verse Name	Verse No.	Item Name	Item Length	Relative Index	Comments
		KEY	2	0	Key=33
		spare	2	2	
DATA	1		2044	4	Event data.
			2048		

Verse number: 1 of Chapter 33
Verse name: DATA

Item Name	Item Length	Relative Index	Comments
NMVN	2	0	Number of events in this record (<=40).
IEB	2	2	
EVNT	240	4	NMVN times, in A/B format (40 by 60).
		2044	

Chapter number: 34
Chapter name: FSTAT1

Verse Name	Verse No.	Item Name	Item Lenght	Relative Index	Comments
		KEY	2	0	Key=34
		spare	2	2	
STAT	1		124	4	General status.
RATE	2		954	128	HIST rates.
VCNT1	3		200	1082	Specified event counts.
				1282	

Verse number: 1 of Chapter 34
Verse name: STAT

Item Name	Item Length	Relative Index	Comments
LTIME	4	0	Time of last data record in interval.
NDREC	4	4	Number of data records in interval.
STS	32	8	Command status.
ETMP	2	40	Electronic temperature (units 0.1 deg. C).
TT	2	42	Telescope temperature (" " ").
SP	2	44	Spin period.
BRT	1	46	Bit rate.
spare	1	47	
CMDCNT	16	52	
PRWRN	4	68	
EOTFLG	4	72	Interval ended by EOT.
GAP	2	76	# of gaps in data.
XGSE	2	78	Position in units of 100 km.
YGSE	2	80	" " " .
ZGSE	2	82	" " .
spare	4	84	
ABVT	2	88	A/B event count.
AEVT	2	90	A event count.
VCNT	22	92	Event counts by buffer.
VQL	8	114	Event counts by quality.
spare	2	122	
		124	

Verse number: 2 of Chapter 34
Verse name: RATE

Item Name	Item No.	Relative Index	Comments
RTDT	636	0	159 HIST rates.
TMDT	318	636	# of subcoms per rate.
		954	

Verse number: 3 of Chapter 34
Verse name: VCNT1

Item Name	Item Length	Relative Index	Comments
VNCT	200	0	Specified event counts.
		200	

Chapter number: 35
Chapter name: FSTAT2

Verse Name	Verse No.	Item Name	Item Length	Relative Index	Comments
		KEY	2	0	Key =35
		spare	2	2	
STAT	1		124	4	General status. Described in chap.
RATE	2		954	128	HIST rates. Described in chap. 34.
VCNT2	3		756	1082	All count rates possible.
				1838	

Verse number: 3 of Chaper 35
Verse name: VCNT2

Item Name	Item Length	Relative Index	Comments
ZCNT	720	0	180 event counts in [4][5][9] matrix.
HCNT	16	720	Range > 4 counts.
MH	20	736	Multiple hodoscope events by range.
		756	

Chapter number: 36
Chapter name: HISTDC

Verse Name	Verse No.	Item Name	Item Length	Relative Index	Comments
		KEY	2	0	Key=36
		spare	2	0	
TIME	1		12	4	Time & status information.
CNT	2		36	16	Event count rates.
RATE	3		144	52	Rate & rate uncertainties.
FLX	4		72	196	Flux & flux uncertainties.
MISC	5		8	268	Livetime, hodoscope event fractions.
				276	

Verse number: 1 of Chapter 36
Verse name: TIME

Item Name	Item Length	Relative Index	Comments
IYR	2	0	Year >= 78.
IDY	2	2	Day of year.
IHR	2	4	Hour.
ITIME	4	6	Year, day and hour.
IMODE	2	10	Instrument operation mode.
		12	

Verse number: 2 of Chapter 36
Verse name: CNT

Item Name	Item Length	Relative Index	Comments
HCNT	16	0	Event counts R0-R3 hydrogen.
HECNT	20	16	Event counts R0-R4 helium.
		36	

Verse number: 3 of Chapter 36
Verse name: RATE

Item Name	Item Length	Relative Index	Comments
LOZR	4	0	Lo_z rate.
LOZ	20	4	Lo_z R0-R4.
HIZ	20	24	Hi_z R0-R4.

M	8	44	M1, M2.
D	20	52	D1-D5.
ULOZR	4	72	Uncertainties in Lo_z rate.
ULOZ	20	76	" " Lo_z R0-R4.
UHIZ	20	96	" " Hi_z R0-R4.
UM	8	116	" " M1, M2.
UD	20	124	" " D1-D5.
		144	

Verse number: 4 of Chapter 36
Verse name: FLX

Item Name	Item Length	Relative Index	Comments
HFLX	16	0	Flux R0-R3 hydrogen.
HEFLX	20	16	Flux R0-R4 helium.
UHFLX	16	36	Hydrogen flux uncertainty.
UHEFLX	20	52	Helium flux uncertainty.
		72	

Verse number 5 of Chapter 36
Verse name: MISC

Item Name	Item Length	Relative Index	Comments
LZLT	4	0	Lo_z livetime in seconds.
MHF	4	4	Multiple hodoscope event fractions.
		8	

Chapter number: 51
Chapter name: CKSTAT

Verse Name	Verse No.	Item Name	Item Length	Relative Index	Comments
		KEY	2	0	Key=C4=51
	1	RMIN	2	2	Parameter of CRUSH (10 MV).
CST	2		10x2	4	Status
				24	

Verse number: 2 of Chapter 51
Verse name: CST

Item Name	Item Length	Relative Index	Comments
SCS80	2	0	
SCS81	2	2	
SCS82	2	4	
SCS83	2	6	
SCS96	2	8	
SCS97	2	10	
SCS98	2	12	
SCS99	2	14	
SCS125	2	16	
SCS127	2	18	
		20	

Chapter number: 52
Chapter name: CKMAJ

Verse Name	Verse No.	Item Name	Item Length	Relative Index	Comments
		KEY	2	0	Key=52
CTIM	1		10	2	Data from MJTIM.
CATT	2		12	12	Data from MJAT.
CKRT	3		24	24	Cerenkov rates.
ORTYP	4		4	48	Orbit data types.
				52	

Verse number: 1 of Chapter 52
Verse name: CTIM

Item Name	Item Length	Relative Index	Comments
RBNO	2	0	
TMSC	4	2	32-msec units.
SCCK	4	6	
		10	

Verse number: 2 of Chapter 52
Verse name: CATT

Item Name	Item Length	Relative Index	Comments
BANG	2x2	0	
BMAG	4	4	
THTE	2	8	
PHIE	2	10	
		12	

Verse number: 3 of Chapter 52
Verse name: CKRT

Item Name	Item Length	Relative Index	Comments
LFC4	2	0	Left C4 coincidence rate.
LFC2	2	2	Left C2 coincidence rate.
LFC1D	2	4	Left D singles rate.
LFC1C	2	6	Left C singles rate.
LFC1B	2	8	Left B singles rate.
LFC1A	2	10	Left A single rate.
RTC4	2	12	Right C4 coincidence rate.
RTC2	2	14	Right C2 coincidence rate.
RTC1D	2	16	Right D singles rate.
RTC1C	2	18	Right C singles rate.
RTC1B	2	20	Right B singles rate.
RTC1A	2	22	Right A singles rate.
		24	

Verse number: 4 of Chapter 52
Verse name: ORTYP

Item Name	Item Length	Relative Index	Comments
TP1	2	0	Type of first orbit record.
TP2	2	2	Type of second orbit record.
		4	

Chapter number: 53
Chapter name: CKVNT

Verse Name	Verse No.	Item Name	Item Length	Relative Index	Comments
		KEY	2	0	Key-52
CTG	1		14	2	Tag data.
CPSN	2		22	16	Hodo & orbit data.
CSG	3		38	38	Signal data.
				76	

Verse number: 1 of Chapter 53
Verse name: CTG

Item Name	Item Length	Relative Index	Comments
MFNO	2	0	Minor frame no. in orbit.
CTRK	2	2	+1 --> from +y.
NFIRE	2	4	What was hit.
NQUAL	2	6	Number hit.
HTAG	2	8	
BTAG	2	10	
ZCI	2	12	
		14	

Word Index: 4 of Verse 1 of Chapter 53
Word name: NFIRE

Bit No.	Bit Name	Comments
15	X1	
14	Z1	
13	X2	
12	Z2	Hodo
11	X3	
10	Z3	
9	X4	
8	Z4	
7	I1	Ion chamber.
6	I2	
5	I3	
4	I4	
3	I5	
2	I6	
1	RAD1	Radiator.

0	RAD2

Verse number: 2 of Chapter 53
Verse name: CPSN

Item Name	Item Length	Relative Index	Comments
XCN	2	0	
ZCN	2	2	
X1	2	4	
X2	2	6	Position in radiators
Z1	2	8	1 & 2 in mm.
Z2	2	10	
SCEL	2	12	
LCKV	2x2	14	
STRM	2x2	18	
		22	

Verse number: 3 of Chapter 53
Verse name: CSG

Item Name	Item Length	Relative Index	Comments
ICHK	2	0	I1/(I1+I6)x16K
CKOV	8x4	2	
EPRM	4	34	
		38	

Chapter number: 55
Chapter name: CMAP

Verse Name	Verse No.	Item Name	Item Length	Relative Index	Comments
		KEY	2	0	Key=55.
		spare	2	2	
MPDAT	1		20	4	
				24	

Verse number: 1 of Chapter 55
Verse name: MPDAT

Item Name	Item Length	Relative Index	Comments
IX	2	0	X-coordinate of bin.
IZ	2	2	Z-coordinate of bin.
SUM	4	4	Sum of signals in bin.
NUM	4	8	Number of events in bin.
SQ	4	12	Sum of squared signals in bin.
CUB	4	16	Sum of cubed signals in bin.
		20	

Chapter number: 70
Chapter name: PARAMS

Verse Name	Verse No.	Item Name	Item Length	Relative Index	Comments
		KEY	2	0	Key=70
PTIME	1		30	2	Star, end & interval time.
PPARM	2		32	32	Parameter selections.
PCOM	3		512	64	Comment string.
				576	

Verse number: 1 of Chapter 70
Verse name: PTIME

Item Name	Item Length	Relative Index	Comments
BYR	2	0	Begin time - year.
BDY	2	2	Begin time - day of year.
BMS	4	4	Begin time - msec. of day truncated to second.
BHR	2	8	BMS in hours.
BMIN	2	10	BMS in minutes.
EYR	2	14	End time - year.
EDY	2	14	End time - day of year.
EMS	4	16	End time - msec. of day truncated to seconds.
EHR	2	20	EMS in hours.
EMIN	2	22	EMS in minutes.
IDY	2	24	Interval time - day.
IHR	2	26	Interval time - hours.
IMIN	2	28	Interval time - minutes.
		30	

Verse number: 2 of Chapter 70
Verse name: PPARM

Item Name	Item Length	Relative Index	Comments
CSON	2	0	Command status.
CSOFF	2	2	
SPLO	2	4	Spin period low bound (msec.).
SPHI	2	6	Spin period high bound.
OAON	2	8	OA mode.
TMON	2	10	TM mode.
BITHI	2	12	High bitrate.
BITLO	2	14	Low bitrate.
ATXON	2	16	Analog transmitter.
ATXOFF	2	18	

Item Name	Item Length	Relative Index	Comments
PTXON	2	20	PCM transmitter.
PTXOFF	2	22	
BOTHON	2	24	Both transmitters.
BOTHOFF	2	26	
spare	4	28	
		32	

Verse number: 3 of Chapter 70
Verse name: PCOM

Item Name	Item Length	Relative Index	Comments
COMM	512	0	Null terminated ascii string for comments.
		512	

Chapter number: 71
Chapter name: PEVNT

Verse Name	Verse No.	Item Name	Item Length	Relative Index	Comments
		KEY	2	0	Key-71
NUM	1		4	2	Event, copyflag.
COM	2		64	6	Comment field.
SPEC	3		34	70	Specifications.
				104	

Verse number: 1 of Chapter 71
Verse name: NUM

Item Name	Item Length	Relative Index	Comments
NM	2	0	Event number.
COPY	2	2	Copy flag (1=copy,0=just count).
		4	

Verse number: 2 of Chapter 71
Verse name: COM

Item Name	Item Length	Relative Index	Comments
COMT	64	0	Null terminated ascii string.
		64	

Verse number: 3 of Chapter 71
Verse name: SPEC

Item Name	Item Length	Relative Index	Comments
NSTD	2	0	Not a "standard" event.
YISA	2	2	Reverse A & B axis tests for trapezoid.
RON	2	4	Detectors must be on.
ROFF	2	6	Detectors must be off.
ALOW	2	8	Low cutoff for Apha.
AHIGH	2	10	High cutoff for Apha.
B1LOW	2	12	
B1HIGH	2	14	
B2LOW	2	16	
B2HIGH	2	18	
SON	2	20	Sectors accepted.
DQON	2	22	Data quality accepted.
ATON	2	24	Analysis types accepted.
PRON	2	26	Priority accepted.
ETON	2	28	Event types accepted.
MBON	2	30	Misc. bits must be on.
MBOFF	2	32	Misc. bits must be off.
		34	

Chapter number: 72
Chapter name: ISTAT

Verse Name	Verse No.	Item Name	Item Length	Relative Index	Comments
		KEY	2	0	Key=72
TIME	1		16	2	Time information.
SRC	2		20	18	Data source.
STAT	3		12	38	Label block parameters.
				50	

Verse number: 1 of Chapter 72
Verse name: TIME

Item Name	Item Length	Relative Index	Comments
PSC	4	0	Pseudo sequence counter.
GAP	1	4	# missing albums.
YR	1	5	Year (72=1972).
DAY	2	6	Day of year.
MSC	4	8	Millisecond of day.
HR	1	12	GMT hour (0-23).
MIN	1	13	GMT minute (0-59).
TQF	1	14	Time quality flag.
RBN	1	15	Orbit number.
		16	

Verse number: 2 of Chapter 72
Verse name: SRC

Item Name	Item Length	Relative Index	Comments
ATN	8	0	Abstract tape name.
XTN	6	8	Exp. tape name.
XFN	2	14	Exp. tape file #.
XRN	4	16	Exp. record numbers.
		20	

Verse number: 3 of Chapter 72
Verse name: STAT

Item Name	Item Length	Relative Index	Comments
ONF	1	0	Exp. power (0=on,1=off).

BRT	1	1	Bit rate (0=high,1=low).
OTM	1	2	OA/TM.
spare	1	3	
TMP	2	4	Temperature (0.1 deg C).
SP	2	6	Spin period (msec.).
CST	2	8	Command status.
ATX	1	10	Analog transmitter.
PTX	1	11	PCM transmitter.
		12	

Chapter number: 73
Chapter name: EVNT

Verse Name	Verse No.	Item Name	Item Length	Relative Index	Comments
		KEY	2	0	Key=73
NUM	1		2	2	Number of valid events.
EV	2		2040	4	170 events @ 12 bytes.
				2044	

Chapter number: 74
Chapter name: RATE

Verse Name	Verse No.	Item Name	Item Length	Relative Index	Comments
		KEY	2	0	Key=74
COUNT	1		480	2	Rate counts.
TIME	2		480	2	Accumulative time (msec.).
NORM	3		480	962	Counts/time (sec.).
ERR	4		480	1442	Err squared.
				1922	

Chapter number: 75
Chapter name: FSTAT

Verse Name	Verse No.	Item Name	Item Length	Relative Index	Comments
		KEY	2	0	Key=75
TIME	1		16	2	Time information.
SRC	2		20	18	Data source.
STAT	3		12	38	Label block parameters.
ECNT	4		256	50	Event counts.
				306	

Verses 1-3 are described in Chapter 72.

Verse number: 4 of Chapter 75
Verse name: ECNT

Item Name	Item Length	Relative Index	Comments
CNTS	256	0	Counts for each of the 64 events specified.
		256	

Chapter number: 98
Chapter name: INHIST

Verse Name	Verse No.	Item Name	Item Length	Relative Index	Comments
		KEY	2	0	
EXDT	1		8	2	Execution date.
TPNM	2		132	10	Input Tapename.
				142	

Chapter number: 99
Chapter name: RJCN

Verse Name	Verse No.	Item Name	Item Length	Relative Index	Comments
		KEY	2	0	
TPNM	1		8	2	Tapename.
RJCN	2		400	10	Reject counts.
				410	

Chapter number: 100 & 101
Chapter name: EOMJ & EOR

Verse Name	Verse No.	Item Name	Item Length	Relative Index	Comments
		KEY	2	0	Key=100 or 101
		RECNO	2	2	Record number.
				4	

Note: These chapters flag end of major frame and end of physical tape record.

Chapter number: 102
Chapter name: EOI

Verse Name	Verse No.	Item Name	Item Length	Relative Index	Comments
		KEY	2	0	Key=102
		MFCNT	2	2	Major frame count.
				4	

Note: This chapter flags end of summary interval. It is not used by LIBGEN.

Chapter number: 103
Chapter name: EOT

Verse Name	Verse No.	Item Name	Item Length	Relative Index	Comments
		KEY	2	0	Key=103.
		RECNO	2	2	Record number.
				4	

Note: Chapter 103 flags both end of tape and EOR.

Chapter number: 120
Chapter name: HISTO

Verse Name	Verse No.	Item Name	Item Length	Relative Index	Comments
		KEY	2	0	Key=120.
H01	1		24	2	program parameters
				26	

Verse number: 1 of Chapter 120
Verse name: H01

Item Name	Item Length	Relative Index	Comments
HNAME	20	0	program name
HGTAG	2	20	gtag
	2	22	spare
		24	

Chapter number: 121
Chapter name: HIST1

Verse Name	Verse No.	Item Name	Item Length	Relative Index	Comments
		KEY	2	0	Key=121.
H11	1		120	2	reject counts
H12	2		(var)	122	htimes data
				122+(var)	

Verse number: 1 of Chapter 121
Verse name: H11

Item Name	Item Length	Relative Index	Comments
REJC	120	0	rejcnt[30]
		120	

Verse number: 2 of Chapter 121
Verse name: H12

Item Name	Item Length	Relative Index	Comments
HTIM	(var)	0	start/stop times with gaps in fyrdy.
		(var)	

Chapter number: 122
Chapter name: HIST2

Verse Name	Verse No.	Item Name	Item Length	Relative Index	Comments
		KEY	2	0	Key=122.
H21	1		30	2	histogram parameters
H22	2		(var)	32	histogram data
				32+(var)	

Verse number: 1 of Chapter 122
Verse name: H21

Item Name	Item Length	Relative Index	Comments
PLOT	2	0	plot no.
NARR	2	2	array no.; 1=hist,2=var,3=cnt
NBIN	2	4	no. of bins
NNRM	6x4	6	nnrm,nhiz,ncnt,nrate,hcnt,hrate
		30	

Verse number: 2 of Chapter 122
Verse name: H22

Item Name	Item Length	Relative Index	Comments
HARR	4xnbin	0	hist/var/cnt array
		4xnbin	

The heao verify program reads a tape in chapter/verse format and records:

        start + stop times,
        time gaps in excess of a specified interval,
        number of tape records,
        chapter counts,
        read errors.

Execution is in two stages. First run verify, which will request a minimun gap time and the tape unit number. Next run prverify, which reads the output files vtimes and rejchp99, and prints out the results.

To compile:

```
cc -c getchp.c; cc -c request.c; cc -c chapters.c
cc getchp.o request.o chapters.o (magtape.o) verify.c
cc prverify.c
```

Magtape.o is a magtape interface, to be supplied by the user, that must contain three subroutines:

1) mtread(unit,buff,bytes)
   unit= tape drive unit number
   buff= address of input buffer
   bytes= number of bytes to read

   Mtread should return the number of bytes actually read. In the event that number is less than the number requested, no error condition should be set. On an EOF, the value 0 should be returned; on a read error, a negative number.

2) mtrew(unit)
   This call should rewind the tape on the specified unit.

3) mtclose(unit)
   This closes the file descriptor associated with the I/O device. It may be a dummy call if such action is not appropriate.

Files included:

chap.h	(#include file for programs)
chapters.c	(reads and prints chapter numbers)
clook.c	
getchp.c	
prverify.c	
request.c	
verify.c	
+note	

```
/* compile with:
        cc getchp.o request.o chapters.o (magtape.o) verify.c
 */

/* make summmary files of chp tapes, use prverify to print out
 *
 * add #bytes, #rec      3-7-83
 * also chp 20 summary
 * write 18 bytes for exec. date + 10 (new) byte name  3-23-83
 */

#include <stdio.h>
#include <chap.h>

int     chpsize[125];
long    tbytes,trec;
long    chpcnt[125],rejcntl[100],sum20[5];
double  lfyrdy,fyrdy;

main(){
        short   *ip;
        int     i,j,chp,day,first,id,idt,crfl;
        long    *msc,*lp;
        float   fgap;
        double  fdif;

        chpsize[0]= 64;
        first=1;

        printf("fractional day gap: ");
        scanf("%f",&fgap);
        if(fgap < .1){
                fgap=.1;
                printf("WE are making fgap .1     -OK ??\n");
                }

        idt=creat("vtimes",0666);
        write(idt,&fgap,4);
        while((chp=getchp()) != C_END){
             if(chp>=0 && chp< 124){
                  tbytes += chpsize[chp];
                  chpcnt[chp]++;
                  }
             else{
                  fprintf(stderr,"**** chp= %d ??\n");
                  exit();
                  }
             switch(chp){
                  case 0:
                          ip= getvrs(2);
                          if((chp= ip[0]) < 124)
                                  chpsize[chp]= ip[1];
                          else{
                               fprintf(stderr,"**** chp 0 for chp %d ??\n",chp);
                               exit();
                               }
```

```
				if(first){
					ip=getvrs(1);
					write(idt,ip+4,18);
					first=0;
					}
				break;
			case C_ERR:
				chpcnt[124]++;
				break;
			case 1:
				ip= getvrs(1);
				day= ip[2];
				msc= &ip[3];
				fyrdy=1000.*ip[1]+day+ *msc/86400000.;
				if((fdif=fyrdy-lfyrdy)>fgap || fdif<0.)
					write(idt,&lfyrdy,16);
				lfyrdy=fyrdy;
				break;
			case 20:
				ip= getvrs(1);
				crfl= ip[10];
				if(crfl & 1) sum20[0]++;
				if(crfl & 2) sum20[1]++;
				if(crfl & 4) sum20[2]++;
				if(crfl & 03400) sum20[3]++;
				else if((crfl & 03407)==0) sum20[4]++;
				break;
			case 99:
				ip= chapter[99];
				if(*ip == 410) lp= getvrs(1)+8;
				else lp= getvrs(1);
				for(i=0;i<100;i++)
					rejcntl[i] += *lp++;
				break;
			case 101:
				trec++;
				break;
				}
			}

	fyrdy=0.;
	write(idt,&lfyrdy,16);

	id= creat("rejchp99",0666);
	write(id,&tbytes,8);
	write(id,chpcnt,4*125);
	write(id,rejcntl,400);
	write(id,sum20,20);
	}
```

DUMP OF TAPE AT8 11

DUMP OF D-76226

Start Time = 8/5/80

INPUT TAPE AT8 11 ON HTO
DATA INPUT F9 FL 1 3 STOP

VX STD LIB6 02-2-2-81 BINK 8008

8008

FILE 1 RECORD 1 LENGTH 7888 BYTES

( )	7678	7374646C	696243	30322D32	322D3837	62696E6B	383 3038	00000000	01001000	12000000
(4)	[illegible]	00000000	[illegible]	00000000	00000000	01000000	00007678	7374646C	69624300	30322D32
(8)	322D3837	62696E6B	383 3038	00000000	02008400	02000400	00000000	00000000	00000000	00000000
(12)	[illegible]	2	7678	7374646C	696243	3 322D32	322D3837	62696E6B	383 3038	00000000
(16)	030 C800	04000800	20 038	50 68	800 98	B 00000	00000000	09000000	00007678	7374646C
(20)	69624300	30322D32	322D3837	62696E6B	38303038	00000000	0400B400	04001400	3C008C00	9C000000
(24)	[illegible]	[illegible]	[illegible]	5	00007678	7374646C	69624300	30322D32	322D3837	62696E6B
(28)	383 3038	[illegible]	5 28	40	00002000	00020000	00000000	00000000	00000000	01000000
(32)	00007678	7374646C	69624300	30322D32	322D3837	62696E6B	38303038	00000000	06008000	02000000
(36)	[illegible]	00000100	00000000	00000000	00000000	01000000	00007678	7374646C	69624300	30322D32
(40)	322D3837	62696E6B	383 3 38	00000000	070 78	04 01600	22003E00	00000000	00000000	00000000
(44)	[illegible]	04000000	00007678	7374646C	69624300	30322D32	322D3837	62696E6B	38303038	00000000
(48)	0E0 0400	02000000	00000000	00000000	00000000	00000000	00000000	01000000	00007678	7374646C
(52)	696243	3 322D32	322D3837	62696E6B	38303038	00000000	09004000	04000000	00000000	00000000
(56)	[illegible]	[illegible]	[illegible]	01000000	00007678	7374646C	69624300	30322D32	322D3837	62696E6B
(60)	383 3038	00000000	CA001C00	02000000	00000000	00000000	00000000	00000000	00000000	01000000
(64)	00007678	7374646C	69624300	30322D32	322D3837	62696E6B	38303038	00000000	0B00B400	04001600
(68)	22 36	78	[illegible]	[illegible]	[illegible]	05000000	00007678	7374646C	69624300	30322D32
(72)	322D3837	62696E6B	383 3 38	00000000	0C00C800	04001600	22003600	78008C00	00000000	00000000
(76)	000 0000	06000000	00007678	7374646C	69624300	30322D32	322D3837	62696E6B	38303038	00000000
(80)	0D 054	04001800	00000000	00000000	00000000	00000000	00000000	02000000	00007678	7374646C
(84)	696243	3 322D32	322D3837	62696E6B	383 3 38	00000000	0E00C800	04001600	22003600	78008C00
(88)	000 0000	00000000	00000000	06	00007678	7374646C	69624300	30322D32	322D3837	62696E6B
(92)	383 3038	00000000	0F 0036 0	02000000	00000000	00000000	00000000	00000000	00000000	01000000
(96)	7678	7374646C	696243	3 322D32	322D3837	62696E6B	38303038	00000000	10004000	02000E00
(100)	2A	[illegible]	[illegible]	[illegible]	[illegible]	03 00000	00007678	7374646C	69624300	30322D32
(104)	322D3837	62696E6B	38303038	00000000	14002C00	02001800	28000000	00000000	00000000	00000000
(108)	[illegible]	03000000	00007678	7374646C	69624300	30322D32	322D3837	62696E6B	38303038	00000000
(112)	15 4	2	[illegible]	[illegible]	[illegible]	[illegible]	00000000	01000000	00007678	7374646C
(116)	69624300	30322D32	322D3837	62696E6B	38303038	00000000	1C001000	02000000	00000000	00000000
(120)	[illegible]	00000000	00000000	01000000	00007678	7374646C	69624300	30322D32	322D3837	62696E6B
(124)	383 3 38	[illegible]	62 8E 0	0200 A00	00000000	00000000	00000000	00000000	00000000	02000000
(128)	7678	7374646C	696243 0	30322D32	322D3837	62696E6B	38303038	00000000	E3005AC1	0200 AC0
(132)	000 0000	00000000	00000000	0000000C	00000000	02000000	00007678	7374646C	69624300	30322D32
(136)	322D3837	62696E6B	383 3 38	00000000	64000400	02000000	00000000	00000000	00000000	00000000
(140)	[illegible]	1	7678	7374646C	69624300	3 322D32	322D3837	62696E6B	38303038	00000000
(144)	65 4	2	[illegible]	[illegible]	00000000	00 00000	00000000	01000000	00007678	7374646C
(148)	69624300	30322D32	322D3837	62696E6B	38303038	00000000	66000400	02000000	00000000	00000000
(152)	000 0000	00000000	00000000	01000000	00007678	7374646C	69624300	30322D32	322D3837	62696E6B
(156)	383 3 38	[illegible]	67 4	02	00000000	00000000	00000000	00000000	00000000	01000000
(160)	00007678	7374646C	696243	30322D32	322D3837	62696E6B	38303038	00000000	69000400	02000000
(164)	[illegible]	00000000	00000000	00000000	00000000	01000000	00007678	7374646C	69624300	30322D32
(168)	322D3837	62696E6B	383 3 38	000	6A000400	02000000	00000000	00000000	00000000	00000000
(172)	[illegible]	1	7678	7374646C	696243	3 322D32	322D3837	62696E6B	38303038	00000000
(176)	6B 0400	02000000	00000000	00000000	00000000	00000000	00000000	01000000	00007678	7374646C
(180)	696243	30322D32	322D3837	62696E6B	38303038	00000000	6C000400	02000000	00000000	00000000
(184)	[illegible]	[illegible]	[illegible]	01	00007678	7374646C	69624300	30322D32	322D3837	62696E6B
(188)	383 3038	[illegible]	6D 4	02	00000000	00000000	00000000	00000000	00000000	01000000
(192)	60DA	38003982	93 3922	DA000100	00000900	571C78C3	2C78C32D	32C30C70	00000000	0000DA00
(196)	1	92 14	14 5	434A3082	5844	00000000	DE460CAC	1A3C2773	2E43E053	42444E6B
(200)	AC4618BF	7744EA39	85C1FC12	C043AAA8	CA41BEEF	8843EC8E	58C6DA48	4244245A	4244B962	434A3082
(204)	5844	AE41A819	01 2213	5000DA00	77813800	00742705	2BA0D45D	CD022FFE	F2324D33	14001414
(208)	F8 BA	EB 8	8	[illegible]	14000200	77BCEFF0	7BBDDFF0	FF00FFFF	FF000023	FA00FA00
(212)	64 3	1 2213	5 DA	772139	80742705	2BA5D45D	D90267FE	8C32F0F6	14000000	F4 0BF00
(216)	E20 5C0	C8001200	12	00000000	F7BCEFF0	FBBDDFF0	FF00FFFF	FF 0023	FA00FA20	10006804
(220)	0708C1 1	00001 19	3120BD41	86CA0010	000CC42	9EA1CC01	320181F9	FF2E3801	A1011006	5B0ACC42
(224)	9EA1	D842	8642D842	8642	FFFF	15 8114	10006804	07FAB803	00033189	51A00000
(228)	A541	D5E7CD42	AAB78EFF	D2 2F 1	4E243D 1	98 10104	F54FCD42	AAB7CA42	B1310000	00000000

7909
79+0
8009

77=4D
78=4E
79=4F
80=50
81=51
82=52

Day 218
year 1980

481 TYPE

514 start

TYPC

(752)	[illegible]6A77B8	7[illegible]7[illegible]8F	F7[illegible]	F7[illegible]	F7[illegible]	F7[illegible]7A[illegible]	F7[illegible]67[illegible]	F768836[illegible]	F7[illegible]800	2F[illegible]11C69
(756)	C17186A6	15003E01	1C[illegible]3E[illegible]1	30C03070	04044040	81FF0081	64008400	01002213	5000DA0C	77216600
(76[illegible])	8[illegible]9827[illegible]5	2B[illegible]DD65D	[illegible]DFDA6[illegible]A	3448BAFF	14[illegible]	D8[illegible]181[illegible]1	0D02360[illegible]	C9[illegible]12B[illegible]	2C[illegible]	[illegible]0000
(764)	F7BCEFF	FBBDDFF	FF[illegible]FFFF	FF[illegible]23	FA[illegible]FA[illegible]	1[illegible]6E[illegible]2	[illegible]B[illegible]4F[illegible]4	[illegible]48851	116[illegible]7242	11C3F741
(768)	[illegible]8DC3542	[illegible]C3D7BFE	4B[illegible]1E2FB	4D3BBF00	9E001D[illegible]6	AD[illegible]E842	CD71CE42	9DDBF642	6E3F[illegible]F43	E9D2BD42
(772)	82534E[illegible]1	15[illegible]8[illegible]8	[illegible]8[illegible]A[illegible]8	1[illegible]C65[illegible]C	0B4[illegible]E904	[illegible]A1C91	11200542	A15[illegible]0542	56AEC941	C1BE9AEE
(776)	E2[illegible]4D[illegible]4	BE37C1[illegible]	9E[illegible]9[illegible]5	3216[illegible]	[illegible]	[illegible]	[illegible]000C[illegible]	[illegible]000C[illegible]	0000000C	15001C08
(78[illegible])	[illegible]8[illegible]1E1C	1[illegible]65[illegible]8	[illegible]B3BF8[illegible]3	[illegible]61F89	20[illegible]	[illegible]09842	369EDB41	B97527FE	C9[illegible]17[illegible]	6E3A9E[illegible]
(784)	C3[illegible]BA[illegible]5	55[illegible]B[illegible]	[illegible]0	00000000	00000000	[illegible]00000	00000000	15[illegible]09F[illegible]8	0800219F	1000600 0
(788)	[illegible]723F8[illegible]3	[illegible]063B99	212[illegible]	[illegible]0B741	FEF68542	772B5EFE	E2016FFB	5C28A4[illegible]	BB001705	A60E0000
(792)	[illegible]	[illegible]B842	EA318F42	D5F5[illegible]	[illegible]039[illegible]2	15[illegible]BB14	650[illegible]2[illegible]			

EOJ STOP REQUESTED IN FILE 1

EOJ DUMP STOPPED AFTER FILE 1 # OF PERMANENT READ ERRORS 0

START TIME 4/[illegible]2/92 06:50:24 STOP TIME 04/02/92 06:51:32

$$

$EXE TPDUMP BS

REQ. AGENT	RAND NO.	ACQ. AGENT
RLR		SJK

HEAO-3

HEAO C-3 VERIFY PROGRAM

79-082A-03C SPIS-00006

This data set catalog consists of 1 tapes. The tapes are 6250 bpi, 9-track, multifiled, binary, created on the IBM 360. The tape is a verify program for the data sets 79-082A-03A and 79-082A-03A. The D and C numbers, time spans, and number of files are as follows:

D#	C#	FILES
D-76250	C-29139	08

REQ.AGENT	RAND NO.	ACQ. AGENT
DEW	V0190	CHB

HEAO-1

A-2 LED SOFT X-RAY SKY CATALOG

77-075A-02F ASXR-00064

THIS DATA SET CONSIST OF ONE TAPE. THE TAPE IS 800 BPI, 9 TRACK, EBCDIC WITH ONE FILE OF DATA. THE TAPE WAS CREATED ON THE IBM COMPUTER.

D#	C#
D-57541	C-23135

THE PENNSYLVANIA STATE UNIVERSITY
525 DAVEY LABORATORY
UNIVERSITY PARK, PENNSYLVANIA 16802

College of Science
Department of Astronomy

Area Code 814
865-0418

July 29, 1982

Dr. Maureen C. Locke
National Space Sciences Data Center
Goddard Space Flight Center
Code 601
Greenbelt, MD 20771

Dear Dr. Locke:

Enclosed you will find a magnetic tape containing the HEAO-1 A-2 LED Soft X-ray Source Catalog for submission to the NSSDC. The data in the catalog are the same as we have submitted for publication in the Astrophysical Journal Supplement Series.

I also include a brief description to facilitate reading the tape and one copy of the catalog paper preprint. If any more information is required call me at (814) 865-0418.

Sincerely yours,

Dr. J. A. Nousek

JAN:kkb

Enclosures

Magnetic Tape Containing HEAO-1 LED Soft X-ray Sky Catalog

The enclosed magnetic tape contains the HEAO-1 LED Soft X-ray Catalog published in the Astrophysical Journal Supplement Series. The tape is written as a nine-track tape at 800 bpi density, using EBCDIC characters.

The data are organized to directly mimic the appearance of the printed page in the catalog. Each record contains 132 bytes and represents one printed line of catalog. At IBM installations the data control block parameter looks like this: DCB = (LRECL=132, BLKSIZE=132, RECFM=FB).

To interpret the fields, a program must first recognize that the data are grouped into pseudo-'pages' with 49 records (lines) per page. On each page the first seven (7) lines correspond to a header (the same for each page). The remaining 42 lines consist of data for 7 sources, grouped with 6 lines per source. Decoding of the data fields within each line is relatively obvious after examination of the attached sample page (Fig. 1).

A possible FORTRAN code reading each source is the following:

```
      READ 10, H1, H2, F1, F2, C1, C2, C3, C4, FA, FB, HC, H3
10    FORMAT (A8,1X,A16,2(1X,F6.2),1X,4(1X,F6.2),1X,F4.2,2X,F4.1,3X,A30,1X,A8)
```

The meaning of each variable changes depending on which line within the source block is being read. The definitions are the following:

ON SOURCE LINE 1:

F1 = Galactic Longitude(l^{II}) of center of overlap error box (OEB)

F2 = Right Ascension (RA) of center of OEB

C1 = RA of top left corner of OEB

C2 = RA of top right corner of OEB

C3 = RA of bottom right corner of OEB

C4 = RA of bottom left corner of OEB

FB = Source intensity (cts-s^{-1}) in 1 keV band ('<' means source was not detected in this band)

HC = Comments

ON SOURCE LINE 2:

F1 = Galactic Latitude (b^{II}) of center of OEB

F2 = Declination (DEC) of center of OEB

C1 = DEC of top left corner of OEB

C2 = DEC of top right corner of OEB

C3 = DEC of bottom right corner of OEB

C4 = DEC of bottom left corner of OEB

FA = Area of OEB in square degrees

FB = 1σ uncertainty in 1 keV band intensity

HC = Comment

ON SOURCE LINE 3:

H1 = HEAO A-2 LED Source names

H2 = Other names

H3 = HEAO A-2 LED Source names (repeat of H1)

ON SOURCE LINE 4:

F1 = l^{II} of center of best fit error box (BEB)

F2 = RA of center of BEB

C1 = RA of top left corner of BEB

C2 = RA of top right corner of BEB

C3 = RA of bottom right corner of BEB

C4 = RA of bottom left corner of BEB

(If F1 to FA are blank then no best fit box could be determined).

FA = Area of BEB

FB = Source intensity in 1/4 keV band ('<' means source not detected in 1/4 keV band.)

HC = Comments

ON SOURCE LINE 5:

F1 = b^{II} of center of BEB

F2 = DEC of center of BEB

C1 = DEC of top left corner of BEB

C2 = DEC of top right corner of BEB

C3 = DEC of bottom right corner of BEB

C4 = DEC of bottom left corner of BEB

FB = 1σ error in source intensity

HC = Comments, including reference index

ON SOURCE LINE 6:

Blank

To summarize, this nine-track 800 bpi tape written in EBCDIC contains the HEAO-1 A-2 LED sky catalog in 132 byte records. Each 49 records constitute a page unit, grouped as follows:

LINES	DATA		LINE	
1-7	Header			
8-B	Source #1	=	8,9	Overlap Box
			10	Names
			11,12	Best Fit Box
			13	Blank Divider
14-19	Source #2			
20-25	Source #3			
26-31	Source #4			
32-37	Source #5			
38-43	Source #6			
44-49	Source #7			

Fig 1 HEAO A-2 Soft ay Catalog

HEAO A-2 Name	Other Names	Center lII / bII	Center RA (1950) / Dec (1950)	Corners				Box Area	Int/Err (Overlap Box: 1 keV / Best Fit Box: 1/4 keV)	Comments	HEAO A-2 Name
		120.00	5.40	3.72	6.68	7.30	4.34		8.1	SNR	
		1.17	63.61	63.11	64.39	64.09	62.83	.72	1.0		
H0021+63	TYCHO SNR										H0021+63
									<		
									1.6	Ref. 24	
		302.49	13.53	11.27	14.54	15.59	12.41		3.0	in SMC	
		-44.00	-73.40	-74.22	-72.40	-72.55	-74.39	.72	.5	SMC X-2 ?	
H0054-73											H0054-73
		302.03	14.58	13.70	14.39	15.45	14.77	.16	<		
		-44.60	-72.78	-72.91	-72.49	-72.64	-73.07		1.4		
		296.57	24.15	22.69	21.66	24.27	25.22		<	variable source	
		-48.09	-68.71	-70.15	-69.96	-68.18	-68.35	.80	.8		
H0136-68	3A0143-601										H0136-68
									2.6		
									.5		
		132.75	33.03	35.69	32.21	32.02	36.60		3.0	SNR	
		1.65	62.61	62.94	62.09	62.25	63.11	.33	.3		
H0215+62	HB3										H0215+62
									<		
									.5	Ref. 13	
		285.39	36.44	35.13	37.17	37.69	35.66		<	confused with H0305-65	
		-51.40	-62.57	-63.21	-61.76	-61.92	-63.37	.50	1.0	and H0248-63	
H0225-62											H0225-62
		284.97	36.77	36.19	36.82	37.34	36.71	.16	4.8		
		-51.50	-62.33	-62.48	-62.03	-62.18	-62.64		.7		
		136.24	41.81	44.33	40.08	39.31	43.64		1.4	QSO ?	
		2.84	62.37	62.45	61.53	62.24	63.18	1.76	.3		
H0247+62	3A0241+622										H0247+62
									<		
									1.0		
		145.77	41.87	39.16	44.22	44.60	39.60		3.6	AWM7	
		-16.12	41.20	40.97	42.28	41.36	40.00	3.82	.9	NGC1129 CD group	
H0247+41	3A0251+414										H0247+41
		145.81	41.93	41.10	42.36	42.76	41.61	.95	<		
		-16.00	41.22	41.50	41.83	40.92	40.60		2.7		

1 10 27 34 42 49 56 63 70 76 83 114

```
$NOP
$NOP
$NOP ******************  EBCDIC LIST OF DO-1  ****************
$EXE TPLIST BS

INPUT PARAMETERS ARE:  ED SR=1=5

 TAPE NO.   1              FILE NO.   1
 RECORD   1                LENGTH   132


 TAPE NO.   1              FILE NO.   1
 RECORD   2                LENGTH   132
                            -------------  Overlap Box  -------------------  1 keV

 TAPE NO.   1              FILE NO.   1
 RECORD   3                LENGTH   132
HEAO A-2       Other        Center  Center                             Box
               HEAO A-2

 TAPE NO.   1              FILE NO.   1
 RECORD   4                LENGTH   132
  Name         Names          lII   RA (1950)         Corners          Area Int/Err           Comment
s                Name

 TAPE NO.   1              FILE NO.   1
 RECORD   5                LENGTH   132
                              bII   Dec(1950)


***** JOB DONE.
 EO LPS

$$
```

D57541
Heao-1

HEAO-3
79-082A-06A

HEAO-3

GAMMA-RAY SPEC SHEILDING

79-082A-06A ASGR-00001

THIS DATA SET CONSISTS OF 17 TAPES. THE TAPES ARE 9-TRACK, 1600 BPI, BINARY WITH 36 FILES OF DATA. THE TAPES WERE CREATED ON AN IBM COMPUTER THEY CONTAIN ONE DAY OF DATA PER FILE. THE DC TAPES ARE 3480 CARTRIDGES. THE DD AND DC NUMBERS AND TIMESPANS ARE AS FOLLOWS:

DD #	DC #	FILES	TIMESPAN
D-84424	C-28827	36	09/23/79-10/28/79
D-84425	C-28828	36	10/29/79-12/03/79
D-84426	C-28829	36	12/04/80-01/08/80
D-84427	C-28830	36	01/09/80-02/13/80
D-84428	C-28831	36	02/14/80-03/20/80
D-84429	C-28832	36	03/21/80-04/25/80
D-84430	C-28833	36	04/26/80-05/31/80
D-84431	C-28834	36	06/01/80-07/06/80
D-84432	C-28835	36	07/07/80-08/11/80
D-84433	C-28836	36	08/12/80-09/16/80
D-84434	C-28837	36	09/17/80-10/22/80
D-84435	C-28838	36	10/23/80-11/27/80
D-84436	C-28839	36	11/28/80-01/02/81
D-84437	C-28840	36	01/03/81-02/07/81
D-84438	C-28841	36	02/08/81-03/15/81
D-84439	C-28842	36	03/16/81-04/20/81
D-84440	C-28843	36	04/21/81-05/29/81

79-082A-06A

New Burst Search
Logical Record Format - 07/18/88

Word	Description
1	Orbit number(I4)
2	Absolute major frame number(I4)
3	Year of major frame(I4)
4	Day of year of major frame(I4)
5	Seconds of day of start of major frame(I4)
6	Microseconds of start of major frame(I4)
7	Spacecraft X-position in meters(I4)
8	Spacecraft Y-position in meters(I4)
9	Spacecraft Z-position in meters(I4)
10	McIlwain L parameter in (earth radii)/1000000-(I4)
11-14	Right Ascension of Y-axis in radians/1000000-(4I4)
15-18	Declination of Y-axis in radians/1000000-(4I4)
19-22	Right Ascension of Z-axis in radians/1000000-(4I4)
23-26	Declination of Z-axis in radians/1000000-(4I4)
27	Error sum for the major frame(I4)
28	Error sum for attitude data(I4)
29-30	Command status for the frame(4I2)
31-46	Shield 1 LLD counts(32I2)
47-62	Shield 2 LLD counts(32I2)
63-78	Shield 3 LLD counts(32I2)
79-94	Shield 4 LLD counts(32I2)
95-110	Collimator LLD counts(32I2)
111-126	Or'd LLD counts(32I2)
127-128	Shield 1 window counts(4I2)
129-130	Shield 2 window counts(4I2)
131-132	Shield 3 window counts(4I2)
133-134	Shield 4 window counts(4I2)
135-136	Collimator window counts(4I2)
137-138	CPD LLD counts(4I2)
139-140	CPD ULD counts(4I2)

Note: The data in words 31-140 have been time shifted one position. Thus the accumulated number of counts in the time interval t_1 to t_2 appear at time t_1.

Note: Missing data in words 31-140 is indicated by the pattern 4ZFFFF.

Note: Except for words 127-134 all the rate counters can enter time mode. This is indicated by the most significant bit being set.

DUMP OF TAPE KM2 .1

D-84424
79-082A-06A

INPUT TAPE KM2 01 ON FT
DATA INPUT ES NE 36 FL=1=1=1 SR 36 . . SR 36 LAST 1

FILE 1 RECORD 1 LENGTH 1979 36 BYTES 2066

(0)	000 002F	0000 1AD8	00 79B	0001 A	000 BE3	716E6	FFDCDF3C	FFA9D97	03 1F45	1640 3
(4)	159948	01696CD	0169470	0169265	0106848	1 07 4D	11107892	111C8110	42EFDA2	2EFD47
(8)	02EBD38	02EBD A	24 F	2FDB	2D09	0F6	[illegible]	[illegible]	FDFCFDFC	FDFCFDFC
(120)	08AA0877	08EE0941	860 726	6 D 6E3	974 886	831 7E6	7ED 884	83 682	875 84C	7E5 8C4
(160)	08720951	0921 897	8C2 6A6	82A 8A1	8F4 79F	8C2 979	9970A9F	0A33 A0C	9E28844	0809 92
(2)	5E5 9AA	982 A17	975 316	9A3 [illegible]	A6B 9C	9D6 9E9	9D1 A1A	4B66 9E5	987 A88	0A4F 9E9
(240)	AA7 99A	9F 382	956 A07	58A A01	A4C 975	1 F7 489	ABF B8D	PB2 6B6	97A A5C	AB9 AF
(280)	0A8C0AF6	0A37CAE7	0AFA BF8	C3A 991	4A82 BE2	0A9AJB3E	0BBE1A4E	0A510688	3A4 B5C	0C7 06E
(320)	0B420AD9	AAD0AE9	AD A64	A8 0B81	1A9B C1	1AFE 1B8E	1B840BBE	0AD9 E57	A8B AE2	C A AA6
(360)	E01 B07	B57 BE9	B6F AA	C76 0E9	12631274	14FD134E	13D411E4	14521 FC	12E211F9	120B11A1
(400)	11F812DA	12F 1217	1300120A	11DC103F	137E144C	17 81141	12211479	131 1475	14B 1389	128F15D2
(440)	25C626A3	28C02874	27112513	2B7D24DB	274C25D8	26B425C8	24AB2778	25412744	273F2679	25402771
(480)	27A728B4	2CF924C9	26592882	265B27B4	29722681	27912AFF	13 DC382	0368 37F	3AE 3F2	3F8 446
(520)	43E 3E9	431 4 8	3A 3	3A5 3DC	F7E EA7	F87 FB3	14671 1A	14051 07	135 F2	1 2 12
(560)	000 002F	0000 1AD9	00 7 B	0001 A	000 0C0	67A77	FFE FAEF	FFA9A6F9	328474	17 C5
(600)	0169084	0168EEA	01680 0	0168C3C	11C8954	1C92F6	11C9C23	11C9C0	2EFCC8	2EFCC0
(640)	02EBBF7	02EBB6C	3 A	329E	3248	3249	[illegible]	[illegible]	FDFCFDFC	FDFCFDFC
(680)	0873 838	93A 8E5	949 9	8CA 8C2	982 8A0	93E 8A8	8C5 8EE	83E 9	96D 9	97 949
(720)	08CC093E	0A64 97F	99B 97D	905 92C	91F 9FB	9EC09FA	09A60A15	0A77 A72	AA60A02	A 0A41
(760)	0A750 9EC	0A8B0A3B	0B1B 0A0	0957 A01	0A8E0A47	0A0640A36	0AED0B41	4B6A0AD3	0AC40A70	0A630827
(800)	AB2 ACD	B68 B43	C1E F	C64 A	FA8 B1	740B22	BC5 A9E	88 F3	AF1 AF	4 CE
(840)	0C150B11	0B5B0B54	C40 C9	0B8F 0538	0C0 C6	0A15 BB9	874 C48	F6 C6	0A380A86	0BF 048
(880)	0B8 0BEC	0B 8E 0E	C3 B3	C52 876	F46 C1A	C72 B71	C97 AC	CBD B	CF2 C2	C9A 84
(920)	0C720C76	0AE60C16	0BFA C8B	0CAA0C6	137F1458	13641534	132413BC	13401417	146F132E	14F014CB
(960)	13081436	142417E9	13 A1	1E6	140714 F	1 1340	14991 FD	1340130	13DE1309	1FB019
(1000)	2826287B	28702 3BB	28A527A8	27512B7F	29 2C6C2	29E128FC	28942886	283C28F	29402856	20A378AA
(1040)	2A6A29FB	2BAE2888	29FB2AC9	27482AC6	28662950	20022EF9	13650354	13FF 13A6	1325 0418	041F 43F
(1080)	45 47A	42B 444	394 3 3	3E6 4 4	F6 1 77	1 1 15E	1 4 1	1 4E1 CD	12 119	120 14
(1120)	000 002F	0001ADA	7 B	1 A	03F	DE77	FFEB2413	FFA59834	34D4DF	18CD3
(1160)	00168B3C	00168A74	001689AE	0016880B	000CAF57	000CB941	000C0C16E	000C0C858	042EBACA	042EBA13
(1200)	02EB928	02EB8 6	328E	328B	323A	031CB	[illegible]	[illegible]	FDFCFDFC	FDFCFDFC
(1240)	9B4 9C5	9A3 943	A C B	978 803	A C43	AC 994	9984 BD	A5F 949	A B 9C4	B F AC5
(1280)	0924093C	09E80A0E	A2F 933	956 A89	AE A1F	B5E B 8	BAE ABA	B F B5	B87 B7F	BAA AD8
(1320)	0B240CA8	0B3 AB2	0BA4 AD8	C44 BEF	BE9 C21	CE8 C2C	0B88 BB2	0BC4 B4D	0695 BD7	0B17 C65
(1360)	C9C AD6	C4 C A	C 4 D7	DE2 C0	C34 B48	C97 C7C	BAF CE3	C38 CCC	C68 C3	E3A C56
(1400)	CC9 D76	DA4 C6F	C17 C04	C67 DA4	D3A CD7	C99 CFC	D4C C3D	DC0 E5C	CD4 CCF	D 8F3
(1440)	0CCDCC1	0D160BFD	C9 C78	C9E C9	C62 B96	D5 CF8	D8E D28	CCA D	C7C D2F	C 7 E2F
(1480)	0DF90D5C	0BEB0DFF	D5 C1	E51 E3E	157F1434	14051425	1551144E	18431307	171C1595	140A1514
(1520)	171F1578	16F 176E	1720150	16FF1610	141 16F	15931FC	16E5116D	16871697	16D714ED	175017EF
(1560)	2A782A05	2B6529EC	2BE0 A93	2E1A2B9D	2C73 E53	2A882E49	20122A71	2DEB2D4B	2DE52D3E	2E212B94
(1600)	2A4A2C4A	2BDC2DE2	2E4C2DFA	2C8C2E39	2D202B15	2F2E2E6E	03B0388	0392 3BF	419 473	042 493
(1640)	459 46	488 49E	3D9 4	42 426	1 96121F	11F61249	11DE113C	11281 12F	1138140	4152140
(1680)	00 002F	1ADB	7 B	1 A	C F	41F8	FFE9BFAD	FFA9C3E	37 1DC	03 89E
(1720)	00168835	0016873B	016803E	016A6C2	00CCF74	0CD6BD	000CBA6A	00CBF20	2EB6D6	2EA7B
(1760)	002EBAB8	002EC5A8	3114	3138F	3 3D	2729	[illegible]	[illegible]	FDFCFDFC	FDFCFDFC
(18)	A52 A9A	8C3 A 2	A8A A C	81C 9DE	A84 8CF	3 95C	AF8 FA1	ACC B6B	A96 ACE	A5E A33
(1840)	A7C B8A	A31 ADC	AF A76	899 A8	B38 B66	97 BA7	BA7 BEB	DA1 CEC	547 C8	A7 CA1
(1880)	0C1C0E8E	0C29 C1D	CBB C07	D81 C81	CC2 D3	D9 C94	CB24CB7	C1E 0EA	DA60C7	DD D71
(1920)	E5E DC4	0571D26	CFC C7F	D87 D 2	DFA C2	58 CCF	C024E26	D2B D6D	E25 EA7	E3C D6D
(1960)	CF4 D21	DD4 E4C	D97 DED	C82 DE7	E4 E	EE8 E	121E4E46	065 E1	E4C DE4	E73 D74
(2000)	0D920D73	0D8F0D30	CEA EFF	DBF D14	F3C F29	097 F5D	E45 DC3	D4D D7F	DEF DEE	DD D3E
(2040)	0E45 E96	0DD7 EBE	E 0 E 4	E 8A CA7	15D 16A6	1 E8178E	15E 1581	13D817E5	176A1A2A	17651757
(2080)	1C6 17AA	16FC1A81	187A 6 D	172 70	17071810	1 9 176	191C178F	1928166	19 A1979	193F1928
(2120)	2D162DFF	32962091	2E89 D 1	31402EAC	2DB 2E	2E8 2E49	33423 09	2F443378	31 72DF1	2E4 E70
(2160)	2DF 3002	2D782EDA	3134 F	31383174	36203146	31483190	3333 3D	3306 4 9	464 468	48F 40E
(2200)	0469 488	04A4 407	422 47	045 437	13121286	10281307	11331166	14881 E3	163 168	144 16D
(2240)	00 002F	1ADC	7	1 A	CB7	AAF89	FFEDA622	FFAA1837	0791390	11 8A87
(2280)	016B BB	016866D	16 705	16 964	04AB	AF465	98841	BBAB	2FCA	2FC8D

```
( [illegible])  [illegible]
( 364[illegible])  [illegible]
( 368 )  [illegible]
( 372 )  [illegible]
( 376 )  000 0000  00000000  [illegible]
( 38[illegible])  [illegible]
( 384 )  [illegible]
( 388 )  [illegible]
( 392 )  [illegible]
( 396 )  [illegible]
( 4[illegible])  [illegible]
( 404 )  [illegible]
( 408 )  [illegible]
( 412 )  [illegible]
( 416 )  [illegible]
( 42[illegible])  [illegible]
( 424 )  [illegible]
( 428 )  [illegible]
( 432 )  00000000  [illegible]
( 436 )  [illegible]
( 44[illegible])  [illegible]
( 444 )  [illegible]
( 448 )  00000000  00000000  [illegible]
( 452 )  [illegible]
( 456 )  [illegible]
( 460 )  [illegible]
( 464 )  [illegible]
( 468 )  [illegible]
( 472 )  [illegible]
( 476 )  [illegible]
( 48[illegible])  [illegible]
( 484 )  [illegible]
( 488 )  [illegible]
( 492 )  [illegible]
( 496 )  [illegible]
( 5[illegible])  [illegible]
( 504 )  [illegible]
( 508 )  [illegible]
( 512 )  [illegible]
( 516 )  [illegible]
( 520 )  [illegible]
( 524 )  [illegible]
( 528 )  [illegible]
( 532 )  [illegible]
( 536 )  [illegible]
( 54[illegible])  [illegible]
( 544 )  [illegible]
( 548 )  [illegible]
( 552 )  [illegible]
( 556 )  [illegible]

     FILE   INPUT     DATA RECORDS     MAX.
            RECS.        INPUT         SIZE          READ ERROR SUMMARY
       36    185          186          [illegible]   PERM  ZERO B  SHORT  UNDEF.   INPUT RETRIES
                                                                                #RECS.  TOTAL#
EOJ        DUMP STOPPED AFTER FILE  [illegible]      # OF PERMANENT READ ERRORS

START TIME [illegible]1/22/92  [illegible]4:03:1[illegible]      STOP TIME  1/22/92  [illegible]4:[illegible]7:[illegible]

$$
$ASS  IN HT1
$EXE  TPNRCF BS
```